The Dissertation Committee for Travis H. Mercker
certifies that this is the approved version of the following dissertation:

Adaptive Estimation and Control Algorithms for Certain Classes of Large-Scale Sensor and Actuator Uncertainties

Committee:

Maruthi R. Akella, Supervisor

Ari Arapostathis

David G. Hull

E. Glenn Lightsey

Belinda G. Marchand

Adaptive Estimation and Control Algorithms for Certain Classes of Large-Scale Sensor and Actuator Uncertainties

by

Travis H. Mercker, B.S.As.E; M.S.E.

DISSERTATION

Presented to the Faculty of the Graduate School of

The University of Texas at Austin

in Partial Fulfillment

of the Requirements

for the Degree of

DOCTOR OF PHILOSOPHY

THE UNIVERSITY OF TEXAS AT AUSTIN

May 2012

Learn from yesterday, live for today, hope for tomorrow.
-Albert Einstein

To Natalie,
My partner on life's great journey

Acknowledgments

First and foremost, I want to thank my advisor Dr. Maruthi R. Akella. It has been the greatest honor and privilege to be able to work with him for the past six years. I have always felt nothing but unwavering support from him both in my research as well as my personal life. I could not have asked for a better mentor, and I will always be grateful for the work we have accomplished together.

I would personally like to thank the members of my committee: Dr. Ari Arapostathis, Dr. David G. Hull, Dr. E. Glenn Lightsey, and Dr. Belinda G. Marchand for taking the time out of their busy schedules to read through my dissertation and take part in my defense. Any feedback that they had certainly contributed to the end product of this dissertation. I would also like to thank all the professors as well as the staff of the Aerospace Engineering Department that I have encountered over the past decade. The support and opportunities that have been bestowed on me has contributed so much to my education and life.

I would be remiss not to acknowledge all of colleagues who also suffer through the daily grind of being a graduate student. To those who have gone: Dr. Kyle Demars, Dr. Tyler Summers, Dr. Srikant "Pudding" Sukumar, Hector Escobar, and Jorge Alvarez. And to those still left behind: Apurva Chunodkar, Divya Thakur, Sara Scaritt, Kelley Hutchins, Sung-Pil Yang, and Miki Szmuk. I will certainly remember (only sometimes fondly) the time we have spent working together. In addition, I want to thank any teaching assistants that I have had for their effort in helping me with my courses.

Last and certainly not least, I want to extend the deepest gratitude to my friends and my entire family. I could never properly put into words how much your support means to me (even though I know no one understands what it is I actually do). Specifically, to my Mom and Dad, it is because of you that I am the person I

am today and that I have been able to accomplish so much. I sincerely hope that you will take everything that I have done as a confirmation that you did things right. To everyone, it is through the individual sacrifices of all of you that I have been able to chase my dreams. For that, I will always be eternally grateful.

Adaptive Estimation and Control Algorithms for Certain Classes of Large-Scale Sensor and Actuator Uncertainties

Publication No. _____

Travis H. Mercker, Ph.D.
The University of Texas at Austin, 2012

Supervisor: Maruthi R. Akella

This dissertation considers the general problem of controlling dynamic systems subject to large-scale sensor and actuator uncertainties. The assumption is made that the uncertainty is limited to either pure rotation (i.e. special orthogonal matrix) or that each axis is rotated *independently*. Although uncertainty can appear in more general forms, this representation describes a "net-effect" when the ideal axes have become misaligned that is of fundamental importance to the control of numerous systems. Adaptive observers and controllers are introduced that guarantee perfect reference trajectory tracking even with the appearance of these large-scale uncertainties.

The specific contributions of this dissertation are as follows: (I) the problem of rigid-body attitude tracking with vector measurements, unknown gyro bias, and unknown body inertia matrix is addressed for the first time. In this problem, the body attitude acts as unknown special orthogonal matrix (i.e. sensor uncertainty). A set of adaptive observers and an adaptive controller is presented that guarantees perfect tracking as well as convergence of the attitude and bias estimates through a Lyapunov stability analysis. (II) An adaptive observer is developed for the scenario where the control is pre-multiplied by an unknown constant scaling and rotation matrix which gives a non-affine representation of the uncertainty. The observer is shown to be

convergent given a certain persistence of excitation condition on the input signal and using a smooth projection scheme on the estimate of the unknown scaling. In addition, the observer is combined with a stabilizing control to guarantee perfect tracking which establishes a separation like property. (III) The class of uncertainties where each axis of the control is independently misaligned is examined. The problem is split into studies of in-plane and out-of-plane misalignment angles given that they exhibit fundamental technical differences in establishing convergence. Where possible, rigorous stability proofs are given for a series of adaptive observers. The structure of the observers assure that the estimates do not introduce any singularities into the control problem other than those inherent from the misalignment geometry. The inherent singularities are avoided through the use of projection schemes which allow for extension to the control problem. This work represents the first significant effort to develop adaptive observers and controllers for this class of misalignments.

Table of Contents

List of Figures

Chapter 1

Introduction

1.1 Motivation

Technological advancements over the past few decades has seen a rapid increase in the ability to collect and share large amounts of data. Of particular interest, especially from a military stand point, is using the data to create Situational Awareness (SA); that is to determine information in a dynamic environment such that decisions can be made as defined by Nofi in [1]. In a battlefield scenario, SA is achieved through a variety of agents including: soldiers, unmanned aerial vehicles (UAV), and satellites. The main issue with any space assets is that their use is not mission specific and as such, is not as useful in rapidly evolving environments. Moreover, the number of space assets is typically limited. UAVs, on the other hand, are designed for specific missions and can be rapidly deployed to assist in achieving the necessary SA. Therefore, a need to shift the space asset paradigm from catch-all satellites to more mission specific, rapidly deployable space vehicles was introduced as described by Cebrowski and Raymond [2]. This new idea has become known as "Responsive Space." * The Department of Defense has taken an active interest in responsive space through the Operationally Responsive Space (ORS) office † which was started in 2007. The mission of ORS is the development of architectures and technologies such that space assets can be launched and mission ready within days to weeks as opposed to years. This will allow for better, mission specific information to be provided from the space assets in obtaining SA. Although responsive space systems clearly apply to the military, responsive space has been accepted throughout the broader aerospace

*More recently, this has been referred to as "Reinventing Space"

†`http://ors.csd.disa.mil`

community as a necessity for the future. The rising cost of launching and developing space assets has led to a call for less expensive alternatives to the current generation of satellites. Of particular interest is smaller but equally as capable teams of satellites which are easier to service and cheaper to replace.

The concept of very short lead times for launch is appealing; however, there is a significant cost especially when it comes to designing and implementing the underlying control system. Currently, satellites are assembled and prepped for years before being deployed. During this time, a good deal of time and effort is spent determining the inertia properties (e.g. mass distribution) and checking that there are no issues with the alignment of sensors and actuators. If a satellite is assembled, calibrated, and launched in a matter of weeks for a specific mission, it is expected that there could be large uncertainties across all components of the system. To perform accurate control of such a system, these uncertainties need to be accounted for while on orbit, otherwise, the stabilities properties and/or performance of the overall closed-loop control system could be severely compromised. Therefore, an artifact of the idea of responsive space is that the control system will have to be adaptive and on-board tunable to ensure closed-loop stability with acceptable performance.

To create an adaptive controller with good performance, the effect of the uncertainties on the system dynamics must be well understood. Significant work has been performed on controlling systems with unknown mass properties; however, far less attention has been paid to uncertain sensor or actuator misalignments, which can be just as detrimental to the stability of the overall control system. Since these uncertainties are introduced either through the available measurements or the implementation of the control system itself, their overall effect on the dynamics is quite different that that of uncertain plant parameters. A rigorous examination of sensor and actuator misalignments is noticeably lacking from current literature on adaptive estimation and control and is the main focus of this dissertation. Any results contained herein are directly applicable to responsive space systems as well as to any other dynamic systems which are susceptible to sensor and actuator alignment uncertainties.

1.2 Literature Review

In this section, the existing literature is introduced for the two main problems examined in this dissertation. The first review covers the literature related to the use of adaptive control for the rigid-body attitude tracking problem. The second examines the existing work related to control of dynamic systems with control uncertainties.

1.2.1 Rigid-Body Attitude Tracking

The problem of rigid-body/spacecraft attitude tracking has been studied extensively over the past decades with varying technical complexities. A wide range of controller and observer-controller combinations have been developed for different problem formulations. The difference between the formulations usually lies with either presence of unmodeled dynamics/disturbances or the availability and accuracy of certain measurements relating to the state or parameters of the rigid-body. In this dissertation, the formulation of the rigid-body attitude tracking problem is extended to include the scenario where the measured angular velocity has an unknown constant bias and the attitude (represented by a quaternion) is estimated through a set of vector measurements. In addition, inertia matrix uncertainties are included to further extend the scope of the problem under consideration.

The state-vector of the attitude tracking control problem includes the body angular rates and some representation of the attitude (quaternion, Modified Rodrigues Parameters (MRPs), direction cosine matrix). To have full-state feedback, the entire state must be available and perfectly known. A solution for the spacecraft attitude control problem with full-state feedback using a quaternion representation has been available for nearly two decades as introduced by Wen and Delgado [3]. As an alternative, Wie et al. [4] established that the optimal eigenaxis rotation could be applied through a judicious choice of the control gains. The full-state feedback problem has been extended to account for an unknown spacecraft inertia matrix using a certainty equivalence framework by Sastry and Bodson [5] and non-certainty equivalence framework by Seo and Akella [6] which both meet the control objective of perfect tracking

but require suitable persistence of excitation (PE) conditions on the attitude reference trajectory to ensure convergence of the inertia estimates to their corresponding true values. This problem has been extended further by Sanyal et. al [7] to include unknown constant or known frequency harmonic disturbance torques while still meeting the tracking control objectives. In addition to the full-state formulation, it has been shown that given perfect knowledge of the attitude, the control problem can be solved without the use of any angular rate information as found by Lizzeralde and Wen [8] due to certain passivity properties of the rigid-body attitude dynamics established by Tsiotras [9]. This has been shown by Akella [10] and Tayebi [11] to be applicable to the MRPs and quaternion representations of the attitude, respectively. It should be noted that this result has been expanded by Costic et. al [12] to allow for unknown inertia parameters. In addition to these results, there are a large number of results which include additional complexities such as: flexible dynamics, control saturation, actuator dynamics, and unknown external disturbances [13–21] . Although these results are useful, the shortcoming of each of these results is that in practice, perfect attitude measurements are seldom directly available to the controller, and angular rate measurements are inevitably corrupted by bias and noise. Thus, the control problem needs to be reformulated to include necessary observers that synthesize the attitude and angular velocity from more realistic measurement models. Since the attitude control problem is nonlinear and in general the separation property is not applicable, the solutions are not as straightforward as combining a stable observer with a stabilizing controller.

Viewed inside an observer-based framework, attitude quaternion and gyro-bias estimation can be performed using a variety of methods as surveyed recently by Crassidis et. al [22]. In practice, spacecraft attitude is estimated using a least squares approach or some form of the Kalman Filter. Lefferts et. al [23], Crassidis and Markley [24], and Fan and You [25] develop a Kalman Filter, an Unscented Kalman Filter and a Sigma Point Filter, respectively for attitude estimation. Although these are valid observers, it can be difficult to develop mathematically rigorous convergence proofs for these filter formulations because they assume a stochastic and noise

driven system. Moreover, the Kalman Filter results are based on a linear analysis and as such can only be local results. Thus, the general Kalman Filter approach is not considered in this dissertation. Boskovic et. al [26] have attempted to directly use the kinematics to derive a nonlinear estimator. Similarly, both Akella et. al [27] and Mahony et al. [28] use the topological properties of the special orthogonal group $SO(3)$ which describe the body orientation to independently arrive at a nonlinear observer that guarantees convergence of the attitude estimates. The latter results are of particular interest because the Lyapunov analysis used to prove convergence of the estimates is often amenable to extensions for the closed-loop control problem. Akella et al. [27] show convergence of the estimated attitude to the true attitude given a time-varying reference direction but assuming there is no angular rate bias, where as Mahony et al. [28] proves convergence of both the attitude and bias estimates using a constant reference direction. The formulation of [27] was used by Seo and Akella [29] to solve the attitude tracking problem with vector measurements albeit with perfect angular-rate measurements. Separately, the attitude tracking problem with unknown angular velocity bias has been completed by Thienel and Sanner [30] but under the restrictive assumption of direct measurement of the attitude quaternion. A similar result but including actuator saturation has been proposed by Boskovic et. al [31]. The combined problem of controlling a spacecraft with unknown angular velocity bias as well as with attitude available only through vector attitude measurements has been studied previously by Hamel, Pounds, and Mahoney [32, 33]. Both use an adaptation of passivity based control to develop controller-observer combinations for the problem. By their own admission, Pounds et. al [33] suggest that there are unresolved issues related to the implementability of the control law in [32]. Reference [33], however, has no such implementability issues, and the work therein is most related to this dissertation. The resulting controller of [33] contains an inverse of the body of inertia matrix that makes the system performance particularly susceptible to measurement noise; moreover, the result cannot be directly applied when the inertia matrix is unknown. The controller described herein obtained through immersion and invariance has an affine representation of the inertia matrix that is less affected by

measurement noise and requires less control effort to achieve approximately the same rate of convergence. In addition, the affine representation allows for extension to the case of constant unknown inertia which has not been shown previously.

1.2.2 Control of System with Actuator Misalignments

The use of adaptive algorithms to estimate uncertain parameters has been more widely studied in the past few decades as a means to ensure both closed-loop stability and robust performance. For most typical adaptive control formulations, the parameter uncertainty is restricted to be affine (i.e., linear) within the plant dynamics while the control signal is assumed be perfectly applied. In practice, one can also expect there to be unknown and non-negligible actuator uncertainties. It is just as important to estimate these uncertainties during application of the control signal. In the general case of controlling three degrees of freedom motion via three independent actuator inputs, the uncertainty could be mathematically represented as a constant unknown matrix that pre-multiplies the control vector in the form of a high-frequency gain. Viewed in this framework, the ideal case is when the control vector is pre-multiplied by an identity matrix. The adaptive estimation problem is then to determine the unknown values of the uncertainty matrix while ensuring desirable boundedness and convergence properties for the overall estimation process. Such adaptive estimation can be performed through any of the classical parameter estimation schemes available in literature dealing with identification theory; however, there are important practical considerations when introducing the resulting estimate values into the closed-loop control signal. The obvious choice is the invocation of the standard certainty equivalence formalism [5, 34, 35] that allows for use of estimate values to eliminate as closely as possible the unknown matrix by taking the inverse. This action requires that the estimated matrix be invertible to begin with, but also have a small condition number because this could otherwise lead to large demands on the required control signal. Furthermore, the estimates should to be continuous to avoid discontinuities or high-frequency chattering effects within the control signal. Thus, the estimation problem must be approached with due caution.

An alternate approach to representing the uncertainty as a pre-multiplying matrix is to derive the specific dynamics of the actuator and determine which particular unknown parameters represent the uncertainty . A specific example of this approach is the use of a control-moment gyro (CMG) to perform actuation of a spacecraft as studied by Chakrabotty et. al [36] and Yoon and Tsiotras [37]. One potential issue with this approach is that the control signal is now part of the internal dynamics of the system. This serves the purpose of absorbing the uncertainties to make them appear in the form of plant parameters, albeit at the price of overparameterization, which makes it amenable within the classical adaptive control framework. Through this overparameterization based approach, however, broader generalizations cannot be made to larger classes of control uncertainties regardless of the actuator dynamics.

In this dissertation, the problem is restricted to directly estimating the uncertainty matrix. The most general adaptive control problem where the input scaling matrix can assume unknown values provided that the misalignment matrix is nonsingular is typically referred to as the unknown high-frequency gain problem. In the case that the gain is scalar, the problem has been solved with a variety dynamics (i.e. linear and nonlinear) and somewhat standard assumptions on the uncertain gain [38–40]. It has been widely studied and resolved when the high frequency gain is a matrix under the framework of model reference adaptive control (MRAC) by Ioannou and Sun [41] and model reference adaptive control with immersion and invariance by Ortega and Astolfi [42]. Both of these aforementioned approaches present restricting conditions that require additional a priori information on the control uncertainties although the immersion and invariance schemes typically need weaker hypotheses for ensuring global adaptive stabilization. The structure of the underlying adaptive estimation problem is such that the uncertainty matrix is affine in the input-output relationship which allows for the use of the standard certainty-equivalence framework [5]. Despite the generality of these classical MRAC results, there are no guarantees on the time evolution of the estimates that would readily allow for direct use in the control problem. More specifically, closing the control loop becomes a formidable technical challenge given that the inverse of the pointwise-in-time estimated matrix could be-

come singular. Fortunately, the focus of the estimation problem can be shifted to physically meaningful actuator uncertainties. As an example, the uncertainty matrix could be represented as a diagonal-like matrix, which might represent performance degradation of the actuators. This type of problem is more in the realm of fault-tolerant control [26, 43–46] than adaptive estimation since the uncertainty manifests as a scaling as opposed to a shift of the control axes which represents a misalignment. Thus, a possible special case of the uncertainty would be a pure rotation misalignment matrix. This has been examined using an Extended Kalman Filter (EKF) approach by Fosbury and Nebelecky [47] but is limited to the estimation problem so there is no consideration of time-evolution of the estimates for the control problem. The certainty-equivalence framework could be used in this case; however, there exists a non-linear adaptive estimation algorithm [27, 28] that ensures that the time-varying adaptive estimate also evolves as a rotation matrix. Since the estimate is a rotation matrix, it is always invertible and can be used in the control signal. The main issue with this result is that it is highly unlikely that all three of the control axes would be subject to the same rotational misalignment. A more general misalignment is that each control axis is misaligned *independently*. That is, if the ideal is the standard $(\mathbf{i}, \mathbf{j}, \mathbf{k})$ basis (in three dimensions), there exists unit vectors $(\mathbf{i}', \mathbf{j}', \mathbf{k}')$ which define the misaligned control axes which are a non-orthogonal basis. This simplifies the problem to estimating rotations of the individual axes which has been considered with a small angle approach by Peck [48] and by estimating the rotations through a simplified set of MRP's by Norman et. al [49]. Both of these representations were investigated as part of a larger EKF implementation and the corresponding closed-loop stability problem due to control implementation has largely been left unexplored.

Thus, existing literature has not addressed the problem of estimating an unknown high-frequency gain which represents independent misalignments on the control axes. In the event that a stabilizing observer can be developed, the extension to the control problem requires that the estimates avoid singularity conditions in the control that do not occur during estimation of uncertain plant parameters. Both of these problems are open questions that will be examined in this dissertation. In ad-

dition, it is noteworthy that the actuator misalignment problem can be thought of as a dual problem to the sensor misalignment problem. The main difference is that the measurement equation will be directly available in the sensor misalignment problem; hence, any observers developed for the actuator misalignment problem directly apply to the sensor misalignment problem but without the additional constraint that the control singularity be avoided. Therefore, the results shown in this dissertation also address the sensor misalignment problem.

1.3 Dissertation Outline

The remainder of the dissertation is organized as follows: Chapter 2 discusses pertinent information that will be used throughout the dissertation. The general estimation and control problems are formulated for an unknown 3×3 matrix. In addition to several necessary definitions, background is given on existing results that are used with the dissertation. These results include estimation of unknown special orthogonal matrices, control design through filtering, and implementation of smooth parameter projection. Each of these results are applied in portions of the dissertation and are introduced to better familiarize the reader with these well-established processes and to remove redundancy throughout the subsequent chapters.

Chapter 3 introduces the rigid-body attitude tracking problem where the attitude is available through vector measurements and the angular velocity measurements are subject to a constant unknown bias. A control scheme is first introduced for the case where the body inertia matrix is known. The corresponding Lyapunov stability analysis shows that in addition to the control objectives being met, all of the estimation errors converge to their true values *without* any additional requirements on the reference trajectory. The performance of the control scheme is compared with existing results and is shown to be less susceptible to measurement noise because of the affine appearance of the inertia matrix in the control signal. This also allows for direct inclusion of unknown body inertia which is not available in the existing literature. The generalized adaptive control scheme for this unknown inertia case is

then introduced with a corresponding stability analysis.

Chapter 4 begins the study of unknown actuator misalignments which continues through the remainder of the dissertation. To begin, the actuator misalignment is restricted to be a rotation matrix. An observer already exists for the estimation problem, but extension to the control problem requires using a filter design to recover the necessary measurement equation. This problem is further generalized by the introduction of an unknown actuator scaling which could represent a performance degradation or measurement unit conversion error. The combination of the scaling and rotation makes the uncertainty representation non-affine. Both the estimation and control problems are shown to be stable through the use of parameter projection to ensure boundedness of the control signal. The stability of the control scheme is shown for prototypical second-order dynamics as well as for the rigid-body attitude tracking problem.

In Chapter 5, the class of actuator misalignments is extended to the case where there are *independent* misalignments on two [‡] of the control axes. To begin, the misalignments are assumed to be predominately in the plane. The restriction to the plane allows for stability proofs for both the estimation and control problems by limiting the range of allowable misalignments and their estimates. In Chapter 6, the misalignments are considered to be out of the plane which introduces serious challenges into the stability analysis. Thus, the techniques of Chapter 5 cannot be readily extended to Chapter 6. After a thorough discussion of the geometric issues with the out-of-plane problem, several alternative observers are proposed which guarantee convergence for both the estimation and control problems. Unfortunately, these alternative methods do not readily extend when more uncertain misalignment angles are included with the pair of out-of-plane misalignments. Therefore, the amount of scenarios which can be proven to be stable is limited.

Chapter 7 builds upon the insights drawn from Chapters 5 and 6 to solve a set of problems where there are independent uncertainties on all three axes. The

[‡]The third axis is assumed to be ideal

difficulties with out-of-plane components limits the set of three-axis problems that can be proven to converge. Specifically, there exist four three-axis misalignment scenarios for which convergence can be proven. Unfortunately, this does not include the full three-axis misalignment problem; however, a numerical analysis of the full problem is discussed that indicates the proposed observer converges for a large set of misalignments. This result indicates that the only issue lies with the stability analysis used to prove convergence.

Chapter 8 summarizes the key results of the dissertation. A statement of original contributions is made along with future research directions. An Appendix is included which has the completion of several proofs that were deemed to impede the basic flow of thought in the main text.

Chapter 2

Background

As a preliminary to discussing the completed research, a formal statement of the problem under consideration is introduced. In addition, several existing results will be discussed which are relevant to the proposed methods and appear several times throughout this dissertation. These are included to help the reader and reduce the amount of repetition in this work.

2.1 Problem Formulation

Consider the problem of determining an unknown constant matrix, $\mathbf{\Psi} \in \mathbb{R}^{3\times 3}$, available through the measurement equation

$$\mathbf{y} = \mathbf{\Psi}\mathbf{u}_f \tag{2.1}$$

where $\mathbf{u}_f \in \mathbb{R}^3$ is a known bonded input and $\mathbf{y} \in \mathbb{R}^3$ is a measured output. In general, the elements of $\mathbf{\Psi}$ can take on any real values and can be time-varying; however, for this work, $\mathbf{\Psi}$ will be restricted to certain special structures which will be discussed in the appropriate sections. The goal of this estimation problem is to develop an update law on the parameter estimate $\hat{\mathbf{\Psi}}(t)$ such that $\hat{\mathbf{\Psi}}(t)$ remains bounded and possibly ensure $\hat{\mathbf{\Psi}}(t) \to \mathbf{\Psi}$ as $t \to \infty$.

In addition to the estimation problem, the following control problem can be examined. Consider the problem of performing tracking of a reference trajectory for the class of double-integrator dynamics with a drift term given by

$$\dot{\mathbf{x}}_1 = \mathbf{x}_2 \tag{2.2a}$$

$$\dot{\mathbf{x}}_2 = \mathbf{f}(\mathbf{x}_1, \mathbf{x}_2) + \mathbf{\Psi}\mathbf{u} \tag{2.2b}$$

where $\mathbf{x}_1, \mathbf{x}_2 \in \mathbb{R}^3$, $\mathbf{f}(\cdot,\cdot) \in \mathbb{R}^3$, $\mathbf{u} \in \mathbb{R}^3$ is an external control, and $\boldsymbol{\Psi}$ is a constant unknown actuator misalignment matrix. The assumption is made that $\mathbf{f}$ is a function that is locally Lipschitz. Admittedly, the system represents a particular class of dynamics; however, the methods described herein on this particular system can be extended to other systems. As an example, the problem of rigid-body attitude tracking will be studied which does not have the same form dynamics as (2.2). The system of (2.2) was simply chosen to highlight the overall process and will be used exclusively unless otherwise noted. Thus, given a bounded and $\mathcal{C}^2$ reference trajectory * $\mathbf{r} \in \mathbb{R}^3$, define the tracking error as

$$\mathbf{e}_1 \equiv \mathbf{x}_1 - \mathbf{r} \tag{2.3a}$$

$$\mathbf{e}_2 \equiv \mathbf{x}_2 - \dot{\mathbf{r}} \tag{2.3b}$$

Differentiating (2.3) with respect to time, the error dynamics are given by

$$\dot{\mathbf{e}}_1 = \mathbf{e}_2 \tag{2.4a}$$

$$\dot{\mathbf{e}}_2 = \mathbf{g} + \boldsymbol{\Psi}\mathbf{u} \tag{2.4b}$$

where the function $\mathbf{g} \in \mathbb{R}^3$ is defined for convenience as

$$\mathbf{g} \equiv \mathbf{f} - \ddot{\mathbf{r}} \tag{2.5}$$

The goal is to determine a control law, $\mathbf{u}$ and an update law for the parameter estimate $\hat{\boldsymbol{\Psi}}$ in order to achieve boundedness of all closed-loop signals and convergence of the tracking errors

$$\lim_{t\to\infty} \begin{bmatrix} \mathbf{e}_1(t) \\ \mathbf{e}_2(t) \end{bmatrix} = \mathbf{0}$$

for all admissible reference trajectories $\mathbf{r}$ and initial conditions $[\mathbf{x}_1(0),\ \mathbf{x}_2(0)]^\top$. The assumption is made that both $\mathbf{x}_1$ and $\mathbf{x}_2$ are available through perfect measurements. Note that for the remainder of the paper the time argument, t, is left out for notational simplicity unless for point of emphasis.

*All reference trajectories which satisfy these conditions are considered to be admissible reference trajectories

2.2 Unknown High Frequency Gain Problem

The main motivation of this work is to focus on the idea of control uncertainty, which is manifested here through the unknown matrix $\mathbf{\Psi}$, using adaptive control. As mentioned in Section 1.2.2, an abundance of literature is available on the "Unknown High Frequency Gain" problem. This problem can be stated more formally as regulation to zero of the system

$$\dot{\mathbf{x}} = \mathbf{\Psi}\mathbf{u} \tag{2.6}$$

where $\mathbf{\Psi}$ is unknown and non-singular. If the stabilization problem is considered for simplicity and $\mathbf{\Psi}$ were assumed to be known, then the control law

$$\mathbf{u} = -k\mathbf{\Psi}^{-1}\mathbf{x} \tag{2.7}$$

provides asymptotic convergence of $\mathbf{x}$ to zero. When $\mathbf{\Psi}$ is unknown, the true value of $\mathbf{\Psi}$ in (2.7) is replaced with the estimate $\hat{\mathbf{\Psi}}$. Consequently, it is required that $\hat{\mathbf{\Psi}}$ remain non-singular for all time in order to ensure that the control signal remains bounded. This is an inherent complexity that exists when controlling systems with control uncertainties. In the area of adaptive controls, there are two established methods to enforcing invertibility of the estimates: direct and indirect adaptive control.

Using direct adaptive control, the dynamics are reformulated such that it is possible to estimate $\hat{\mathbf{\Psi}}^{-1}$ *directly* which removes concern on the invertibility of the estimate. The proof of convergence, however, requires that certain "matching conditions" be met in order to eliminate sign indefinite terms in the Lyapunov analysis and ultimately guarantee stability. Using standard MRAC, the symmetry condition

$$\mathbf{\Psi}\mathbf{\Gamma}^{\top} = \mathbf{\Gamma}\mathbf{\Psi}^{\top} > 0 \tag{2.8}$$

is required for stability where $\mathbf{\Gamma}$ is a non-singular matrix [41]. Thus, to ensure stabilization of (2.6), there must be a priori information available on the unknown high frequency gain. For example, if $\mathbf{\Psi}$ is an unknown scalar, then the sign of $\mathbf{\Psi}$ must be known. Accordingly, the matching conditions place restrictions on the control uncertainty that must be known. It should be noted that a weaker matching condition is

found when using MRAC with Immersion and Invariance as [42]

$$\mathbf{\Psi\Gamma}^\top + \mathbf{\Gamma\Psi}^\top > 0 \tag{2.9}$$

This is a weaker condition since the requirement of symmetry has been removed; however, information is still required on the unknown gain.

Indirect adaptive control requires estimating $\hat{\mathbf{\Psi}}$ and using its inverse in the control law. Therefore, boundedness of the control signal is not guaranteed as with direct adaptive control. By not estimating the inverse, it is possible to eliminate the matching conditions and ultimately the restrictive information that must be known about the high frequency gain; however, the non-singularity of the estimate must be actively enforced through some other means. In general, this is accomplished by bounding the estimates through some projection scheme. Thus, the time evolution of the values of $\hat{\mathbf{\Psi}}$ must be constrained such that the columns of $\hat{\mathbf{\Psi}}$ remain linearly independent. Admittedly, both direct and indirect adaptive control have limitations when it comes to the unknown high frequency gain problem. It is emphasized that these restrictions are inherent any time there are control uncertainties and cannot be avoided. In this dissertation, indirect adaptive control will be applied which will inevitably lead to the use of a projection scheme.

2.3 Applicable Results

The following existing results will be used either as motivation or directly in the proposed methods. Before discussing these results, a few definitions are introduced. First, the following classical definition is presented for persistence of excitation [5].

Definition 2.3.1. The scalar signal $s : \mathbb{R} \to \mathbb{R}$ is said to be persistently exciting if there exists finite positive constants ϵ and T such that

$$\epsilon \leq \int_t^{t+T} s^2(\tau)\, d\tau \qquad \forall\, t \tag{2.10}$$

A portion of the proceeding analysis will be dependent on persistence of excitation (PE) conditions. Second, the notion of input-to-state stability (ISS) as discussed

in [50] is presented. Before defining ISS, it is necessary to introduce the definitions of class $\mathcal{K}$ and class $\mathcal{KL}$ functions.

Definition 2.3.2. A continuous function $\gamma : [0, a) \to [0, \infty)$ is said to belong to class $\mathcal{K}$ if it is strictly increasing and $\gamma(0) = 0$.

Definition 2.3.3. A continuous function $\beta : [0, a) \times [0, \infty) \to [0, \infty)$ is said to belong to class $\mathcal{KL}$ if, for each fixed s, the mapping $\beta(r, s)$ belongs to class $\mathcal{K}$ with respect to r and, for each fixed r, the mapping $\beta(r, s)$ is decreasing with with respect to s and $\beta(r, s) \to 0$ as $s \to \infty$.

Using the two preceding definitions, it is possible to make a formal definition of input-to-state stability as follows:

Definition 2.3.4. The system $\dot{\mathbf{x}} = \mathbf{f}(t, \mathbf{x}, \mathbf{u})$ is said to be input-to-state stable if there exist a class $\mathcal{KL}$ function β and a class $\mathcal{K}$ function γ such that for any initial state $\mathbf{x}(t_0)$ and any bounded input $\mathbf{u}(t)$, the solution $\mathbf{x}(t)$ exists for all $t \geq t_0$ and satisfies

$$||\mathbf{x}(t)|| \leq \beta\left(||\mathbf{x}(t_0)||, t - t_0\right) + \gamma\left(\sup_{t_0 \leq \tau \leq t} ||\mathbf{u}(\tau)||\right) \tag{2.11}$$

The inequality of (2.11) guarantees that for any bounded input $\mathbf{u}(t)$, the state $\mathbf{x}(t)$ will also be bounded. This definition can be thought of as the extension of bounded-input, bounded-output (BIBO) stability to nonlinear systems. Note that ISS implies that the origin of the unforced system $\dot{\mathbf{x}} = \mathbf{f}(t, \mathbf{x}, \mathbf{0})$ be at minimum globally uniformly asymptotically stable.

2.3.1 Estimation of Unknown Special Orthogonal Matrices

Consider the estimation problem of (2.1) where $\mathbf{\Psi}$ belongs to the special orthogonal group (i.e. a rotation matrix). Both Akella et. al [27] and Mahony et. al [28] propose the update law on $\hat{\mathbf{\Psi}}$ which for $\mathbb{R}^3$ is given by

$$\dot{\hat{\mathbf{\Psi}}} = -\gamma S(\mathbf{y} \times \hat{\mathbf{y}})\hat{\mathbf{\Psi}} \tag{2.12}$$

where $\gamma > 0$ is a scalar gain, $S(\cdot)$ is the skew-symmetric matrix operator which represents the cross-product operation between any two vectors ($S(\mathbf{x})\mathbf{y} = \mathbf{x} \times \mathbf{y}$ for all $\mathbf{x}, \mathbf{y} \in \mathbb{R}^3$), and $\hat{\mathbf{y}}$ can be calculated as

$$\hat{\mathbf{y}} = \hat{\mathbf{\Psi}}\mathbf{u}_f \tag{2.13}$$

The fact that the nonlinear update law in (2.12) has the structure of a Poisson's differential equation guarantees given an initial guess $\hat{\mathbf{\Psi}}(0) \in SO(3)$ that $\hat{\mathbf{\Psi}}$ will evolve as a rotation matrix for all time. This fact cannot be duplicated by existing linear observers. In [27] for $SO(3)$, the convergence properties are examined using a quaternion formulation. Let $\mathbf{q}$ and $\hat{\mathbf{q}}$ be the parameterizations of $\mathbf{\Psi}$ and $\hat{\mathbf{\Psi}}$, respectively. Then define the error as the rotation matrix $\mathbf{\Psi}(\mathbf{q})^\top \mathbf{\Psi}(\hat{\mathbf{q}})$ which is parameterized through the quaternion $\mathbf{z}$. Thus, if $\mathbf{\Psi}^\top \hat{\mathbf{\Psi}} \to \mathbf{I}$, $z_0 \to 1$ and $\mathbf{z}_v \to \mathbf{0}$. The error dynamics in $\mathbf{z}$ can be derived as in [29] as

$$\dot{z}_0 = \gamma z_0 ||\mathbf{z}_v \times \mathbf{u}_f||^2 \tag{2.14a}$$

$$\dot{\mathbf{z}}_v = \gamma \left[z_0^2 \left(\mathbf{z}_v \times \mathbf{u}_f \right) \times \mathbf{u}_f - \left(\mathbf{u}_f^\top \mathbf{z} \right) S(\mathbf{z}) \left(\mathbf{z}_v \times \mathbf{u}_f \right) \right] \tag{2.14b}$$

Then the Lyapunov candidate function

$$V_{\text{Ak}} = \frac{\mathbf{z}_v^\top \mathbf{z}_v}{2\gamma z_0^2} \tag{2.15}$$

with $z_0 \neq 0$ is chosen and has the derivative

$$\dot{V}_{\text{Ak}} = -||\mathbf{z}_v \times \mathbf{u}_f||^2 \tag{2.16}$$

which is negative semi-definite. Accordingly, using signal chasing arguments, it can be shown that $\lim_{t\to\infty} \mathbf{z}_v \times \mathbf{u}_f = 0$ which guarantees that $\mathbf{z}_v$ goes to zero asymptotically provided that $\mathbf{u}_f$ is PE. Therefore $\hat{\mathbf{\Psi}}(t) \to \mathbf{\Psi}$ as $t \to \infty$. Mahony et. al [28] assume that $\mathbf{u}_f$ is constant and determine that $\tilde{\mathbf{\Psi}}$ converges asymptotically provided two independent $\mathbf{u}_f$'s are available. To complete their proof, they use the Lyapunov candidate function which has the structure

$$V_{\text{Ma}} = 1 - \mathbf{y}^\top \hat{\mathbf{y}} \tag{2.17}$$

and the derivative

$$\dot{V}_{\text{Ma}} = -\gamma ||\mathbf{y} \times \hat{\mathbf{y}}||^2 \tag{2.18}$$

Both of these results give different insights into estimating rotation matrices and will be used in the remainder of the paper.

2.3.2 Filter Design in Adaptive Control Problems

As part of the controller design, the idea of using filtered variables is introduced to ensure that the control objectives are met. The use of filtered variables is consistent with Immersion and Invariance adaptive control for linear multivariable systems presented by Astolfi and Ortega [42]. As a practical example, the filter design process has been used by Seo and Akella [6] for the spacecraft attitude tracking problem. To highlight the filtering process, consider the error dynamics of (2.4). Define filtered signals $\mathbf{e}_{2,f}$ and $\mathbf{g}_f$ which are obtained from the stable first-order linear low-pass filter dynamics

$$\dot{\mathbf{e}}_{2,f} = -\alpha \mathbf{e}_{2,f} + \mathbf{e}_2 \tag{2.19a}$$

$$\dot{\mathbf{g}}_f = -\alpha \mathbf{g}_f + \mathbf{g} \tag{2.19b}$$

$$\dot{\mathbf{u}}_f = -\alpha \mathbf{u}_f + \mathbf{u} \tag{2.19c}$$

with arbitrary initial conditions $\mathbf{e}_{2,f}(0) \in \mathbb{R}^3$, $\mathbf{g}_f(0) \in \mathbb{R}^3$, $\mathbf{u}_f(0) \in \mathbb{R}^3$ and some scalar constant $\alpha > 0$. Note that the filtered signal of $\mathbf{u}_f$ will only be used for analysis purposes. Differentiating both sides of the filter dynamics in (2.19a) followed by substitution of the filter definitions in (2.19b) and (2.19c) yields

$$\begin{aligned}
\ddot{\mathbf{e}}_{2,f} &= -\alpha \dot{\mathbf{e}}_{2,f} + \dot{\mathbf{e}}_2 \\
&= -\alpha \dot{\mathbf{e}}_{2,f} + \mathbf{g} + \boldsymbol{\Psi} \mathbf{u} \\
&= -\alpha \dot{\mathbf{e}}_{2,f} + \dot{\mathbf{g}}_f + \alpha \mathbf{g}_f + \boldsymbol{\Psi} \left(\dot{\mathbf{u}}_f + \alpha \mathbf{u}_f \right)
\end{aligned} \tag{2.20}$$

This can be arranged to obtain the differential equation

$$\frac{d}{dt} \left(\dot{\mathbf{e}}_{2,f} - \mathbf{g}_f - \boldsymbol{\Psi} \mathbf{u}_f \right) = -\alpha \left(\dot{\mathbf{e}}_{2,f} - \mathbf{g}_f - \boldsymbol{\Psi} \mathbf{u}_f \right) \tag{2.21}$$

which has the solution

$$\dot{\mathbf{e}}_{2,f} = \mathbf{g}_f + \mathbf{\Psi}\mathbf{u}_f + \left[\dot{\mathbf{e}}_{2,f}(0) - \mathbf{g}_f(0) - \mathbf{\Psi}\mathbf{u}_f(0)\right] e^{-\alpha t} \tag{2.22}$$

The exponential term on the right hand side can be ignored if the initial conditions of the filter states are chosen such that the the preceding constant is zero. In general, this will not be possible since $\mathbf{\Psi}$ is unknown. Fortunately, it will be shown through the analysis that the exponentially decaying term does not effect stability and can be ignored. For now, however, assume that the exponentially decaying term will effect the stability. To avoid any increased complexity assume that $\mathbf{\Psi}$ is known and is a constant, non-singular matrix. Choose the filtered control as a standard proportional-derivative (PD) controller given by

$$\mathbf{u}_f = -\mathbf{\Psi}^{-1}\left(\mathbf{g}_f + k_p\mathbf{e}_1 + k_v\mathbf{e}_{2,f}\right) \tag{2.23}$$

The filtered version of the $\mathbf{e}_2$ dynamics becomes

$$\dot{\mathbf{e}}_{2,f} = -k_p\mathbf{e}_1 - k_v\mathbf{e}_{2,f} + \mathbf{w} \tag{2.24}$$

where $\mathbf{w} = \left[\dot{\mathbf{e}}_{2,f}(0) - \mathbf{g}_f(0) - \mathbf{\Psi}\mathbf{u}_f(0)\right] e^{-\alpha t}$. Note that $\dot{\mathbf{w}} = -\alpha\mathbf{w}$. Consider the Lyapunov-like function,

$$V = \frac{1}{2}\mathbf{e}_1^\top\mathbf{e}_1 + \frac{1}{2}\mathbf{e}_{2,f}^\top\mathbf{e}_{2,f} + \frac{\lambda}{2}\mathbf{w}^\top\mathbf{w} \tag{2.25}$$

where λ is a positive scalar constant. Assume that $\alpha = k_p + k_v$. Then the Lyapunov-like function has the derivative

$$\begin{aligned}
\dot{V} &= \mathbf{e}_1^\top\dot{\mathbf{e}}_1 + \mathbf{e}_{2,f}^\top\dot{\mathbf{e}}_{2,f} + \lambda\mathbf{w}^\top\dot{\mathbf{w}} \\
&= \mathbf{e}_1^\top\left(\alpha\mathbf{e}_{2,f} + \dot{\mathbf{e}}_{2,f}\right) + \mathbf{e}_{2,f}^\top\dot{\mathbf{e}}_{2,f} - \lambda\alpha\mathbf{w}^\top\mathbf{w} \\
&= \alpha\mathbf{e}_1^\top\mathbf{e}_{2,f} + \left(\mathbf{e}_1 + \mathbf{e}_{2,f}\right)^\top\left(-k_p\mathbf{e}_1 - k_v\mathbf{e}_{2,f} + \mathbf{w}\right) - \lambda\alpha\mathbf{w}^\top\mathbf{w} \\
&= -k_p||\mathbf{e}_1||^2 - k_v||\mathbf{e}_{2,f}||^2 - \lambda\alpha||\mathbf{w}||^2 + \left(\alpha - k_p - k_v\right)\mathbf{e}_1^\top\mathbf{e}_{2,f} + \left(\mathbf{e}_1 + \mathbf{e}_{2,f}\right)^\top\mathbf{w} \\
&\leq -k_p\left(1 - \frac{1}{2k_p\lambda\alpha}\right)||\mathbf{e}_1||^2 - k_v\left(1 - \frac{1}{2k_v\lambda\alpha}\right)||\mathbf{e}_{2,f}||^2 \\
&\quad - \frac{\lambda\alpha}{2}\left[||\mathbf{w}|| - \left(\frac{1}{\lambda\alpha}\right)||\mathbf{e}_1||\right]^2 - \frac{\lambda\alpha}{2}\left[||\mathbf{w}|| - \left(\frac{1}{\lambda\alpha}\right)||\mathbf{e}_{2,f}||\right]^2
\end{aligned}$$

$$\dot{V} \leq -k_p \left(1 - \frac{1}{2k_p\lambda\alpha}\right) ||\mathbf{e}_1||^2 - k_v \left(1 - \frac{1}{2k_v\lambda\alpha}\right) ||\mathbf{e}_{2,f}||^2 \tag{2.26}$$

where the filter definitions have been used as well as the assumption on α. Equation (2.26) is negative semi-definite if $(1 - 1/2k_p\lambda\alpha) > 0$ and $(1 - 1/2k_v\lambda\alpha) > 0$. This is trivially satisfied since λ can be chosen as large as necessary *without* effecting the system performance. Therefore, any time there is an exponentially decaying term, it can be ignored because it does not effect the stability analysis as mentioned previously, and the filtered error dynamics can simply be represented as

$$\dot{\mathbf{e}}_{2,f} = -k_p\mathbf{e}_1 - k_v\mathbf{e}_{2,f} \tag{2.27}$$

Returning to (2.26), the Lyapunov-like function derivative is negative semi-definite. Using standard signal chasing arguments, [†] the errors $\mathbf{e}_1$ and $\mathbf{e}_2$ are shown to converge asymptotically to zero and the control objective is met. The final step would be to recover the true control signal $\mathbf{u}$ through (2.19c) as

$$\begin{aligned}
\mathbf{u} &= \alpha\mathbf{u}_f + \dot{\mathbf{u}}_f \\
&= -\alpha\boldsymbol{\Psi}^{-1}\left(\mathbf{g}_f + k_p\mathbf{e}_1 + k_v\mathbf{e}_{2,f}\right) - \boldsymbol{\Psi}^{-1}\left(\dot{\mathbf{g}}_f + k_p\dot{\mathbf{e}}_1 + k_v\dot{\mathbf{e}}_{2,f}\right) \\
&= -\boldsymbol{\Psi}^{-1}\left(\mathbf{g} + k_v\mathbf{e}_2 + \alpha k_p\mathbf{e}_1 + k_p\mathbf{e}_2\right) \\
\mathbf{u} &= -\boldsymbol{\Psi}^{-1}\left(\mathbf{g} + \alpha k_p\mathbf{e}_1 + \alpha\mathbf{e}_2\right)
\end{aligned} \tag{2.28}$$

Note that for this problem, the implementation of any of the filter variables is not necessary. As will be seen, the filter variables must be implemented when estimating uncertain plant parameters.

The development of the control design for all of the investigated problems will involve using the filter process. Moreover, it will become clear that the implementation of filters is necessary when trying to estimate the unknown actuator misalignment matrix $\boldsymbol{\Psi}$. Regardless of the individual problem, the filter construction will be practically the same; accordingly, the majority of the steps in the filter construction will be skipped except where there are important differences from this section.

[†] These will be included in the remainder of the dissertation but are left out here for brevity

2.3.3 Smooth Parameter Projection

A practical consideration to estimating uncertain parameters is the inclusion of known a priori bounds on the parameters or avoiding singularity conditions, as will be seen in controlling a system with unknown actuator misalignment. To bound the estimates, a parameter projection scheme is needed. A simple non-smooth projection scheme has been developed by Bakker and Annaswamy [51]. Unfortunately, the non-smooth nature of the projection can lead to discontinuities in the time-derivative of the control signal. Accordingly, a smooth parameter projection scheme is adopted as introduced by Akella and Subbarao [52] which insures that the estimates are $\mathcal{C}^\infty$. Given an unknown parameter ρ that needs to be bounded within $\rho_{\min}$ and $\rho_{\max}$ and a stabilizing update law $\dot{\hat{\rho}}$, the separate unknown parameter ξ can be estimated through the relation

$$\rho = \frac{\rho_{\max} - \rho_{\min}}{2}\left(1 - \tanh\xi\right) + \rho_{\min} \tag{2.29a}$$

$$\hat{\rho} = \frac{\rho_{\max} - \rho_{\min}}{2}\left(1 - \tanh\hat{\xi}\right) + \rho_{\min} \tag{2.29b}$$

Note that the use of the hyperbolic tangent functions forces the estimate $\hat{\rho} \in (\rho_{\min}, \rho_{\max})$, where as, $\hat{\xi}$ is not constrained. In fact as $\hat{\xi}$ goes to ∞, $\hat{\rho}$ goes to $\rho_{\min}$ and as $\hat{\xi}$ goes to $-\infty$, $\hat{\rho}$ goes to $\rho_{\max}$. Using the Lyapunov-like function

$$V = \frac{\rho_{\max} - \rho_{\min}}{2}\left[\log\left(\cosh\hat{\xi}\right) - \tilde{\xi}\tanh\xi\right] \geq 0 \tag{2.30}$$

which is bounded, the derivative can be found to be

$$\dot{V} = -\tilde{\rho}\,\dot{\hat{\xi}} \tag{2.31}$$

Without parameter projection, the standard form of the Lyapunov function for parameter estimates is $V = \tilde{\rho}^2/2$ which has the derivative $\dot{V} = \tilde{\rho}\dot{\hat{\rho}}$. An appropriate choice of $\dot{\hat{\rho}}$ would contribute to the overall Lyapunov function being negative semi-definite and show convergence for the system. Thus by relating $\dot{\hat{\xi}}$ to $\dot{\hat{\rho}}$, the stability established for the unbounded estimates can be recovered for the projected estimates. [‡]

[‡]A possible example is $\dot{\hat{\xi}} = -\dot{\hat{\rho}}$ which recovers the Lyapunov derivative $\dot{V} = \tilde{\rho}\,\dot{\hat{\rho}}$ from (2.31)

This projection scheme will be required to ensure boundedness of the control signal throughout this work.

Chapter 3

Rigid-Body Attitude Tracking with Vector Measurements and Unknown Gyro Bias

In this chapter, the problem of rigid-body attitude tracking where the attitude is available through a set of vector measurements and the angular velocity measurements are corrupted by an unknown bias is examined. This problem fits into the generalized measurement equation of (2.1) where $\mathbf{\Psi} \in SO(3)$ and represents the attitude of the rigid-body. In this case, $\mathbf{\Psi}$ is unknown and time-varying. In general, adaptive control results often assume perfect measurements of the attitude representation (i.e. Direction Cosine Matrix, quaternion, etc.) and the angular velocity. In practice, however, direct measurements of the attitude are not available and gyro rates can be corrupted by bias. Thus solving this problem represents a step to a more realistic adaptive control methods for rigid-body attitude tracking.

The problem of rigid-body attitude tracking with only vector measurements has been presented by Seo and Akella [29]. Mahoney et. al [28] solved the problem of estimating both the attitude and the unknown gyro bias. This work was extended to the attitude tracking problem by Hamel and Mahoney [32] and Pounds et. al [33]. Both use an adaptation of passivity based control to develop controller-observer combinations for the problem. By the authors' own admission in [33], there exists unresolved issues related to the implementability of the control law in [32]. In [33], however, there are no such issues and [33] is viewed as a viable solution to this problem. The focus of [33] is to perform attitude control of micro-air vehicles; accordingly, a premium is placed on computational efficiency. As a result, the vehicle's attitude is not explicitly estimated and is unavailable for use in the control law where the vector attitude measurements are used directly. Although the same basic framework is used, the methodologies employed in the proposed method and those

of [33] yield different control structures. Admittedly, the lack of attitude estimation and auxiliary signals make [33] a computationally efficient algorithm for resource limited devices; however, it is clear that this also leads to a control structure which is more susceptible to control saturation and noise on vector measurements because of an inverse term on the rigid-body inertia matrix inside the control law that would be undesirable for more precise applications particularly for bodies with small inertia. The proposed method does not suffer such limitations and has a control structure that is affine only in the inertia matrix which makes the control structure amenable for extension to the unknown inertia matrix problem as shown in [53, 54] which is not available with the any other existing results.

The remainder of the chapter is organized as follows. Section 3.1 formally states the attitude tracking problem. Section 3.2 develops the observer and controller with stability analysis for the case of vector measurements and unknown gyro bias with *known* body inertia matrix. Section 3.3 extends the analysis for an unknown inertia matrix. Section 3.4 shows numerical simulations which highlight the proposed methods performance using a comparison of the algorithm shown in [33] when the inertia is known. Simulations are presented that consider noise on the measurements as well as time-varying bias. Finally, Section 3.5 contains some remarks about this problem.

3.1 Problem Statement

Consider the problem of performing attitude tracking for a rigid spacecraft. The rigid-body attitude dynamics in terms of the angular velocity, $\boldsymbol{\omega} \in \mathbb{R}^3$ prescribed in a body fixed reference frame, $\mathcal{F}_B$, are governed by Euler's rotational equations of motion given by

$$\mathbf{J}\dot{\boldsymbol{\omega}} = -S\left(\boldsymbol{\omega}\right)\mathbf{J}\boldsymbol{\omega} + \mathbf{u} \tag{3.1}$$

where $\mathbf{J} = \mathbf{J}^\top \in \mathbb{R}^{3\times 3}$ is the constant positive-definite inertia matrix and $\mathbf{u} \in \mathbb{R}^3$ is the external control torque. The corresponding kinematic differential equations

governing the attitude motion (as a quaternion) are given by

$$\dot{\mathbf{q}} = \frac{1}{2} E\left(\mathbf{q}\right) \boldsymbol{\omega}; \qquad E(\mathbf{q}) = \begin{bmatrix} -\mathbf{q}_v^\top & q_0 \mathbf{I}_{3\times 3} + S(\mathbf{q}_v) \end{bmatrix}^\top \tag{3.2}$$

where $\mathbf{q} = \begin{bmatrix} q_0 & \mathbf{q}_v^\top \end{bmatrix}^\top$ is the four-dimensional unit-norm constrained quaternion comprised of the scalar (q_0) and vector ($\mathbf{q}_v$) part, respectively. The quaternion represents the attitude of $\mathcal{F}_B$ with respect to the inertial frame, $\mathcal{F}_I$. The direction cosine matrix transforming $\mathcal{F}_I$ to $\mathcal{F}_B$ can be obtained from the quaternion vector through

$$\mathbf{C}(\mathbf{q}) = \mathbf{I}_{3\times 3} - 2q_0 S(\mathbf{q}_v) + 2S^2(\mathbf{q}_v) \tag{3.3}$$

Note that $\boldsymbol{\Psi} = \mathbf{C}(\mathbf{q})$, and the choice to use $\mathbf{C}$ was made since that is the convention in most existing literature. The bounded reference angular velocity $\boldsymbol{\omega}_r$, is assumed to be specified in its own reference frame, $\mathcal{F}_R$. The transformation between $\mathcal{F}_R$ and the inertial frame $\mathcal{F}_I$ is denoted by the quaternion, $\mathbf{q}_r$, which has the dynamics

$$\dot{\mathbf{q}}_r = \frac{1}{2} E\left(\mathbf{q}_r\right) \boldsymbol{\omega}_r \tag{3.4}$$

Define the attitude and angular velocity tracking errors as follows:

$$\mathbf{C}(\delta\mathbf{q}) = \mathbf{C}(\mathbf{q})\mathbf{C}^\top(\mathbf{q}_r); \qquad \delta\boldsymbol{\omega} = \boldsymbol{\omega} - \mathbf{C}(\delta\mathbf{q})\boldsymbol{\omega}_r \tag{3.5}$$

In terms of the direction cosine matrix $\mathbf{C}(\cdot)$, the analogous matrix version of (3.2) can be derived as

$$\frac{d}{dt}\mathbf{C}(\mathbf{q}) = -S(\boldsymbol{\omega})\mathbf{C}(\mathbf{q}) \tag{3.6}$$

Using (3.1), (3.5), and (3.6) along with a few identities leads to the true attitude tracking errors dynamics and kinematics [55]:

$$\delta\dot{\mathbf{q}} = \frac{1}{2} E(\delta\mathbf{q})\delta\boldsymbol{\omega} \tag{3.7}$$

$$\mathbf{J}\delta\dot{\boldsymbol{\omega}} = -S(\boldsymbol{\omega})\mathbf{J}\boldsymbol{\omega} + \mathbf{u} + \mathbf{J}\left[S(\delta\boldsymbol{\omega})\mathbf{C}(\delta\mathbf{q})\boldsymbol{\omega}_r - \mathbf{C}(\delta\mathbf{q})\dot{\boldsymbol{\omega}}_r\right] \tag{3.8}$$

For this problem, we assume that neither the true attitude nor the true angular velocity are exactly measured. Instead, the attitude is available through the n measurement equations

$$\mathbf{y}_i = \mathbf{C}(\mathbf{q})\mathbf{p}_i + \boldsymbol{\mu}_i \tag{3.9}$$

where $\mathbf{p}_i$ is a known constant unit-norm vector governing the inertial direction of the observation and $\boldsymbol{\mu}_i$ is zero-mean, white noise for $i = 1, \cdots, n$. For this problem $\mathbf{p}$ has taken the place of $\mathbf{u}_f$ since $\mathbf{u}_f$ has a different meaning. Note that by definition, in the absence of noise, $\mathbf{y}_i$ must also be a unit vector. Equation (3.9) is typical for single input-output type measurement sensors such as star trackers and sun sensors. The measurement equation for the angular velocity is given by

$$\boldsymbol{\omega}_m = \boldsymbol{\omega} + \mathbf{b} + \boldsymbol{\nu} \tag{3.10}$$

where $\mathbf{b} \in \mathbb{R}^3$ is an unknown bias and $\boldsymbol{\nu}$ is zero-mean, white noise.

For feedback control implementation purposes, it thus becomes necessary to estimate the attitude of the spacecraft as well as the bias. Accordingly, we introduce the quaternion estimate, $\hat{\mathbf{q}}$ and the bias estimate, $\hat{\mathbf{b}}$. The quaternion estimate represents the attitude between the estimated body frame, $\mathcal{F}_E$, and the inertial frame, $\mathcal{F}_I$. The adaptive control objective is then to determine the external control torque $\mathbf{u}$ and stable update laws for $\hat{\mathbf{q}}$ and $\hat{\mathbf{b}}$ while assuming the measurements of (3.9) and (3.10) to be perfect (no noise) so as to achieve boundedness of all closed-loop signals and convergence of tracking errors

$$\lim_{t\to\infty} \begin{bmatrix} \delta\mathbf{q}_v(t) \\ \delta\boldsymbol{\omega}(t) \end{bmatrix} = \mathbf{0}$$

for all possible reference trajectories $\begin{bmatrix} \boldsymbol{\omega}_r^\top & \mathbf{q}_r^\top \end{bmatrix}^\top$ and initial conditions $\begin{bmatrix} \boldsymbol{\omega}(0)^\top & \mathbf{q}(0)^\top \end{bmatrix}^\top$.

3.2 Adaptive Attitude Tracking Control with Unknown Bias

In this section, an adaptive control method for the attitude tracking problem with n attitude vector measurements and unknown angular velocity bias is introduced. To facilitate discussion of the theorem and ensuing stability proof, some notation and definitions are presented. Define the matrix attitude error as

$$\tilde{\mathbf{C}} \equiv \hat{\mathbf{C}}^\top \mathbf{C} \tag{3.11}$$

Note that $\tilde{\mathbf{C}} \rightarrow \mathbf{I}_{3\times 3}$ is equivalent to $\hat{\mathbf{C}} \rightarrow \mathbf{C}$. Next, borrowing from [28] let the matrix $\mathbf{M}_0 \in \mathbb{R}^{3\times 3}$ be given by

$$\mathbf{M}_0 = \sum_{i=1}^{n} k_i \mathbf{p}_i \mathbf{p}_i^\top \tag{3.12}$$

where k_i are scalar constants to be discussed later. Finally, $\mathbf{M}_0$ can be decomposed into $\mathbf{M}_0 = \mathbf{U}_0 \mathbf{\Lambda} \mathbf{U}_0^\top$ where $\mathbf{U}_0 \in SO(3)$ and $\mathbf{\Lambda}$ is the diagonal matrix consisting of the eigenvalues of $\mathbf{M}_0$. Note that for $n = 2$, the three eigenvalues are given by

$$0, \frac{1}{2}(k_1 + k_2) \pm \frac{1}{2}\sqrt{k_1^2 + k_2^2 + k_1 k_2 (2 - 4p')}$$

where $p' = (p_{11}p_{22} - p_{12}p_{21})^2 + (p_{11}p_{23} - p_{13}p_{21})^2 + (p_{12}p_{23} - p_{13}p_{22})^2$.

3.2.1 Observer/Controller Design

To begin, the parameter estimate $\hat{\boldsymbol{\theta}} = [\hat{\mathbf{b}} \quad \hat{\mathbf{B}}]^\top$ is introduced which contains the bias estimate as well as the estimate for the overparameterized term $\mathbf{B} = S(\mathbf{b})\mathbf{J}\mathbf{b}$. Let the regressor matrix $\mathbf{W} \in \mathbb{R}^{3\times 6}$ be defined as

$$\mathbf{W} = [\mathbf{W}_b \quad \mathbf{W}_B] = [S(\boldsymbol{\omega}_m)\mathbf{J} - S(\mathbf{J}\boldsymbol{\omega}_m) \quad -\mathbf{I}_{3\times 3}] \tag{3.13}$$

where the subscripts correspond to the 3×3 sub-matrices associated with the two members of the parameter estimate. Next, define filtered signals $\mathbf{W}_f$ and $\hat{\boldsymbol{\omega}}_f$ which are obtained from the stable first-order linear filter dynamics:

$$\dot{\hat{\boldsymbol{\omega}}}_f = -\alpha \hat{\boldsymbol{\omega}}_f + \delta \hat{\boldsymbol{\omega}} \tag{3.14}$$

$$\dot{\mathbf{W}}_f = -\alpha \mathbf{W}_f + \mathbf{W} \tag{3.15}$$

with arbitrary initial conditions $\mathbf{W}_f(0) \in \mathbb{R}^{3\times 6}$, $\boldsymbol{\omega}_f(0) \in \mathbb{R}^3$ and some $\alpha > 0$. Also, let $\boldsymbol{\beta} = [\boldsymbol{\beta}_b \quad \boldsymbol{\beta}_B]^\top$ be an auxiliary signal given by

$$\boldsymbol{\beta} = -\tau \mathbf{W}_f^\top \hat{\boldsymbol{\omega}}_f; \tag{3.16}$$

which has derivative

$$\dot{\boldsymbol{\beta}} = \tau \mathbf{W}_f^\top (2\alpha \hat{\boldsymbol{\omega}}_f - \delta \hat{\boldsymbol{\omega}}) - \tau \mathbf{W}^\top \hat{\boldsymbol{\omega}}_f \tag{3.17}$$

where τ is a positive scalar constant. Equations (3.14) - (3.17) appear due to the attracting-manifold design and the non-certainty equivalence framework and are vital to proving convergence of the error signals. The estimated attitude and angular velocity tracking errors are

$$\mathbf{C}(\delta\hat{\mathbf{q}}) = \mathbf{C}(\hat{\mathbf{q}})\mathbf{C}^{\top}(\mathbf{q}_r) \tag{3.18}$$

$$\delta\hat{\boldsymbol{\omega}} = \hat{\boldsymbol{\omega}} - \mathbf{C}(\delta\hat{\mathbf{q}})\boldsymbol{\omega}_r = \boldsymbol{\omega}_m - \hat{\mathbf{b}} + \boldsymbol{\beta}_b - \mathbf{C}(\delta\hat{\mathbf{q}})\boldsymbol{\omega}_r \tag{3.19}$$

Finally, let $\boldsymbol{\Omega}$ be the signal defined as

$$\boldsymbol{\Omega} = \sum_{i=1}^{n} k_i \left(\mathbf{y}_i \times \hat{\mathbf{y}}_i\right); \qquad k_i > 0 \tag{3.20}$$

where k_i are user-defined positive scalar constants which can be thought of as weights on the confidence of the measurement. Then, $\hat{\mathbf{y}}_i$ is defined as

$$\hat{\mathbf{y}}_i = \mathbf{C}(\hat{\mathbf{q}})\mathbf{p}_i \tag{3.21}$$

Using these implementable signals, let the control torque $\mathbf{u}$ be determined through

$$\mathbf{u} = S(\boldsymbol{\omega}_m)\mathbf{J}\boldsymbol{\omega}_m - \mathbf{J}\left[S\left(\delta\hat{\boldsymbol{\omega}} + \gamma\boldsymbol{\Omega}\right)\mathbf{C}(\delta\hat{\mathbf{q}})\boldsymbol{\omega}_r - \mathbf{C}(\delta\hat{\mathbf{q}})\dot{\boldsymbol{\omega}}_r + \dot{\boldsymbol{\beta}}_b - \dot{\hat{\mathbf{b}}}\right] + \mathbf{v} \tag{3.22a}$$

$$\begin{aligned}\mathbf{v} = &-k_v\mathbf{J}\delta\hat{\boldsymbol{\omega}} - k_p\mathbf{J}\left(\alpha\delta\hat{\mathbf{q}}_v + \frac{1}{2}\left[\delta\hat{q}_0\mathbf{I} + S\left(\delta\hat{\mathbf{q}}_v\right)\right]\left(\delta\hat{\boldsymbol{\omega}} + \gamma\boldsymbol{\Omega}\right)\right) \\ &- \mathbf{W}\left(\hat{\boldsymbol{\theta}} - \boldsymbol{\beta}\right) - \mathbf{W}_f\left(\dot{\hat{\boldsymbol{\theta}}} - \dot{\boldsymbol{\beta}}\right)\end{aligned} \tag{3.22b}$$

wherein $k_p, k_v, \gamma > 0$ and are scalar constants, and let the observer be given by

$$\dot{\hat{\mathbf{q}}} = \frac{1}{2}E(\hat{\mathbf{q}})\left(\hat{\boldsymbol{\omega}} + \gamma\boldsymbol{\Omega}\right) \tag{3.23a}$$

$$\dot{\hat{\boldsymbol{\theta}}} = \begin{bmatrix}\dot{\hat{\mathbf{b}}} \\ \dot{\hat{\mathbf{B}}}\end{bmatrix} = \begin{bmatrix}-\lambda\boldsymbol{\Omega} \\ 0\end{bmatrix} + \tau\mathbf{W}_f^{\top}\left[k_p\delta\hat{\mathbf{q}}_v + \left(\alpha + k_v\right)\hat{\boldsymbol{\omega}}_f\right] - \tau\mathbf{W}^{\top}\hat{\boldsymbol{\omega}}_f \tag{3.23b}$$

The quaternion estimate update is equivalent to the matrix update law

$$\dot{\hat{\mathbf{C}}} = -S\left[\hat{\boldsymbol{\omega}} + \gamma\sum k_i(\mathbf{y}_i \times \mathbf{y})\right]\hat{\mathbf{C}}$$

which is consistent with the discussion of estimation special orthogonal matrices in Section 2.3.1. Note that despite the algebraic complexity of the controller, the control signal $\mathbf{u}$ essentially contains feedforward terms to eliminate the naturally occurring dynamics due to the attitude reference trajectory tracking. Additionally, $\mathbf{v}$ has the negative feedback terms of the attitude, angular velocity, and parameter estimates which have extra terms due to the filter process. The parameter observer in (3.23b) occurs by eliminating terms in the Lyapunov analysis along with employing the non-certainty equivalence framework.

Theorem 3.2.1. *Consider the attitude tracking error system of (3.7) and (3.8) with $n \geq 2$ linearly independent measurements and choose $k_i > 0$ for $i = 1, \cdots, n$ such that $\mathbf{M}_0$ has three distinct eigenvalues. Further assume that $(\boldsymbol{\omega}(t), \tilde{\mathbf{C}}^\top(t))$ are asymptotically independent and that there is no measurement noise and that the bias is constant. Suppose that the adaptive control torque $\mathbf{u}$ is given by (3.22) with constraints on k_p, k_v, and α such that*

$$k_p > \frac{9\gamma}{8}, \qquad k_v > \frac{9k_p}{2\left(\frac{8\tau k_p}{\lambda} - 9\right)}, \qquad \alpha = k_p + k_v \tag{3.24}$$

Furthermore, suppose that the attitude quaternion and parameter estimates are available from (3.23), then the convergence condition

$$\lim_{t\to\infty} \begin{bmatrix} \delta\mathbf{q}_v(t) \\ \delta\boldsymbol{\omega}(t) \end{bmatrix} = \mathbf{0}$$

is applicable for all reference trajectories $\begin{bmatrix} \boldsymbol{\omega}_r^\top & \mathbf{q}_r^\top \end{bmatrix}^\top$, all $\hat{\mathbf{B}}(0)$, all $\hat{\mathbf{b}}(0)$ and $\hat{\mathbf{q}}(0)$ such that

$$\mathbf{C}(\hat{\mathbf{q}})(0) \neq \mathbf{U}_0\mathbf{D}_i\mathbf{U}_0^\top\mathbf{C}(\mathbf{q})(0) \tag{3.25}$$

for $i = 1, 2, 3$ where

$$\mathbf{D}_1 = \mathrm{diag}(1, -1, -1); \qquad \mathbf{D}_2 = \mathrm{diag}(-1, 1, -1); \qquad \mathbf{D}_3 = \mathrm{diag}(-1, -1, 1)$$

*and "*diag*" is the diagonal matrix operator. In addition to meeting the control objective, it is guaranteed that $\hat{\mathbf{q}} \to \mathbf{q}$, $\hat{\mathbf{b}} \to \mathbf{b}$, and $\hat{\mathbf{B}} \to \mathbf{B}$ as $t \to \infty$.*

Proof. Consider the Euler rotational equations and realizing that $\boldsymbol{\omega} = \boldsymbol{\omega}_m - \mathbf{b}$, equation (3.1) can be rewritten as

$$\begin{aligned}\mathbf{J}\dot{\boldsymbol{\omega}} &= -S\left(\boldsymbol{\omega}_m - \mathbf{b}\right)\mathbf{J}\left(\boldsymbol{\omega}_m - \mathbf{b}\right) + \mathbf{u} \\ &= -S\left(\boldsymbol{\omega}_m\right)\mathbf{J}\boldsymbol{\omega}_m + \left[S(\boldsymbol{\omega}_m)\mathbf{J} - S(\mathbf{J}\boldsymbol{\omega}_m)\right]\mathbf{b} - S(\mathbf{b})\mathbf{J}\mathbf{b} + \mathbf{u} \\ &= -S\left(\boldsymbol{\omega}_m\right)\mathbf{J}\boldsymbol{\omega}_m + \mathbf{W}\boldsymbol{\theta} + \mathbf{u} \end{aligned} \tag{3.26}$$

Using the estimated attitude error of (3.18), the estimated attitude error dynamics can be determined as

$$\delta\dot{\hat{\mathbf{q}}} = \frac{1}{2}E(\delta\hat{\mathbf{q}})\left(\delta\hat{\boldsymbol{\omega}} + \gamma\boldsymbol{\Omega}\right) \tag{3.27}$$

Differentiating the estimated angular velocity error of (3.19), using (3.26), and (3.22a) where $\mathbf{v} \in \mathbb{R}^3$ is a to be determined control signal leads to the estimated angular velocity error dynamics

$$\delta\dot{\hat{\boldsymbol{\omega}}} = \mathbf{J}^{-1}\left(\mathbf{v} + \mathbf{W}\boldsymbol{\theta}\right) \tag{3.28}$$

In addition to the filters of (3.14) and (3.15), the stable first-order filter dynamics on $\mathbf{v}$ are introduced (only for analysis purposes)

$$\dot{\mathbf{v}}_f = -\alpha\mathbf{v}_f + \mathbf{v} \tag{3.29}$$

Using the same arguments of Section 2.3.2, the filtered angular velocity error dynamics are given by

$$\dot{\hat{\boldsymbol{\omega}}}_f = \mathbf{J}^{-1}\left(\mathbf{v}_f + \mathbf{W}_f\boldsymbol{\theta}\right) + \left[\dot{\hat{\boldsymbol{\omega}}}_f(0) - \mathbf{J}^{-1}\left(\mathbf{v}_f(0) + \mathbf{W}_f(0)\boldsymbol{\theta}\right)\right]e^{-\alpha t} \tag{3.30}$$

As shown previously in Chapter 2, the exponential term does not effect the stability analysis, and the filtered estimated error dynamics are reduced to

$$\dot{\hat{\boldsymbol{\omega}}}_f = \mathbf{J}^{-1}\left(\mathbf{v}_f + \mathbf{W}_f\boldsymbol{\theta}\right) \tag{3.31}$$

Suppose that the filtered control signal $\mathbf{v}_f$ is chosen as

$$\mathbf{v}_f = -\mathbf{J}\left(k_p\delta\hat{\mathbf{q}}_v + k_v\hat{\boldsymbol{\omega}}_f\right) - \mathbf{W}_f\left(\hat{\boldsymbol{\theta}} - \boldsymbol{\beta}\right) \tag{3.32}$$

where $\boldsymbol{\beta} \in \mathbb{R}^3$ is a still to be determined signal and $k_p, k_v > 0$ are scalar constants. The control filter dynamics of (3.29) will be enforced later to recover the control, $\mathbf{v} = \dot{\mathbf{v}}_f + \alpha \mathbf{v}_f$, which is implemented in the control law. Next, define a parameter estimation error as

$$\tilde{\boldsymbol{\theta}} \equiv \boldsymbol{\theta} - \hat{\boldsymbol{\theta}} + \boldsymbol{\beta} = \begin{bmatrix} \tilde{\mathbf{b}} \\ \tilde{\mathbf{B}} \end{bmatrix} = \begin{bmatrix} \mathbf{b} - \hat{\mathbf{b}} + \boldsymbol{\beta}_b \\ \mathbf{B} - \hat{\mathbf{B}} + \boldsymbol{\beta}_B \end{bmatrix} \tag{3.33}$$

Substituting (3.32) into (3.31) yields

$$\dot{\hat{\boldsymbol{\omega}}}_f = -k_p \delta \hat{\mathbf{q}}_v - k_v \hat{\boldsymbol{\omega}}_f + \mathbf{J}^{-1} \mathbf{W}_f \tilde{\boldsymbol{\theta}} \tag{3.34}$$

Suppose that $\boldsymbol{\beta}$ is chosen as in (3.16). Differentiating and substituting (3.15) and (3.34) gives

$$\dot{\boldsymbol{\beta}} = \tau \mathbf{W}_f^\top \left[k_p \delta \hat{\mathbf{q}}_v + (\alpha + k_v) \, \hat{\boldsymbol{\omega}}_f \right] - \tau \mathbf{W}^\top \hat{\boldsymbol{\omega}}_f - \tau \mathbf{W}_f^\top \mathbf{J}^{-1} \mathbf{W}_f \tilde{\boldsymbol{\theta}} \tag{3.35}$$

Note that this expression differs from $\dot{\boldsymbol{\beta}}$ in (3.17). Both results are algebraically equivalent, however, the version shown in (3.17) is implementable where as (3.35) is not. Next, taking the derivative of (3.33) and replacing $\dot{\hat{\boldsymbol{\theta}}}$ with (3.23b) and $\dot{\boldsymbol{\beta}}$ with (3.35) produces

$$\dot{\tilde{\boldsymbol{\theta}}} = \dot{\boldsymbol{\theta}} - \dot{\hat{\boldsymbol{\theta}}} + \dot{\boldsymbol{\beta}} = \begin{bmatrix} \lambda \boldsymbol{\Omega} \\ 0 \end{bmatrix} - \tau \mathbf{W}_f^\top \mathbf{J}^{-1} \mathbf{W}_f \tilde{\boldsymbol{\theta}} \tag{3.36}$$

Consider the Lyapunov-like function

$$V_E = \sum_{i=1}^{n} k_i \left(1 - \mathbf{y}_i^\top \hat{\mathbf{y}}_i \right) + \frac{1}{2\lambda} \tilde{\boldsymbol{\theta}}^\top \tilde{\boldsymbol{\theta}} \geq 0 \tag{3.37}$$

which has time derivative

$$\begin{aligned}
\dot{V}_E &= -\sum_{i=1}^{n} k_i \left(\dot{\mathbf{y}}_i^\top \hat{\mathbf{y}}_i + \mathbf{y}_i^\top \dot{\hat{\mathbf{y}}}_i \right) + \frac{1}{\lambda} \tilde{\boldsymbol{\theta}}^\top \dot{\tilde{\boldsymbol{\theta}}} \\
&= -\sum_{i=1}^{n} k_i \left[\mathbf{y}_i^\top S(\boldsymbol{\omega}) \hat{\mathbf{y}}_i - \mathbf{y}_i^\top S(\hat{\boldsymbol{\omega}} + \gamma \boldsymbol{\Omega}) \hat{\mathbf{y}}_i \right] + \frac{1}{\lambda} \tilde{\boldsymbol{\theta}}^\top \left(\begin{bmatrix} \lambda \boldsymbol{\Omega} \\ 0 \end{bmatrix} - \tau \mathbf{W}_f^\top \mathbf{J}^{-1} \mathbf{W}_f \tilde{\boldsymbol{\theta}} \right) \\
&= -\sum_{i=1}^{n} k_i \mathbf{y}_i^\top S(\tilde{\mathbf{b}} + \gamma \boldsymbol{\Omega}) \hat{\mathbf{y}}_i + \begin{bmatrix} \tilde{\mathbf{b}} & \tilde{\mathbf{B}} \end{bmatrix} \begin{bmatrix} \boldsymbol{\Omega} \\ \mathbf{0} \end{bmatrix} - \frac{\tau}{\lambda} \tilde{\boldsymbol{\theta}}^\top \mathbf{W}_f^\top \mathbf{J}^{-1} \mathbf{W}_f \tilde{\boldsymbol{\theta}}
\end{aligned}$$

$$
\begin{aligned}
&= -\left(\tilde{\mathbf{b}} + \gamma\boldsymbol{\Omega}\right)^{\top} \sum_{i=1}^{n} k_i \left(\mathbf{y}_i \times \hat{\mathbf{y}}_i\right) + \tilde{\mathbf{b}}^{\top}\boldsymbol{\Omega} - \frac{\tau}{\lambda}\tilde{\boldsymbol{\theta}}^{\top}\mathbf{W}_f^{\top}\mathbf{J}^{-1}\mathbf{W}_f\tilde{\boldsymbol{\theta}} \\
&= -\gamma||\boldsymbol{\Omega}||^2 - \frac{\tau}{\lambda}||\mathbf{J}^{-1}\mathbf{W}_f\tilde{\boldsymbol{\theta}}||^2
\end{aligned} \tag{3.38}
$$

Next, consider the Lyapunov-like function

$$
V_C = \frac{1}{2}\hat{\boldsymbol{\omega}}_f^{\top}\hat{\boldsymbol{\omega}}_f + \left[\left(\delta\hat{q}_0 - 1\right)^2 + \delta\hat{\mathbf{q}}_v^{\top}\delta\hat{\mathbf{q}}_v\right] \geq 0 \tag{3.39}
$$

which has time derivative

$$
\begin{aligned}
\dot{V}_C &= \hat{\boldsymbol{\omega}}_f^{\top}\dot{\hat{\boldsymbol{\omega}}}_f + 2\left(\delta\hat{q}_0 - 1\right)\delta\dot{\hat{\mathbf{q}}}_0 + 2\delta\hat{\mathbf{q}}_v^{\top}\delta\dot{\hat{\mathbf{q}}}_v \\
&= \hat{\boldsymbol{\omega}}_f^{\top}\dot{\hat{\boldsymbol{\omega}}}_f + \delta\hat{\mathbf{q}}_v^{\top}\left(\delta\hat{\boldsymbol{\omega}} + \gamma\boldsymbol{\Omega}\right) \\
&= \left(\hat{\boldsymbol{\omega}}_f + \delta\hat{\mathbf{q}}_v\right)^{\top}\left(-k_p\delta\hat{\mathbf{q}}_v - k_v\hat{\boldsymbol{\omega}}_f + \mathbf{J}^{-1}\mathbf{W}_f\tilde{\boldsymbol{\theta}}\right) + \alpha\delta\hat{\mathbf{q}}_v^{\top}\hat{\boldsymbol{\omega}}_f + \gamma\delta\hat{\mathbf{q}}_v^{\top}\boldsymbol{\Omega} \\
&= -k_p\delta\hat{\mathbf{q}}_v^{\top}\delta\hat{\mathbf{q}}_v - k_v\hat{\boldsymbol{\omega}}_f^{\top}\hat{\boldsymbol{\omega}}_f + \left(\alpha - k_p - k_v\right)\delta\hat{\mathbf{q}}_v^{\top}\hat{\boldsymbol{\omega}}_f + \gamma\delta\hat{\mathbf{q}}_v^{\top}\boldsymbol{\Omega} \\
&\quad + \left(\hat{\boldsymbol{\omega}}_f + \delta\hat{\mathbf{q}}_v\right)^{\top}\mathbf{J}^{-1}\mathbf{W}_f\tilde{\boldsymbol{\theta}} \\
&\leq k_p||\delta\hat{\mathbf{q}}_v||^2 - k_v||\hat{\boldsymbol{\omega}}_f||^2 \\
&\quad + \gamma||\delta\hat{\mathbf{q}}_v||\,||\boldsymbol{\Omega}|| + ||\hat{\boldsymbol{\omega}}_f||\,||\mathbf{J}^{-1}\mathbf{W}_f\tilde{\boldsymbol{\theta}}|| + ||\delta\hat{\mathbf{q}}_v||\,||\mathbf{J}^{-1}\mathbf{W}_f\tilde{\boldsymbol{\theta}}||
\end{aligned} \tag{3.40}
$$

where $\alpha = k_p + k_v$ was used from (3.24). Finally, consider the Lyapunov-like function which is the combination of (3.37) and (3.39)

$$
V = V_C + V_E \geq 0 \tag{3.41}
$$

The associated time derivative of V comes from (3.38) and (3.40) and can be manipulated using completion of squares to get the result

$$
\begin{aligned}
\dot{V} \leq &-\frac{k_p}{3}||\delta\hat{\mathbf{q}}_v||^2 - \frac{k_v}{3}||\hat{\boldsymbol{\omega}}_f||^2 - \frac{\gamma}{3}||\boldsymbol{\Omega}||^2 - \frac{\tau}{3\lambda}||\mathbf{J}^{-1}\mathbf{W}_f\tilde{\boldsymbol{\theta}}||^2 \\
&- \frac{2\gamma}{3}\left(1 - \frac{9\gamma}{8k_p}\right)||\boldsymbol{\Omega}||^2 - \frac{\tau}{3\lambda}\left[2 - \frac{9\lambda}{4\tau}\left(\frac{1}{k_p} + \frac{1}{2k_v}\right)\right]||\mathbf{J}^{-1}\mathbf{W}_f\tilde{\boldsymbol{\theta}}||^2 \\
&- \frac{k_p}{3}\left[||\delta\hat{\mathbf{q}}_v|| - \left(\frac{3\gamma}{2k_p}\right)||\boldsymbol{\Omega}||\right]^2 \\
&- \frac{k_p}{3}\left[||\delta\hat{\mathbf{q}}_v|| - \left(\frac{3}{2k_p}\right)||\mathbf{J}^{-1}\mathbf{W}_f\tilde{\boldsymbol{\theta}}||\right]^2 \\
&- \frac{2k_v}{3}\left[||\hat{\boldsymbol{\omega}}_f|| - \left(\frac{3}{4k_v}\right)||\mathbf{J}^{-1}\mathbf{W}_f\tilde{\boldsymbol{\theta}}||\right]^2
\end{aligned}
$$

$$\dot{V} \leq -\frac{k_p}{3}||\delta\hat{\mathbf{q}}_v||^2 - \frac{k_v}{3}||\hat{\boldsymbol{\omega}}_f||^2 - \frac{\gamma}{3}||\boldsymbol{\Omega}||^2 - \frac{\tau}{3\lambda}||\mathbf{J}^{-1}\mathbf{W}_f\tilde{\boldsymbol{\theta}}||^2 \leq 0 \tag{3.42}$$

where the constraints on k_p and k_v in (3.24) have been used to ensure negative definiteness of the derivative. Thus, $\dot{V}$ is negative semi-definite, indicating boundedness for all closed-loop signals. Further, because V is lower-bounded, we know that $\int_0^\infty \dot{V}(t)\,dt$ exists and is finite which taken together with (3.42) implies that $\hat{\boldsymbol{\omega}}_f$, $\delta\hat{\mathbf{q}}_v$, $\boldsymbol{\Omega}$ and $\mathbf{J}^{-1}\mathbf{W}_f\tilde{\boldsymbol{\theta}} \in \mathcal{L}_2 \cap \mathcal{L}_\infty$. This also implies boundedness of $\dot{\hat{\boldsymbol{\omega}}}_f$, $\dot{\delta\hat{\mathbf{q}}}_v$, $\dot{\mathbf{W}}_f$ and $\dot{\tilde{\boldsymbol{\theta}}}$ from (3.14), (3.27), (3.15), and (3.36), respectively. By taking the derivative of $\boldsymbol{\Omega}$ in (3.20), it can be shown that $\dot{\boldsymbol{\Omega}}$ is also bounded. Therefore, invoking Barbalat's Lemma yields

$$\lim_{t\to\infty}[\hat{\boldsymbol{\omega}}_f(t) \quad \delta\hat{\mathbf{q}}_v(t) \quad \boldsymbol{\Omega}(t) \quad \mathbf{J}^{-1}\mathbf{W}_f(t)\tilde{\boldsymbol{\theta}}(t)] = \mathbf{0}$$

Of particular importance is that $\boldsymbol{\Omega}(t) \to 0$ as $t \to \infty$. Note that this equivalent to the condition in [28] that $\mathbb{P}_a(\tilde{\mathbf{C}}\mathbf{M}) \to 0$ where $\tilde{\mathbf{C}}$ is defined in (3.11). Accordingly, given the initial conditions $[\mathbf{C}(\hat{\mathbf{q}})(0) \quad \hat{\mathbf{b}}(0)] \neq [\mathbf{U}_0\mathbf{D}_i\mathbf{U}_0^\top\mathbf{C}(\mathbf{q})(0) \quad \mathbf{b}]$ for $i = 1, 2, 3$, it is guaranteed that $[\tilde{\mathbf{C}} \quad \tilde{\mathbf{b}}] \to [\mathbf{I} \quad \mathbf{0}]$ as $t \to \infty$ (See [28] for a more detailed discussion). Thus, it can be shown that $\boldsymbol{\Omega} \to 0$ leads to $\hat{\mathbf{q}} \to \mathbf{q}$ and $\hat{\mathbf{b}} \to \mathbf{b}$ as $t \to \infty$. Using the definitions of the attitude tracking error, it should also be clear that $\delta\hat{\mathbf{q}} \to \delta\mathbf{q}$ from which it follows that $\lim_{t\to\infty}\delta\mathbf{q}_v = \mathbf{0}$. Next, from the structure of the angular velocity filter definition, $\hat{\boldsymbol{\omega}}_f \to \mathbf{0}$ implies that $\delta\hat{\boldsymbol{\omega}} \to \mathbf{0}$ as $t \to \infty$. Examining the estimated angular velocity error of (3.19) and using the fact that $\tilde{\mathbf{b}} \to 0$, $\delta\hat{\mathbf{q}}_v \to \delta\mathbf{q}_v$, and $\boldsymbol{\beta} \to 0$ since $\hat{\boldsymbol{\omega}}_f \to 0$, $\delta\hat{\boldsymbol{\omega}} \to \delta\boldsymbol{\omega}$ as $t \to \infty$. Thus, $\lim_{t\to\infty}\delta\boldsymbol{\omega} = 0$, and both of the control objectives are met. The final piece comes from examining the $\mathbf{J}^{-1}\mathbf{W}_f\tilde{\boldsymbol{\theta}}$ term. As a result of $\mathbf{J}$ being positive definite constant matrix and $\tilde{\mathbf{b}}$ tending to zero, this term can be rewritten as $\mathbf{W}_{B,f}\tilde{\mathbf{B}} \to 0$. Using the filter definition in (3.15), the filter dynamics for the portion associated with $\mathbf{B}$ are $\dot{\mathbf{W}}_{B,f} = -\alpha\mathbf{W}_{B,f} - \mathbf{I}$. This differential equation can be analytically solved and leads to a steady state value of $\mathbf{W}_{B,f,\infty} = (-1/\alpha)\mathbf{I}$ which is clearly non-zero. Consequently, $\tilde{\mathbf{B}} \to 0$ and $\lim_{t\to\infty}\hat{\mathbf{B}} = \mathbf{B}$. Upon recovering $\mathbf{v}$ through $\mathbf{v} = \dot{\mathbf{v}}_f + \alpha\mathbf{v}_f$ from (3.29), the proof is complete.

□

3.2.2 Remarks

1) The important step of the proof is that the estimated quaternion converges to the true quaternion. If that does not occur, neither the true attitude nor the true angular velocity can be guaranteed to asymptotically converge to zero. It should be noted that the convergence of the estimated attitude is only guaranteed in the case where the number of linearly independent measurements is at least 2. In the case there is only a single measurement, $\mathbf{\Omega}$ reduces to $\mathbf{\Omega} = k\mathbf{y} \times \hat{\mathbf{y}}$, and a stability analysis can only prove that $\mathbf{y} \times \hat{\mathbf{y}} \to 0$ as $t \to \infty$ which *does not guarantee* that $\hat{\mathbf{q}} \to \mathbf{q}$. In this case, we can only infer boundedness on the true angular velocity (although the estimated attitude and angular velocity error will go to zero).

2) The technically mild constraints on the initial guess for the observer terms as in (3.25) occurs because of three unstable equilibria in the attitude filter. This characteristic of the problem is discussed in detail in [28] and is also evident in the similar result published in [27] which uses a different Lyapunov construction.

3) The constraint of choosing the positive constants k_i such that the eigenvalues of M_0 are distinct is non-restrictive. For $n = 2$, this simply amounts to choosing k_1 and k_2 such that $k_1^2 + k_2^2 + k_1 k_2(2 - 4p') \neq 0$ which is a mild condition. Larger values of n have similarly passive conditions although the constraints are more algebraically complex.

4) The proof of convergence of the estimate of $\mathbf{B}$ to its true value is a direct result from the addition of the $\boldsymbol{\beta}$ term into the parameter estimation. Note that $\boldsymbol{\beta}$ plays the role of being an additive disturbance which as was shown in the stability analysis goes to zero with $\hat{\boldsymbol{\omega}}_f$. This is of particular importance since convergence is not dependent on any PE properties or lack thereof for the underlying attitude reference trajectory.

5) The result proves asymptotic convergence for the case where continuous measurements are available and no noise is present. Furthermore, the gyro-bias is assumed to be constant. In practical applications, measurements will be discrete and noise will corrupt both the attitude and angular rate measurements. In addition, it is expected that the gyro-bias will likely suffer slow drift over time ($\dot{\mathbf{b}}$ will be non-zero). Although

these characteristics are not explicitly considered and no proofs are given, it is expected that presence of measurement noise would create a residual set which would be dependent on the maximum values of the noise. The proposed control scheme would thus converge to the residual set and then would remain inside the set. The same behavior is expected for a time-varying bias except the set would depend on the time rate of change of the bias parameter. If the gyro-bias were slowly-varying, the effect on the convergence would be negligible. Both of these ideas are considered empirically in the simulations section.

6) The proposed controller of 3.22 is affine in the inertia matrix. This differs from the controller presented in [33] which contains a $\mathbf{J}^{-1}$ term for the control torque. The inertia affine control law derived here makes extension to the unknown inertia matrix problem rather straightforward as shown in the sequel. Furthermore, the $\mathbf{J}^{-1}$ term naturally injects a high-gain into the system for vehicles with smaller inertia values. This can lead to amplification of measurement noise as well as torque saturation which is not a concern in the proposed method. Also note that if an estimate is needed for any other operations, the proposed method provides an attitude estimate through (3.23a)whereas the method in [33] does not provide any explicit measure of the body's attitude.

3.3 Adaptive Attitude Tracking Control with Unknown Bias and Inertia

In this section, the adaptive controller is extended to account for uncertainty in the inertia matrix, $\mathbf{J}$. Note that unless otherwise stated, signals are the same as presented in the previous section.

3.3.1 Observer/Controller Design

For the purpose of simplicity, let $\hat{\mathbf{b}}$ be the estimate of the gyro bias and $\hat{\boldsymbol{\theta}}$ be the estimate of all other uncertain quantities. Define a new regressor matrix $\mathbf{W} \in \mathbb{R}^{3\times 21}$

such that

$$\mathbf{W}\boldsymbol{\theta} = \mathbf{J}\left[S(\delta\hat{\boldsymbol{\omega}} + \gamma\boldsymbol{\Omega})\mathbf{C}(\delta\hat{\mathbf{q}})\boldsymbol{\omega}_r - \mathbf{C}(\delta\hat{\mathbf{q}})\dot{\boldsymbol{\omega}}_r - \dot{\hat{\mathbf{b}}} + k_v\delta\hat{\boldsymbol{\omega}} + k_p\left(\delta\dot{\hat{\mathbf{q}}}_v + \alpha\delta\hat{\mathbf{q}}_v\right)\right] - S(\boldsymbol{\omega}_m)\mathbf{J}\boldsymbol{\omega}_m + S(\boldsymbol{\omega}_m)\mathbf{A} - \mathbf{I}_{3\times 3}\mathbf{B} + \mathbf{D}\boldsymbol{\omega}_m \tag{3.43}$$

where $\mathbf{A} = \mathbf{J}\mathbf{b}$, $\mathbf{B} = S(\mathbf{b})\mathbf{J}\mathbf{b}$, $\mathbf{D} = S(\mathbf{b})\mathbf{J}$ and

$$\boldsymbol{\theta} = [J_{11}, J_{12}, J_{13}, J_{22}, J_{23}, J_{33}, A_1, A_2, A_3, B_1, B_2, B_3, D_{11}, D_{12}, D_{13}, D_{21}, D_{22}, D_{23}, D_{31}, D_{32}, D_{33}]^\top$$

Note that $\boldsymbol{\theta}$ contains the 6 unique values of the inertia matrix along with 15 parameters which are combinations of the uncertain inertia and gyro bias. Also, define the new angular velocity tracking error as

$$\delta\hat{\boldsymbol{\omega}} = \boldsymbol{\omega}_m - \hat{\mathbf{b}} - \mathbf{C}(\delta\hat{\mathbf{q}})\boldsymbol{\omega}_r \tag{3.44}$$

which no longer contains a part of the auxiliary signal $\boldsymbol{\beta}$ since the bias will not appear linearly as a plant uncertainty as in the known inertia problem. Let the control torque $\mathbf{u}$ be determined through

$$\mathbf{u} = -\mathbf{W}\left(\hat{\boldsymbol{\theta}} - \boldsymbol{\beta}\right) + \tau\mathbf{W}_f\mathbf{W}_f^\top\left[k_p\left(\hat{\boldsymbol{\omega}}_f - \delta\hat{\mathbf{q}}_v\right) - \delta\hat{\boldsymbol{\omega}}\right] \tag{3.45}$$

along with the observer

$$\dot{\hat{\mathbf{q}}} = \frac{1}{2}E(\hat{\mathbf{q}})\left(\hat{\boldsymbol{\omega}} + \gamma\boldsymbol{\Omega}\right) \tag{3.46a}$$

$$\dot{\hat{\boldsymbol{\theta}}} = \tau\mathbf{W}_f^\top\left[k_p\delta\hat{\mathbf{q}}_v + (\alpha + k_v)\,\hat{\boldsymbol{\omega}}_f\right] - \tau\mathbf{W}^\top\hat{\boldsymbol{\omega}}_f \tag{3.46b}$$

$$\dot{\hat{\mathbf{b}}} = -\lambda\boldsymbol{\Omega} \tag{3.46c}$$

where the attitude quaternion update law is the same as the known inertia problem.

Theorem 3.3.1. *Consider the attitude tracking error system of (3.7) and (3.8) where the inertia is now unknown. As before, we require $n \geq 2$ linearly independent measurements, and choose $k_i > 0$ for $i = 1, \cdots, n$ such that $\mathbf{M}_0$ has three distinct eigenvalues. In addition, assume that $(\boldsymbol{\omega}(t), \tilde{\mathbf{C}}^\top(t))$ are asymptotically independent and that there is no measurement noise and that the bias is constant. Suppose that the adaptive*

control torque $\mathbf{u}$ *is chosen as (3.45) with the control gain constraints of (3.24). Furthermore, suppose that the attitude quaternion, gyro bias, and parameter estimates are available from (3.46) then the convergence condition*

$$\lim_{t\to\infty} \begin{bmatrix} \delta\mathbf{q}_v(t) \\ \delta\boldsymbol{\omega}(t) \end{bmatrix} = \mathbf{0}$$

is applicable for all reference trajectories $\begin{bmatrix} \boldsymbol{\omega}_r^\top & \mathbf{q}_r^\top \end{bmatrix}^\top$*, all* $\hat{\mathbf{A}}(0)$*, all* $\hat{\mathbf{B}}(0)$*, all* $\hat{\mathbf{D}}(0)$*, all* $\hat{\mathbf{b}}(0)$*, and* $\hat{\mathbf{q}}(0)$ *such that the same constraint as (3.25) is not violated. In addition to meeting the control objective, it is guaranteed that* $\hat{\mathbf{q}} \to \mathbf{q}$ *and* $\hat{\mathbf{b}} \to \mathbf{b}$ *as* $t \to \infty$*.*

Proof. Using the angular velocity error estimate of (3.44), differentiating $\mathbf{J}\delta\hat{\boldsymbol{\omega}}$, and using (3.26), yields

$$\begin{aligned}
\mathbf{J}\dot{\delta\hat{\boldsymbol{\omega}}} &= \mathbf{J}\dot{\boldsymbol{\omega}}_r - \mathbf{J}\dot{\hat{\mathbf{b}}} - \mathbf{J}\left[\dot{\mathbf{C}}(\delta\hat{\mathbf{q}})\boldsymbol{\omega}_r - \mathbf{C}(\delta\hat{\mathbf{q}})\dot{\boldsymbol{\omega}}_r\right] \\
&= -S(\boldsymbol{\omega})\mathbf{J}\boldsymbol{\omega} + \mathbf{u} + \mathbf{J}\left[S(\delta\hat{\boldsymbol{\omega}} + \gamma\boldsymbol{\Omega})\mathbf{C}(\delta\hat{\mathbf{q}})\boldsymbol{\omega}_r - \mathbf{C}(\delta\hat{\mathbf{q}})\dot{\boldsymbol{\omega}}_r - \dot{\hat{\mathbf{b}}}\right] \\
&= \mathbf{u} - S\left(\boldsymbol{\omega}_m\right)\mathbf{J}\boldsymbol{\omega}_m + \left[S(\boldsymbol{\omega}_m)\mathbf{J} - S(\mathbf{J}\boldsymbol{\omega}_m)\right]\mathbf{b} - S(\mathbf{b})\mathbf{J}\mathbf{b} \\
&\quad + \mathbf{J}\left[S(\delta\hat{\boldsymbol{\omega}} + \gamma\boldsymbol{\Omega})\mathbf{C}(\delta\hat{\mathbf{q}})\boldsymbol{\omega}_r - \mathbf{C}(\delta\hat{\mathbf{q}})\dot{\boldsymbol{\omega}}_r - \dot{\hat{\mathbf{b}}}\right] \\
&= \mathbf{u} - S\left(\boldsymbol{\omega}_m\right)\mathbf{J}\boldsymbol{\omega}_m + S(\boldsymbol{\omega}_m)\mathbf{A} - \mathbf{I}_{3\times 3}\mathbf{B} + \mathbf{D}\boldsymbol{\omega}_m \\
&\quad + \mathbf{J}\left[S(\delta\hat{\boldsymbol{\omega}} + \gamma\boldsymbol{\Omega})\mathbf{C}(\delta\hat{\mathbf{q}})\boldsymbol{\omega}_r - \mathbf{C}(\delta\hat{\mathbf{q}})\dot{\boldsymbol{\omega}}_r - \dot{\hat{\mathbf{b}}}\right]
\end{aligned} \tag{3.47}$$

Adding and subtracting $\mathbf{J}\left[k_v\delta\hat{\boldsymbol{\omega}} + k_p\left(\delta\dot{\hat{\mathbf{q}}}_v + \alpha\delta\hat{\mathbf{q}}_v\right)\right]$ into (3.47) and applying the definition of the regressor matrix $\mathbf{W}$ of (3.43) leads to

$$\begin{aligned}
\mathbf{J}\dot{\delta\hat{\boldsymbol{\omega}}} &= \mathbf{u} - \mathbf{J}\left[k_v\delta\hat{\boldsymbol{\omega}} + k_p\left(\delta\dot{\hat{\mathbf{q}}}_v + \alpha\delta\hat{\mathbf{q}}_v\right)\right] - S\left(\boldsymbol{\omega}_m\right)\mathbf{J}\boldsymbol{\omega}_m + S(\boldsymbol{\omega}_m)\mathbf{A} - \mathbf{I}_{3\times 3}\mathbf{B} + \mathbf{D}\boldsymbol{\omega}_m \\
&\quad + \mathbf{J}\left[S(\delta\hat{\boldsymbol{\omega}} + \gamma\boldsymbol{\Omega})\mathbf{C}(\delta\hat{\mathbf{q}})\boldsymbol{\omega}_r - \mathbf{C}(\delta\hat{\mathbf{q}})\dot{\boldsymbol{\omega}}_r - \dot{\hat{\mathbf{b}}} + k_v\delta\hat{\boldsymbol{\omega}} + k_p\left(\delta\dot{\hat{\mathbf{q}}}_v + \alpha\delta\hat{\mathbf{q}}_v\right)\right] \\
&= \mathbf{u} - \mathbf{J}\left[k_v\delta\hat{\boldsymbol{\omega}} + k_p\left(\delta\dot{\hat{\mathbf{q}}}_v + \alpha\delta\hat{\mathbf{q}}_v\right)\right] + \mathbf{W}\boldsymbol{\theta}
\end{aligned} \tag{3.48}$$

Multiplying (3.48) by $\mathbf{J}^{-1}$ gives the expression for the estimated angular velocity error

$$\dot{\delta\hat{\boldsymbol{\omega}}} = -k_v\delta\hat{\boldsymbol{\omega}} - k_p\left(\delta\dot{\hat{\mathbf{q}}}_v + \alpha\delta\hat{\mathbf{q}}_v\right) + \mathbf{J}^{-1}\left(\mathbf{W}\boldsymbol{\theta} + \mathbf{u}\right) \tag{3.49}$$

Define the same stable first order filters of (3.14) and (3.15). In addition, define a filter for the control signal, $\mathbf{u}$. Using the same arguments as previously, the filtered angular velocity error is given by

$$\dot{\hat{\boldsymbol{\omega}}}_f = -k_p \delta \hat{\mathbf{q}}_v - k_v \hat{\boldsymbol{\omega}}_f + \mathbf{J}^{-1} \left(\mathbf{W}_f \boldsymbol{\theta} + \mathbf{u}_f \right) \tag{3.50}$$

Let the filtered control be determined through

$$\mathbf{u}_f = -\mathbf{W}_f \left(\hat{\boldsymbol{\theta}} + \boldsymbol{\beta} \right) \tag{3.51}$$

then the filtered angular velocity error becomes

$$\dot{\hat{\boldsymbol{\omega}}}_f = -k_p \delta \hat{\mathbf{q}}_v - k_v \hat{\boldsymbol{\omega}}_f + \mathbf{J}^{-1} \mathbf{W}_f \tilde{\boldsymbol{\theta}} \tag{3.52}$$

It is important to note that these are the same dynamics as in the known inertia problem. The only difference is an alternate version of the regressor matrix has been used. Finally, the dynamics of the parameter estimation error are

$$\dot{\tilde{\boldsymbol{\theta}}} = \dot{\boldsymbol{\theta}} - \dot{\hat{\boldsymbol{\theta}}} + \dot{\boldsymbol{\beta}} = -\tau \mathbf{W}_f^\top \mathbf{J}^{-1} \mathbf{W}_f \tilde{\boldsymbol{\theta}} \tag{3.53}$$

which only slightly differs from the known inertia problem because the estimation of the bias has been removed from the regressor. Now consider a Lyapunov-like function on the estimation terms given by

$$V_E' = \sum_{i=1}^{n} k_i \left(1 - \mathbf{y}_i^\top \hat{\mathbf{y}}_i \right) + \frac{1}{2\lambda} \tilde{\mathbf{b}}^\top \tilde{\mathbf{b}} + \frac{1}{2\lambda} \tilde{\boldsymbol{\theta}}^\top \tilde{\boldsymbol{\theta}} \geq 0 \tag{3.54}$$

where an additional term has been added to V_E of (3.37) to account for the separate estimation of the bias. Despite the change, it can be easily found that $\dot{V}_E' = \dot{V}_E$. Moreover, the control Lyapunov-like function, V_C, does not need to be changed since the bias estimation does not directly effect any of the values in V_C. Therefore, defining the joint Lyapunov-like function as $V' = V_E' + V_C$ will yield the negative semi-definite derivative $\dot{V}' = \dot{V}$. Then using the same arguments as previously, it can be shown that

$$\lim_{t \to \infty} \begin{bmatrix} \delta \mathbf{q}_v(t) & \delta \boldsymbol{\omega}(t) & \tilde{\mathbf{b}}(t) & \mathbf{q}(t) - \hat{\mathbf{q}}(t) & \mathbf{J}^{-1} \mathbf{W}_f(t) \tilde{\boldsymbol{\theta}}(t) \end{bmatrix}^\top = \mathbf{0}$$

for the same set of conditions as the known inertia problem. After recovering the true control signal through the filter definitions, the proof is complete. □

3.3.2 Remarks

1) The presence of uncertainty in the inertia matrix does not greatly alter the overall structure of the control law except that there is no affine parameterization of the gyro bias, $\mathbf{b}$, in the rotational equations of motion. Thus, there are no additional terms that become a part of the gyro bias estimation, and the gyro bias update law is the same as in [28]. On the other hand, the $\mathbf{A}$, $\mathbf{B}$, and $\mathbf{D}$ terms that must be estimated are non-affine combinations of both $\mathbf{J}$ and $\mathbf{b}$. This greatly increases the overall dimension of the adaptive control problem, especially from a computation stand-point.

2) The main difference between the known and unknown inertia cases is the regressor matrix, $\mathbf{W}$. The control law of (3.45) for the unknown inertia appears to be simpler than the controller for the known inertia in (3.22); however, the structure of the unknown inertia problem requires the control terms to be absorbed into the regressor as opposed to appearing directly in the control law since they are dependent on the inertia matrix. Thus, there are many additional terms that appear linearly in $\mathbf{J}$ which renders derivation of the regressor matrix to be algebraically tedious.

3) The form of the resulting adaptive estimator still guarantees that $\tilde{\mathbf{b}} = \mathbf{b} - \hat{\mathbf{b}} \to 0$ as $t \to \infty$ irrespective of any persistence properties on the reference trajectory. Clearly absent from the unknown inertia case is any guarantee on $\tilde{\boldsymbol{\theta}}$ also converging to zero. As before, the stability analysis leads to the fact that $\mathbf{W}_f \tilde{\boldsymbol{\theta}} \to 0$ as $t \to \infty$. Since the bias error is not contained in $\tilde{\boldsymbol{\theta}}$ as in Theorem 3.2.1, no manipulations can be made to prove convergence of the other estimation errors because $\tilde{\boldsymbol{\theta}} \to 0$ is not inherent in the condition $\mathbf{W}_f \tilde{\boldsymbol{\theta}} \to 0$. The only way to achieve $\tilde{\boldsymbol{\theta}} \to 0$ as $t \to \infty$ is for $\mathbf{W}_f$ to be persistently exciting. This condition manifests itself in having a suitably rich reference signal for the attitude reference trajectory. It should be noted that regardless of the convergence of $\hat{\boldsymbol{\theta}}$ to $\boldsymbol{\theta}$, the attitude tracking control objectives are still met.

3.4 Numerical Simulations

To demonstrate the performance of the controller-observer combination, a series of numerical simulations were performed. The simulations include: known inertia

without noise or time-varying bias, known inertia with noise and without time-varying bias, known inertia without noise and with time-varying bias, and unknown inertia without noise and time-varying bias. The true values of the inertia matrix $\mathbf{J}$ and bias $\mathbf{b}$ were chosen as

$$\mathbf{J} = \begin{bmatrix} 0.0797 & 0 & 0 \\ 0 & 0.0797 & 0 \\ 0 & 0 & 0.1490 \end{bmatrix} \qquad \mathbf{b} = \begin{bmatrix} 0.2 \\ 0.1 \\ -0.1 \end{bmatrix}$$

to be consistent with [33]. Although the proposed algorithm uses quaternions to represent attitude, the results are presented using Euler angles (yaw, pitch, roll) = (ψ,θ,ϕ) to be consistent with [33] and to be more visually appealing to the reader. The initial conditions of the rigid body were set to $[\psi, \theta, \phi] = [20^\circ, 0, 5^\circ]$ and $[\dot{\psi}, \dot{\theta}, \dot{\phi}] = [0, 0.1, -0.02]$ rad/s along with initial filter conditions $\hat{\boldsymbol{\omega}}_f(0) = [0 \quad 0 \quad 0]^\top$ and $\mathbf{W}_f(0) = \mathbf{0}_{3\times N}$, where N is the number of parameters being estimated for the particular problem. Additionally, the initial estimate for the attitude was chosen as $[\psi, \theta, \phi] = [0, 0, 0]$. The initial bias estimates were chosen as $\hat{\mathbf{b}}(0) = \mathbf{0}$ and $\hat{\mathbf{B}}(0) = \mathbf{0}$. In order to simulate $\boldsymbol{\Omega}$, it was assumed that two vector measurements were available:

$$\mathbf{p}_1 = [0 \quad 0 \quad 1]^\top \qquad \mathbf{p}_2 = [1 \quad 1 \quad 1]^\top/\sqrt{3}$$

with gains $k_1 = k_2 = 1$. The remainder of the values will be discussed in the appropriate section.

3.4.1 Known Inertia Simulations

The performance characteristics when the body inertia matrix, $\mathbf{J}$, is known is examined first. In order to highlight the performance characteristics, the proposed control method of (3.13)-(3.23) are compared to the control solution introduced in [33], which will be referred to as "Comparison" in the proceeding simulations. The comparison method is given by

$$\mathbf{u} = -k_\epsilon \boldsymbol{\epsilon} - k_R \mathbf{J}^{-1}\boldsymbol{\Omega}' - \hat{\mathbf{B}} - \boldsymbol{\tau}^d + S(\hat{\mathbf{b}})\mathbf{J}\hat{\mathbf{b}} + S(\mathbf{J}\boldsymbol{\omega}^d)\left(\boldsymbol{\omega}_m - \hat{\mathbf{b}}\right) \tag{3.55a}$$

$$\dot{\hat{\mathbf{B}}} = k_B \mathbf{J}\boldsymbol{\epsilon} \tag{3.55b}$$

$$\dot{\hat{\mathbf{b}}} = k_b k_R \boldsymbol{\Omega}' + k_b \left[S(\mathbf{J}\boldsymbol{\omega}_m) - \mathbf{J} S(\boldsymbol{\omega}_m) \right] \mathbf{J}\boldsymbol{\epsilon} \tag{3.55c}$$

where k_ϵ, k_R, k_b, and k_B are positive scalar constants and the signals $\boldsymbol{\epsilon}$ and $\boldsymbol{\Omega}'$ are

$$\boldsymbol{\epsilon} = \boldsymbol{\omega}_m - \boldsymbol{\omega}^d - \hat{\mathbf{b}} \tag{3.56}$$

$$\boldsymbol{\Omega}' = -\frac{1}{2} \sum_{i=1}^{n} k_i \left(\mathbf{C}_d^\top \mathbf{p}_i \right) \times \left(\mathbf{C}^\top \mathbf{p}_i \right) \tag{3.57}$$

where $\mathbf{C}$ is the direction cosine matrix of the attitude. Note that a script d indicates the desired trajectory. For more information refer to [33]. Both controllers rely on different feedforward terms (partly because of how the reference trajectory is defined for each method) as well as a feedback of the estimated angular velocity. The most notable feature of the comparison method is that there is no estimation of the attitude, rather, the vector measurements are used directly. As a result, the controller in (3.55a) is computationally less intrusive, but it does not use the estimated attitude to perform feedback.

For the proceeding known inertia simulations, the attitude stabilization problem ($\boldsymbol{\omega}_r = \dot{\boldsymbol{\omega}}_r = \boldsymbol{\omega}^d = \boldsymbol{\tau}^d = \mathbf{0}$, $\mathbf{C} = \mathbf{I}$ and $\mathbf{q}_r = [1, 0, 0, 0]^\top$) is considered. Both methods were tuned to provide a 2% settling time within 5 seconds for the attitude, angular rate, and bias errors to create a fair comparison between the methods. The resulting gains for the proposed method were

$$k_p = 10 \qquad k_v = \gamma = \tau = \lambda = 5$$

and for the comparison method, the gains were

$$k_\epsilon = 5 \qquad k_R = 8 \qquad k_b = 2 \qquad k_B = 1$$

The results of the simulation are shown in Figure 3.1, Figure 3.2, and Figure 3.3. The performance of the control methods with respect to the attitude, angular rates, and bias estimation is approximately the same, and both meet the settling time requirements. There is a drastic difference, however, in the estimation of $\mathbf{B}$ as can be seen in Figure 3.2(b). The proposed method inherently meets the settling time imposed on the other errors, but the comparison method has a relatively slow rate of

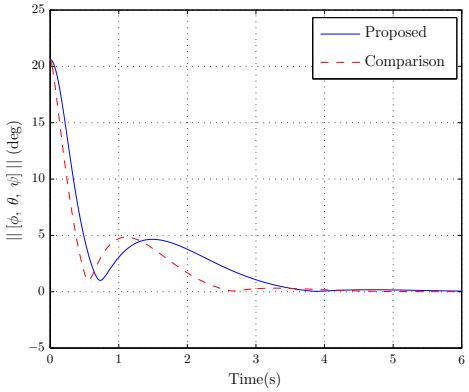

(a) Euler angles

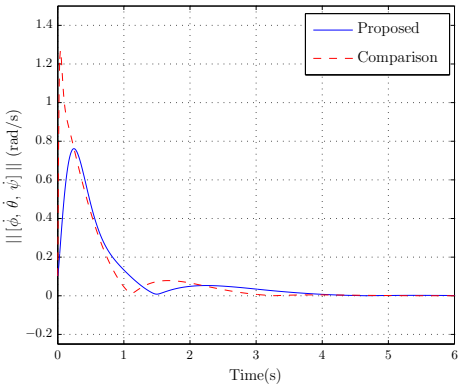

(b) Euler angle rates

Figure 3.1: Comparison of simulation results for the Euler angles and their respective rates without noise and time-varying bias. The responses have been tuned to a 2% settling time within 5 seconds.

convergence. When the simulation is run for a considerably longer time period, the comparison $\mathbf{B}$ estimate finally converges around 200 seconds which is a time scale separation of approximately 40. Despite the slow rate, the lack of convergence does not effect the performance of the the control method since the magnitude of the bias is

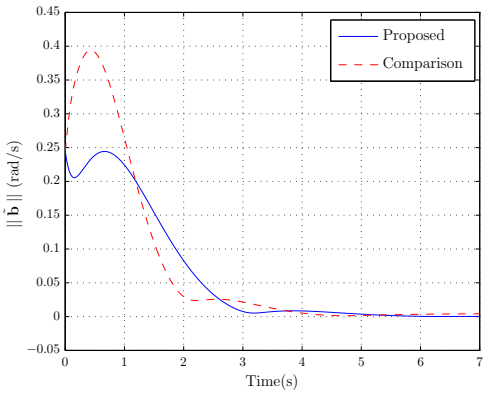

(a) Bias error

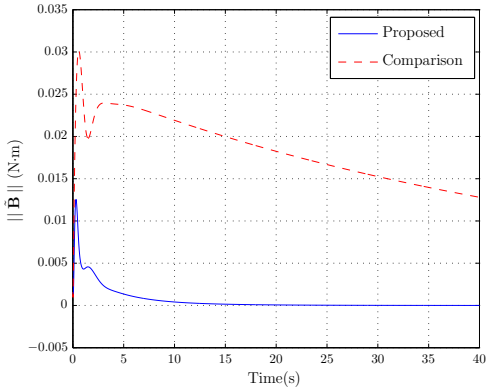

(b) Nonlinear bias term error

Figure 3.2: Comparison of simulation results for the error for the two bias estimation terms without noise or time-varying bias. The gyro-bias response has been tuned to a 2% settling time within 5 seconds. The nonlinear bias term error has not been tuned

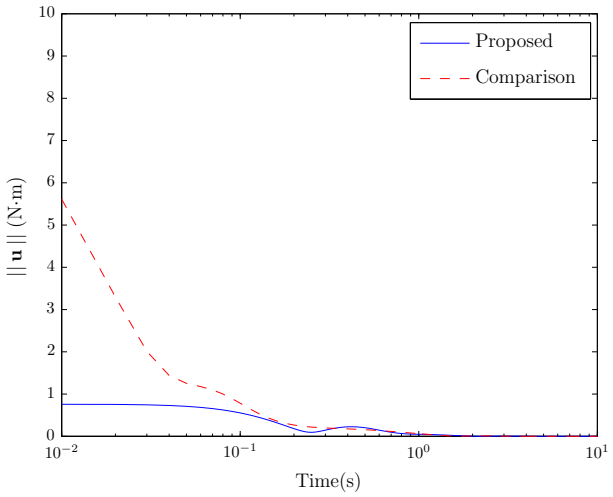

Figure 3.3: Comparison of simulation results for the magnitude of the control torque without noise or time-varying bias

small. If the bias values were to increase, the convergence rate could lead to degraded performance. It should be noted that the learning rate of $\hat{\mathbf{B}}$, k_B, was increased and led to a faster rate of convergence; however, the resulting performance of the tracking errors did not meet settling time requirements. In addition to the estimate of $\mathbf{B}$, the proposed method has significantly superior performance with regard to the control torque magnitude as visible in Figure 3.3. The proposed method requires a much smaller control torque during the transient. After analyzing, the control structures of both methods, the primary reason for the increased control torque demand in the comparison method is due to the $\mathbf{J}^{-1}$ term. When the inertia values in $\mathbf{J}$ are small (as would be expected with micro aerial vehicles), the values in $\mathbf{J}^{-1}$ are large and automatically lead to larger control torques when compared to the proposed method which is affine in the inertia matrix $\mathbf{J}$. Thus, the proposed method is less susceptible to control saturation issues.

3.4.2 Known Inertia Simulations with Measurement Noise

Although no proofs are given both control methods were tested with zero-mean, white noise on the angular rate measurements as well as the pair of vector

measurements. Each component of the measurement noise ($\boldsymbol{\mu}_1$,$\boldsymbol{\mu}_2$,$\boldsymbol{\nu}$) was chosen to have a variance of $\sigma^2 = 1 \times 10^{-4}$. All of the gains and initial conditions for both methods remain the same. The simulation results are shown for the Euler angles, rates, and control effort in Figure 3.4 and Figure 3.5. The transient behavior and

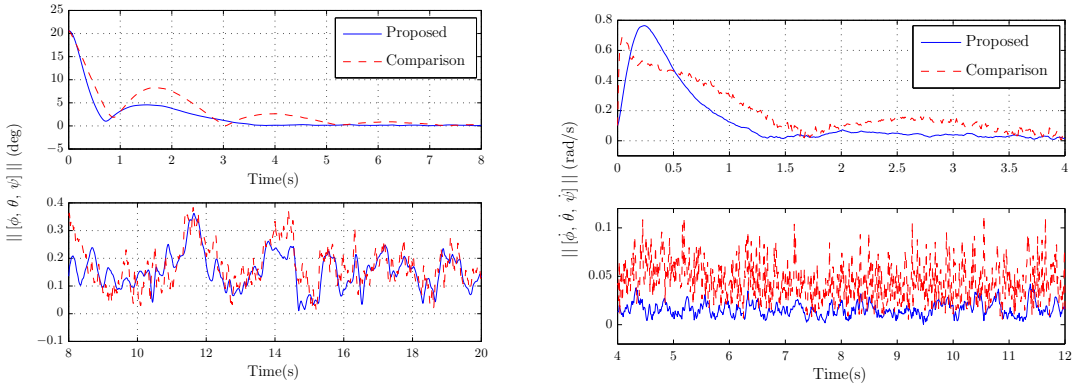

(a) Euler angles

(b) Euler angle rates

Figure 3.4: Comparison of simulation results for the Euler angles and their respective rates with noise but without time-varying bias

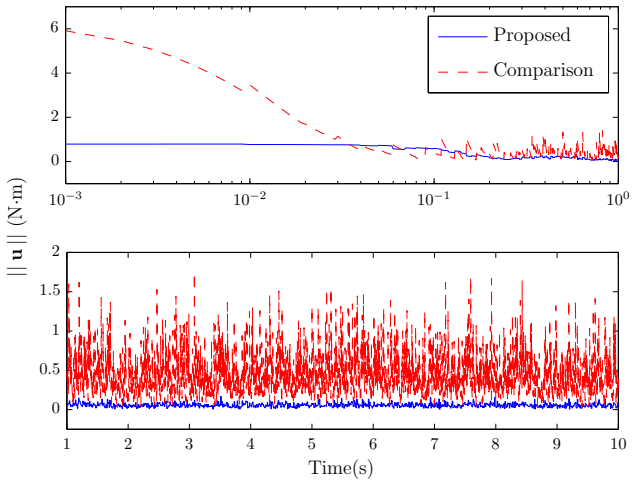

Figure 3.5: Comparison of simulation results for the magnitude of the control torque with noise but without time-varying bias

steady state behavior are shown separately. The added noise does not greatly effect

the transient behavior and the settling time requirements are still met by both methods. It is clear that the attitude and rate errors converge to a residual set for both methods. Similar behavior is found when viewing the bias estimation errors (which are not shown). The residual set of the Euler angles in Figure 3.4(a) appears to be the same for both methods. When examining the Euler angle rates in Figure 3.4(b), however, the proposed method is contained to a smaller residual set than the comparison method by about a full order of magnitude. Furthermore, this difference in the residual sets has a profound effect (again an order of magnitude) on the amount of required control torque to stabilize the attitude as can be seen in the steady state of Figure 3.5. It was found that noise associated with the vector measurements causes the considerable difference between the two methods (when only angular rate noise is added, the difference between the two methods is negligible). Again this behavior can be attributed to the $\mathbf{J}^{-1}$ term in the comparison control law which inherently amplifies any noise in the vector measurements. This phenomena could be avoided by choosing a small value of k_R; consequently, the performance of the tracking errors would degrade considerably. Thus, it is clear at least empirically that the addition of noise to the proposed method causes convergence to a residual set, which will grow or shrink dependent on the variance of the noise, and that the proposed method is structured more advantageously to handle the addition of measurement noise.

3.4.3 Known Inertia Simulations with Time-Varying Bias

In practical applications, the gyro-bias will have a tendency to drift. Accordingly, a simulation was conducted where the gyro-bias was modeled as a random walk to test how both methods responded to a time-varying bias. For the simulation, the random walk had a magnitude change of $0.001||\mathbf{b}||$ every 0.01 seconds. The resulting time history of the bias is shown in Figure 3.6(a) where it is clear that each component was subject to a different random walk. The results of the simulation are shown in Figure 3.6(b) and Figure 3.7. When a time-varying bias is introduced, both methods appear to converge to a residual set of approximately the same magnitude. The size of the residual set is dependent on the size of the change in magnitude

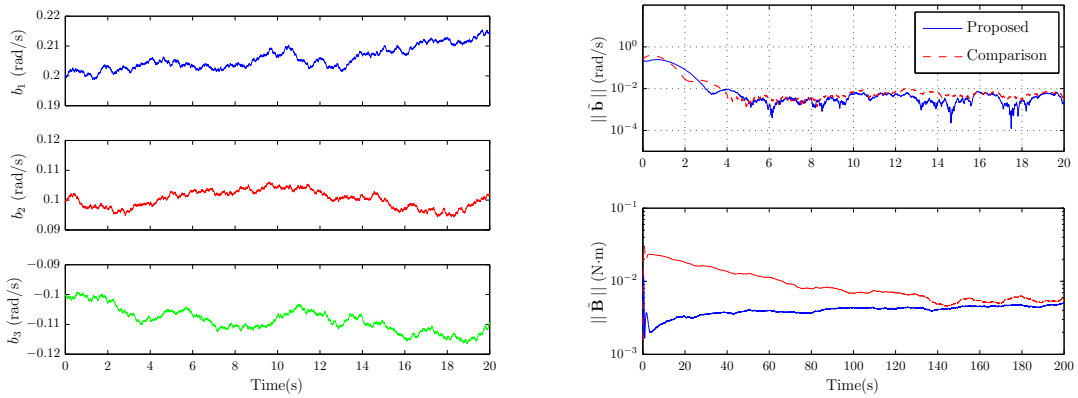

(a) Bias subject to random walk

(b) Error in bias terms

Figure 3.6: Comparison of simulation for the bias estimation errors without noise but with time-varying bias. In addition, the time history of the components of the bias subject to a random walk show how the bias varies with time

of the random walk (essentially the average rate of change of $\mathbf{b}$). In addition, the transient response is not affected by the time-varying bias. It should be noted that as before the proposed method has a much faster rate of convergence for $\mathbf{B}$ and a smaller initial required control torque. Although, the steady state control torque is of

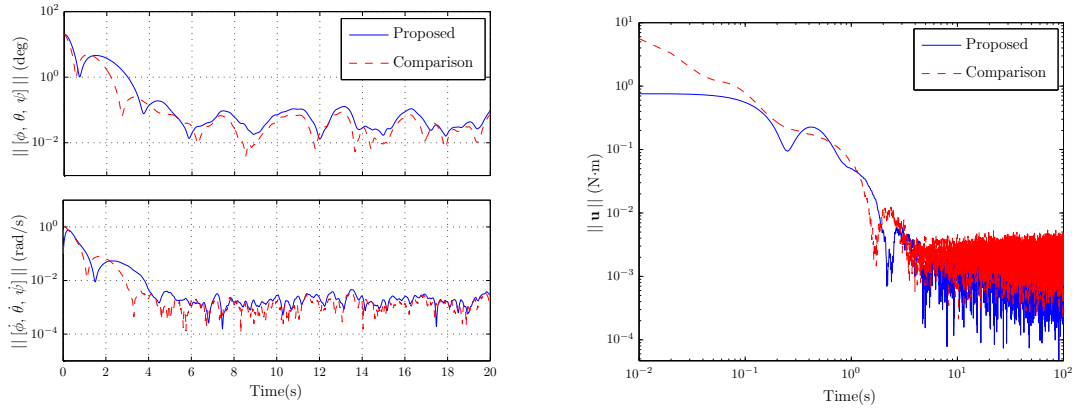

(a) Euler angles and rates

(b) Control torque

Figure 3.7: Comparison of simulation for the bias estimation errors without noise but with time-varying bias

the same magnitude since the time-varying bias does not directly involve the vector measurements unlike with the noise.

3.4.4 Unknown Inertia Simulations

Finally a simulation was performed where the body inertia matrix was assumed to be unknown but constant. Also, it was assumed that no noise was acting on the system, and the bias is constant. Since this is the first result for an unknown inertia, the results will only be for the proposed method. As mentioned previously, the convergence of the inertia parameters is dependent on a persistence of excitation condition. Given that the unknown inertia case requires estimation of 21 parameters, including 15 over-estimated parameters, meeting the PE condition is not straightforward; however, the main interest is in having the six inertia parameters converge. Accordingly, the reference trajectory was selected as

$$\boldsymbol{\omega}_r = [\cos t + 0.5\cos 0.2t, \quad 0.75\sin 2t, \quad \sin 5t\, e^{-0.001t} + \cos 0.5t]^\top$$

with $\mathbf{q}_r(0) = [1 \quad 0 \quad 0 \quad 0]^\top$. The initial bias and inertia estimates were chosen to have a 10% error from the true value. * These estimates were then used to find the initial estimates of $\hat{\mathbf{A}}(0)$, $\hat{\mathbf{B}}(0)$, and $\hat{\mathbf{D}}(0)$. The other initial conditions and values were kept the same as in previous simulations. The tracking errors associated with the Euler angles and rates are shown in Figure 3.8. Examination of the tracking errors actually indicates better performance despite the uncertainty in the inertia matrix and the time-varying reference signal. In addition, the steady state shows a rate of convergence of three orders and two orders of magnitude per 100 seconds for the Euler angles and rates, respectively. The convergence rates of $\boldsymbol{\Omega}$ and the bias converge quite rapidly when compared to the other signals as can be seen in Figure 3.9(a). Accordingly, the estimated states become the true as the parameter values shown in Figure 3.9(b) are still converging. Once the tracking errors converge,

*The choice of 10% error was made to include uncertainties that might be realistic for a practical system. It is emphasized that the initial error can in fact be anything, and perfect tracking will still be guaranteed

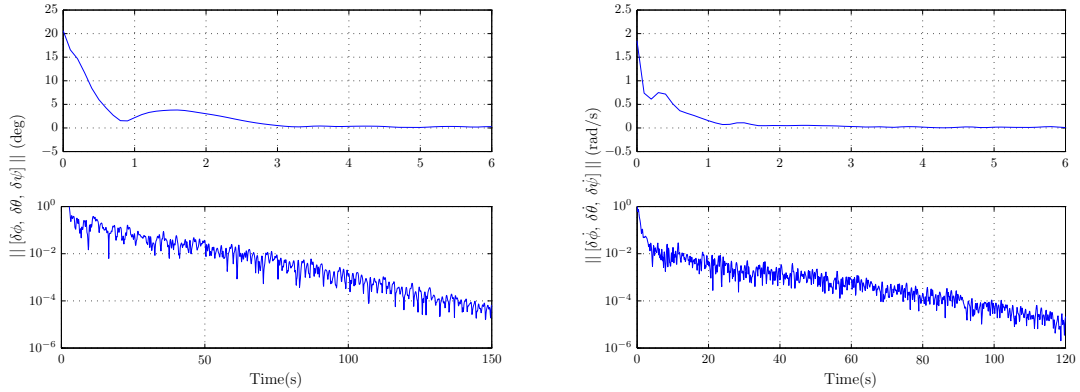

(a) Euler angles (b) Euler angle rates

Figure 3.8: Simulation results of the proposed method with unknown body inertia for the Euler angles and their respective rates without noise and time-varying bias

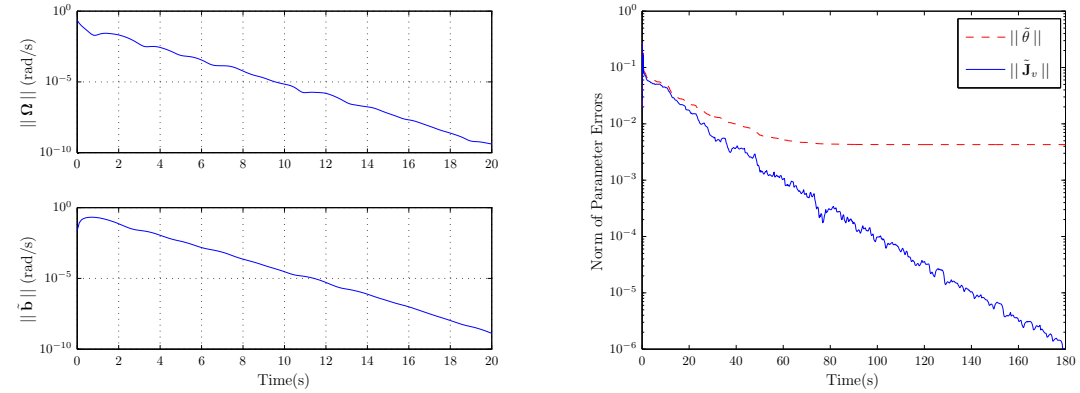

(a) $\boldsymbol{\Omega}$ and bias (b) Parameter errors

Figure 3.9: Simulation results of the proposed method with unknown body inertia for the estimation errors. Note that although not all of the parameter errors converge, the true values of the inertia matrix are recovered

the decay of the parameters errors is attributed only to the richness of the reference signal. Even though it is guaranteed that $||\mathbf{J}^{-1}\mathbf{W}_f\tilde{\boldsymbol{\theta}}||$ asymptotically converges to zero, it is clear that $\tilde{\boldsymbol{\theta}}$ does not because our signal was not able to excite all of the parameters. In fact, only 12 of the 21 parameters converge to their true values, but most importantly, the vector of six inertia errors, $\tilde{\mathbf{J}}_v$, converges whereas some of the redundant parameters do not. It should be noted that it would be possible to design a

"richer" reference trajectory to ensure convergence of all the parameters, provided the estimation scheme satisfies the identifiability condition, by adding more frequencies, but as mentioned previously, it would be unnecessary if the goal is only to ensure reliable tracking of the attitude reference trajectory. Furthermore, it is not required that any of the parameter estimates exactly converge to their unknown true values in order to meet the tracking control objectives. Finally (although not proved), it is expected that the addition of noise or time-varying to the unknown inertia case would show similar behavior to the known inertia case, albeit, with different residual sets.

3.5 Concluding Remarks

This chapter presents a novel control scheme for rigid-body attitude tracking with vector measurements and both unknown gyro bias and unknown body inertia matrix. The simpler problem of known inertia is introduced and compared with an existing control method. Both methods guarantee convergence of the tracking errors as well as the estimation errors on the attitude and the bias. The application of non-certainty equivalence techniques to the proposed method allows for the inertia matrix to appear linearly in the control law. This has two important effects on the system. The first is that the performance of the system is less susceptible to measurement noise and ultimately control saturation when contrasted with the comparison method where the inverse of the inertia matrix appears in the controller. Second, and perhaps more important, is that the control method can be extended to the case where the inertia matrix is uncertain. This work represents the first adaptive control algorithm to include vector measurements, unknown gyro bias, and unknown body inertia. Unfortunately, the structure of the problem requires an additional 15 parameters to be estimated, but the control objectives are met regardless of the convergence of the estimation errors. This result represents another important step to including more realistic measurement models into an adaptive control scheme for attitude tracking.

Chapter 4

Unknown Large-Scale Rotational Misalignments with Unknown Scaling

In this chapter, the problem of constant unknown actuator misalignment is examined. In this case, the misalignment is assumed to be a rotation matrix. Therefore, this problem is the extension of the special orthogonal matrix estimator where the unknown matrix is now a part of the system dynamics and is directly effecting the control signal. This could be a rigid actuation platform that has been installed incorrectly, which would create an equal rotation across all three control axes. As will be seen, the main issue is that a measurement equation is not directly available that allows for the estimation of the actuator misalignment. To do so will require the introduction of the filter variables. To further complicate the problem, an unknown scalar will also be included as a gain on the control signal. Thus, the unknown parameters will be non-affine in the system dynamics. The appearance of two unknowns will complicate the estimation process, but as will be shown, the stability of the system can be guaranteed.

The remainder of this chapter is organized as follows. Section 4.1 examines a control method for the trajectory tracking problem with an unknown rotational misalignment but without a scaling. Section 4.2 introduces the estimation problem where an additional unknown scaling is present. Section 4.3 extends this result to the control problem. Section 4.4 highlights how the control methodology can be easily extended to the rigid-body attitude tracking problem. Section 4.5 shows numerical simulations of the full unknown misalignment and unknown scaling problem. Finally, Section 4.6 gives some concluding remarks.

4.1 Trajectory Tracking with Unknown $SO(3)$ Actuator Misalignment

Consider the error dynamics of the standard system of (2.2) which has the error dynamics of (2.4). Assume that the actuator misalignment matrix belongs to the three-dimensional special orthogonal group. The assumption was made that only $\mathbf{x}_1$ and $\mathbf{x}_2$ are available; accordingly, there is no direct measurement of the unknown misalignment matrix (i.e. there is no $\mathbf{y} = \boldsymbol{\Psi}\mathbf{u}_f$). Using the filter definitions of (2.19), define the signal

$$\mathbf{y} \equiv \dot{\mathbf{e}}_{2,f} - \mathbf{g}_f = \boldsymbol{\Psi}\mathbf{u}_f \tag{4.1}$$

Further define the estimate of $\mathbf{y}$ to be

$$\hat{\mathbf{y}} = -\mathbf{g}_f - k_p\mathbf{e}_1 - k_v\mathbf{e}_{2,f} = \hat{\boldsymbol{\Psi}}\mathbf{u}_f \tag{4.2}$$

where k_p and k_v are positive scalar constants. It is now possible to implement the observer of (2.12)

$$\dot{\hat{\boldsymbol{\Psi}}} = -\gamma S(\mathbf{y} \times \hat{\mathbf{y}})\hat{\boldsymbol{\Psi}}$$

where γ is a positive scalar constant. Let the control be determined through

$$\mathbf{u} = -\hat{\boldsymbol{\Psi}}^\top \left[\mathbf{g} + \alpha\left(k_p\mathbf{e}_1 + \mathbf{e}_2\right) + \gamma S(\mathbf{y} \times \hat{\mathbf{y}})\hat{\boldsymbol{\Psi}}^\top\hat{\mathbf{y}}\right] \tag{4.3}$$

Note that the filters (except the control filter) must be implemented for this controller unlike the controller of (2.28) because there is now uncertainty through the actuator misalignment.

Theorem 4.1.1. *Consider the error system shown in (2.4) with the proper-orthogonal misalignment matrix, $\boldsymbol{\Psi}$, unknown. Suppose that the adaptive control torque $\mathbf{u}$ is determined through (4.3) with the update law on $\hat{\boldsymbol{\Psi}}$ of (2.12), and the filter definitions of (2.19a) and (2.19b) with arbitrary initial conditions $\mathbf{g}_f(0)$ and $\mathbf{e}_{2,f}(0)$. Choose the control gains subject to the condition that $\alpha = k_p + k_v$. Let $\mathbf{q}_{\boldsymbol{\Psi}}$ be the quaternion parameterization of $\boldsymbol{\Psi}$ and $\hat{\mathbf{q}}_{\boldsymbol{\Psi}}$ be its associated estimate. Then for all possible reference trajectories $\mathbf{r}(t)$ where the initial guess of $\hat{\mathbf{q}}_{\boldsymbol{\Psi}}$ is such that $\mathbf{q}_{\boldsymbol{\Psi}}^\top\hat{\mathbf{q}}_{\boldsymbol{\Psi}} \neq 0$, the closed-loop is asymptotically stable, leading to the convergence condition*

$$\lim_{t\to\infty}\begin{bmatrix}\mathbf{e}_1(t)\\ \mathbf{e}_2(t)\end{bmatrix} = \mathbf{0}$$

Proof. Using the filter discussion of Section 2.3.2, the filtered error dynamics can be represented as

$$\dot{\mathbf{e}}_{2,f} = \mathbf{g}_f + \mathbf{\Psi}\mathbf{u}_f \tag{4.4}$$

where $\dot{\mathbf{e}}_{2,f}$ is a known signal as opposed to $\dot{\mathbf{e}}_2$ which is not available. Re-arranging the terms in (4.4), $\mathbf{y}$ can be defined as in (4.1). It is then desirable to define

$$\hat{\mathbf{y}} \equiv \hat{\mathbf{\Psi}}\mathbf{u}_f \tag{4.5}$$

as the estimate of $\mathbf{y}$. Using (2.23) as motivation, choose the filtered control signal as

$$\mathbf{u}_f = -\hat{\mathbf{\Psi}}^\top \left(\mathbf{g}_f + k_p\mathbf{e}_1 + k_v\mathbf{e}_{2,f}\right) \tag{4.6}$$

If the estimate of the misalignment were to converge, $\hat{\mathbf{\Psi}}^\top$ would eliminate the actuator misalignment matrix $\mathbf{\Psi}$ and only the standard control problem would remain. Note that this control brings up a possible constraint on $\hat{\mathbf{\Psi}}$ such that the control does not become unbounded; however, since the observer guarantees that the estimate is a rotation matrix for all time, $\hat{\mathbf{\Psi}}$ is always invertible (and is in fact the transpose). If the observer did not give this guarantee, there could be issues with singularity in the control as discussed via the unknown high frequency gain problem of Section 2.2. Also, note that plugging the $\mathbf{u}_f$ of (4.6) into $\hat{\mathbf{y}}$ of (4.5) recovers the implemented version of $\hat{\mathbf{y}}$ in (4.2).

Consider the Lyapunov-like function,

$$V = \frac{1}{2}\mathbf{e}_1^\top\mathbf{e}_1 + \frac{1}{2}\mathbf{e}_{2,f}^\top\mathbf{e}_{2,f} + \tau\frac{\mathbf{z}_v^\top\mathbf{z}_v}{2z_0^2} \tag{4.7}$$

where $\tau > 0$ is a scalar constant. Taking the derivative (following Section 2.3.2) and realizing that

$$\begin{aligned}
\left(\mathbf{e}_1 + \mathbf{e}_{2,f}\right)^\top \mathbf{\Psi}\left(\mathbf{I} - \mathbf{\Psi}^\top\hat{\mathbf{\Psi}}\right)\mathbf{u}_f &\leq ||\mathbf{e}_1 + \mathbf{e}_{2,f}||\,||\mathbf{\Psi}||\,||\left(\mathbf{I} - \mathbf{\Psi}^\top\hat{\mathbf{\Psi}}\right)\mathbf{u}_f|| \\
&\leq \left(||\mathbf{e}_1|| + ||\mathbf{e}_{2,f}||\right)||2\left[z_0\mathbf{I} - S(\mathbf{z}_v)\right]S(\mathbf{z}_v)\mathbf{u}_f|| \\
&\leq 2\left(||\mathbf{e}_1|| + ||\mathbf{e}_{2,f}||\right)||z_0\mathbf{I} - S(\mathbf{z}_v)||\,||\mathbf{z}_v \times \mathbf{u}_f|| \\
&\leq 4\left(||\mathbf{e}_1|| + ||\mathbf{e}_{2,f}||\right)||\mathbf{z}_v \times \mathbf{u}_f||
\end{aligned}$$

yields

$$
\begin{aligned}
\dot{V} &= \alpha \mathbf{e}_1^\top \mathbf{e}_{2,f} + \left(\mathbf{e}_1 + \mathbf{e}_{2,f}\right)^\top \dot{\mathbf{e}}_{2,f} - \gamma\tau ||\mathbf{z}_v \times \mathbf{u}_f||^2 \\
&= \alpha \mathbf{e}_1^\top \mathbf{e}_{2,f} + \left(\mathbf{e}_1 + \mathbf{e}_{2,f}\right)^\top \left(\mathbf{g}_f + \boldsymbol{\Psi}\mathbf{u}_f\right) - \gamma\tau ||\mathbf{z}_v \times \mathbf{u}_f||^2 \\
&= \alpha \mathbf{e}_1^\top \mathbf{e}_{2,f} + \left(\mathbf{e}_1 + \mathbf{e}_{2,f}\right)^\top \left[\mathbf{g}_f + \hat{\boldsymbol{\Psi}}\mathbf{u}_f + \left(\boldsymbol{\Psi} - \hat{\boldsymbol{\Psi}}\right)\mathbf{u}_f\right] - \gamma\tau ||\mathbf{z}_v \times \mathbf{u}_f||^2 \\
&= \alpha \mathbf{e}_1^\top \mathbf{e}_{2,f} + \left(\mathbf{e}_1 + \mathbf{e}_{2,f}\right)^\top \left[-k_p \mathbf{e}_1 - k_v \mathbf{e}_{2,f} + \boldsymbol{\Psi}\left(\mathbf{I} - \boldsymbol{\Psi}^\top \hat{\boldsymbol{\Psi}}\right)\mathbf{u}_f\right] - \gamma\tau ||\mathbf{z}_v \times \mathbf{u}_f||^2 \\
&= -k_p ||\mathbf{e}_1||^2 - k_v ||\mathbf{e}_{2,f}||^2 - \gamma\tau ||\mathbf{z}_v \times \mathbf{u}_f||^2 + \left(\mathbf{e}_1 + \mathbf{e}_{2,f}\right)^\top \boldsymbol{\Psi}\left(\mathbf{I} - \boldsymbol{\Psi}^\top \hat{\boldsymbol{\Psi}}\right)\mathbf{u}_f \\
&\leq -k_p ||\mathbf{e}_1||^2 - k_v ||\mathbf{e}_{2,f}||^2 - \gamma\tau ||\mathbf{z}_v \times \mathbf{u}_f||^2 + 4\left(||\mathbf{e}_1|| + ||\mathbf{e}_{2,f}||\right)||\mathbf{z}_v \times \mathbf{u}_f|| \\
&\leq -\frac{k_p}{2}||\mathbf{e}_1||^2 - \frac{k_v}{2}||\mathbf{e}_{2,f}||^2 - \gamma\tau\left[1 - \frac{8}{\gamma\tau}\left(\frac{1}{k_p} + \frac{1}{k_v}\right)\right]||\mathbf{z}_v \times \mathbf{u}_f||^2 \\
&\quad - \frac{k_p}{2}\left[||\mathbf{e}_1|| - \left(\frac{4}{k_p}\right)||\mathbf{z}_v \times \mathbf{u}_f||\right]^2 - \frac{k_v}{2}\left[||\mathbf{e}_1|| - \left(\frac{4}{k_v}\right)||\mathbf{z}_v \times \mathbf{u}_f||\right]^2 \\
&\leq -\frac{k_p}{2}||\mathbf{e}_1||^2 - \frac{k_v}{2}||\mathbf{e}_{2,f}||^2 - \gamma'||\mathbf{z}_v \times \mathbf{u}_f||^2 \qquad (4.8)
\end{aligned}
$$

where a selection of τ was made were used to ensure that $\dot{V} \leq 0$. This selection of τ is trivial since it in no way effects the system performance. Thus, $\dot{V}$ is negative semi-definite, indicating boundedness for all closed-loop signals. Further, because V is lower-bounded, $\int_0^\infty \dot{V}(t)\, dt$ exists and is finite which implies that $\mathbf{e}_1$, $\mathbf{e}_{2,f}$ and $\mathbf{z}_v \times \mathbf{u}_f \in \mathcal{L}_2 \cap \mathcal{L}_\infty$. It follows that $\dot{\mathbf{e}}_1$, $\dot{\mathbf{e}}_{2,f}$ and $\dot{\mathbf{z}}_v$ are $\mathcal{L}_\infty$ from (2.4a), (4.4), and (2.14a). Thus by Barbalat's lemma, $\mathbf{e}_{2,f}$ and $\mathbf{e}_1 \to 0$ as $t \to \infty$. Furthermore, because of the definition of the filter of (2.19a), $\mathbf{e}_{2,f} \to 0$ implies $\mathbf{e}_2 \to 0$ as $t \to \infty$. Therefore, the control objective is met. In addition, from Barbalat's lemma, $||\mathbf{z} \times \mathbf{u}_f|| \to 0$ as $t \to 0$. This, however, does not guarantee convergence of $\mathbf{z}_v \to 0$ and ultimately $\hat{\boldsymbol{\Psi}} \to \boldsymbol{\Psi}$ in all cases; yet, it is emphasized that even without convergence of the misalignment matrix, the attitude and angular velocity errors still converge to zero. □

4.1.1 Remarks

1. For the control problem, it would be of particular interest to achieve convergence of the unknown rotation matrix, in addition to the control objectives. As already stated, convergence of $\mathbf{z}_v$ to zero does not immediately follow from convergence of $||\mathbf{z} \times \mathbf{u}_f||$ to zero. For example, in the stabilization problem (constant position and zero velocity),

$\mathbf{u}_f$ can quickly go to zero as stabilization occurs which causes the estimate of $\mathbf{\Psi}$ to remain relatively constant without converging to the true value. The commanded reference trajectory, however, can drive the signal $\mathbf{u}_f$ to meet certain additional PE conditions. In this case, the estimate of $\mathbf{\Psi}$ converges to the true value.

2. Even though our main theorem precludes the initial condition on $\hat{\mathbf{q}}_{\mathbf{\Psi}}(0)$ such that $z_0(0) \neq 0$, it is important to note that $z_0 = 0$ is in fact an unstable manifold. From (2.14a), it is clear that z_0 defines an equilibrium manifold since $z_0(0) = 0$ implies that $z_0(t) = 0$ for all $t \geq 0$. Using the Lyapunov-like function

$$V_E = \frac{1}{2}\mathbf{z}_v^\top \mathbf{z}_v = \frac{1}{2}\left(1 - z_0^2\right) \tag{4.9}$$

that yields the derivative

$$\dot{V}_E = -\gamma z_0^2 ||\mathbf{z}_v \times \mathbf{u}_f||^2 \leq 0 \tag{4.10}$$

it is clear that V_E belongs to the closed interval [0, 1/2] with $V_E = 1/2$ when $z_0 = 0$. In this case, V_E remains constant since $\dot{V}_E = 0$. If $z_0 = \epsilon \neq 0$ with arbitrarily small $|\epsilon|$ ($V_E(0) < 1/2$), then $|z_0(t)| \geq |\epsilon|$ for all $t \geq 0$ from (2.14a). Therefore, it is impossible that $z_0(t) \to 0$ as $t \to \infty$. Since arbitrarily small perturbations drive the solution away from the equilibrium manifold, $z_0 = 0$ is an unstable manifold.

4.2 Estimation of Unknown $SO(3)$ Misalignment with Unknown Scaling

Assume that in addition to the unknown rotation matrix, there is additional constant unknown scaling, c, so that the measurement equation can be represented as

$$\bar{\mathbf{y}} = c\mathbf{\Psi}\mathbf{u}_f \tag{4.11}$$

where $\mathbf{u}_f$ is a known input and $\bar{\mathbf{y}}$ is the measured output. Note that $\bar{\mathbf{y}} = c\mathbf{y}$. The scaling could possibly be a model for performance degradation or an error in units. Let the update law for the rotation matrix be given by

$$\dot{\hat{\mathbf{\Psi}}} = -\gamma S(\bar{\mathbf{y}} \times \hat{\mathbf{y}})\hat{\mathbf{\Psi}} \tag{4.12}$$

where $\hat{\mathbf{y}} = \hat{\mathbf{\Psi}}\mathbf{u}_f$. Further, let the estimate of c, given by $\hat{c}$ be determined through the dynamics

$$\dot{\hat{c}} = -\lambda \left(\hat{c} ||\mathbf{u}_f||^2 - \bar{\mathbf{y}}^\top \hat{\mathbf{y}} \right) \tag{4.13}$$

where $\lambda > 0$ is a scalar gain. Then the following theorem can be stated:

Theorem 4.2.1. *Consider the measurement equation of (4.11). Let the update laws for $\hat{\mathbf{\Psi}}$ and $\hat{c}$ be determined through (4.12) and (4.13), respectively. Then for all initial conditions $\hat{\mathbf{\Psi}}(0)$ and $\hat{c}(0)$ excluding the initial guess of $\hat{\mathbf{q}}_{\mathbf{\Psi}}$ such that $\mathbf{q}_{\mathbf{\Psi}}^\top \hat{\mathbf{q}}_{\mathbf{\Psi}} \neq 0$, the convergence condition*

$$\lim_{t \to \infty} \begin{bmatrix} \hat{\mathbf{\Psi}}(t) - \mathbf{\Psi} \\ \hat{c}(t) - c \end{bmatrix} = \mathbf{0}$$

is valid provided that $\mathbf{u}_f$ is a persistently exciting signal.

Proof. Examining the update law on $\hat{\mathbf{\Psi}}$, the dynamics can be rewritten as

$$\dot{\hat{\mathbf{\Psi}}} = -\gamma c S(\mathbf{y} \times \hat{\mathbf{y}}) \hat{\mathbf{\Psi}} \tag{4.14}$$

Thus, the unknown scaling c acts as an additional gain on the observer and will pass through the analysis without changing the stability properties. Next, define the estimation error on c as

$$\tilde{c} \equiv \hat{c} - c \tag{4.15}$$

In addition, the update law on $\hat{c}$ can be expressed as

$$\begin{aligned} \dot{\tilde{c}} = \dot{\hat{c}} &= -\lambda \left(\hat{c} ||\mathbf{u}_f||^2 - c \mathbf{u}_f^\top \mathbf{\Psi}^\top \hat{\mathbf{\Psi}} \mathbf{u}_f \right) \\ &= -\lambda \left[\tilde{c} ||\mathbf{u}_f||^2 + c \mathbf{u}_f^\top \left(\mathbf{I} - \mathbf{\Psi}^\top \hat{\mathbf{\Psi}} \right) \mathbf{u}_f \right] \end{aligned} \tag{4.16}$$

which has terms related to the estimation error of c and $\mathbf{\Psi}$. Note that if $\hat{\mathbf{\Psi}}$ were to converge to the true value that the estimation error on c would have the dynamics $\dot{\tilde{c}} = -\lambda' \tilde{c}$ which is an exponentially decaying signal. To prove convergence of the estimation errors, consider the Lyapunov-like function

$$V = \frac{\tau \mathbf{z}_v^\top \mathbf{z}_v}{2 c z_0^2} + \frac{1}{2} \tilde{c}^2 \tag{4.17}$$

where $\tau > 0$ is a scalar constant. Given the discussion above and using the update laws of (4.14) and (4.16), the derivative is found to be

$$\begin{aligned}
\dot{V} &= -\frac{\gamma\tau c}{c}||\mathbf{z}_v \times \mathbf{u}_f||^2 + \tilde{c}\dot{\tilde{c}} \\
&= -\gamma\tau||\mathbf{z}_v \times \mathbf{u}_f||^2 - \lambda\tilde{c}^2||\mathbf{u}_f||^2 - \lambda c\tilde{c}\mathbf{u}_f^\top \left(\mathbf{I} - \mathbf{\Psi}^\top\hat{\mathbf{\Psi}}\right)\mathbf{u}_f \\
&\leq -\gamma\tau||\mathbf{z}_v \times \mathbf{u}_f||^2 - \lambda\tilde{c}^2||\mathbf{u}_f||^2 + \lambda|c|\left(\tilde{c}||\mathbf{u}_f||\right)||\left(\mathbf{I} - \mathbf{\Psi}^\top\hat{\mathbf{\Psi}}\right)\mathbf{u}_f|| \\
&\leq -\gamma\tau||\mathbf{z}_v \times \mathbf{u}_f||^2 - \lambda\tilde{c}^2||\mathbf{u}_f||^2 + 4\lambda|c|\left(\tilde{c}||\mathbf{u}_f||\right)||\mathbf{z}_v \times \mathbf{u}_f|| \\
&\leq -\frac{\lambda}{2}\tilde{c}^2||\mathbf{u}_f||^2 - \gamma\tau\left(1 - \frac{8c^2}{\gamma\lambda\tau}\right)||\mathbf{z}_v \times \mathbf{u}_f||^2 \\
&\quad - \frac{\lambda}{2}\left[\tilde{c}||\mathbf{u}_f|| - \left(\frac{4|c|}{\lambda}\right)||\mathbf{z}_v \times \mathbf{u}_f||\right]^2 \\
&\leq -\frac{\lambda}{2}\tilde{c}^2||\mathbf{u}_f||^2 - \gamma\tau\left(1 - \frac{8c^2}{\gamma\lambda\tau}\right)||\mathbf{z}_v \times \mathbf{u}_f||^2
\end{aligned} \tag{4.18}$$

For (4.18) to be negative semi-definite, the condition

$$\tau > \frac{8c^2}{\gamma\lambda}$$

must be satisfied. Fortunately, this condition is trivially satisfied because τ can be increased as much as necessary (provided c is finite) without effecting the performance of the observers. Therefore, the derivative of the Lyapunov like function is given by

$$\dot{V} \leq -\frac{\lambda}{2}\tilde{c}^2||\mathbf{u}_f||^2 - \gamma'||\mathbf{z}_v \times \mathbf{u}_f||^2 \leq 0 \tag{4.19}$$

where γ' is a positive scalar dependent on the choice of τ. Thus, $\dot{V}$ is negative semi-definite, indicating boundedness for all signals. Further, because V is lower-bounded, $\int_0^\infty \dot{V}(t)\,dt$ exists and is finite which implies that $\tilde{c}||\mathbf{u}_f||$ and $\mathbf{z}_v \times \mathbf{u}_f \in \mathcal{L}_2 \cap \mathcal{L}_\infty$. It follows that $\dot{\tilde{c}}$ and $\dot{\mathbf{z}}_v$ are $\mathcal{L}_\infty$ from (4.13), and (2.14a), respectively. Thus by Barbalat's lemma, $\tilde{c}||\mathbf{u}_f||$ and $\mathbf{z}_v \times \mathbf{u}_f \to 0$ as $t \to \infty$. Since the convergence of the estimation errors themselves are dependent on the behavior of $\mathbf{u}_f$, the requirement of persistence of excitation is added to $\mathbf{u}_f$. Accordingly, this implies $\tilde{c}$ and $\mathbf{z}_v \to 0$ as $t \to \infty$. From $\mathbf{z}_v \to 0$, the extension can be made that $\mathbf{\Psi}^\top\hat{\mathbf{\Psi}} \to \mathbf{I}$, and ultimately $\hat{\mathbf{\Psi}} - \mathbf{\Psi} \to 0$ asymptotically which completes the proof. □

4.2.1 Remarks

1) The obvious downside is the requirement of persistence of excitation on $\mathbf{u}_f$ to achieve convergence of the estimation errors. In practice, $\mathbf{u}_f$ simply has to be sufficiently rich to ensure that the errors have had ample opportunity to converge to the true values.

2) Interesting behavior is evident when all the values of $\mathbf{u}_f$ are non-zero constants. From the stability analysis, it is clear that the estimation error on c must converge to zero; however, the best that can be done is to show that $\mathbf{y} \times \hat{\mathbf{y}}$ converges to zero. As mentioned previously, this does not guarantee that $\hat{\mathbf{\Psi}} \to \mathbf{\Psi}$. Thus an additional constant, linearly independent $\mathbf{u}_f$ would have to be available to get convergence of the rotation matrix as in the previous chapter.

4.3 Trajectory Tracking with Unknown $SO(3)$ Actuator Misalignment and Unknown Scaling

Now, consider the control problem where there is a purely rotational unknown actuator misalignment along with an unknown scaling. Updating the standard system of (2.2) to

$$\dot{\mathbf{x}}_1 = \mathbf{x}_2 \tag{4.20a}$$

$$\dot{\mathbf{x}}_2 = \mathbf{f}(\mathbf{x}_1, \mathbf{x}_2) + c\mathbf{\Psi}\mathbf{u} \tag{4.20b}$$

from which the tracking error dynamics can be established as

$$\dot{\mathbf{e}}_1 = \mathbf{e}_2 \tag{4.21a}$$

$$\dot{\mathbf{e}}_2 = \mathbf{g} + c\mathbf{\Psi}\mathbf{u} \tag{4.21b}$$

Before showing the observer and controller for this problem, it should be noted that extension to the control problem introduces a problem with the scaling estimation. Consider the case where c is known. The signal $\mathbf{y}$ can be recovered by dividing $\bar{\mathbf{y}}$ by c, and the estimation of the rotation matrix progresses as before. In order to remove c from the dynamics, however, it is necessary to include a $1/c$ in the control signal

much in the same way a $\mathbf{\Psi}^{-1}$ would be needed to eliminate $\mathbf{\Psi}$. When c is a known constant, there is no chance of $1/c$ becoming an issue, but during the estimation of c, a $1/\hat{c}$ must be included in the control signal. Therefore, it becomes a requirement that the estimate of c can never pass through zero or the desired control will become unbounded. Since $\hat{c}$ cannot become zero, it is necessary to assume the sign of c is known. * Moreover, a projection scheme (as in Section 2.3.3) must be implemented. Thus, let the estimation of the scalar c be replaced by estimation of ξ which has the relations

$$c = \frac{\mu}{2}\left(1 - \tanh \xi\right) + c_{\min} \tag{4.22a}$$

$$\hat{c} = \frac{\mu}{2}\left(1 - \tanh \hat{\xi}\right) + c_{\min} \tag{4.22b}$$

where

$$\mu \equiv c_{\max} - c_{\min} \tag{4.23}$$

and the assumption has been made that there are known bounds such that $0 < c_{\min} \leq c \leq c_{\max}$. By appropriately selecting the bounds, the constraint on the sign of c can be enforced, and $\hat{c}$ will not become zero at any instant in time. Additionally, the scaling can be estimated a different way than in the previous section. In this case, information can be gathered from the system dynamics and the update law

$$\dot{\hat{\xi}} = -\lambda \left(\mathbf{e}_1 + \mathbf{e}_{2,f}\right)^\top \hat{\mathbf{y}} \tag{4.24}$$

where

$$\hat{\mathbf{y}} = -\frac{1}{\hat{c}}\left(\mathbf{g}_f + k_p \mathbf{e}_1 + k_v \mathbf{e}_{2,f}\right) \tag{4.25}$$

can be used as opposed to (4.13). The motivation for this choice will be made clear during the proof. Next, define the signal

$$\bar{\mathbf{y}} \equiv \dot{\mathbf{e}}_{2,f} - \mathbf{g}_f \tag{4.26}$$

frow which the observer on $\hat{\mathbf{\Psi}}$ in (4.12) can still be applied. Finally, let the control signal $\mathbf{u}$ be determined through

$$\mathbf{u} = -\frac{1}{\hat{c}}\hat{\mathbf{\Psi}}^\top \left[\mathbf{g} + \alpha\left(k_p \mathbf{e}_1 + \mathbf{e}_2\right) + \gamma S(\bar{\mathbf{y}} \times \hat{\mathbf{y}})\hat{\mathbf{y}} + \frac{\mu}{2\hat{c}}\left(1 - \tanh^2 \hat{\xi}\right)\dot{\hat{\xi}}\,\hat{\mathbf{\Psi}}^\top \hat{\mathbf{y}}\right] \tag{4.27}$$

*For the proceeding analysis it is assumed that c is positive without loss of generality

which includes an additional term from the non-scaling case of (4.3) due to the estimation of c.

Theorem 4.3.1. *Consider the error system shown in (4.21) with the proper-orthogonal misalignment matrix, $\mathbf{\Psi}$, and scaling c unknown. Suppose that the adaptive control torque $\mathbf{u}$ is determined through (4.27) with the update law on $\hat{\mathbf{\Psi}}$ of (4.12), the update law on $\hat{\xi}$ of (4.24), and the filter definitions of (2.19a) and (2.19b) with arbitrary initial conditions $\mathbf{g}_f(0)$ and $\mathbf{e}_{2,f}(0)$. Choose the control gains subject to the condition $\alpha = k_p + k_v$. Then for all possible reference trajectories $\mathbf{r}(t)$, all $\hat{c}(0)$, and all $\hat{\mathbf{q}}_{\mathbf{\Psi}}(0)$ such that $\mathbf{q}_{\mathbf{\Psi}}^{\top}\hat{\mathbf{q}}_{\mathbf{\Psi}} \neq 0$, the closed-loop is asymptotically stable, leading to the convergence condition*

$$\lim_{t\to\infty} \begin{bmatrix} \mathbf{e}_1(t) \\ \mathbf{e}_2(t) \end{bmatrix} = \mathbf{0}$$

Proof. Using the filter discussion of Section 2.3.2, the filtered error dynamics can be represented as

$$\dot{\mathbf{e}}_{2,f} = \mathbf{g}_f + c\mathbf{\Psi}\mathbf{u}_f \tag{4.28}$$

Re-arranging the terms in (4.28), $\bar{\mathbf{y}}$ can be defined as in (4.26) and the measurement equation of (4.11) is recovered. Then define

$$\hat{\mathbf{y}} \equiv \hat{\mathbf{\Psi}}\mathbf{u}_f \tag{4.29}$$

where $\hat{c}$ has not been included as in the observer. Next, choose the filtered control signal as

$$\mathbf{u}_f = -\frac{1}{\hat{c}}\hat{\mathbf{\Psi}}^{\top}\left(\mathbf{g}_f + k_p\mathbf{e}_1 + k_v\mathbf{e}_{2,f}\right) \tag{4.30}$$

If the estimates were to converge, the unknown values on the control would be eliminated, and only the standard control problem would remain. Consider the Lyapunov-like function on the estimation values given by

$$V_E = \tau\frac{\mathbf{z}_v^{\top}\mathbf{z}_v}{2cz_0^2} + \frac{\mu}{2\lambda}\left[\log\left(\cosh\hat{\xi}\right) - \tilde{\xi}\tanh\xi\right] \tag{4.31}$$

where the second term is consistent with (2.30) and the discussion of the smooth projection scheme. Using the derivatives from (4.18) and (2.31), the rate of change

of the Lyapunov function is

$$\dot{V}_E = -\gamma\tau||\mathbf{z}_v \times \mathbf{u}_f||^2 - \frac{1}{\lambda}\tilde{c}\,\dot{\hat{\xi}} \tag{4.32}$$

Next, consider the Lyapunov function involving the control values

$$V_C = \frac{1}{2}\mathbf{e}_1^\top \mathbf{e}_1 + \frac{1}{2}\mathbf{e}_{2,f}^\top \mathbf{e}_{2,f} \tag{4.33}$$

Taking the derivative of (4.33) and recognizing that $c = \hat{c} - \tilde{c}$ yields

$$\begin{aligned}
\dot{V}_C &= \alpha\mathbf{e}_1^\top \mathbf{e}_{2,f} + (\mathbf{e}_1 + \mathbf{e}_{2,f})^\top \dot{\mathbf{e}}_{2,f} \\
&= \alpha\mathbf{e}_1^\top \mathbf{e}_{2,f} + (\mathbf{e}_1 + \mathbf{e}_{2,f})^\top (\mathbf{g}_f + c\boldsymbol{\Psi}\mathbf{u}_f) \\
&= \alpha\mathbf{e}_1^\top \mathbf{e}_{2,f} + (\mathbf{e}_1 + \mathbf{e}_{2,f})^\top \left[\mathbf{g}_f + c\hat{\boldsymbol{\Psi}}\mathbf{u}_f + c\left(\boldsymbol{\Psi} - \hat{\boldsymbol{\Psi}}\right)\mathbf{u}_f\right] \\
&= \alpha\mathbf{e}_1^\top \mathbf{e}_{2,f} + (\mathbf{e}_1 + \mathbf{e}_{2,f})^\top \left[\mathbf{g}_f + (\hat{c} - \tilde{c})\,\hat{\boldsymbol{\Psi}}\mathbf{u}_f + c\boldsymbol{\Psi}\left(\mathbf{I} - \boldsymbol{\Psi}^\top\hat{\boldsymbol{\Psi}}\right)\mathbf{u}_f\right] \\
&= \alpha\mathbf{e}_1^\top \mathbf{e}_{2,f} + (\mathbf{e}_1 + \mathbf{e}_{2,f})^\top \left[-k_p\mathbf{e}_1 - k_v\mathbf{e}_{2,f} + \tilde{c}\hat{\mathbf{y}} - c\boldsymbol{\Psi}\left(\mathbf{I} - \boldsymbol{\Psi}^\top\hat{\boldsymbol{\Psi}}\right)\mathbf{u}_f\right] \\
&= -k_p||\mathbf{e}_1||^2 - k_v||\mathbf{e}_{2,f}||^2 \\
&\quad + c\,(\mathbf{e}_1 + \mathbf{e}_{2,f})^\top \boldsymbol{\Psi}\left(\mathbf{I} - \boldsymbol{\Psi}^\top\hat{\boldsymbol{\Psi}}\right)\mathbf{u}_f - \tilde{c}\,(\mathbf{e}_1 + \mathbf{e}_{2,f})^\top \hat{\mathbf{y}}
\end{aligned} \tag{4.34}$$

Define the joint Lyapunov-like function V by combining (4.31) and (4.33) as

$$V = V_C + V_E \tag{4.35}$$

which from (4.32) and (4.34) has time derivative

$$\begin{aligned}
\dot{V} &= -k_p||\mathbf{e}_1||^2 - k_v||\mathbf{e}_{2,f}||^2 - \gamma\tau||\mathbf{z}_v \times \mathbf{u}_f||^2 \\
&\quad + c\,(\mathbf{e}_1 + \mathbf{e}_{2,f})^\top \boldsymbol{\Psi}\left(\mathbf{I} - \boldsymbol{\Psi}^\top\hat{\boldsymbol{\Psi}}\right)\mathbf{u}_f - \tilde{c}\left[(\mathbf{e}_1 + \mathbf{e}_{2,f})^\top \hat{\mathbf{y}} + \frac{1}{\lambda}\dot{\hat{\xi}}\right]
\end{aligned} \tag{4.36}$$

This is the point where the update law on $\hat{\xi}$ is chosen such that the term proceeding $\tilde{c}$ is zero. Thus, using the observer for $\hat{\xi}$ in (4.24) and completing squares, equation (4.36) becomes

$$\begin{aligned}
\dot{V} &\leq -k_p||\mathbf{e}_1||^2 - k_v||\mathbf{e}_{2,f}||^2 - \gamma\tau||\mathbf{z}_v \times \mathbf{u}_f||^2 + 4|c|\,(||\mathbf{e}_1|| + ||\mathbf{e}_{2,f}||)\,||\mathbf{z}_v \times \mathbf{u}_f|| \\
&\leq -\frac{k_p}{2}||\mathbf{e}_1||^2 - \frac{k_v}{2}||\mathbf{e}_{2,f}||^2 - \gamma\tau\left[1 - \frac{8c^2}{\gamma\tau}\left(\frac{1}{k_p} + \frac{1}{k_v}\right)\right]||\mathbf{z}_v \times \mathbf{u}_f||^2 \\
&\quad - \frac{k_p}{2}\left[||\mathbf{e}_1|| - \left(\frac{4|c|}{k_p}\right)||\mathbf{z}_v \times \mathbf{u}_f||\right]^2 - \frac{k_v}{2}\left[||\mathbf{e}_1|| - \left(\frac{4|c|}{k_v}\right)||\mathbf{z}_v \times \mathbf{u}_f||\right]^2 \\
&\leq -\frac{k_p}{2}||\mathbf{e}_1||^2 - \frac{k_v}{2}||\mathbf{e}_{2,f}||^2 - \gamma'||\mathbf{z}_v \times \mathbf{u}_f||^2
\end{aligned} \tag{4.37}$$

where the a proper selection of τ ensures that the factor on the rotation error term remains positive. Thus, $\dot{V}$ is negative semi-definite, indicating boundedness for all closed-loop signals. Further, because V is lower-bounded, $\int_0^\infty \dot{V}(t)\,dt$ exists and is finite which implies that $\mathbf{e}_1$, $\mathbf{e}_{2,f}$ and $\mathbf{z}_v \times \mathbf{u}_f \in \mathcal{L}_2 \cap \mathcal{L}_\infty$. It follows that $\dot{\mathbf{e}}_1$, $\dot{\mathbf{e}}_{2,f}$ and $\dot{\mathbf{z}}_v$ are $\mathcal{L}_\infty$ from (4.21a), (4.28), and (2.14a). Thus by Barbalat's lemma, $\mathbf{e}_{2,f}$ and $\mathbf{e}_1 \to 0$ as $t \to \infty$. Furthermore, because of the definition of the filter of (2.19a), $\mathbf{e}_{2,f} \to 0$ implies $\mathbf{e}_2 \to 0$ as $t \to \infty$. Therefore, the control objective is met. In addition, from Barbalat's lemma, $||\mathbf{z}_v \times \mathbf{u}_f|| \to 0$ as $t \to 0$. This, however, does not guarantee convergence of $\mathbf{z}_v \to 0$ and ultimately $\hat{\mathbf{\Psi}} \to \mathbf{\Psi}$ in all cases; yet, it is emphasized that even without convergence of the misalignment matrix, the attitude and angular velocity errors still converge to zero. □

4.4 Extension to the Rigid-Body Attitude Tracking Problem

To complete the discussion, the observer and controller are shown to be stabilizing for the rigid-body attitude tracking problem where the unknown rotation and unknown scaling are applied [56]. This extension will only be shown one time and will be assumed to apply to any results where the standard system dynamics are stabilized. Consider the attitude tracking error kinematics of (3.7) and dynamics of (3.8) with the slight variation

$$\mathbf{J}\delta\dot{\boldsymbol{\omega}} = -S(\boldsymbol{\omega})\mathbf{J}\boldsymbol{\omega} + c\mathbf{\Psi}\mathbf{u} + \mathbf{J}\left[S(\delta\boldsymbol{\omega})\mathbf{C}(\delta\mathbf{q})\boldsymbol{\omega}_r - \mathbf{C}(\delta\mathbf{q})\dot{\boldsymbol{\omega}}_r\right] \tag{4.38}$$

which now includes the unknown misalignment terms. The assumption is made that the angular velocity and attitude quaternion are perfectly measured. Define the signal

$$\mathbf{W} = -S(\boldsymbol{\omega})\mathbf{J}\boldsymbol{\omega} + \mathbf{J}\left[S(\delta\boldsymbol{\omega})\mathbf{C}(\delta\mathbf{q})\boldsymbol{\omega}_r - \mathbf{C}(\delta\mathbf{q})\dot{\boldsymbol{\omega}}_r\right] \tag{4.39}$$

such that the error dynamics can be represented as

$$\mathbf{J}\delta\dot{\boldsymbol{\omega}} = \mathbf{W} + c\mathbf{\Psi}\mathbf{u} \tag{4.40}$$

which is similar to the error dynamics of the standard system. Implement stable first-order filters on $\delta\boldsymbol{\omega}$ through

$$\dot{\boldsymbol{\omega}}_f = -\alpha\boldsymbol{\omega}_f + \delta\boldsymbol{\omega} \tag{4.41}$$

and $\mathbf{W}$ via (3.15) with arbitrary initial conditions. Define the available signals,

$$\bar{\mathbf{y}} = \mathbf{J}\dot{\boldsymbol{\omega}}_f - \mathbf{W}_f \tag{4.42}$$

$$\hat{\mathbf{y}} = -\frac{1}{\hat{c}}\left(\mathbf{W}_f + k_p\mathbf{J}\delta\mathbf{q}_v + k_v\mathbf{J}\boldsymbol{\omega}_f\right) \tag{4.43}$$

then the observer on the rotation matrix can be chosen as in the previous section. It is still necessary to apply a projection scheme on c to avoid unboundedness of the control signal; accordingly, the update law on the projection parameter, ξ, can be chosen as

$$\dot{\hat{\xi}} = -\lambda\left(\boldsymbol{\omega}_f + \delta\mathbf{q}_v\right)^\top \mathbf{J}^{-1}\hat{\mathbf{y}} \tag{4.44}$$

which will have the effect of eliminating the sign indefinite term on $\tilde{c}$ from the Lyapunov function derivative. Finally, let the control signal be determined through

$$\begin{aligned}\mathbf{u} = -\frac{1}{\hat{c}}\hat{\boldsymbol{\Psi}}^\top\Big[&\mathbf{W} + k_v\mathbf{J}\delta\boldsymbol{\omega} + k_p\mathbf{J}\Big(\alpha\delta\mathbf{q}_v + \frac{1}{2}\left[q_0\mathbf{I}_{3\times3} + S(\delta\mathbf{q}_v)\right]\delta\boldsymbol{\omega}\Big)\\ &+ \frac{\mu}{2\hat{c}}\left(1-\tanh^2\hat{\xi}\right)\dot{\hat{\xi}}\,\hat{\boldsymbol{\Psi}}^\top\hat{\mathbf{y}} + \gamma S\left(\bar{\mathbf{y}}\times\hat{\mathbf{y}}\right)\hat{\boldsymbol{\Psi}}^\top\hat{\mathbf{y}}\Big]\end{aligned} \tag{4.45}$$

Note that the feedback terms are slightly different because of the kinematics of the rigid-body attitude problem; however, the terms related to the estimation which appear in the control are unchanged.

Theorem 4.4.1. *Consider the error system shown in (3.7) and (4.40) with the proper-orthogonal misalignment matrix, $\boldsymbol{\Psi}$, and scaling c unknown. Suppose that the adaptive control torque $\mathbf{u}$ is determined through (4.45) with the update law on $\hat{\boldsymbol{\Psi}}$ of (4.12), the update law on $\hat{\xi}$ of (4.44), and the filter definitions of (4.41) and (3.15) with arbitrary initial conditions $\mathbf{g}_f(0)$ and $\mathbf{e}_{2,f}(0)$. Choose the control gains subject to the condition $\alpha = k_p + k_v$. Then for all possible reference trajectories $\begin{bmatrix}\boldsymbol{\omega}_r(t)^\top & \mathbf{q}_r(t)^\top\end{bmatrix}^\top$, all $\hat{c}(0)$, and all $\hat{\mathbf{q}}_{\boldsymbol{\Psi}}(0)$ such that $\mathbf{q}_{\boldsymbol{\Psi}}^\top\hat{\mathbf{q}}_{\boldsymbol{\Psi}} \neq 0$, the closed-loop is asymptotically stable, leading to the convergence condition*

$$\lim_{t\to\infty}\begin{bmatrix}\delta\mathbf{q}_v(t)\\ \delta\boldsymbol{\omega}(t)\end{bmatrix} = \mathbf{0}$$

Proof. The resulting proof is fairly straightforward and follows the development discussed in the previous section. Therefore, the proof is not shown here for reasons of brevity but is available in Appendix A. □

4.5 Numerical Simulations

To demonstrate the performance of the proposed controller with actuator misalignment, a simulation was performed for the rigid-body attitude tracking problem. The inertia and misalignment matrices were chosen as

$$\mathbf{J} = \begin{bmatrix} 20 & 1.2 & 0.9 \\ 1.2 & 17 & 1.4 \\ 0.9 & 1.4 & 15 \end{bmatrix} \qquad \text{and} \qquad \mathbf{\Psi} = \begin{bmatrix} 3/4 & 1/4 & -\sqrt{6}/4 \\ 1/4 & 3/4 & \sqrt{6}/4 \\ \sqrt{6}/4 & -\sqrt{6}/4 & 1/2 \end{bmatrix}$$

which corresponds to a rotation of 60° about the vector $\begin{bmatrix} \sqrt{2}/2 & \sqrt{2}/2 & 0 \end{bmatrix}^\top$. The unknown scaling was chosen as $c = 9.8$ to simulate a gravity-constant error with known bounds 0.1 and 12 for c_{min} and c_{max}, respectively. Furthermore, the commanded attitude reference trajectory is given as

$$\boldsymbol{\omega}_r(t) = \left[0.3\cos t \left(1 - e^{-0.01t^2}\right) + (0.08\pi + 0.006\sin t)\, te^{-0.01t^2}\right] \cdot \begin{bmatrix} 1 & 1 & 1 \end{bmatrix}^\top$$
$$\mathbf{q}_r(t) = \begin{bmatrix} 1 & 0 & 0 & 0 \end{bmatrix}^\top$$

where $\boldsymbol{\omega}_r$ is the reference angular velocity and $\mathbf{q}_r$ is the reference attitude relative to the inertial frame. The initial conditions for the spacecraft are $\boldsymbol{\omega}(0) = \begin{bmatrix} 0.4 & 0.2 & -0.3 \end{bmatrix}^\top$ and $\mathbf{q}(0) = \begin{bmatrix} (2\sqrt{2})/3 & 1/(3\sqrt{3}) & 1/(3\sqrt{3}) & 1/(3\sqrt{3}) \end{bmatrix}^\top$. The initial estimate, $\hat{\mathbf{\Psi}}$, was set to $\mathbf{I}_{3\times 3}$, and the initial estimate was $\hat{c} = 1$.

A simulation was performed using the control method from Section 4.4 with the control parameters $k_p = k_v = 0.4$, $\gamma = 0.05$ and $\lambda = 30$. The simulation was run for 200 seconds to examine the steady state behavior and allow for convergence of the unknown parameters. In addition to establish a benchmark for the situation of perfectly determined actuator misalignment parameters and scale factors, we also simulated a second control law given by

$$\mathbf{u}_2 = -\frac{1}{c}\mathbf{\Psi}^\top \left[\mathbf{W} + k_v \mathbf{J}\delta\boldsymbol{\omega} + k_p \mathbf{J}\left(\beta\delta\mathbf{q}_v + \frac{1}{2}\left[q_0\mathbf{I}_{3\times 3} + S(\delta\mathbf{q}_v)\right]\delta\boldsymbol{\omega}\right)\right] \tag{4.46}$$

This particular control law is a standard choice [6, 20] that ensures asymptotic tracking for all prescribed reference trajectories. No formal proof is given in the interest of brevity. As can be seen in Figure 4.1, the proposed controller provides convergence of the attitude and velocity errors to zero for the unknown misalignment. Both

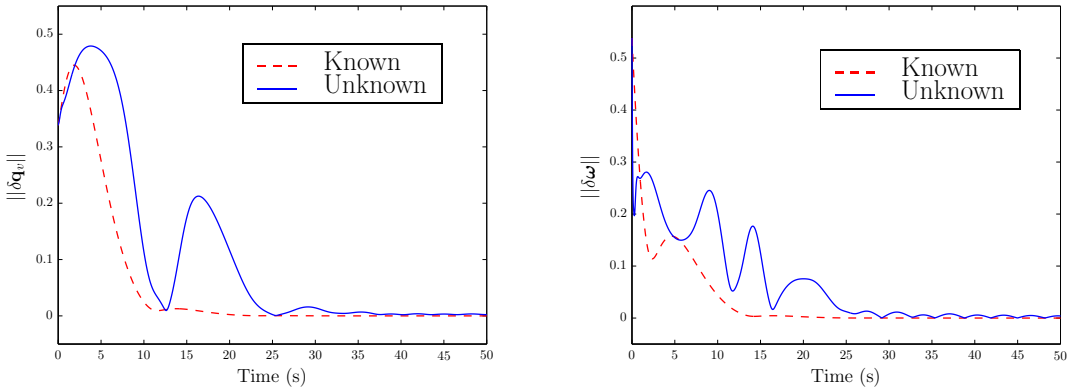

(a) Quaternion attitude error

(b) Angular velocity error

Figure 4.1: Simulation results using the controller from (4.45) compared with those from the known parameter controller in (4.46). The quaternion attitude and angular velocity errors converge to zero despite the presence of the unknown actuator misalignment

the quaternion attitude error and angular velocity error converge as expected. In general, the simulation with known controller converges quicker than with unknown parameter controller and does not have the oscillations associated with estimating the unknown terms. The magnitude of the controller effort for the known and unknown cases is shown in Figure 4.2. For the unknown case, the initial required control effort is rather large when compared to the steady state value. The increased magnitude occurs due to the poor guess of the spacecraft's misalignment matrix. As the simulation reaches steady state, the magnitude for the unknown case approaches the known case. Finally, we examine the behavior of the parameter estimation for the unknown misalignment simulation. The behavior of $\mathbf{z}_v$, the vector part of the quaternion that parameterizes $\boldsymbol{\Psi}^\top \hat{\boldsymbol{\Psi}}$ is shown in Figure 4.3(a). Although convergence of the estimate of $\boldsymbol{\Psi}$ cannot be guaranteed in general, in this case, we are able to converge to the true parameter values since the commanded reference trajectory causes $\mathbf{u}_f$ to be a periodic signal in the steady-state. We see similar convergence for the scaling parameter $\hat{c}$ in Figure 4.3(b). During the transient, the parameter estimate is more active, but once the attitude and velocity errors approach zero, the rate of convergence decreases. It is reiterated that even though the parameters converged, it is not a requirement in

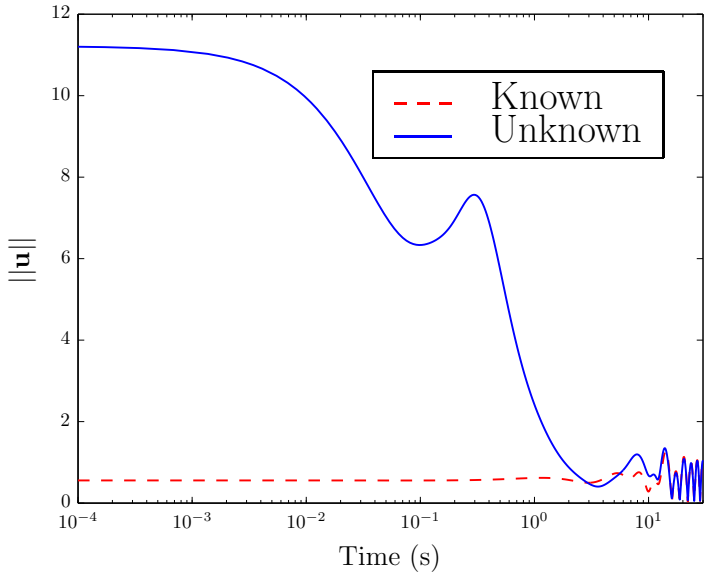

Figure 4.2: Simulation results for the norm of the control effort using the controller from (4.45) compared with those from the known parameter controller in (4.46). When $\boldsymbol{\Psi}$ is unknown, the initial guess of $\hat{\boldsymbol{\Psi}}$ can lead to a potentially large initial control effort; however, the unknown simulation effort eventually reduces to the known simulation effort

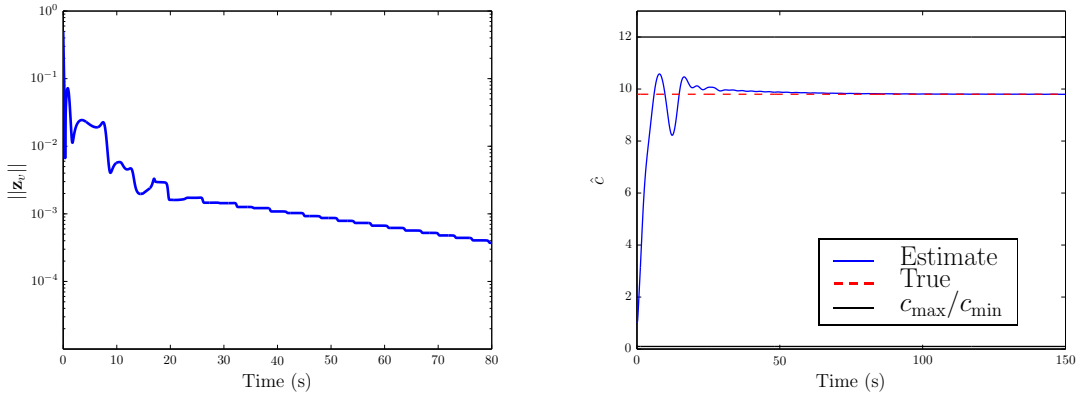

(a) Rotation Error, z_v

(b) Estimate of c

Figure 4.3: Simulation results for the unknown parameter estimates. In both cases the estimates converge to the true values

order to meet the control objectives.

4.6 Concluding Remarks

This chapter presents the problem of controlling a system with an unknown proper orthogonal matrix acting as an actuator misalignment. In addition, an unknown scaling is introduced which causes the uncertainty on the control to be non-affine in the parameters. The control problem requires the use of filters in order to recover the measurement equation needed to estimate the unknown rotation matrix. This estimation can be performed through a standard update law whether the unknown scaling is present or not. When the scaling is present, it acts as an additional gain which will either increase or decrease the rate of convergence. The use of the nonlinear update law guarantees that estimate of the rotation matrix remains in $SO(3)$ for all time and ensures that the estimate is always invertible and does not create any issues in the control problem. The estimation of the scaling can be approached through the measurement equation as was seen in Section 4.2 or by using the information available from the system dynamics in the control problem as was seen in Section 4.3. The addition of the scaling to the control problem requires that a projection scheme be used to avoid the estimate passing through zero and causing the control to become unbounded. The design of the controller through the filter dynamics completes the control method and guarantees convergence of the tracking errors for all but a mild set of constraints for both the standard system as well as the rigid-body attitude tracking problem. The convergence of the estimation errors requires persistence of excitation on the measurement equation input. In the control problem, this condition manifests itself as a richness requirement on the reference trajectory. Regardless of the behavior of the estimation error, the control objectives are always met.

Chapter 5

Independent Two-Axis, In-Plane Misalignments

In this chapter, the problem of determining unknown actuator misalignments is extended to a more general class of misalignments. From a practical standpoint, the actuation system would not be a rigid body. Accordingly, the actuator system would not be rotated equally across all three axes. Generally, the system would be designed to give independent control across all three of the body axes; therefore, it is more realistic to examine misalignments where the uncertainty appears independently across each of the three axes. As a beginning step, the problem of independent misalignments across two axes is studied. Moreover, it is assumed that the misalignments are in-plane. * In general, each misalignment is a vector which has been rotated from an ideal position to the misalignment position. Unfortunately, the minimal set of parameters to represent a rotation is three; however, if the problem is reformulated as simply estimating an unknown unit vector, the minimal set can be reduced to two because of the unit-norm constraint. Thus, each misalignment can be examined through two angles. To make the misalignment physically meaningful, the misalignment can be represented as an in-plane and an out-of-plane angle. This is the reason for the shift away from general rotations.

The problem is always approached in a two-step process. First, determine the specific observer and find for which set of misalignments the estimation process is guaranteed to converge. Second, the observer is combined with a stabilizing controller to ensure trajectory tracking for the standard dynamics of (2.2). As will be seen, this is a fairly straightforward process when the misalignments are restricted to the plane;

*For this particular study, the x and y axes are examined, and in-plane refers to the xy-plane without loss of generality

however, this is not a universal solution as will be highlighted in the proceeding chapter.

The remainder of the chapter is organized as follows. Section 5.1 introduces the problem of two-axis misalignments which are *strictly* in-plane. Section 5.2 shows the results for a certainty-equivalence like observer where region of attraction arguments are used to guarantee stability. In addition, the results for the control problem are shown. Section 5.3 investigates the same problem but adds a projection scheme to the misalignment estimation to expand the set of possible misalignments. Section 5.4 introduces the problem of two-axis misalignments where both axes have in-plane misalignments, but one axis also has an out-of-plane misalignment. Section 5.5 shows the stability analysis for both the estimation and control problems. Section 5.6 highlights the performance of the proposed methods through numerical simulations. Finally, Section 5.7 discusses some concluding remarks.

5.1 Strictly In-Plane Misalignment Problem

In general, the problem of estimating $\mathbf{\Psi}$ from the measurement equation of (2.1) is still valid. In the previous chapter, $\mathbf{\Psi}$ was restricted to be a special orthogonal matrix. From now on, $\mathbf{\Psi}$ is restricted to the class of matrices where each of the columns is a unit vector. Note that a rotation matrix falls into this class of matrices, but rotation matrices are also such that $\mathbf{\Psi}^\top \mathbf{\Psi} = \mathbf{\Psi}\mathbf{\Psi}^\top = \mathbf{I}$. Thus, the structure of $\mathbf{\Psi}$ in three dimensions is such that

$$\mathbf{\Psi} = \begin{bmatrix} \mathbf{\Psi}_A & \mathbf{\Psi}_B & \mathbf{\Psi}_C \end{bmatrix} \tag{5.1}$$

where $\mathbf{\Psi}_* \in \mathbb{R}^3$ and $||\mathbf{\Psi}_*|| = 1$ with $* = A, B, C$. Thus, each column of $\mathbf{\Psi}$ is a unit-vector which acts on each of the control directions independently. For the remainder of the dissertation, the subscripts A, B, and C will refer to the misalignment in the x, y, and z directions. For the strictly in-plane problem, the columns of $\mathbf{\Psi}$ are given by

$$\mathbf{\Psi}_A = \begin{bmatrix} \cos\theta_A \\ \sin\theta_A \\ 0 \end{bmatrix} \qquad \mathbf{\Psi}_B = \begin{bmatrix} -\sin\theta_B \\ \cos\theta_B \\ 0 \end{bmatrix} \qquad \mathbf{\Psi}_C = \begin{bmatrix} 0 \\ 0 \\ 1 \end{bmatrix} \tag{5.2}$$

where the misalignment on the x and y axes can be parameterized through the angles θ_A and θ_B, respectively. The z-axis is assumed to be ideal. This scenario is represented graphically in Figure 5.1. Since the control axes are no longer orthogonal, there is a

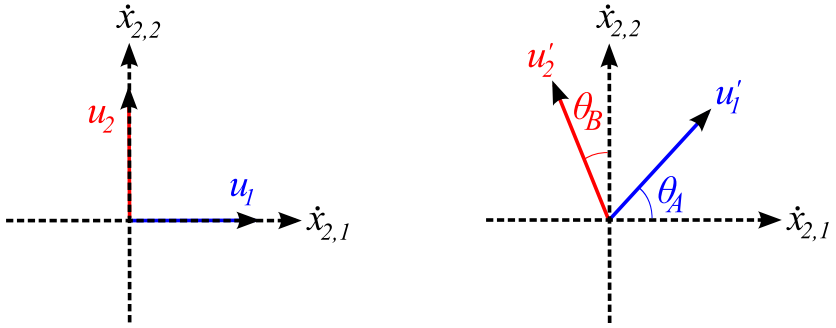

(a) $\mathbf{\Psi}_{xy} = \mathbf{I}_{2\times 2}$ (b) $\mathbf{\Psi}_{xy} \neq \mathbf{I}_{2\times 2}$

Figure 5.1: Graphical representation of the effect of $\mathbf{\Psi}$ on the independent control axes wherein misalignments are restricted to be inside the xy-plane. Notice that there is a cross-coupling that occurs, and the control axes are non-orthogonal

cross-coupling that will occur in the control problem. As the control axes becomes closer together, it can be increasingly difficult to control the system. Recall from the filter design process that to eliminate the misalignment from the system, the control of (2.23) includes the term $\hat{\mathbf{\Psi}}^{-1}$ which requires that $\hat{\mathbf{\Psi}}$ be non-singular. Using the representation of $\mathbf{\Psi}$ in (5.2) the determinant of $\hat{\mathbf{\Psi}}$ can be determined as $\cos(\hat{\theta}_A - \hat{\theta}_B)$. The determinant clearly becomes zero when $\hat{\theta}_A - \hat{\theta}_B = \pm\pi/2$. This same condition is manifested as the x and y control axes being in the same direction; that is, there is no difference in the control applied through the x and y directions. This condition will appear several times in the proceeding analysis and always must be considered to ensure boundedness of the control signal.

5.2 Observer/Controller without Parameter Projection

In this section, an adaptive control method is introduced for the tracking error problem when the actuator misalignment is restricted to the xy-plane, and parameter projection is not used to bound the estimates.

5.2.1 Estimation Problem

To begin, consider the standard estimation problem of (2.1)

$$\mathbf{y} = \mathbf{\Psi}\mathbf{u}_f$$

where $\mathbf{u}_f$ is a known input, $\mathbf{y}$ is the measured output, and $\mathbf{\Psi}$ is as stated in (5.1) and (5.2). If $\mathbf{u}_f$ is written as $\mathbf{u}_f = \begin{bmatrix} u_{f,A} & u_{f,B} & u_{f,C} \end{bmatrix}^\top$, then $\mathbf{y}$ can be represented as

$$\mathbf{y} = \mathbf{\Psi}_A \, u_{f,A} + \mathbf{\Psi}_B \, u_{f,B} + \mathbf{\Psi}_C \, u_{f,C} \tag{5.3a}$$

$$\mathbf{y} = \quad \mathbf{y}_A \quad + \quad \mathbf{y}_B \quad + \quad \mathbf{y}_C \tag{5.3b}$$

Next, update laws for the estimates of $\hat{\mathbf{\Psi}}_A$ and $\hat{\mathbf{\Psi}}_B$ need to be developed which will ultimately be update laws on $\hat{\theta}_A$ and $\hat{\theta}_B$. Note that $\mathbf{\Psi}_C$ is known in this case and does not require an estimate. Define the estimate of $\mathbf{y}$ to be

$$\hat{\mathbf{y}} \equiv \hat{\mathbf{\Psi}}\mathbf{u}_f \tag{5.4}$$

which can be written as

$$\hat{\mathbf{y}} = \hat{\mathbf{\Psi}}_A \, u_{f,A} + \hat{\mathbf{\Psi}}_B \, u_{f,B} + \mathbf{\Psi}_C \, u_{f,C} \tag{5.5a}$$

$$\hat{\mathbf{y}} = \quad \hat{\mathbf{y}}_A \quad + \quad \hat{\mathbf{y}}_B \quad + \quad \mathbf{y}_C \tag{5.5b}$$

where $\hat{\mathbf{\Psi}}_A, \hat{\mathbf{\Psi}}_B \in \mathbb{R}^3$ are unit vectors given by

$$\hat{\mathbf{\Psi}}_A = \begin{bmatrix} \cos\hat{\theta}_A \\ \sin\hat{\theta}_A \\ 0 \end{bmatrix} \qquad \hat{\mathbf{\Psi}}_B = \begin{bmatrix} -\sin\hat{\theta}_B \\ \cos\hat{\theta}_B \\ 0 \end{bmatrix} \tag{5.6}$$

If one of these two misalignments were perfectly known (e.g. B), an update law of the form

$$\begin{aligned} \dot{\hat{\mathbf{\Psi}}}_A &= -S\left[(\mathbf{y} - \mathbf{y}_B - \mathbf{y}_C) \times \hat{\mathbf{y}}_A\right] \hat{\mathbf{\Psi}}_A \\ &= -S\left(\mathbf{y}_A \times \hat{\mathbf{y}}_A\right) \hat{\mathbf{\Psi}}_A \end{aligned} \tag{5.7}$$

can be used which is motivated by the observer for an unknown proper orthogonal matrix as stated in (2.12). Note that in this case that $\hat{\mathbf{\Psi}}_A$ is a unit vector and not an

orthogonal matrix but convergence to the true value $\mathbf{\Psi}_A$ is guaranteed for all initial conditions modulo a set of negligible measure. [†] Furthermore, the particular form of the update law given in (5.7) assures that the estimate will remain a unit-vector for all time provided that the initial estimate is a unit-vector. Motivated by these insights, certainty-equivalence like update laws are proposed as

$$\dot{\hat{\mathbf{\Psi}}}_A = -\gamma S\left[(\mathbf{y} - \hat{\mathbf{y}}_B - \mathbf{y}_C) \times \hat{\mathbf{y}}_A\right] \hat{\mathbf{\Psi}}_A \tag{5.8a}$$

$$\dot{\hat{\mathbf{\Psi}}}_B = -\gamma S\left[(\mathbf{y} - \hat{\mathbf{y}}_A - \mathbf{y}_C) \times \hat{\mathbf{y}}_B\right] \hat{\mathbf{\Psi}}_B \tag{5.8b}$$

where the learning rate parameter $\gamma > 0$ is a scalar constant. Note that if $\hat{\mathbf{y}}_A$ and $\hat{\mathbf{y}}_B$ converge to their true values, i.e., if we have that $(\mathbf{y} - \hat{\mathbf{y}}_B - \mathbf{y}_C) \to \mathbf{y}_A$ and $(\mathbf{y} - \hat{\mathbf{y}}_A - \mathbf{y}_C) \to \mathbf{y}_B$, the desired form for convergence is recovered as in (5.7). Note also that (5.8) can be algebraically manipulated yielding convenient updates laws on the angles $\hat{\theta}_A$ and $\hat{\theta}_B$ given by

$$\dot{\hat{\theta}}_A = \gamma\left[\hat{\mathbf{y}}_{A,1}\left(\mathbf{y} - \hat{\mathbf{y}}_B - \mathbf{y}_C\right)_2 - \left(\mathbf{y} - \hat{\mathbf{y}}_B - \mathbf{y}_C\right)_1 \hat{\mathbf{y}}_{A,2}\right] \tag{5.9a}$$

$$\dot{\hat{\theta}}_B = \gamma\left[\hat{\mathbf{y}}_{B,1}\left(\mathbf{y} - \hat{\mathbf{y}}_A - \mathbf{y}_C\right)_2 - \left(\mathbf{y} - \hat{\mathbf{y}}_A - \mathbf{y}_C\right)_1 \hat{\mathbf{y}}_{B,2}\right] \tag{5.9b}$$

It is important to recognize here that all the signals that appear are available, and thus, the observer is implementable.

Theorem 5.2.1. *Assume that the components of $\mathbf{u}_f$ are such that $u_{f,A}$, $u_{f,B}$ and $u_{f,C}$ and their respective derivatives are bounded. Suppose also that $u_{f,A}$ and $u_{f,B}$ are PE signals and thus cannot remain indefinitely at zero. Then, given the measurement relation of (5.3) together with the update laws of (5.9), the estimation scheme guarantees that $\hat{\theta}_A \to \theta_A$ and $\hat{\theta}_B \to \theta_B$ as $t \to \infty$ provided that $|\theta_A|, |\theta_B| < \pi/8$ and $\hat{\theta}_A(0) = \hat{\theta}_B(0) = 0$.*

Proof. Define the parameter error in θ_* as

$$\tilde{\theta}_* \equiv \hat{\theta}_* - \theta_* \tag{5.10}$$

[†]Recall that the columns of a rotation matrix are unit vectors. Therefore, the stability analysis for the rotation matrix could have focused on convergence of each of the columns of the matrix and reached the same conclusion

for $* = A, B$. Using (5.3)-(5.6), the update laws on $\hat{\theta}_*$ of (5.9) can be re-written as

$$\dot{\tilde{\theta}}_A = \dot{\hat{\theta}}_A = -\gamma \sin\tilde{\theta}_A \, u_{f,A}^2 - \gamma\sigma_A \sin\tilde{\theta}_B \, u_{f,A} \, u_{f,B} \tag{5.11a}$$

$$\dot{\tilde{\theta}}_B = \dot{\hat{\theta}}_B = -\gamma \sin\tilde{\theta}_B \, u_{f,B}^2 - \gamma\sigma_B \sin\tilde{\theta}_A \, u_{f,A} \, u_{f,B} \tag{5.11b}$$

where

$$\sigma_A = \frac{\sin\left[\frac{1}{2}\left(\hat{\theta}_A - \hat{\theta}_B\right) + \frac{1}{2}\left(\hat{\theta}_A - \theta_B\right)\right]}{\cos\left(\frac{1}{2}\tilde{\theta}_B\right)} \tag{5.12a}$$

$$\sigma_B = \frac{\sin\left[\frac{1}{2}\left(\hat{\theta}_A - \hat{\theta}_B\right) + \frac{1}{2}\left(\theta_A - \hat{\theta}_B\right)\right]}{\cos\left(\frac{1}{2}\tilde{\theta}_A\right)} \tag{5.12b}$$

Next, define a scalar variable η such that

$$\eta = |\sigma_A + \sigma_B| \tag{5.13}$$

It will become necessary that η be less than two in order to use completion of squares to dominate the sign indefinite term in the upcoming stability analysis. A simple calculation shows that $\eta = 2$ when $\hat{\theta}_A - \hat{\theta}_B = \pm\pi/2$. In the $\hat{\theta}_A\hat{\theta}_B$ plane, these are the two lines $\hat{\theta}_B = \hat{\theta}_A \pm \pi/2$. This is verified by plotting the contour of η at 2 as can be seen in Figure 5.2. Of particular importance is that these two lines are fixed regardless of the true misalignments. Clearly there are additional parts to the contour that appear near the corners of Figure 5.2. This part of the contour changes based on the values of the true misalignments; however, these parts are either outside the fixed lines or coincide with very large values for the estimates (e.g. $|\hat{\theta}_A|, |\hat{\theta}_B| > \pi/2$) which is considered outside the region of interest of $(-\pi/4, \pi/4)$. Thus, the remainder of the contour does not contribute to region of attraction analysis and is ignored. The region of attraction is then entirely determined by the fixed lines $\hat{\theta}_B = \hat{\theta}_A \pm \pi/2$. Perhaps the most interesting aspect of these two lines is that they coincide with the singularity condition of the control problem. Therefore, proving stability for the estimation scheme here will automatically contain the estimates for the control problem and avoid the singularity condition. In any case, this information on η will

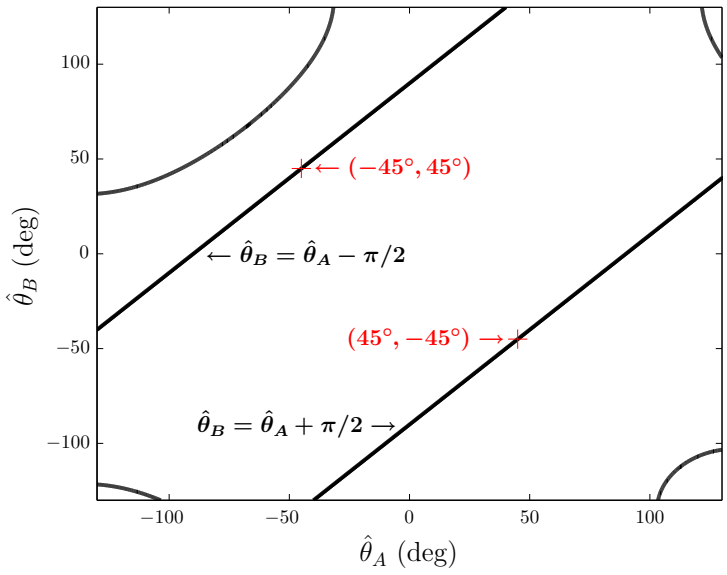

Figure 5.2: Plot of the $\eta = 2$ contour. The important part to notice is that the fixed lines $\hat{\theta}_B = \hat{\theta}_A \pm \pi/2$ are the boundaries for $\eta < 2$.

be used momentarily to show a region of attraction for this problem. Along with η, define the scalar value β as

$$\beta \equiv \frac{1}{2}\left(1 - \frac{\eta^2}{4}\right) \tag{5.14}$$

Note that if $\eta < 2$, β is strictly positive. Finally, let the signal $\mathbf{z}_n$ be defined as

$$\mathbf{z}_n(\tilde{\theta}) = \begin{bmatrix} \sin\left(n\tilde{\theta}_A\right) u_{f,A} \\ \sin\left(n\tilde{\theta}_B\right) u_{f,B} \\ 0 \end{bmatrix} \tag{5.15}$$

where n is any non-zero scalar value. In the case that $n = 1$, $\mathbf{z}_1$ is represented as simply $\mathbf{z}$.

Consider the Lyapunov-like function

$$V_E = 2\sin^2\left(\frac{1}{2}\tilde{\theta}_A\right) + 2\sin^2\left(\frac{1}{2}\tilde{\theta}_B\right) \geq 0 \tag{5.16}$$

The subscript E indicates the estimation problem under consideration here. Consider bounding θ_A and θ_B such that $|\theta_A|, |\theta_B| < \theta_P$ for some $0 < \theta_P \leq \pi/4$ and assume that the initial guess of the estimates is $\hat{\theta}_A(0) = \hat{\theta}_B(0) = 0$. Since there is no a

priori information available on the misalignments, it is logical to start the estimation process as if there is no misalignment. Thus, $|\tilde{\theta}_A(0)|, |\tilde{\theta}_B(0)| < \theta_P$ would make $V_E(0) < 4\sin^2(\theta_P/2)$. If the derivative of V_E is such that $\dot{V}_E$ is negative semi-definite, then V_E is non-increasing and is a level curve that the estimates may not pass through. As mentioned, the derivative of V_E will be shown to be negative semi-definite provided that $\eta < 2$. Therefore, the largest level curve such that $\eta < 2$ defines a region of attraction for this problem. The region of attraction can be found by solving a constrained optimization problem. Specifically, the problem is to maximize $V_E(0)$ subject to the constraints that $\hat{\theta}_A - \pi/2 \leq \hat{\theta}_B \leq \hat{\theta}_A + \pi/2$ and $V_E \leq V_E(0)$. The solution to this optimization problem is $\theta_P = \pi/8$. This result is confirmed by plotting a set of level curves as can be seen in Figure 5.3. Thus, $\theta_P = \pi/8$ is the level curve the

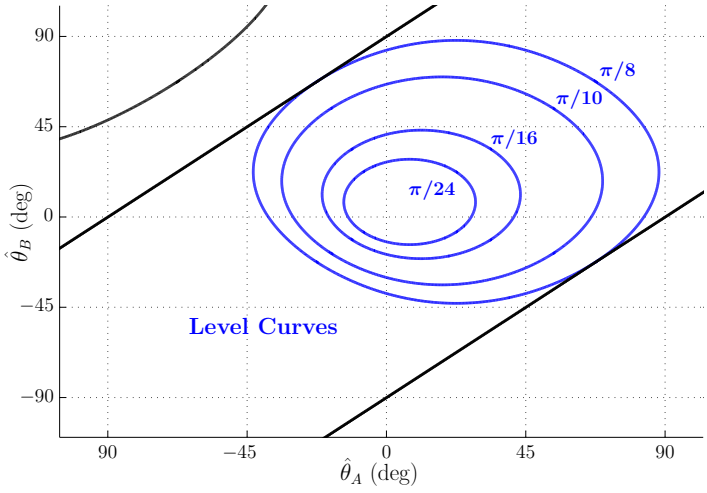

Figure 5.3: Plot of the level curves associated with the strictly in-plane misalignment problem for increasing values of the misalignment. $\theta_P = \pi/8$ is the last contour which does not cross the $\eta = 2$ contour.

meets the $\eta = 2$ contour at only one point (on each side). Consequently, if $\theta_P < \pi/8$, it is guaranteed that $\eta < 2$. The last step to be shown is that the Lyapunov derivative is negative semi-definite for the stated conditions. This can be done by taking the time derivative of (5.16) which yields

$$\dot{V}_E = \sin\tilde{\theta}_A\dot{\hat{\theta}}_A + \sin\tilde{\theta}_B\dot{\hat{\theta}}_B$$

Substituting the $\hat{\theta}_*$ update laws of (5.11)

$$\begin{aligned}
\dot{V}_E &= -\gamma \sin^2 \tilde{\theta}_A \, u_{f,A}^2 - \gamma \sin^2 \tilde{\theta}_B \, u_{f,B}^2 \\
&\quad - \gamma \left(\sigma_A \sin \tilde{\theta}_A \, \sin \tilde{\theta}_B + \sigma_B \sin \tilde{\theta}_B \, \sin \tilde{\theta}_A \right) u_{f,A} \, u_{f,B} \\
&\leq -\gamma |\sin \tilde{\theta}_A \, u_{f,A}|^2 - \gamma |\sin \tilde{\theta}_B \, u_{f,B}|^2 + \gamma |\sigma_A + \sigma_B| \, |\sin \tilde{\theta}_A \, u_{f,A}| \, |\sin \tilde{\theta}_B \, u_{f,B}| \\
&\leq -\gamma |\sin \tilde{\theta}_A \, u_{f,A}|^2 - \gamma |\sin \tilde{\theta}_B u_{f,B}|^2 + \gamma\eta \, |\sin \tilde{\theta}_A \, u_{f,A}| \, |\sin \tilde{\theta}_B \, u_{f,B}|
\end{aligned}$$

From the structure, completion of squares is attempted to dominate the cross-term. This action requires that η be less than 2 which is guaranteed given the conditions discussed previously.

$$\begin{aligned}
\dot{V}_E \leq \gamma \Bigg(& -\beta |\sin \tilde{\theta}_A u_{f,A}|^2 - \left[1 - \frac{\eta^2}{4\,(1-\beta)} \right] |\sin \tilde{\theta}_B u_{f,B}|^2 \\
& - (1-\beta) \left[|\sin \tilde{\theta}_A u_{f,A}| - \frac{\eta}{2\,(1-\beta)} |\sin \tilde{\theta}_B u_{f,B}| \right]^2 \Bigg)
\end{aligned}$$

From the completion of squares, the constants on the quadratic terms in $\sin^2 \tilde{\theta}_A$ and $\sin^2 \tilde{\theta}_B$ must be less than zero. The first condition requires $\beta > 0$ while the second condition results in our choice of β in (5.14).

$$\begin{aligned}
\dot{V}_E &\leq -\gamma\beta \left(|\sin \tilde{\theta}_A u_{f,A}|^2 + |\sin \tilde{\theta}_B u_{f,B}|^2 \right) \\
&\leq -\gamma\beta ||\mathbf{z}(\tilde{\theta})||^2 \leq 0
\end{aligned} \tag{5.17}$$

Thus, $\dot{V}_E$ is negative semi-definite, indicating boundedness for all closed-loop signals. Further, because V_E is lower-bounded, $\int_0^\infty \dot{V}_E(t)\, dt$ exists and is finite which taken together with (5.17) implies that $\mathbf{z}(\tilde{\theta}) \in \mathcal{L}_2 \cap \mathcal{L}_\infty$. Examining $\dot{\mathbf{z}}$ indicates that boundedness of $\dot{\mathbf{z}}$ is only dependent on boundedness of $\dot{\tilde{\theta}}_A$ and $\dot{\tilde{\theta}}_B$ (as all other values are bounded by definition). From (5.9), it is clear that $\dot{\tilde{\theta}}_A, \dot{\tilde{\theta}}_B \in \mathcal{L}_\infty$ which implies $\dot{\mathbf{z}} \in \mathcal{L}_\infty$. Therefore, invoking Barbalat's Lemma yields

$$\lim_{t \to \infty} \mathbf{z}(t) = \mathbf{0}$$

Since the components $u_{f,A}$ and $u_{f,B}$ are persistently exciting, this implies that

$$\lim_{t \to \infty} \begin{bmatrix} \sin \tilde{\theta}_A \\ \sin \tilde{\theta}_B \end{bmatrix} = \mathbf{0}$$

which considering the definitions on $\tilde{\theta}_*$ implies

$$\lim_{t\to\infty} \begin{bmatrix} \tilde{\theta}_A \\ \tilde{\theta}_B \end{bmatrix} = \begin{bmatrix} \hat{\theta}_A - \theta_A \\ \hat{\theta}_B - \theta_B \end{bmatrix} = \mathbf{0}$$

and the proof is complete. □

5.2.1.1 Remarks

a) A direct consequence of the convergence of $\hat{\theta}_A$ and $\hat{\theta}_B$ to their respective true values is the convergence of $\hat{\mathbf{\Psi}}$ to $\mathbf{\Psi}$. This is necessary to eventually eliminate the misalignment from the control problem.

b) The main restriction in this result is that the unknown axes misalignments must be no greater than $\pi/8$ to ensure that their time-varying adaptive estimates are such that $\hat{\theta}_A - \hat{\theta}_B < \pi/2$. Although this was just shown to ensure that the initial estimates are in an invariant set, it is also necessary to restrict the estimates to this region for the control problem so as to ensure non-singularity for the $\hat{\mathbf{\Psi}}$ matrix. Further, this result occurs naturally without any need for additional projection mechanisms to contain the estimates although, as will be shown, the region of allowable misalignments can be increased through projection

c) Although it was not necessary, the proof of convergence of the observer in the estimation problem was shown for completeness. The convergence of the estimator will not directly effect convergence in the control problem although part of the preceding Lyapunov-like analysis will again be useful. An interesting side note to convergence in the estimation problem is that when $\mathbf{u}_f$ is constant and non-zero, there exist multiple equilibria where $\hat{\mathbf{y}} = \mathbf{y}$ but $\hat{\theta}_* \neq \theta_*$. This amounts to a different misalignment that has the same "net effect" on the dynamics. When $\mathbf{u}_f$ is not constant with time, the only equilibria are solutions to $\sin\tilde{\theta}_* = 0$ which are equivalent. In either case, the bounding of the estimates eliminates convergence to any of the other equilibria when the inputs are non-zero constants with time.

5.2.2 Control Problem

Now consider the control problem for the error system of (2.4) and attempt to determine a control law to perform perfect tracking. Assuming use of the filtered signals on $\mathbf{e}_2$ and $\mathbf{g}$ as shown in (2.19a) and (2.19b) and defining $\mathbf{y}$ as

$$\mathbf{y} \equiv \dot{\mathbf{e}}_{2,f} - \mathbf{g}_f \tag{5.18}$$

let the control $\mathbf{u}$ be determined through

$$\mathbf{u} = -\hat{\mathbf{\Psi}}^{-1}\left(\mathbf{g} + \alpha\left(k_p\mathbf{e}_1 + \mathbf{e}_2\right) - \begin{bmatrix} -\sin\hat{\theta}_A & -\cos\hat{\theta}_B & 0 \\ \cos\hat{\theta}_A & -\sin\hat{\theta}_B & 0 \\ 0 & 0 & 0 \end{bmatrix}\begin{bmatrix} \dot{\hat{\theta}}_A & 0 & 0 \\ 0 & \dot{\hat{\theta}}_B & 0 \\ 0 & 0 & 0 \end{bmatrix}\hat{\mathbf{\Psi}}^{-1}\hat{\mathbf{y}}\right) \tag{5.19}$$

wherein $k_p, k_v > 0$ are scalar constants. As mentioned previously the control law is dependent on the inverse of $\hat{\mathbf{\Psi}}$. Thus, the estimated misalignment matrix becomes singular when $\hat{\theta}_A - \hat{\theta}_B = \pm\pi/2$. Accordingly, since $-\pi/2 < \hat{\theta}_A - \hat{\theta}_B < \pi/2$ as is guaranteed by observer formulated in the preceding developments, the control signal will be implementable.

Theorem 5.2.2. *Consider the tracking error dynamics of (2.4). Suppose that the adaptive control law is given by (5.19) with the update laws of (5.9). Then the convergence condition*

$$\lim_{t\to\infty}\begin{bmatrix}\mathbf{e}_1(t) \\ \mathbf{e}_2(t)\end{bmatrix} = \mathbf{0}$$

holds for all admissible reference trajectories $\mathbf{r}$ *and initial conditions* $[\mathbf{x}_1(0),\ \mathbf{x}_2(0)]^\top$ *provided that the gain* α *is chosen such that* $\alpha = k_p + k_v$, $|\theta_A|, |\theta_B| < \pi/8$, *and* $\hat{\theta}_A(0) = \hat{\theta}_B(0) = 0$.

Proof. Recall the filter discussion of Section 2.3.2 and that the filtered dynamics of $\mathbf{e}_2$ can be represented as

$$\dot{\mathbf{e}}_{2,f} = \mathbf{g}_f + \mathbf{\Psi}\mathbf{u}_f \tag{5.20}$$

where the standard filter definitions have been used. Next, choose the filtered control signal as

$$\mathbf{u}_f = -\hat{\mathbf{\Psi}}^{-1}\left(\mathbf{g}_f + k_p\mathbf{e}_1 + k_v\mathbf{e}_{2,f}\right) \tag{5.21}$$

Let $\Lambda \in \mathbb{R}^{3\times 3}$ be given by

$$\Lambda = \begin{bmatrix} \sin\left[\frac{1}{2}\left(\theta_A + \hat{\theta}_A\right)\right] & \cos\left[\frac{1}{2}\left(\theta_B + \hat{\theta}_B\right)\right] & 0 \\ -\cos\left[\frac{1}{2}\left(\theta_A + \hat{\theta}_A\right)\right] & \sin\left[\frac{1}{2}\left(\theta_B + \hat{\theta}_B\right)\right] & 0 \\ 0 & 0 & 0 \end{bmatrix} \tag{5.22}$$

Note that the $||\Lambda|| < 1$, since the largest eigenvalue of $\Lambda^\top \Lambda$ is 1. Consider the Lyapunov function on the control terms

$$V_C = \frac{1}{2}\mathbf{e}_1^\top \mathbf{e}_1 + \frac{1}{2}\mathbf{e}_{2,f}^\top \mathbf{e}_{2,f} \geq 0 \tag{5.23}$$

Taking the time derivative of (5.23) yields

$$\begin{aligned}
\dot{V}_C &= \mathbf{e}_1^\top \dot{\mathbf{e}}_1 + \mathbf{e}_{2,f}^\top \dot{\mathbf{e}}_{2,f} \\
&= \alpha \mathbf{e}_1^\top \mathbf{e}_{2,f} + (\mathbf{e}_1 + \mathbf{e}_{2,f})^\top (\mathbf{g}_f + \mathbf{\Psi}\mathbf{u}_f) \\
&= \alpha \mathbf{e}_1^\top \mathbf{e}_{2,f} + (\mathbf{e}_1 + \mathbf{e}_{2,f})^\top \left[\mathbf{g}_f + \hat{\mathbf{\Psi}}\mathbf{u}_f + \left(\mathbf{\Psi} - \hat{\mathbf{\Psi}}\right)\mathbf{u}_f\right] \\
&= \alpha \mathbf{e}_1^\top \mathbf{e}_{2,f} + (\mathbf{e}_1 + \mathbf{e}_{2,f})^\top \left[-k_p \mathbf{e}_1 - k_v \mathbf{e}_{2,f} + \left(\mathbf{\Psi} - \hat{\mathbf{\Psi}}\right)\mathbf{u}_f\right] \\
&= -k_p \mathbf{e}_1^\top \mathbf{e}_1 - k_v \mathbf{e}_{2,f}^\top \mathbf{e}_{2,f} + (\alpha - k_p - k_v)\, \mathbf{e}_1^\top \mathbf{e}_{2,f} + (\mathbf{e}_1 + \mathbf{e}_{2,f})^\top \left(\mathbf{\Psi} - \hat{\mathbf{\Psi}}\right)\mathbf{u}_f \\
&= -k_p ||\mathbf{e}_1||^2 - k_v ||\mathbf{e}_{2,f}||^2 + 2\,(\mathbf{e}_1 + \mathbf{e}_{2,f})^\top \Lambda \mathbf{z}_{1/2}(\tilde{\theta}) \\
&\leq -k_p ||\mathbf{e}_1||^2 - k_v ||\mathbf{e}_{2,f}||^2 + 2||\mathbf{e}_1 + \mathbf{e}_{2,f}||\, ||\Lambda||\, ||\mathbf{z}_{1/2}(\tilde{\theta})|| \\
&\leq -k_p ||\mathbf{e}_1||^2 - k_v ||\mathbf{e}_{2,f}||^2 + 2\sqrt{2}\,(||\mathbf{e}_1|| + ||\mathbf{e}_{2,f}||)\, ||\mathbf{z}(\tilde{\theta})||
\end{aligned} \tag{5.24}$$

where the constraint on α has been used. Additionally, note that $||\mathbf{z}_{1/2}|| \leq ||\mathbf{z}||$ for all $\tilde{\theta}_A, \tilde{\theta}_B < \pi/2$ which is automatically enforced due to the constraint on the estimates.

Consider the joint Lyapunov-like function which combines the estimation and control functions of (5.16) and (5.23)

$$V = V_C + \tau V_E \geq 0 \tag{5.25}$$

where τ is a positive scalar constant. The associated derivative of V comes from (5.17) and (5.24) and can be manipulated using completion of squares to get the result

$$\dot{V} = \dot{V}_C + \tau \dot{V}_E$$

$$
\begin{aligned}
&\leq -k_p||\mathbf{e}_1||^2 - k_v||\mathbf{e}_{2,f}||^2 - \gamma\beta\tau||\mathbf{z}(\tilde{\theta})||^2 + 2\sqrt{2}||\mathbf{e}_1||\,||\mathbf{z}|| + 2\sqrt{2}||\mathbf{e}_{2,f}||\,||\mathbf{z}(\tilde{\theta})|| \\
&\leq -\frac{k_p}{2}||\mathbf{e}_1||^2 - \frac{k_v}{2}||\mathbf{e}_{2,f}||^2 - \gamma\beta\tau\left[1 - \frac{1}{\gamma\beta\tau}\left(\frac{1}{k_p} + \frac{1}{k_v}\right)\right]||\mathbf{z}(\tilde{\theta})||^2 \\
&\quad - \frac{k_p}{2}\left(||\mathbf{e}_1|| - \frac{2\sqrt{2}}{k_p}||\mathbf{z}||\right)^2 - \frac{k_v}{2}\left(||\mathbf{e}_{2,f}|| - \frac{2\sqrt{2}}{k_v}||\mathbf{z}(\tilde{\theta})||\right)^2 \\
&\leq -\frac{k_p}{2}||\mathbf{e}_1||^2 - \frac{k_v}{2}||\mathbf{e}_{2,f}||^2 - k_z||\mathbf{z}(\tilde{\theta})||^2 \leq 0
\end{aligned} \tag{5.26}
$$

where τ has been selected to be large enough to ensure that the estimation error term is negative semi-definite. Note that $k_z > 0$ is a scalar constant whose value depends on the choice of gains. Thus, $\dot{V}$ is negative semi-definite, indicating boundedness for all closed-loop signals. Further, because V is lower-bounded, it is known that $\int_0^\infty \dot{V}(t)\,dt$ exists and is finite which taken together with (5.26) implies that $\mathbf{e}_1, \mathbf{e}_{2,f}, \mathbf{z}(\tilde{\theta}) \in \mathcal{L}_2 \cap \mathcal{L}_\infty$. This also implies that $\dot{\mathbf{e}}_1, \dot{\mathbf{e}}_{2,f} \in \mathcal{L}_\infty$ from (2.4a) and (5.20). Again, it can be shown that $\dot{\mathbf{z}} \in \mathcal{L}_\infty$ as in the estimation result. Therefore, invoking Barbalat's Lemma yields

$$\lim_{t\to\infty}[\mathbf{e}_1 \quad \mathbf{e}_{2,f} \quad \mathbf{z}(t)] = \mathbf{0}$$

By construction of the filter dynamics, $\mathbf{e}_{2,f} \to \mathbf{0}$ implies $\mathbf{e}_2 \to \mathbf{0}$ as $t \to \infty$, and the control objectives are met. The stability analysis reveals that $\mathbf{z}$ also goes to zero asymptotically; however, this does not inherently lead to convergence of the parameter estimates to their true values. Thus, no additional guarantees can be made, and upon recovering the control through $\mathbf{u} = \alpha\mathbf{u}_f + \dot{\mathbf{u}}_f$, the proof is complete. □

5.2.2.1 Remarks

a) The dependence of $\mathbf{z}$ on both the parameter errors and the components of $\mathbf{u}_f$ does not allow for any additional guarantees to be made on parameter convergence. Since $\mathbf{u}_f$ has a physical meaning in this problem, it is certainly possible that $\mathbf{u}_f \to 0$ faster than the parameter errors. A perfect example of this phenomenon occurs in the stabilization problem where $\mathbf{x}_1$ and $\mathbf{x}_2$ converge to zero. In the case of trajectory tracking, $\mathbf{u}_f$ is less likely to go to zero because of the possibility for richness of the reference trajectory $\mathbf{r}$. In the case that signal $\mathbf{g}$ meets necessary PE conditions, it is

then possible that $\tilde{\theta}_A$ and $\tilde{\theta}_B$ converge to zero asymptotically. It is emphasized, however, that convergence of the parameter estimates to the true values is not necessary to meet the control objectives.

b) The leading term in the control law of (5.19) is $\hat{\mathbf{\Psi}}^{-1}$ which attempts to cancel out the $\mathbf{\Psi}$ in the system dynamics. As mentioned, $\hat{\mathbf{\Psi}}^{-1}$ becomes singular when $\cos(\hat{\theta}_A - \hat{\theta}_B) = 0$ which occurs at $\hat{\theta}_A - \hat{\theta}_B = \pi/2$ and $\hat{\theta}_A - \hat{\theta}_B = -\pi/2$. This manifests to the condition that the estimates have the control axes being parallel as is shown in Figure 5.4. Fortunately, convergence of the estimation problem is dependent on the

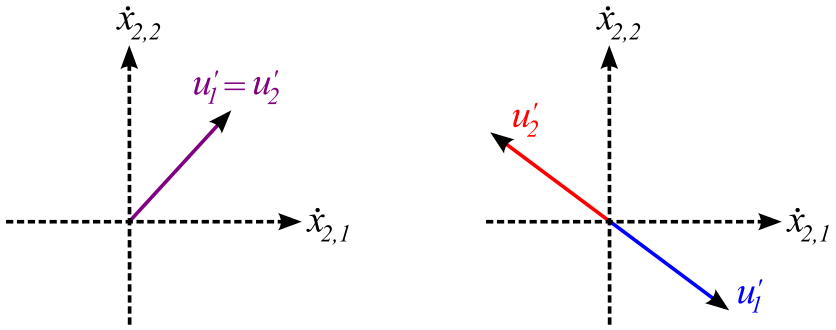

(a) $\hat{\theta}_A - \hat{\theta}_B = \pi/2$ (b) $\hat{\theta}_A - \hat{\theta}_B = 3\pi/2$

Figure 5.4: The two conditions where the control effort will become infinitely large due to the singular condition of $\mathbf{\Psi}$

exact same conditions. Thus, the singularity condition for the control is automatically avoided.

5.3 Observer/Controller with Parameter Projection

In this section, an adaptive control method is introduced for the tracking error problem when the actuator misalignment is restricted to the xy-plane and parameter projection is used to bound the estimates. Note that bounding is not necessary to avoid the singularity condition as mentioned in the previous section; rather, parameter projection can be used in the stability analysis to increase the range of allowable misalignment angles.

5.3.1 Estimation Problem

Consider the exact same estimation problem as the previous section but let the estimates on θ_* be replaced by estimates of the projection variables ξ_* where the two estimates are related through

$$\theta_* = \frac{\mu_*}{2}\left(1 - \tanh \xi_*\right) + \theta_{*,\min} \tag{5.27a}$$

$$\hat{\theta}_* = \frac{\mu_*}{2}\left(1 - \tanh \hat{\xi}_*\right) + \theta_{*,\min} \tag{5.27b}$$

where $* = A, B$ and $\mu_* = \theta_{*,\max} - \theta_{*,\min}$. Furthermore let the update laws on $\hat{\xi}_*$ be determined as

$$\dot{\hat{\xi}}_* = -\dot{\hat{\theta}}_* \tag{5.28}$$

where the update laws on $\hat{\theta}_*$ are consistent with the previous section and are given in (5.9). The following theorem can now be stated:

Theorem 5.3.1. *Assume that the components of $\mathbf{u}_f$ are such that $u_{f,A}$, $u_{f,B}$ and $u_{f,C}$ and their respective derivatives are bounded. Suppose also that $u_{f,A}$ and $u_{f,B}$ are PE signals and thus cannot remain indefinitely at zero. Then, given the measurement relation of (5.3) together with the projection scheme of (5.27) and update laws of (5.28), the estimation scheme guarantees that $\hat{\theta}_A \to \theta_A$ and $\hat{\theta}_B \to \theta_B$ as $t \to \infty$ provided that $|\theta_A|, |\theta_B| < \pi/4$ and $|\hat{\theta}_A(0)|, |\hat{\theta}_B(0)| < \pi/4$.*

Proof. Let the value η_2 be given by

$$\eta_2 = \left| \sqrt{\frac{\tilde{\theta}_A \sin \tilde{\theta}_B}{\tilde{\theta}_B \sin \tilde{\theta}_A}}\, \sigma_A + \sqrt{\frac{\tilde{\theta}_B \sin \tilde{\theta}_A}{\tilde{\theta}_A \sin \tilde{\theta}_B}}\, \sigma_B \right| \tag{5.29}$$

where σ_* is the same as in (5.12). Note that the ratio of $\tilde{\theta}_*/\sin\tilde{\theta}_*$ and $\sin\tilde{\theta}_*/\tilde{\theta}_*$ approaches one as the error goes to zero. Thus, there is only an issue if $\tilde{\theta}_*$ becomes $\pi/2$ which is outside the region being investigated. Let $\theta_A = \theta_B = \theta_P$. Consider the problem of maximizing $J = \theta_P^2$ (i.e. the area of the projection region), subject to the constraints that $\eta_2 \leq 2$, $\hat{\theta}_A \leq \theta_P^2$, and $\hat{\theta}_B \leq \theta_P^2$. Thus, the optimization problem solves for the largest set of misalignments such that $\eta_2 \leq 2$. The solution to this

optimization problem is $\theta_P = \pi/4$ which means that the projected estimates must be bounded within the singularity condition of the control problem. This is confirmed by plotting the contour of $\eta_2 = 2$ and the projection region as can be seen in Figure 5.5. Accordingly, the optimization problem solution demonstrates that if $|\theta_P| < \pi/4$ then

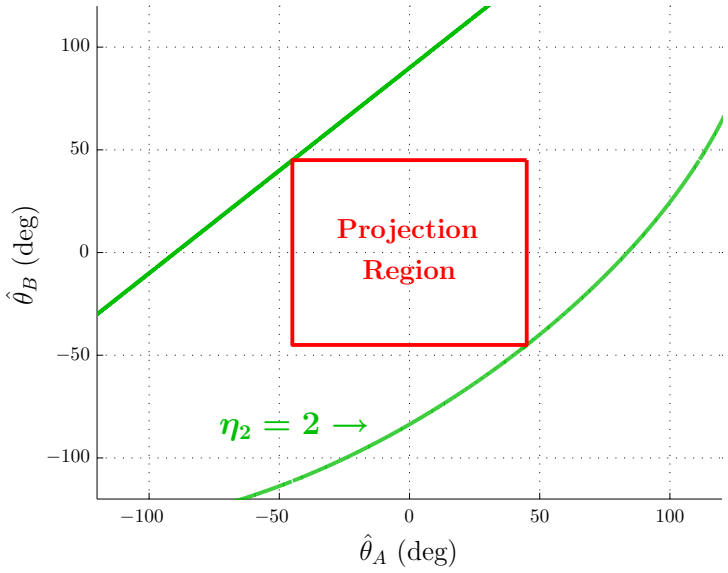

Figure 5.5: Plot of the contour when $\eta_2 = 2$ compared with the projection region for $\theta_P = \pi/4$

$\eta_2 < 2$. Again, this is a necessary condition to prove stability of the observer. Let the scalar value β_2 be defined as

$$\beta_2 = \frac{1}{2}\left(1 - \frac{\eta_2^2}{4}\right) \tag{5.30}$$

Note again that if $\eta_2 < 2$, β_2 is strictly positive.

Consider the Lyapunov-like function

$$V_E = \frac{\mu_A}{2}\left[\log\left(\cosh\hat{\xi}_A\right) - \tilde{\xi}_A \tanh\xi_A\right] + \frac{\mu_B}{2}\left[\log\left(\cosh\hat{\xi}_B\right) - \tilde{\xi}_B \tanh\xi_B\right] \geq 0 \tag{5.31}$$

which is consistent with the smooth projection scheme discussed in Section 2.3.3. Taking the time derivative of (5.31) yields

$$\dot{V}_E = -\tilde{\theta}_A\dot{\hat{\xi}}_A - \tilde{\theta}_B\dot{\hat{\xi}}_B$$

$$
\begin{aligned}
&= \tilde{\theta}_A \dot{\tilde{\theta}}_A + \tilde{\theta}_B \dot{\tilde{\theta}}_B \\
&= -\gamma \tilde{\theta}_A \sin\tilde{\theta}_A \, u_{f,A}^2 - \gamma \tilde{\theta}_B \sin\tilde{\theta}_B \, u_{f,B}^2 - \gamma \left(\sigma_A \tilde{\theta}_A \, \sin\tilde{\theta}_B + \sigma_B \tilde{\theta}_B \, \sin\tilde{\theta}_A \right) u_{f,A} u_{f,B} \\
&= -\gamma \left(\sqrt{\tilde{\theta}_A \sin\tilde{\theta}_A} \, u_{f,A} \right)^2 - \gamma \left(\sqrt{\tilde{\theta}_B \sin\tilde{\theta}_B} \, u_{f,B} \right)^2 \\
&\quad - \gamma \left(\sqrt{\frac{\tilde{\theta}_A \sin\tilde{\theta}_B}{\tilde{\theta}_B \sin\tilde{\theta}_A}} \sigma_A + \sqrt{\frac{\tilde{\theta}_B \sin\tilde{\theta}_A}{\tilde{\theta}_A \sin\tilde{\theta}_B}} \sigma_B \right) \left(\sqrt{\tilde{\theta}_A \sin\tilde{\theta}_A} \, u_{f,A} \right) \left(\sqrt{\tilde{\theta}_B \sin\tilde{\theta}_B} \, u_{f,B} \right) \\
&\leq \gamma \Bigg(- \left(\sqrt{\tilde{\theta}_A \sin\tilde{\theta}_A} \, u_{f,A} \right)^2 - \left(\sqrt{\tilde{\theta}_B \sin\tilde{\theta}_B} \, u_{f,B} \right)^2 \\
&\quad + \eta_2 \left| \sqrt{\tilde{\theta}_A \sin\tilde{\theta}_A} \, u_{f,A} \right| \left| \sqrt{\tilde{\theta}_B \sin\tilde{\theta}_B} \, u_{f,B} \right| \Bigg) \\
&\leq \gamma \Bigg(- \beta_2 \left| \sqrt{\tilde{\theta}_A \sin\tilde{\theta}_A} \, u_{f,A} \right|^2 - \left[1 - \frac{\eta_2^2}{4\,(1-\beta_2)} \right] \left| \sqrt{\tilde{\theta}_B \sin\tilde{\theta}_B} \, u_{f,B} \right|^2 \\
&\quad - (1-\beta_2) \left[\left| \sqrt{\tilde{\theta}_A \sin\tilde{\theta}_A} \, u_{f,A} \right| - \frac{\eta_2}{2\,(1-\beta_2)} \left| \sqrt{\tilde{\theta}_B \sin\tilde{\theta}_B} \, u_{f,B} \right| \right]^2 \Bigg) \\
&\leq -\gamma \beta_2 \left(\left| \sqrt{\tilde{\theta}_A \sin\tilde{\theta}_A} \, u_{f,A} \right|^2 + \left| \sqrt{\tilde{\theta}_B \sin\tilde{\theta}_B} \, u_{f,B} \right|^2 \right) \\
&\leq -\gamma \beta_2 \left(\left| \sin\tilde{\theta}_A u_{f,A} \right|^2 + \left| \sin\tilde{\theta}_B u_{f,B} \right|^2 \right) \\
&\leq -\gamma \beta_2 ||\mathbf{z}(\tilde{\theta})||^2 \leq 0
\end{aligned} \tag{5.32}
$$

where an appropriate choice for β_2 in (5.30) was used. Thus, $\dot{V}_E$ is negative semi-definite, indicating boundedness for all closed-loop signals. Further, because V_E is lower-bounded, $\int_0^\infty \dot{V}_E(t)\, dt$ exists and is finite which taken together with (5.32) implies that $\mathbf{z}(\tilde{\theta}) \in \mathcal{L}_2 \cap \mathcal{L}_\infty$. Examining $\dot{\mathbf{z}}$ indicates that boundedness of $\dot{\mathbf{z}}$ is only dependent on boundedness of $\dot{\tilde{\theta}}_A$ and $\dot{\tilde{\theta}}_B$ (as all other values are bounded by definition). From Eq. (5.9), it is clear that $\dot{\tilde{\theta}}_A, \dot{\tilde{\theta}}_B \in \mathcal{L}_\infty$ which implies $\dot{\mathbf{z}} \in \mathcal{L}_\infty$. Therefore, invoking Barbalat's Lemma yields

$$\lim_{t\to\infty} \mathbf{z}(t) = \mathbf{0}$$

Since the components $u_{f,A}$ and $u_{f,B}$ are not zero for all time, this implies that

$$\lim_{t\to\infty} \begin{bmatrix} \sin\tilde{\theta}_A \\ \sin\tilde{\theta}_B \end{bmatrix} = \mathbf{0}$$

which considering the projection scheme guarantees that

$$\lim_{t\to\infty}\begin{bmatrix}\tilde{\theta}_A\\ \tilde{\theta}_B\end{bmatrix} = \begin{bmatrix}\hat{\theta}_A - \theta_A\\ \hat{\theta}_B - \theta_B\end{bmatrix} = \mathbf{0}$$

and the proof is complete. □

5.3.1.1 Remarks

a) The increase in the region of allowable misalignment angles is a direct result of the projection scheme and the fact that the implemented estimates are not allowed leave the projection region. Comparing η with η_2, it should be clear that for a fixed values of the estimates that $\eta_2 \geq \eta$; however, the range of values that the projection estimates can take is significantly smaller than without projection. Accordingly, θ_P can be increased from $\pi/8$ to $\pi/4$ by including the projection. A comparison of the regions with and without projection is shown in Figure 5.6. The area of the blue

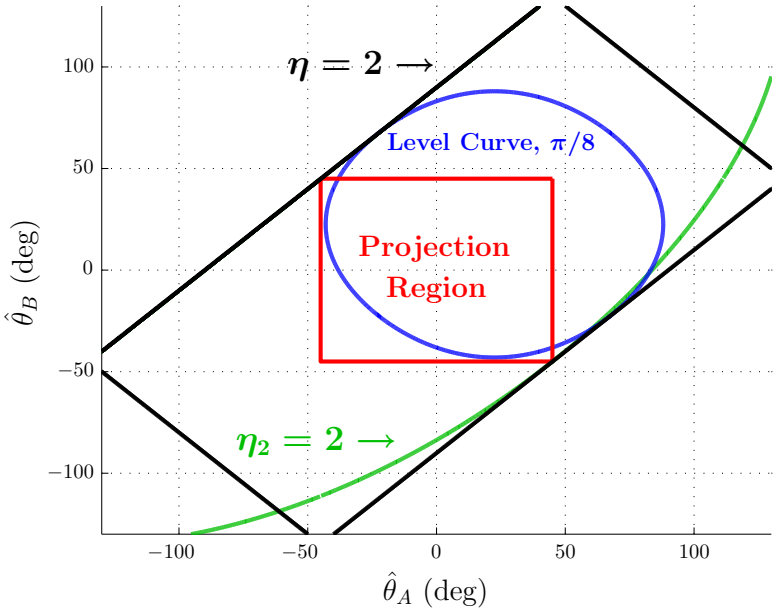

Figure 5.6: Comparison of the bounding region created by projection and the region of attraction without projection

region is actually greater than the red region which means the region of attraction

without projection includes more initial estimates; however, since the true misalignments are unknown, most of these initial guesses would never be used. Although the projection region is smaller by comparison, the shape of the projection region allows for the increase in the magnitude of allowable misalignment to the maximum value of $\pi/4$.

b) The constraint that $\hat{\theta}_A(0) = \hat{\theta}_B(0) = 0$ is noticeably absent from the proof with projection. This occurs because the initial error directly relates to the size of the level curve used to determine the region of attraction. Recall that to establish the region of attraction, the initial errors were taken to be $\tilde{\theta}_A(0) = -\theta_P$ and $\tilde{\theta}_B(0) = -\theta_P$. If an initial guess were made such that the estimate were closer to the true value, that is $-\theta_P < \tilde{\theta}_A(0) < 0$, the initial point would be within the region of attraction, and the solution would converge. On the other hand, if the initial guess increased the initial error (e.g. $\tilde{\theta}_A(0) < -\theta_P$), the size of the level curve would increase, and the initial point could be outside of the region of attraction. Fortunately, the guess of the initial estimates should be no worse than $\hat{\theta}_A(0) = 0$ and $\hat{\theta}_B(0) = 0$ which assumes no knowledge on the misalignments. When projection is included, the initial estimates are only required to lie between $-\theta_P$ and θ_P because the estimates will always remain between the artificial bounds instead of being free to evolve anywhere in the level curve.

c) In practice, the projection bound on the misalignment may need to be kept smaller than just below $\pi/4$ since this will be very close to the singularity condition of the control problem. The only effect will be that the true misalignment must be less than the bounding value (i.e. decreasing the size of allowable misalignments), but there is no effect on the convergence.

5.3.2 Control Problem

The extension to the control problem is practically the same as the previous section. The only slight change occurs because of the use of the projection scheme to update the estimates. Thus, let the control signal be determined as

$$\mathbf{u} = -\hat{\mathbf{\Psi}}^{-1}\left(\mathbf{g} + \alpha\left(k_p\mathbf{e}_1 + \mathbf{e}_2\right) - \begin{bmatrix} -\sin\hat{\theta}_A & -\cos\hat{\theta}_B & 0 \\ \cos\hat{\theta}_A & -\sin\hat{\theta}_B & 0 \\ 0 & 0 & 0 \end{bmatrix}\begin{bmatrix} \frac{\dot{\hat{\theta}}_A}{\cosh^2\xi_A} & 0 & 0 \\ 0 & \frac{\dot{\hat{\theta}}_B}{\cosh^2\xi_B} & 0 \\ 0 & 0 & 0 \end{bmatrix}\hat{\mathbf{\Psi}}^{-1}\hat{\mathbf{y}}\right) \tag{5.33}$$

The only change is the inclusion of $1/\cosh^2\xi_*$ terms in the denominator of the term associated with the estimation. This has the effect of limiting the contribution of the estimates to the control when the estimates approach the boundaries. In this case, the values of ξ_* will be large which will make $\cosh^2\xi_*$ very large.

Theorem 5.3.2. *Consider the tracking error dynamics of (2.4). Suppose that the adaptive control law is given by (5.33) with the projection scheme of (5.27) and update laws of (5.28). Then the convergence condition*

$$\lim_{t\to\infty}\begin{bmatrix}\mathbf{e}_1(t) \\ \mathbf{e}_2(t)\end{bmatrix} = \mathbf{0}$$

is applicable for all admissible reference trajectories $\mathbf{r}$ *and initial conditions* $[\mathbf{x}_1(0), \mathbf{x}_2(0)]^\top$ *provided that the gain* α *is chosen such that* $\alpha = k_p + k_v$, $|\theta_A|, |\theta_B| < \pi/4$ *and* $|\hat{\theta}_A(0)|, |\hat{\theta}_B(0)| < \pi/4$.

Proof. The proof is identical to the scenario without projection. Therefore, the reader is referred to the proof of Theorem 5.2.2. □

5.4 In-Plane with Single Out-of-Plane Component Misalignment Problem

To increase complexity, an out-of-plane misalignment is now added to the strictly in-plane problem. The out-of-plane misalignment is only included on one of the axes [‡] while the other axis remains strictly in the plane. This class of misalign-

[‡]For the remainder of this section the out-of-plane component will appear on the x-axis without loss of generality

ments has the structure

$$\mathbf{\Psi}_A = \begin{bmatrix} \cos\theta_A \cos\phi_A \\ \sin\theta_A \cos\phi_A \\ \sin\phi_A \end{bmatrix} \qquad \mathbf{\Psi}_B = \begin{bmatrix} -\sin\theta_B \\ \cos\theta_B \\ 0 \end{bmatrix} \qquad \mathbf{\Psi}_C = \begin{bmatrix} 0 \\ 0 \\ 1 \end{bmatrix} \tag{5.34}$$

where the in-plane misalignments are again given by θ_* for $* = A, B$ and ϕ_A represents the out-of-plane misalignment of the x-axis. The z-axis is assumed to be ideal. This scenario is represented graphically in Figure 5.7. The representation of the x-

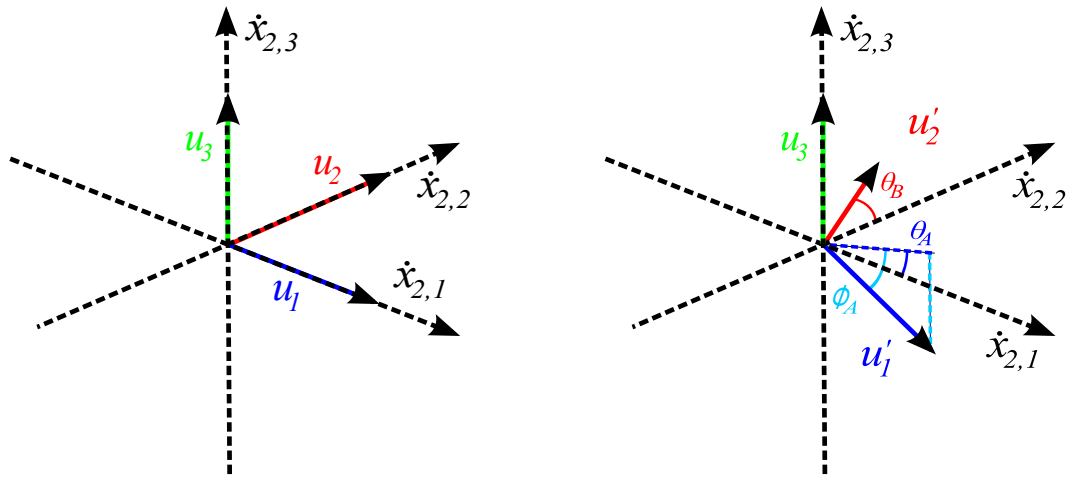

(a) $\mathbf{\Psi} = \mathbf{I}_{3\times3}$ (b) $\mathbf{\Psi} \neq \mathbf{I}_{3\times3}$

Figure 5.7: Graphical representation of the effect of $\mathbf{\Psi}$ for an in-plane misalignment on two axes and an out-of-plane misalignment on one axis. Note the out-of-plane misalignment is shown on the x-axis.

axis misalignment was reached by first considering the rotation in-plane followed by the out-of-plane rotation. This choice was made to be consistent with azimuth and elevation. It is noted that this is not the only two parameter option for the misalignment, but the choice was made because azimuth and elevation seemed to be the most physically meaningful representation. As before, there is a singularity condition with this class of $\mathbf{\Psi}$. The determinant of $\hat{\mathbf{\Psi}}$ can be found to be $\cos\hat{\phi}_A \cos(\hat{\theta}_A - \hat{\theta}_B)$ which gives two geometrically meaningful conditions for which $\hat{\mathbf{\Psi}}$ is not invertible. The first is the same as the strictly in-plane problem and corresponds to the axes becoming parallel in the plane. The second condition is that the out-of-plane misalignment

becomes $\pm\pi/2$. This is the case where the x-axis becomes parallel to the z-axis, but more importantly, it is the point where the in-plane angle cannot be determined since there is no in-plane component (i.e. the in-plane angle cannot be uniquely determined). The addition of this extra singularity condition will not have a significant impact since the first condition requires smaller angles.

5.5 Observer/Controller with Parameter Projection

In the section, the estimation and control problems are presented for the case that both axes have an in-plane misalignment, and one axis also has an out-of-plane misalignment. Based off the strictly in-plane results, an observer with parameter projection is the only estimation scheme considered. The parameter projection gives a larger set of allowable misalignments; moreover, the inclusion of the additional unknown angle will add an extra term to the Lyapunov analysis which will significantly reduce the size of the level curve and the resulting region of attraction. Thus, the result without projection is not presented.

5.5.1 Estimation Problem

To begin, consider the standard estimation problem for $\mathbf{\Psi}$ with the structure in (5.34). Using the vector update laws of (5.8) given by

$$\dot{\hat{\mathbf{\Psi}}}_A = -\gamma S\left[(\mathbf{y} - \hat{\mathbf{y}}_B - \mathbf{y}_C) \times \hat{\mathbf{y}}_A\right] \hat{\mathbf{\Psi}}_A$$
$$\dot{\hat{\mathbf{\Psi}}}_B = -\gamma S\left[(\mathbf{y} - \hat{\mathbf{y}}_A - \mathbf{y}_C) \times \hat{\mathbf{y}}_B\right] \hat{\mathbf{\Psi}}_B$$

where $\hat{\mathbf{\Psi}}_A$ and $\hat{\mathbf{\Psi}}_B$ are the unit vectors

$$\hat{\mathbf{\Psi}}_A = \begin{bmatrix} \cos\hat{\theta}_A \cos\hat{\phi}_A \\ \sin\hat{\theta}_A \cos\hat{\phi}_A \\ \sin\hat{\phi}_A \end{bmatrix} \qquad \hat{\mathbf{\Psi}}_B = \begin{bmatrix} -\sin\hat{\theta}_B \\ \cos\hat{\theta}_B \\ 0 \end{bmatrix} \tag{5.35}$$

Let $\hat{\mathbf{y}}_* = \hat{\mathbf{\Psi}}_* \mathbf{u}_{f,*}$, and define the signals

$$\bar{\mathbf{y}} = \begin{bmatrix} y_1 \\ y_2 \end{bmatrix} \qquad \hat{\bar{\mathbf{y}}}_* = \begin{bmatrix} \hat{y}_{*,1} \\ \hat{y}_{*,2} \end{bmatrix} \tag{5.36}$$

where $* = A, B$, and the subscript numeral indicates the value in the 3×1 vector. Using (5.35), Equation (5.8) can be manipulated to yield update laws on the estimates of the angles given by

$$\dot{\hat{\theta}}_A = -\frac{\gamma}{\cos^2 \hat{\phi}_A} \hat{\bar{\mathbf{y}}}_A^\top \mathbf{\Gamma}_A \left(\bar{\mathbf{y}} - \hat{\bar{\mathbf{y}}}_B \right) \tag{5.37a}$$

$$\dot{\hat{\phi}}_A = \gamma u_{f,A} \left(\frac{1}{\cos \hat{\phi}_A} \left(y_3 - u_{f,C} \right) - \left[\left(\mathbf{y} - \hat{\mathbf{y}}_B - \mathbf{y}_C \right)^\top \hat{\mathbf{\Psi}}_A \right] \tan \hat{\phi}_A \right) \tag{5.37b}$$

$$\dot{\hat{\theta}}_B = -\gamma \hat{\mathbf{y}}_B^\top \mathbf{\Gamma}_{\boldsymbol{B}} \left(\mathbf{y} - \hat{\mathbf{y}}_A - \mathbf{y}_C \right) \tag{5.37c}$$

where

$$\mathbf{\Gamma}_A = \begin{bmatrix} 0 & -1 \\ 1 & 0 \end{bmatrix} \qquad \mathbf{\Gamma}_B = \begin{bmatrix} 0 & -1 & 0 \\ 1 & 0 & 0 \\ 0 & 0 & 0 \end{bmatrix}$$

It is important to recognize here that all the signals that appear are available and can be implemented. Let the estimates on θ_* and ϕ_A be replaced by estimates of the projection variables $\xi_{*,\theta}$ and $\xi_{A,\phi}$, respectively. The relation between the projection variables and the true variables is the same as (5.27) and the discussion of Section 2.3.3. Furthermore, let the update laws on $\hat{\xi}_{*,\theta}$ be determined as

$$\dot{\hat{\xi}}_{*,\theta} = -\dot{\hat{\theta}}_* \tag{5.38}$$

and the update law on $\xi_{A,\phi}$ be given by

$$\dot{\hat{\xi}}_{A,\phi} = -\dot{\hat{\phi}}_A \tag{5.39}$$

where the update laws on the true variables have been chosen as in (5.37).

Theorem 5.5.1. *Assume that the components of $\mathbf{u}_f$ are such that $u_{f,A}$, $u_{f,B}$ and $u_{f,C}$ and their respective derivatives are bounded. Suppose also that $u_{f,A}$ and $u_{f,B}$ are PE signals and thus cannot remain indefinitely at zero. Then, given the measurement relation of (5.3) together with the smooth projection scheme for θ_* and ϕ_A and update laws of (5.38) and (5.39), the estimation scheme guarantees that $\hat{\theta}_A \to \theta_A$, $\hat{\theta}_B \to \theta_B$, and $\hat{\phi}_A \to \phi_A$ as $t \to \infty$ provided that $|\theta_A|, |\theta_B|, |\phi_A| < 33^\circ$ $(180\pi/33)$ and $|\hat{\theta}_A(0)|, |\hat{\theta}_B(0)|, |\hat{\phi}_A(0)| < 33^\circ$.*

Proof. Using the definition of the in-plane angle error in (5.10), and defining the out-of-plane angle error as

$$\tilde{\phi}_* \equiv \hat{\phi}_* - \phi_* \tag{5.40}$$

and the values $\bar{\theta}_*$ and $\bar{\phi}_*$ as

$$\bar{\theta}_* \equiv \hat{\theta}_* + \theta_* \qquad \bar{\phi}_* \equiv \hat{\phi}_* + \phi_* \tag{5.41}$$

the update laws can be rewritten in term of the errors as [§]

$$\dot{\tilde{\theta}}_A = \dot{\hat{\theta}}_A = -\gamma \left(\frac{\cos\phi_A}{\cos\hat{\phi}_A} \right) \sin\tilde{\theta}_A \, u_{f,A}^2 - \gamma \left(\frac{\sigma_A}{\cos\hat{\phi}_A} \right) \sin\tilde{\theta}_B \, u_{f,A} \, u_{f,B} \tag{5.42a}$$

$$\begin{aligned} \dot{\tilde{\phi}}_A = \dot{\hat{\phi}}_A = &-\gamma \sin\tilde{\phi}_A \, u_{f,A}^2 + \gamma \left[\tan\left(\frac{1}{2}\tilde{\theta}_A \right) \sin\hat{\phi}_A \cos\phi_A \right] \sin\tilde{\theta}_A \, u_{f,A}^2 \\ &- \gamma \left[\frac{\sin\hat{\phi}_A \cos\left(\hat{\theta}_A - \frac{1}{2}\bar{\theta}_B \right)}{\cos\left(\frac{1}{2}\tilde{\theta}_B \right)} \right] \sin\tilde{\theta}_B \, u_{f,A} \, u_{f,B} \end{aligned} \tag{5.42b}$$

$$\begin{aligned} \dot{\tilde{\theta}}_B = \dot{\hat{\theta}}_B = &-\gamma \sin\tilde{\theta}_B \, u_{f,B}^2 - \gamma \left[\sigma_B \cos\left(\frac{1}{2}\tilde{\phi}_A \right) \cos\left(\frac{1}{2}\bar{\phi}_A \right) \right] \sin\tilde{\theta}_A \, u_{f,A} \, u_{f,B} \\ &- \gamma \left[\frac{\sin\left(\frac{1}{2}\bar{\phi}_A \right) \cos\left(\frac{1}{2}\tilde{\theta}_A \right) \cos\left(\frac{1}{2}\bar{\theta}_A - \hat{\theta}_B \right)}{\cos\left(\frac{1}{2}\tilde{\phi}_A \right)} \right] \sin\tilde{\phi}_A \, u_{f,A} \, u_{f,B} \end{aligned} \tag{5.42c}$$

where σ_* is the same as (5.12) for in the strictly in-plane formulation. As a shorthand notation define the values

$$\delta_{\tilde{\theta}_A, \tilde{\theta}_B} = \frac{\sigma_A}{\cos\hat{\phi}_A} \tag{5.43a}$$

$$\delta_{\tilde{\phi}_A, \tilde{\theta}_A} = \tan\left(\frac{1}{2}\tilde{\theta}_A \right) \sin\hat{\phi}_A \cos\phi_A \tag{5.43b}$$

$$\delta_{\tilde{\phi}_A, \tilde{\theta}_B} = \frac{\sin\hat{\phi}_A \cos\left(\hat{\theta}_A - \frac{1}{2}\bar{\theta}_B \right)}{\cos\left(\frac{1}{2}\tilde{\theta}_B \right)} \tag{5.43c}$$

$$\delta_{\tilde{\theta}_B, \tilde{\theta}_A} = \sigma_B \cos\left(\frac{1}{2}\tilde{\phi}_A \right) \cos\left(\frac{1}{2}\bar{\phi}_A \right) \tag{5.43d}$$

$$\delta_{\tilde{\theta}_B, \tilde{\phi}_A} = \frac{\sin\left(\frac{1}{2}\bar{\phi}_A \right) \cos\left(\frac{1}{2}\tilde{\theta}_A \right) \cos\left(\frac{1}{2}\bar{\theta}_A - \hat{\theta}_B \right)}{\cos\left(\frac{1}{2}\tilde{\phi}_A \right)} \tag{5.43e}$$

[§] After a great deal of tedious algebra and trigonometric identities

This allows for (5.42) to be presented in the much more compact form of

$$\dot{\tilde{\theta}}_A = \dot{\hat{\theta}}_A = -\gamma \left(\frac{\cos\phi_A}{\cos\hat{\phi}_A} \right) \sin\tilde{\theta}_A \, u_{f,A}^2 - \gamma \delta_{\tilde{\theta}_A,\tilde{\theta}_B} \sin\tilde{\theta}_B \, u_{f,A} \, u_{f,B} \tag{5.44a}$$

$$\dot{\tilde{\phi}}_A = \dot{\hat{\phi}}_A = -\gamma \sin\tilde{\phi}_A \, u_{f,A}^2 + \gamma \delta_{\tilde{\phi}_A,\tilde{\theta}_A} \sin\tilde{\theta}_A \, u_{f,A}^2 - \gamma \delta_{\tilde{\phi}_A,\tilde{\theta}_B} \sin\tilde{\theta}_B \, u_{f,A} \, u_{f,B} \tag{5.44b}$$

$$\dot{\tilde{\theta}}_B = \dot{\hat{\theta}}_B = -\gamma \sin\tilde{\theta}_B \, u_{f,B}^2 - \gamma \delta_{\tilde{\theta}_B,\tilde{\theta}_A} \sin\tilde{\theta}_A \, u_{f,A} \, u_{f,B} - \gamma \delta_{\tilde{\theta}_B,\tilde{\phi}_A} \sin\tilde{\phi}_A \, u_{f,A} \, u_{f,B} \tag{5.44c}$$

Now consider the Lyapunov-like function involving the three projected parameter errors

$$\begin{aligned} V_E = {} & \frac{\mu_{A,\theta}}{2} \left[\log\left(\cosh\hat{\xi}_{A,\theta} \right) - \tilde{\xi}_{A,\theta} \tanh\xi_{A,\theta} \right] + \frac{\mu_{A,\phi}}{2} \left[\log\left(\cosh\hat{\xi}_{A,\phi} \right) - \tilde{\xi}_{A,\phi} \tanh\xi_{A,\phi} \right] \\ & + \frac{\mu_{B,\theta}}{2} \left[\log\left(\cosh\hat{\xi}_{B,\theta} \right) - \tilde{\xi}_{B,\theta} \tanh\xi_{B,\theta} \right] \geq 0 \end{aligned} \tag{5.45}$$

Using the expressions in (5.44) the derivative can be found to be

$$\begin{aligned} \dot{V}_E &= -\tilde{\theta}_A \dot{\tilde{\xi}}_{A,\theta} - \tilde{\phi}_A \dot{\tilde{\xi}}_{A,\phi} - \tilde{\theta}_B \dot{\tilde{\xi}}_{B,\theta} \\ &= \tilde{\theta}_A \dot{\tilde{\theta}}_A + \tilde{\phi}_A \dot{\tilde{\phi}}_A + \tilde{\theta}_B \dot{\tilde{\theta}}_B \\ &= -\gamma \left(\frac{\cos\phi_A}{\cos\hat{\phi}_A} \right) \tilde{\theta}_A \sin\tilde{\theta}_A \, u_{f,A}^2 - \gamma \tilde{\phi}_A \sin\tilde{\phi}_A \, u_{f,A}^2 - \gamma \tilde{\theta}_B \sin\tilde{\theta}_B \, u_{f,B}^2 \\ &\quad - \gamma \delta_{\tilde{\theta}_A,\tilde{\theta}_B} \tilde{\theta}_A \sin\tilde{\theta}_B \, u_{f,A} \, u_{f,B} \\ &\quad + \gamma \delta_{\tilde{\phi}_A,\tilde{\theta}_A} \tilde{\phi}_A \sin\tilde{\theta}_A \, u_{f,A}^2 - \gamma \delta_{\tilde{\phi}_A,\tilde{\theta}_B} \tilde{\phi}_A \sin\tilde{\theta}_B \, u_{f,A} \, u_{f,B} \\ &\quad - \gamma \delta_{\tilde{\theta}_B,\tilde{\theta}_A} \tilde{\theta}_B \sin\tilde{\theta}_A \, u_{f,A} \, u_{f,B} - \gamma \delta_{\tilde{\theta}_B,\tilde{\phi}_A} \tilde{\theta}_B \sin\tilde{\phi}_A \, u_{f,A} \, u_{f,B} \\ &= -\gamma \left[\sqrt{\left(\frac{\cos\phi_A}{\cos\hat{\phi}_A} \right) \tilde{\theta}_A \sin\tilde{\theta}_A} \, u_{f,A} \right]^2 - \gamma \left(\sqrt{\tilde{\phi}_A \sin\tilde{\phi}_A} \, u_{f,A} \right)^2 - \gamma \left(\sqrt{\tilde{\theta}_B \sin\tilde{\theta}_B} \, u_{f,B} \right)^2 \\ &\quad + \gamma \Delta_{\tilde{\theta}_A,\tilde{\phi}_A} \left[\sqrt{\left(\frac{\cos\phi_A}{\cos\hat{\phi}_A} \right) \tilde{\theta}_A \sin\tilde{\theta}_A} \, u_{f,A} \right] \left(\sqrt{\tilde{\phi}_A \sin\tilde{\phi}_A} \, u_{f,A} \right) \\ &\quad - \gamma \Delta_{\tilde{\theta}_A,\tilde{\theta}_B} \left[\sqrt{\left(\frac{\cos\phi_A}{\cos\hat{\phi}_A} \right) \tilde{\theta}_A \sin\tilde{\theta}_A} \, u_{f,A} \right] \left(\sqrt{\tilde{\theta}_B \sin\tilde{\theta}_B} \, u_{f,B} \right) \\ &\quad - \gamma \Delta_{\tilde{\phi}_A,\tilde{\theta}_B} \left(\sqrt{\tilde{\phi}_A \sin\tilde{\phi}_A} \, u_{f,A} \right) \left(\sqrt{\tilde{\theta}_B \sin\tilde{\theta}_B} \, u_{f,B} \right) \end{aligned} \tag{5.46}$$

where the Δ's are defined as

$$\Delta_{\tilde{\theta}_A,\tilde{\phi}_A} = \sqrt{\frac{\cos\hat{\phi}_A}{\cos\phi_A}}\sqrt{\frac{\tilde{\theta}_A\sin\tilde{\phi}_A}{\tilde{\phi}_A\sin\tilde{\theta}_A}}\delta_{\tilde{\phi}_A,\tilde{\theta}_A} \tag{5.47a}$$

$$\Delta_{\tilde{\theta}_A,\tilde{\theta}_B} = \sqrt{\frac{\cos\hat{\phi}_A}{\cos\phi_A}}\left(\sqrt{\frac{\tilde{\theta}_A\sin\tilde{\theta}_B}{\tilde{\theta}_B\sin\tilde{\theta}_A}}\delta_{\tilde{\theta}_A,\tilde{\theta}_B} + \sqrt{\frac{\tilde{\theta}_B\sin\tilde{\theta}_A}{\tilde{\theta}_A\sin\tilde{\theta}_B}}\delta_{\tilde{\theta}_B,\tilde{\theta}_A}\right) \tag{5.47b}$$

$$\Delta_{\tilde{\phi}_A,\tilde{\theta}_B} = \sqrt{\frac{\tilde{\phi}_A\sin\tilde{\theta}_B}{\tilde{\theta}_B\sin\tilde{\phi}_A}}\delta_{\tilde{\phi}_A,\tilde{\theta}_B} + \sqrt{\frac{\tilde{\theta}_B\sin\tilde{\phi}_A}{\tilde{\phi}_A\sin\tilde{\theta}_B}}\delta_{\tilde{\theta}_B,\tilde{\phi}_A} \tag{5.47c}$$

The main difficulty (other than the shear amount of algebra) in (5.46) is that there are three negative definite (i.e. quadratic) terms and three sign indefinite terms which are the cross terms of the quadratic terms. For the strictly in-plane problem, there were two quadratic terms and only *one* cross term. Therefore, the condition to be able to "dominate" the cross term with the good terms was $\eta < 2$. The problem in this case is that two portions of each good term must be used to dominate all of the cross terms. Moreover, the amount that needs to be taken from each good term is dependent on the value of each of the Δ's since it is not expected that they will be exactly the same. Equal parts could be taken from each good term but this will result in a conservative estimate on the set of allowable misalignments. Accordingly, extreme diligence must be taken to understand the Δ terms to develop a far less conservative result. The assumption is made that it is desired to have an equal range of allowable misalignments across all angles. Thus, the goal is to determine θ_P such that $|\theta_A|, |\theta_B|, |\phi_A| < \theta_P$. After some algebraic manipulation and bounding of individual terms, upper bounds can be found in terms of θ_P as ¶

$$\Delta^{\max}_{\tilde{\theta}_A,\tilde{\phi}_A} = \sqrt{\theta_P\tan\theta_P}\,\tan\theta_P \tag{5.48a}$$

$$\Delta^{\max}_{\tilde{\theta}_A,\tilde{\theta}_B} = \frac{1}{2}\left(\frac{2}{\cos\theta_P} + \sqrt{2}\right)\tan\theta_P \tag{5.48b}$$

$$\Delta^{\max}_{\tilde{\phi}_A,\tilde{\theta}_B} = 2\sqrt{\theta_P\tan\theta_P} \tag{5.48c}$$

This process used to find these values was extremely tedious. As a result, the analysis is left out of the proof but is available in Appendix B. To better understand the

¶From (B.2), (B.4), and (B.7)

behavior of these upper bounds as a function of θ_P, the functions can be plotted as shown in Figure 5.8. Thus, there is one term which is considerably smaller than

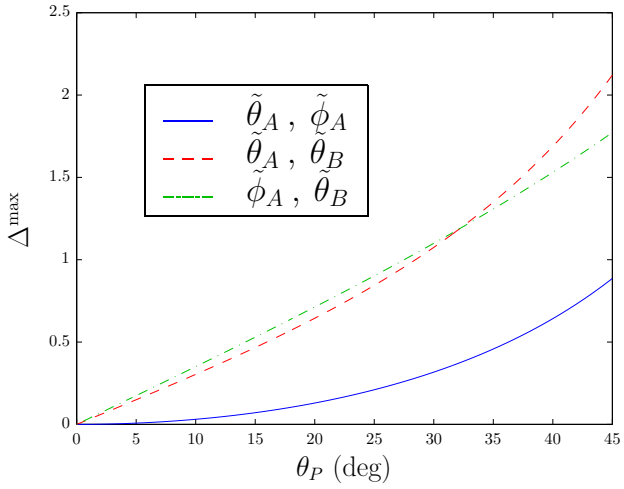

Figure 5.8: Plot of the upper bounds for increasing θ_P

the other two terms; moreover, the other two terms are approximately the same magnitude. To complete squares, define the value

$$\beta = 1 - \frac{1}{2}\Delta^{\max}_{\tilde{\theta}_A,\tilde{\phi}_A} \tag{5.49}$$

which is the amount left over on the quadratic terms of $\tilde{\theta}_A$ and $\tilde{\phi}_A$ to successfully dominate the cross term involving $\Delta_{\tilde{\theta}_A,\tilde{\phi}_A}$. The derivative of (5.46) can then be manipulated to become

$$\begin{aligned}
\dot{V}_E \leq & -\gamma\beta\left[\sqrt{\left(\frac{\cos\phi_A}{\cos\hat{\phi}_A}\right)\tilde{\theta}_A \sin\tilde{\theta}_A}\, u_{f,A}\right]^2 - \gamma\beta\left(\sqrt{\tilde{\phi}_A \sin\tilde{\phi}_A}\, u_{f,A}\right)^2 - \gamma\left(\sqrt{\tilde{\theta}_B \sin\tilde{\theta}_B}\, u_{f,B}\right)^2 \\
& + \gamma\Delta^{\max}_{\tilde{\theta}_A,\tilde{\theta}_B}\left|\sqrt{\left(\frac{\cos\phi_A}{\cos\hat{\phi}_A}\right)\tilde{\theta}_A \sin\tilde{\theta}_A}\, u_{f,A}\right|\left|\sqrt{\tilde{\theta}_B \sin\tilde{\theta}_B}\, u_{f,B}\right| \\
& + \gamma\Delta^{\max}_{\tilde{\phi}_A,\tilde{\theta}_B}\left|\sqrt{\tilde{\phi}_A \sin\tilde{\phi}_A}\, u_{f,A}\right|\left|\sqrt{\tilde{\theta}_B \sin\tilde{\theta}_B}\, u_{f,B}\right| \\
\leq & -\gamma\left[\beta - \frac{\left(\Delta^{\max}_{\tilde{\theta}_A,\tilde{\theta}_B}\right)^2}{4\left(\frac{1}{2}-\epsilon\right)}\right]\left[\sqrt{\left(\frac{\cos\phi_A}{\cos\hat{\phi}_A}\right)\tilde{\theta}_A \sin\tilde{\theta}_A}\, u_{f,A}\right]^2
\end{aligned}$$

$$-\gamma\left[\beta-\frac{\left(\Delta^{\max}_{\tilde{\phi}_A,\tilde{\theta}_B}\right)^2}{4\left(\frac{1}{2}-\epsilon\right)}\right]\left(\sqrt{\tilde{\phi}_A\sin\tilde{\phi}_A}\,u_{f,A}\right)^2-\gamma\epsilon\left(\sqrt{\tilde{\theta}_B\sin\tilde{\theta}_B}\,u_{f,B}\right)^2 \tag{5.50}$$

The only requirement on ϵ is that it must be greater than zero. Therefore, let ϵ be infinitesimally small such that the following constraints need to be satisfied.

$$\left(\Delta^{\max}_{\tilde{\theta}_A,\tilde{\theta}_B}\right)^2<2\beta \tag{5.51a}$$

$$\left(\Delta^{\max}_{\tilde{\phi}_A,\tilde{\theta}_B}\right)^2<2\beta \tag{5.51b}$$

Using the definitions on $\Delta^{\max}$ and β, $\theta_P\approx 33^\circ$ is the largest value such that (5.51) is satisfied. Note that this value occurs because $\Delta^{\max}_{\tilde{\theta}_A,\tilde{\theta}_B}$ is an active constraint, where as, $\Delta^{\max}_{\tilde{\theta}_A,\tilde{\theta}_B}$ could satisfy a larger value of θ_P before becoming active ($\theta_P\approx 33.5^\circ$). [‖] Therefore, enforcing that the allowable misalignment are less than this value of θ_P, equation (5.50) can be simplified to

$$\begin{aligned}\dot{V}_E &\leq -\gamma_1'\left[\sqrt{\left(\frac{\cos\phi_A}{\cos\hat{\phi}_A}\right)\tilde{\theta}_A\sin\tilde{\theta}_A}\,u_{f,A}\right]^2-\gamma_2'\left(\sqrt{\tilde{\phi}_A\sin\tilde{\phi}_A}\,u_{f,A}\right)^2\\ &\quad-\gamma_3'\left(\sqrt{\tilde{\theta}_B\sin\tilde{\theta}_B}\,u_{f,B}\right)^2\\ &\leq -\gamma_1'\cos\theta_P\sin^2\tilde{\theta}_A\,u_{f,A}^2-\gamma_2'\sin^2\tilde{\phi}_A\,u_{f,A}^2-\gamma_3'\sin^2\tilde{\theta}_B\,u_{f,B}^2\\ &\leq -\gamma_1''\sin^2\tilde{\theta}_A\,u_{f,A}^2-\gamma_2'\sin^2\tilde{\phi}_A\,u_{f,A}^2-\gamma_3'\sin^2\tilde{\theta}_B\,u_{f,B}^2\\ &\leq -\gamma'||\mathbf{z}'(\tilde{\theta},\tilde{\phi})||^2\end{aligned} \tag{5.52}$$

where $\gamma'=\min(\gamma_1'',\gamma_2',\gamma_3')$ and $\mathbf{z}_n'$ is defined as

$$\mathbf{z}_n'(\tilde{\theta},\tilde{\phi})=\begin{bmatrix}\sin\left(n\tilde{\theta}_A\right)u_{f,A}\\ \sin\left(n\tilde{\phi}_A\right)u_{f,A}\\ \sin\left(n\tilde{\theta}_B\right)u_{f,B}\end{bmatrix} \tag{5.53}$$

Thus, $\dot{V}_E$ is negative semi-definite, indicating boundedness for all closed-loop signals. Further, because V_E is lower-bounded, $\int_0^\infty \dot{V}_E(t)\,dt$ exists and is finite which taken

[‖] The real solution for θ_P is about 33.3° and the $\Delta^{\max}_{\tilde{\theta}_A,\tilde{\theta}_B}$ constraint becomes active at 33.7°. These values are reduced to smaller values to simplify the presentation while excluding a negligible set of misalignments

together with (5.50) implies that $\mathbf{z}'(\tilde{\theta}, \tilde{\phi}) \in \mathcal{L}_2 \cap \mathcal{L}_\infty$. Examining $\dot{\mathbf{z}}'$ indicates that boundedness of $\dot{\mathbf{z}}'$ is only dependent on boundedness of $\dot{\hat{\theta}}_A$, $\dot{\hat{\theta}}_B$, and $\dot{\hat{\phi}}_A$ (as all other values are bounded by definition). From (5.37), it is clear that $\dot{\hat{\theta}}_A, \dot{\hat{\theta}}_B, \dot{\hat{\phi}}_A \in \mathcal{L}_\infty$ which implies $\dot{\mathbf{z}}' \in \mathcal{L}_\infty$. Therefore, invoking Barbalat's Lemma yields

$$\lim_{t\to\infty} \mathbf{z}'(t) = \mathbf{0}$$

Since the components $u_{f,A}$ and $u_{f,B}$ are not zero for all time, this implies that

$$\lim_{t\to\infty} \begin{bmatrix} \sin\tilde{\theta}_A \\ \sin\tilde{\phi}_A \\ \sin\tilde{\theta}_B \end{bmatrix} = \mathbf{0}$$

which considering the projection scheme guarantees that

$$\lim_{t\to\infty} \begin{bmatrix} \tilde{\theta}_A \\ \tilde{\phi}_A \\ \tilde{\theta}_B \end{bmatrix} = \begin{bmatrix} \hat{\theta}_A - \theta_A \\ \hat{\phi}_A - \phi_A \\ \hat{\theta}_B - \theta_B \end{bmatrix} = \mathbf{0}$$

and the proof is complete. □

5.5.1.1 Remarks

a) The inclusion of the single out-of-plane misalignment reduces the region of allowable misalignments from 45° to 33°. Although θ_P does not reach its maximum value as determined by the control singularity, the reduction was not unexpected because as more misalignments are added more pieces of the quadratic terms must be shared by an increasing number of cross terms. This phenomenon is simply an artifact of the nonlinear stability analysis. It should certainly be noted that an allowable range of misalignments of 33° is impressive in itself and is well outside the small-angle approximation.

b). The result on θ_P involves two forms of conservatism. The first is that the determining of the upper bounds in Appendix B occurred by dividing the larger terms into smaller terms which themselves were upper bounded. This allows for upper bounds on a single variable to simultaneously satisfy two conditions. Since this is

not possible, the upper bounds are automatically conservative. In addition, the process of dominating the cross terms caused only two of three constraints to be active. Therefore, part of the quadratic terms was leftover which could have been used to increase θ_P. Unfortunately, finding the values necessary to use up as much of the quadratic terms as possible is even more tedious than the process already presented; accordingly, removing this second form of conservatism was not addressed.

5.6 Control Problem

As seen previously, once the convergence condition has been established for the estimation problem, the extension to the control problem is fairly simple. The only difference is a slight change to the estimation term of the control law. Let the control signal be determined through

$$\mathbf{u} = -\hat{\boldsymbol{\Psi}}^{-1}\left[\mathbf{g} + \alpha\left(k_p\mathbf{e}_1 + \mathbf{e}_2\right) - \dot{\hat{\boldsymbol{\Psi}}}\hat{\boldsymbol{\Psi}}^{-1}\hat{\mathbf{y}}\right] \tag{5.54}$$

where

$$\dot{\hat{\boldsymbol{\Psi}}} = \begin{bmatrix} -\sin\hat{\theta}_A\cos\hat{\phi}_A & -\cos\hat{\theta}_B & -\cos\hat{\theta}_A\sin\hat{\phi}_A \\ \cos\hat{\theta}_A\cos\hat{\phi}_A & -\sin\hat{\theta}_B & -\sin\hat{\theta}_A\sin\hat{\phi}_A \\ 0 & 0 & \cos\hat{\phi}_A \end{bmatrix} \begin{bmatrix} \frac{\dot{\hat{\theta}}_A}{\cosh^2\xi_{A,\theta}} & 0 & 0 \\ 0 & \frac{\dot{\hat{\theta}}_B}{\cosh^2\xi_{B,\theta}} & 0 \\ \frac{\dot{\hat{\phi}}_A}{\cosh^2\xi_{A,\phi}} & 0 & 0 \end{bmatrix} \tag{5.55}$$

which is similar to the last section but with the addition of the estimate of the out-of-plane angle.

Theorem 5.6.1. *Consider the tracking error dynamics of (2.4). Suppose that the adaptive control law is given by (5.54) with the smooth projection scheme for θ_* and ϕ_A and update laws of (5.38) and (5.39). Then the convergence condition*

$$\lim_{t\to\infty}\begin{bmatrix}\mathbf{e}_1(t)\\ \mathbf{e}_2(t)\end{bmatrix} = \mathbf{0}$$

is applicable for all admissible reference trajectories $\mathbf{r}$ and initial conditions $[\mathbf{x}_1(0), \mathbf{x}_2(0)]^\top$ provided that the gain α is chosen such that $\alpha = k_p + k_v$, $|\theta_A|, |\theta_B|, |\phi_A| < 33^\circ$ and $|\hat{\theta}_A(0)|, |\hat{\theta}_B(0)|, |\hat{\phi}_A(0)| < 33^\circ$.

Proof. This proof is nearly identical to the strictly in-plane problem with a few minor changes. Therefore, a condensed proof is presented which highlights the only changes. Let $\Lambda' \in \mathbb{R}^{3\times 3}$ be given by

$$\Lambda' = \begin{bmatrix} \sin\left(\frac{1}{2}\bar{\theta}_A\right)\cos\left(\frac{1}{2}\tilde{\phi}_A\right)\cos\left(\frac{1}{2}\bar{\phi}_A\right) & \sin\left(\frac{1}{2}\bar{\phi}_A\right)\cos\left(\frac{1}{2}\tilde{\theta}_A\right)\cos\left(\frac{1}{2}\bar{\theta}_A\right) & \cos\left(\frac{1}{2}\bar{\theta}_B\right) \\ -\cos\left(\frac{1}{2}\bar{\theta}_A\right)\cos\left(\frac{1}{2}\tilde{\phi}_A\right)\cos\left(\frac{1}{2}\bar{\phi}_A\right) & \sin\left(\frac{1}{2}\bar{\phi}_A\right)\cos\left(\frac{1}{2}\tilde{\theta}_A\right)\sin\left(\frac{1}{2}\bar{\theta}_A\right) & \sin\left(\frac{1}{2}\bar{\theta}_B\right) \\ 0 & -\cos\left(\frac{1}{2}\bar{\phi}_A\right) & 0 \end{bmatrix}$$

Note that the $||\Lambda'|| < 1$, since the largest eigenvalue of ${\Lambda'}^{\top}\Lambda'$ is 1. Let the Lyapunov like function on the control be defined as in (5.23) at which point the derivative can be represented as

$$\begin{aligned} \dot{V}_C &\leq -k_p||\mathbf{e}_1||^2 - k_v||\mathbf{e}_{2,f}||^2 + 2||\mathbf{e}_1 + \mathbf{e}_{2,f}||\,||\Lambda'||\,||\mathbf{z}'_{1/2}(\tilde{\theta},\tilde{\phi})|| \\ &\leq -k_p||\mathbf{e}_1||^2 - k_v||\mathbf{e}_{2,f}||^2 + 2\sqrt{2}\left(||\mathbf{e}_1|| + ||\mathbf{e}_{2,f}||\right)||\mathbf{z}'(\tilde{\theta},\tilde{\phi})|| \end{aligned} \tag{5.56}$$

Consider the joint Lyapunov-like function which combines the estimation and control functions of (5.16) and (5.45)

$$V = V_C + \tau V_E \geq 0 \tag{5.57}$$

where τ is a positive scalar constant. The associated derivative of V comes from (5.17) and (5.50) and can be manipulated using completion of squares to get the result

$$\dot{V} \leq -\frac{k_p}{2}||\mathbf{e}_1||^2 - \frac{k_v}{2}||\mathbf{e}_{2,f}||^2 - k_z||\mathbf{z}'(\tilde{\theta},\tilde{\phi})||^2 \leq 0 \tag{5.58}$$

where τ has been selected to be large enough to ensure that the estimation error term is negative semi-definite. Using the same signal chasing arguments and invoking Barbalat's Lemma yields

$$\lim_{t\to\infty}[\mathbf{e}_1 \quad \mathbf{e}_{2,f} \quad \mathbf{z}(t)] = \mathbf{0}$$

By construction of the filter dynamics, $\mathbf{e}_{2,f} \to \mathbf{0}$ implies $\mathbf{e}_2 \to \mathbf{0}$ as $t \to \infty$, and the control objectives are met. Upon recovering the control signal, the proof is complete.

□

5.7 Numerical Simulations

To demonstrate the performance of the proposed control schemes, a series of simulations were performed. The length of each simulation was varied to show the convergence of the tracking and parameter errors. For all the simulations, the initial conditions for $\mathbf{g}_f$ and $\mathbf{e}_{2,f}$ were set to zero. In addition, the gains were selected as $k_p = k_v = 3$ and $\gamma = 10$. The system is assumed to have a drift term given by

$$\mathbf{f} = \text{diag}(\mathbf{x}_1)\mathbf{x}_2$$

5.7.1 Strictly In-Plane

To motivate the use of the proposed control schemes, the performance of a system without an observer is considered. As a control law,

$$\mathbf{u} = -\mathbf{g} - \alpha(k_p\mathbf{e}_1 + \mathbf{e}_2)$$

is used which guarantees asymptotic convergence of the tracking errors if $\mathbf{\Psi} = \mathbf{I}$. ** To show this result, the PE reference trajectory

$$\mathbf{r}(t) = \begin{bmatrix} \cos t \\ \sin t \cos 2t \\ \sin t \sin 2t \end{bmatrix}$$

is used. The initial conditions were set as $\mathbf{x}_1(0) = \mathbf{0}$ and $\mathbf{x}_2(0) = \mathbf{0}$. As expected, the tracking errors converge as can be seen in Figure 5.9(a). If an in-plane misalignment of $\theta_A = 8^\circ$ ($2\pi/45$ rads) and $\theta_B = -12^\circ$ ($-3\pi/45$ rads) is included, clearly $\mathbf{\Psi} \neq \mathbf{I}$. Without any adaptation, the tracking errors do not converge as can be seen in Figure 5.9(b). Therefore, a standard control law is not robust to relatively small misalignments. For this particular scenario, the strictly in-plane control method can be used since the misalignments are well within the allowable range. If the initial estimates are taken to be $\hat{\theta}_A(0) = 0$ and $\hat{\theta}_B(0) = 0$ (assuming no misalignment), the same simulation can be performed with the proposed observer. The results of the simulation are shown in Figure 5.10. Implementing the proposed observer, tracking

**This result is shown in Section 2.3.2

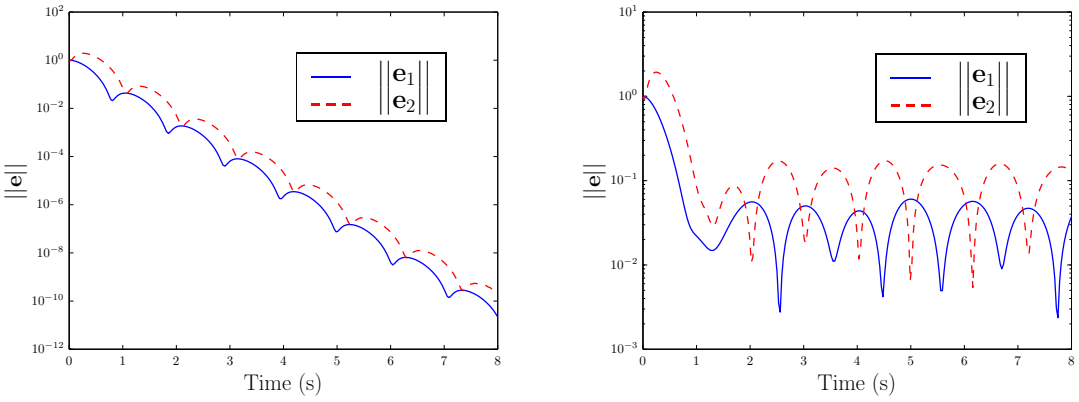

(a) $\mathbf{\Psi} = \mathbf{I}$ (b) $\mathbf{\Psi} \neq \mathbf{I}$

Figure 5.9: Performance of standard control law without any adaptation on the misalignment matrix, $\mathbf{\Psi}$, for the strictly in-plane problem

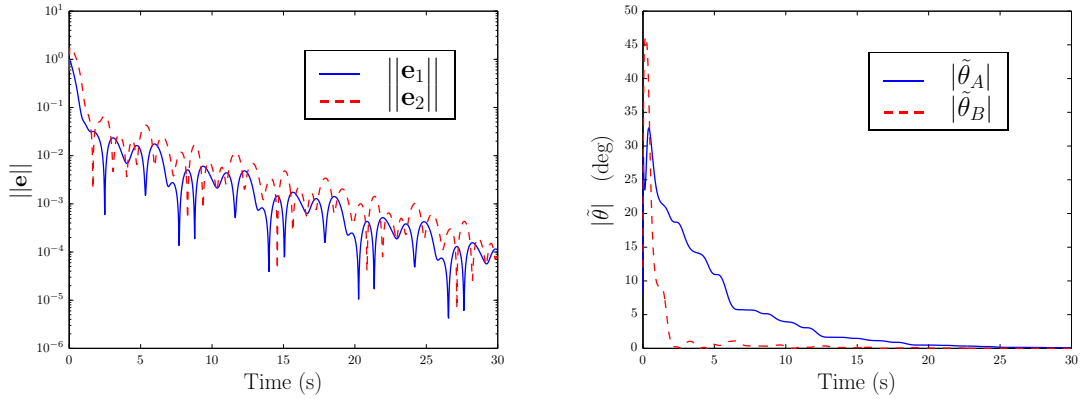

(a) Norm of the tracking errors (b) Norm of the estimation errors

Figure 5.10: Simulation results for the tracking and estimation errors for a PE reference trajectory for the strictly in-plane problem. Note that the estimation errors converge to zero

error convergence is recovered. In addition, the estimation errors are able to converge because of the richness of the reference signal. As stated previously, it is possible to meet the control objectives without convergence of the estimation errors. As an example, consider the problem of stabilization ($\mathbf{r}(t) = \mathbf{0}$). Using the initial conditions $\mathbf{x}_1(0) = \begin{bmatrix} 1 & -0.5 & 0.1 \end{bmatrix}^\top$ and $\mathbf{x}_2(0) = \begin{bmatrix} -0.05 & -0.05 & 0 \end{bmatrix}^\top$, the in-plane control

method was simulated as shown in Figure 5.11. Note that the values of the misalign-

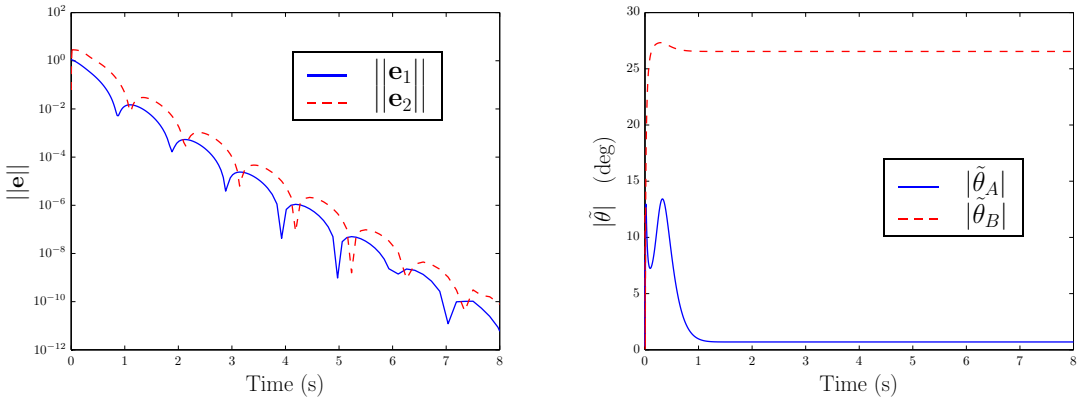

(a) Norm of the tracking errors

(b) Norm of the estimation errors

Figure 5.11: Simulation results for the tracking and estimation errors for stabilization in the strictly in-plane problem. Note that the estimation errors do not converge because the stabilization does not make the filtered control signal sufficiently rich

ments has not changed. As guaranteed by the stability analysis, the tracking errors converge to zero, but the estimates of the misalignments do not converge to the true values. This occurs because the process of stabilizing causes $\mathbf{u}$ and ultimately $\mathbf{u}_f$ to converge to zero before the estimates have had the opportunity to converge. Since $\mathbf{u}_f$ goes to zero, the estimation of the misalignments stops; however, even in this case, the control objectives are still met.

5.7.2 In-Plane with Single Out-of-Plane

Now the performance is examined for the in-plane misalignment problem with an additional out-of-plane component. The true misalignments were taken to be $\theta_A = 10^\circ$ ($\pi/18$ rads), $\theta_B = -20^\circ$ ($-\pi/9$ rads), and $\phi_A = 25^\circ$ ($5\pi/36$ rads) which are fairly large-scale. The PE reference trajectory was used with the same initial conditions and gains as the strictly in-plane simulation. The results are shown in Figure 5.12. As expected, the tracking errors and the estimation errors converge to zero because of the PE reference trajectory. Despite the addition of the out-of-plane misalignment, the convergence rate of the estimation errors is approximately

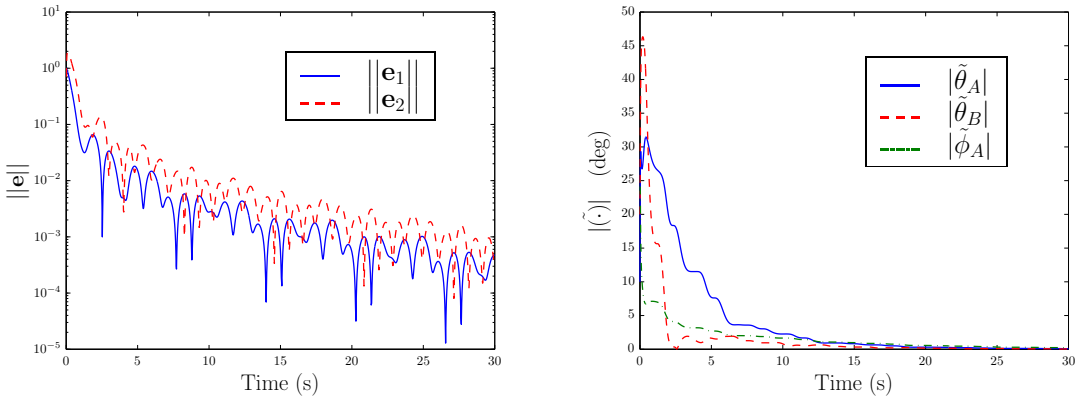

(a) Norm of the tracking errors

(b) Norm of the estimation errors

Figure 5.12: Simulation results for the tracking and estimation errors for a PE reference trajectory for the in-plane with one out-of-plane component problem. Note that the estimation errors converge to zero

the same, and the rate of the tracking error convergence has only slightly reduced. To add some extra insight into the behavior of the proposed method, stabilization is considered, but the drift term is changed to $\mathbf{f} = \mathbf{x}_2$ and the control gains are changed to $k_p = k_v = 0.01$. The estimation gain, γ, is kept the same. The results of the simulation are shown in Figure 5.13. The significant reduction in the control gains has the effect of reducing the rate of convergence of the tracking errors. In fact, the convergence rate is slow enough that $\tilde{\theta}_B$ and $\tilde{\phi}_A$ are able to converge to zero ($\tilde{\theta}_A$ is close to zero). Thus, convergence of the estimation errors can still occur without a PE reference trajectory if the rate for the estimation error is faster than the rate of $\mathbf{u}_f$ approaching zero. Note that this is not just dependent on the values of the control gains but also the dynamics of the system through the drift term.

5.8 Concluding Remarks

This chapter examines the problem of controlling a system subject to a class of actuation misalignments where the control axes are independently misaligned. For this class of misalignments, the uncertainty is predominately in the plane. When the misalignments are restricted to the plane, there is an issue when the two control axes

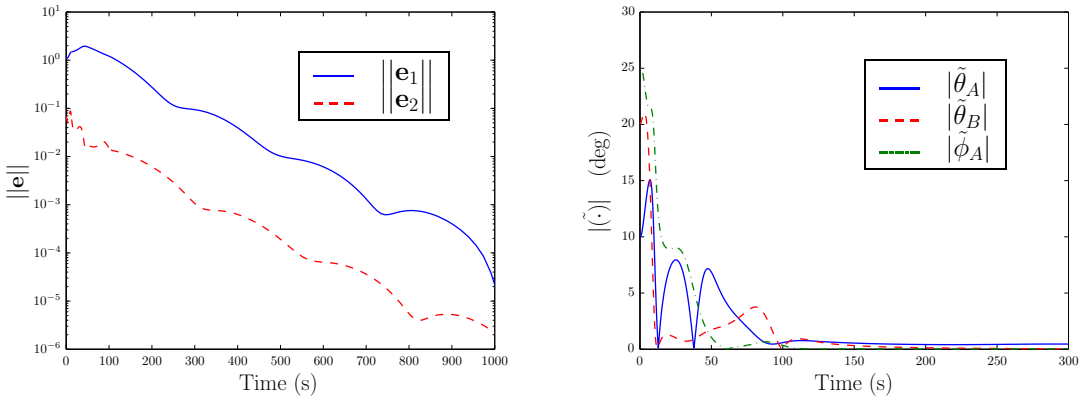

(a) Norm of the tracking errors

(b) Norm of the estimation errors

Figure 5.13: Simulation results for the tracking and estimation errors for stabilization in the in-plane with one out-of-plane component problem. Note that the estimation errors nearly converge despite the stabilization objective, albeit slowly

become parallel. This manifests itself as a singularity condition in the control problem that would cause the control signal to become unbounded. Therefore, the observer must actively avoid this condition. If the choice is made to not use a projection scheme, the actual misalignments must be restricted to be less than $\pi/8$ to guarantee that the initial estimates start in the region of attraction. The inclusion of the smooth projection scheme expands the set of allowable misalignments to its maximum value of $\pi/4$. In either case, the observer can be combined with a controller to ensure convergence of the tracking errors although the projection scheme does add some complexity to the control system. An out-of-plane component was then added to the strictly in-plane problem. Using the projection scheme and a similar stability analysis, the observer was shown to be valid such that all three misalignment angles are less than $180\pi/33$ (33°). This result is slightly conservative (i.e. not to the maximum as with the strictly in-plane result), but still allows for significantly large misalignments. Moreover, the addition of the out-of-plane misalignment does not greatly effect the extension to the control problem, and perfect error tracking is guaranteed. This is perhaps the most tractable of the independent misalignment problems; however, the proofs represent an important first step to understanding the more general problem.

Chapter 6

Independent Two-Axis, Out-of-Plane Misalignments

In this chapter, the problem of determining unknown actuator misalignments that are out of the plane is studied. In reality, it would be expected that the misalignments would occur both in and out of the plane. Interestingly, when both axes are assumed to have out-of-plane misalignments, the problem becomes fundamentally different than the in-plane problem, and thus, the discussion of the in-plane misalignments will not be directly applicable. In the previous chapter, convergence was proven by restricting the allowable range of misalignments and their corresponding estimates. Thus, the proof is fairly simple for misalignment angles with small magnitudes. As will be seen, the out-of-plane problem has formidable technical issues regardless of the magnitude of the misalignments. In fact, even when the out-of-plane misalignments are infinitesimally small, the proof of convergence is not straightforward. These issues arise because of a fundamental difference in how the observer handles the in-plane and out-of-plane components. Accordingly, a new set of observers and controllers are proposed that guarantee convergence of the estimation errors. As in the last chapter, the problem will be approached by considering both the estimation and control problem for specific classes of misalignments involving out-of-plane misalignments.

The remainder of the chapter is organized as follows. Section 6.1 introduces the problem of two-axis misalignments which are *strictly* out-of-plane. Section 6.2 discusses the fundamental differences between the in-plane and out-of-plane as it relates to the certainty-equivalence like observer. Furthermore, the out-of-plane problem is examined in detail to motivate possible solutions. Section 6.3 introduces a new solution that can be used in the control problem through a scheduled switching control. Section 6.4 discusses a switching observer that is guaranteed to have a finite number

of switches and guarantees convergence of the estimation errors. Section 6.5 extends idea of the switching observer to develop a hybrid observer which has the behavior of the switching observer but guarantees that the control signal remains continuous. Section 6.6 discusses the addition of a single in-plane misalignment component to the problem. Section 6.7 highlights the performance of the proposed methods through numerical simulations. Finally, Section 6.8 presents some concluding remarks.

6.1 Strictly Out-of-Plane Misalignment Problem

Consider the class of misalignments such that the misalignment on the x-axis is restricted to the xz-plane, and the misalignment on the y-axis is restrained to the yz-plane. * As a result, the misalignment matrix has the form

$$\boldsymbol{\Psi}_A = \begin{bmatrix} \cos\phi_A \\ 0 \\ \sin\phi_A \end{bmatrix} \qquad \boldsymbol{\Psi}_B = \begin{bmatrix} 0 \\ \cos\phi_B \\ \sin\phi_B \end{bmatrix} \qquad \boldsymbol{\Psi}_C = \begin{bmatrix} 0 \\ 0 \\ 1 \end{bmatrix} \tag{6.1}$$

where ϕ_* signifies the out-of-plane misalignment angles. Again, the z-axis is assumed to have no misalignment. A graphical representation is shown in Figure 6.1. As before, the representation of the angles introduces a singularity into the problem that needs to be avoided to ensure controllability for the corresponding control problem. The determinant of $\hat{\boldsymbol{\Psi}}$ is given by $\det(\hat{\boldsymbol{\Psi}}) = \cos\hat{\phi}_A \cos\hat{\phi}_B$; consequently, $\hat{\boldsymbol{\Psi}}$ becomes singular when $\hat{\phi}_* = \pm\pi/2$. As mentioned previously, this condition occurs when either the x-axis or the y-axis becomes aligned with the z-axis. In addition, the representation has issues because there is no longer an in-plane component, and the idea of an in-plane angle loses all meaning. Fortunately, a misalignment as large as $\pm\pi/2$ would not be expected for any realistic practical system; however, the analysis is performed to determine the largest set of misalignments possible which must consider these singularities.

*Note that this is done without loss of generality since the same arguments could be made for any combination of two of the three axes

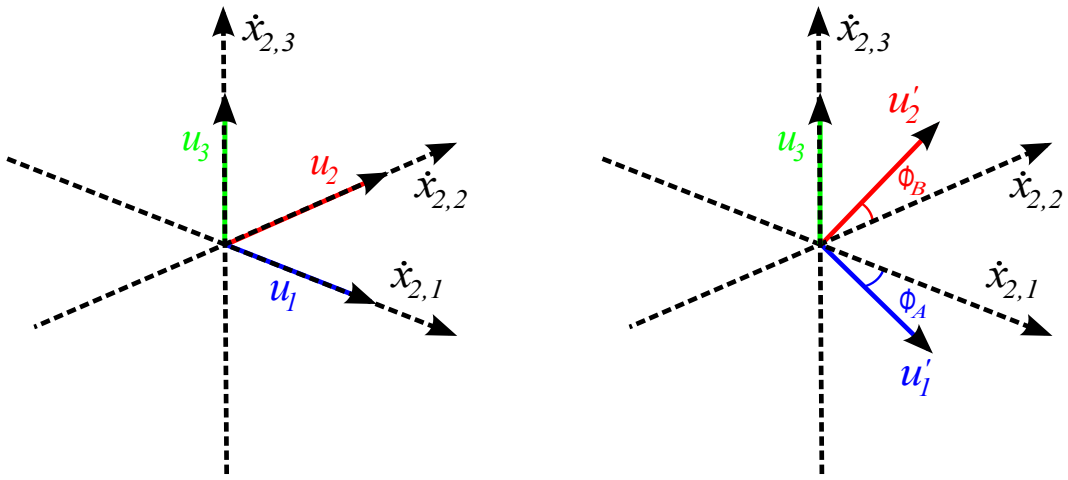

(a) $\mathbf{\Psi} = \mathbf{I}_{3\times 3}$ (b) $\mathbf{\Psi} \neq \mathbf{I}_{3\times 3}$

Figure 6.1: Graphical representation of the effect of $\mathbf{\Psi}$ for the strictly out-of-plane problem on the independent control axes

6.2 Issues in Estimating Pairs of Out-of-Plane Components

In this section, a detailed description of the technical difficulties in extending the previous in-plane only results to misalignments with pairs of out-of-plane components is given. Note that the discussion only relates to estimating out-of-plane components when other out-of-plane components exist. When there is only a single out-of-plane misalignment component, there are no issues other than bounding the estimates as in Section 5.5. These difficulties can be attributed to the peculiar geometry of the out-of-plane problem with respect to the structure of the proposed observer. Fortunately, there are also certain positive aspects to the geometry that motivate different approaches to estimating the uncertain out-of-plane only misalignments. The proceeding discussion will also highlight these aspects.

6.2.1 Direct Extension of In-Plane Results

A significant part of the stability analysis for the certainty-equivalence like observer in-plane was the completion of squares where the non-positive quadratic terms were used to "dominate" the sign indefinite cross terms. Fortunately, the

values associated with the cross-terms (i.e. η's and Δ's) could be bounded by simply constraining the estimates below some maximum value. Recall that for the strictly in-plane problem $\eta = |\sigma_A + \sigma_B|$ needed to be less than two. Substituting in values, η is given by

$$\eta = \left| \frac{\sin\left(\hat{\theta}_A - \frac{1}{2}\bar{\theta}_B\right)}{\cos\left(\frac{1}{2}\tilde{\theta}_B\right)} + \frac{\sin\left(\frac{1}{2}\bar{\theta}_A - \hat{\theta}_B\right)}{\cos\left(\frac{1}{2}\tilde{\theta}_A\right)} \right|$$

The structure of η indicates that if the $\sin(\cdot)$ term in the numerator can be kept small enough and the $\cos(\cdot)$ term in the numerator can be kept large enough then η is less than two. This can be done by ensuring that the misalignments and the estimates (and ultimately the errors) remain "small enough" as in the previous chapter. Without going any deeper into the algebraic details at this point, a similar η' can be established for the strictly out-of-plane problem as follows

$$\eta' = \left| \frac{\cos\hat{\phi}_A \cos\left(\frac{1}{2}\bar{\phi}_B\right)}{\cos\left(\frac{1}{2}\tilde{\phi}_B\right)} + \frac{\cos\hat{\phi}_B \cos\left(\frac{1}{2}\bar{\phi}_A\right)}{\cos\left(\frac{1}{2}\tilde{\phi}_A\right)} \right| \tag{6.2}$$

Using the same analysis as with η, η' would be small enough if the numerator terms were "small" and the denominator terms were "large"; however, this creates a clear obstruction since the numerator can only be small when the misalignment and estimates are large due to the appearance of only $\cos(\cdot)$ terms. For this to be the case, the errors could also be large which would make the denominator small. Accordingly, the structure of the out-of-plane problem has introduced the possibility that $\eta' > 2$ even for infinitesimally small misalignments which is not evident in the strictly in-plane problem (or with a single out-of-plane component). This phenomenon occurs because of the geometric interpretation of the proposed observer.

Recall that the convergence proof of the strictly in-plane observer was based off the Lyapunov-like function $V = 2\sin(\tilde{\theta}_A/2) + 2\sin(\tilde{\theta}_B/2)$. Consider an alternative Lyapunov-like function given by

$$V' = \left(1 - \mathbf{\Psi}_A^\top \hat{\mathbf{\Psi}}_A\right) + \left(1 - \mathbf{\Psi}_B^\top \hat{\mathbf{\Psi}}_B\right) \tag{6.3}$$

Using the same observer discussed throughout the dissertation and assuming that the misalignments associated with the B term are known, the time derivative of V' taken along (5.8) can be found to be

$$\dot{V}' = -\gamma ||\boldsymbol{\Psi}_A \times \hat{\boldsymbol{\Psi}}_A||^2 \, u_{f,A}^2$$

Recall that the norm of the cross-product can be related to the angle between the vectors, ρ such that the derivative can be re-written as

$$\dot{V}' = -\gamma \sin^2 \rho_A \;\; u_{f,A}^2$$

Now assume that the B terms are also uncertain, then the time derivative of V' in (6.3) would be

$$\begin{aligned}\dot{V}' = &-\gamma \sin^2 \rho_A \, u_{f,A}^2 - \gamma \sin^2 \rho_B \, u_{f,B}^2 - \gamma \frac{||\tilde{\boldsymbol{\Psi}}_B \times \hat{\boldsymbol{\Psi}}_A||}{\cos\left(\frac{1}{2}\rho_B\right)} \sin \rho_A u_{f,A} \, u_{f,B} \\ &+ \frac{||\tilde{\boldsymbol{\Psi}}_A \times \hat{\boldsymbol{\Psi}}_B||}{\cos\left(\frac{1}{2}\rho_A\right)} \sin \rho_B \, u_{f,A} \, u_{f,B}\end{aligned}$$

If ν_{BA} and ν_{AB} were taken to be angles between vectors $\tilde{\boldsymbol{\Psi}}_B$ and $\hat{\boldsymbol{\Psi}}_A$ and $\tilde{\boldsymbol{\Psi}}_A$ and $\hat{\boldsymbol{\Psi}}_B$, respectively, then the final form of the derivative is given by

$$\begin{aligned}\dot{V}' = &-\gamma \sin^2 \rho_A \, u_{f,A}^2 - \gamma \sin^2 \rho_B \, u_{f,B}^2 \\ &- \gamma \left[\frac{\sin \nu_{BA}}{\cos\left(\frac{1}{2}\rho_B\right)} + \frac{\sin \nu_{AB}}{\cos\left(\frac{1}{2}\rho_A\right)} \right] \sin \rho_A \sin \rho_B \, u_{f,A} \, u_{f,B}\end{aligned} \tag{6.4}$$

Note that for the strictly in-plane problem, $\rho_A = \tilde{\theta}_A$, $\rho_B = \tilde{\theta}_B$, and η is the same as the term in the squares brackets. In addition, for the strictly out-of-plane problem, $\rho_A = \tilde{\phi}_A$, $\rho_B = \tilde{\phi}_B$, and η' is the same as the term in the squares brackets. This formulation gives an exact geometric interpretation of the contribution of the sign indefinite cross term. Consider the scenario where the x-axis has no misalignment and is known perfectly, and the y-axis has an infinitesimally small misalignment in-plane. Initially, if our estimate of the y-axis misalignment is zero, then the error vector, $\tilde{\boldsymbol{\Psi}}_B$, points in the direction of the x-axis (or opposite) as can be seen in

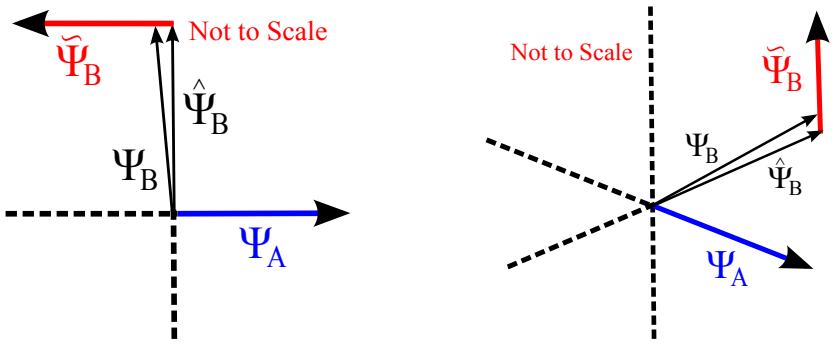

(a) In-plane (b) Out-of-plane

Figure 6.2: Effect of infinitesimal errors on the angle between $\tilde{\mathbf{\Psi}}_B$ and $\mathbf{\Psi}_A$

Figure 6.2(a) and the value of $\sin \nu_{BA}$ is small. [†] Thus, small errors lead to a small value of ν_{BA} which allows for completion of squares. Now, consider the same scenario but the infinitesimally small error is out-of-plane as can be seen in Figure 6.2(b). In this case, the error vector points in the direction of the z-axis (or opposite), which is perpendicular to the x-axis. Accordingly, small errors out-of-plane make $\nu_{BA} \approx 90°$ or $\sin \rho_{BA} \approx 1$ which is detrimental to the bounding step of the Lyapunov-like analysis. Therefore, there could be issues with proving convergence for the proposed observer even for infinitesimally small errors. As previously mentioned, the issues with the out-of-plane estimation are a direct result of the certainty-equivalence like structure of the observer. [‡] Thus, any attempt to prove observer convergence when a pair of out-of-plane misalignments exists cannot directly follow the same process as the strictly in-plane problem.

[†]The same discussion can be made for the other axis

[‡]In fact, a different observer of the form $\dot{\hat{\mathbf{\Psi}}}_A = -\gamma S\left[(\mathbf{y}_A + \mathbf{y}_B \times \hat{\mathbf{y}}_B - \mathbf{y}_C) \times \hat{\mathbf{y}}_A\right] \hat{\mathbf{\Psi}}_A$ was considered where the error was represented through the cross product and not the difference. Although this observer is not implementable, it has the opposite properties of the proposed observer. Specifically, the in-plane problem is susceptible to infinitesimal errors, where as, the out-of-plane problem has no such issues.

6.2.2 Linear Analysis

Before even attempting to tackle the out-of-plane problem, the local stability properties of the certainty-equivalence like observer can be analyzed. To study the local stability and to keep the discussion simple, the inputs were assumed to be constant. Application of the standard update laws of (5.8) with some algebraic manipulation (shown in detail in proceeding section), leads to a representation of the angle update laws in terms of the errors and true misalignments given by

$$\dot{\tilde{\phi}}_A = -\gamma \sin\tilde{\phi}_A \, u_{f,A}^2 - 2\gamma \sin\left(\tfrac{1}{2}\tilde{\phi}_B\right) \cos\left(\tfrac{1}{2}\tilde{\phi}_B + \phi_B\right) \cos\left(\tilde{\phi}_A + \phi_A\right) u_{f,A} \, u_{f,B} \quad \text{(6.5a)}$$

$$\dot{\tilde{\phi}}_B = -\gamma \sin\tilde{\phi}_B \, u_{f,B}^2 - 2\gamma \sin\left(\tfrac{1}{2}\tilde{\phi}_A\right) \cos\left(\tfrac{1}{2}\tilde{\phi}_A + \phi_A\right) \cos\left(\tilde{\phi}_B + \phi_B\right) u_{f,A} \, u_{f,B} \quad \text{(6.5b)}$$

Expanding (6.5) using trigonometric identities, using small angle approximations on the errors, and eliminating quadratic terms and above for the errors, the linearized system in the errors is given by

$$\begin{bmatrix} \dot{\tilde{\phi}}_A \\ \dot{\tilde{\phi}}_B \end{bmatrix} = \gamma \underbrace{\begin{bmatrix} -u_{f,A}^2 & -u_{f,A}u_{f,B} \cos\phi_A \cos\phi_B \\ -u_{f,A}u_{f,B} \cos\phi_A \cos\phi_B & -u_{f,B}^2 \end{bmatrix}}_{\mathbf{M}} \begin{bmatrix} \tilde{\phi}_A \\ \tilde{\phi}_B \end{bmatrix} \qquad (6.6)$$

For the linear system to be locally asymptotically stable, the matrix $\mathbf{M}$ must be negative-definite which for a second-order system requires that the trace($\mathbf{M}$) < 0 and det($\mathbf{M}$) > 0. Examining $\mathbf{M}$, it is clear that

$$\begin{aligned} \text{tr}(\mathbf{M}) &= -u_{f,A}^2 - u_{f,B}^2 < 0 \quad \checkmark \\ \det(\mathbf{M}) &= u_{f,A}^2 u_{f,B}^2 \left(1 - \cos^2\phi_A \cos^2\phi_B\right) \end{aligned}$$

If $u_{f,A}$ and $u_{f,B}$ are both non-zero and *either* ϕ_A or ϕ_B is non-zero such that ϕ_A and ϕ_B both belong to the interval $(-\pi/2, \pi/2)$, then the det($\mathbf{M}$) > 0, and the system is locally asymptotically stable. If $\phi_A = \phi_B = 0$, the det($\mathbf{M}$) $= 0$, and nothing additional can be said about stability because one of the eigenvalues is zero (the other is $-u_{f,A}^2 - u_{f,B}^2$ which is in the open left-half plane). In that case, a center manifold analysis as in [50] is necessary to determine the system stability. The original system can then be viewed as a reduced order system on the order of the number of

eigenvalues which are zero. The stability of the center manifold can be determined by studying the stability of the reduced-order system. In this case, the reduced system of order one, represented through the variable $s(t)$, can be determined [§] as in (C.10) as

$$\dot{s} = -\gamma u_{f,A}^2 u_{f,B}^2 s^3 + O(|s|^5)$$

which can be shown to be asymptotically stable by selecting the standard Lyapunov function $s^2/2$. Thus, the observer is locally asymptotically stable for all non-zero constant inputs and $\phi_A, \phi_B \in (-\pi/2, \pi/2)$. Although this is a restrictive result because it does not apply to time-varying inputs, it does indicate that there is a region of attraction for which the nonlinear system governing the estimation errors is asymptotically stable. If the region of attraction could be better understood then potentially a result could be established that guarantees converge of the proposed observer even for the out-of-plane problem.

6.2.3 Region of Attraction

A region of attraction was determined for the strictly in-plane problem by using a Lyapunov-like function as a level curve and then determining where η (the magnitude associated with the cross term) was equal to two. If the V level curve was entirely contained in the region where η was less than two then the level curve was part of the region of attraction. Using the same logic, it must be determined where η' of (6.2) is equal to two. Unfortunately, there is not a closed-form representation of the curve $\eta' = 2$ [¶] unlike the strictly in-plane problem. A numerical representation of $\eta' = 2$ can be studied by looking at the contour of η' at two for a fixed value of ϕ_A and ϕ_B. Contours for a range of ϕ_* values is shown in Figure 6.3. As the misalignments get larger, the contours grow in size, but the contours are always isolated away from the true misalignments. In fact, all of the contours regardless of the value of the

[§]Following the steps in [50] Chapter 5 and performing a great deal of tedious algebra as shown in Appendix C

[¶]There is not an equation $\hat{\phi}_B = h(\hat{\phi}_A, \phi_A, \phi_B)$. Recall that for the strictly in-plane problem that the $\eta = 2$ contour contained the lines $\hat{\theta}_B = \hat{\theta}_A \pm \pi/2$.

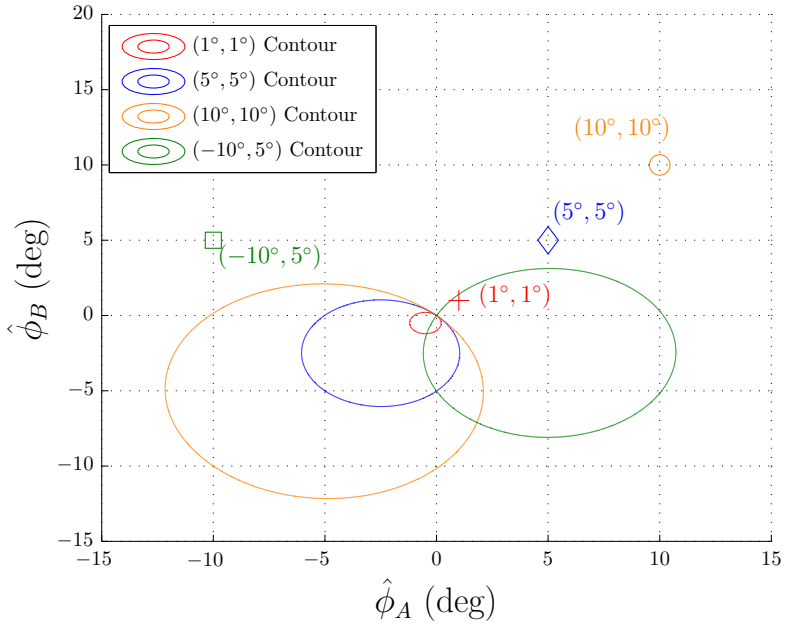

Figure 6.3: Plot of several contours associated with $\eta' = 2$ for varying values of the misalignments. Note that the contour is positioned away from the misalignment and passes through $(0, 0)$

misalignments pass through the origin. This can be easily verified by substituting $\hat{\phi}_A = \hat{\phi}_B = 0$ into η' from which one will find $\eta' = 1 + 1 = 2$. Clearly, a region of attraction exists for all values of the misalignments. The issue is that the region of attraction is a function of the values of the *unknown* misalignments. Moreover, there is not a maximum region of attraction that is valid for a large set of misalignment values like the result for the strictly in-plane problem. In fact, for infinitesimally small misalignment errors, the region of attraction is also infinitesimally small. Despite this issue, there is some hope as to creating a general proof of convergence for the strictly out-of-plane problem. Note that the $\eta' = 2$ contour never enters the quadrant [‖] that contains the true misalignments. Therefore, if an assumption was made that the sign of each misalignment angle is known, a projection scheme could be used to bound the

[‖]The $\hat{\phi}_A\hat{\phi}_B$-plane is divided into four sections by the $\hat{\phi}_A = 0$ and $\hat{\phi}_B = 0$ axes. Each of the four sections is referred to here as a quadrant.

estimates in the correct quadrant and convergence for the estimation errors could be guaranteed. This is an unsatisfying solution because it is not expected that a priori information is known about the sign of the misalignments angles; consequently, this solution is ignored. The second possibility comes from the fact that the contour only passes through and does not contain the origin. Recall that the origin is the point where no knowledge is assumed on the misalignments, and the estimates are guessed as the ideal control axes. Using the standard level curve $V = 2\sin^2(\phi_A/2) + 2\sin^2(\phi_B/2)$ which is the situation where the initial estimates are zero, it is clear that this level curve also passes through the origin. If it could be shown that the level curve and $\eta' = 2$ contour only meet at one point for every set of true misalignments, then V would be a region of attraction for *all* sets of misalignments. Since there is no closed form solution for $\eta' = 2$, finding other possible intersection points analytically is an extremely difficult problem. Unfortunately, the hypothesis that there is only one intersection can be disproved through some simple numerical studies. A plot of the contour and the level curve for $\phi_A = 35°$ and $\phi_B = 15°$ is shown in Figure 6.4. From a macroscopic

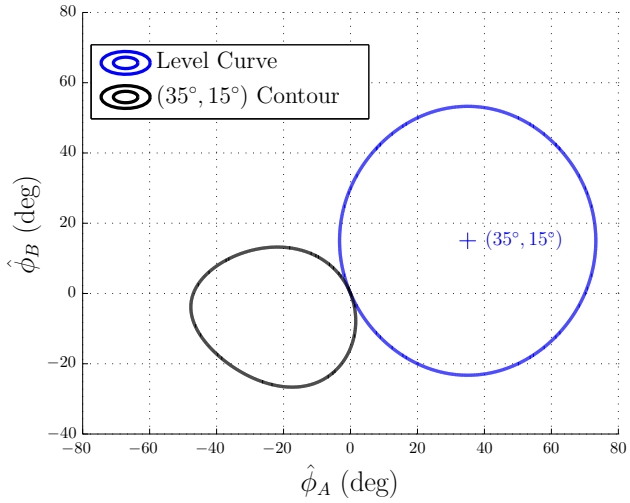

Figure 6.4: Plot of contour associated with $\eta' = 2$ and the level curve associated with V when the true misalignments are $\phi_A = 35°$ and $\phi_B = 15°$

view, it appears as if the two curves only intersect at the origin. At minimum, it is clear that there is not a large region of overlap. To actually see an overlap of the

two curves, the view must be zoomed in considerably as shown in Figure 6.5. For

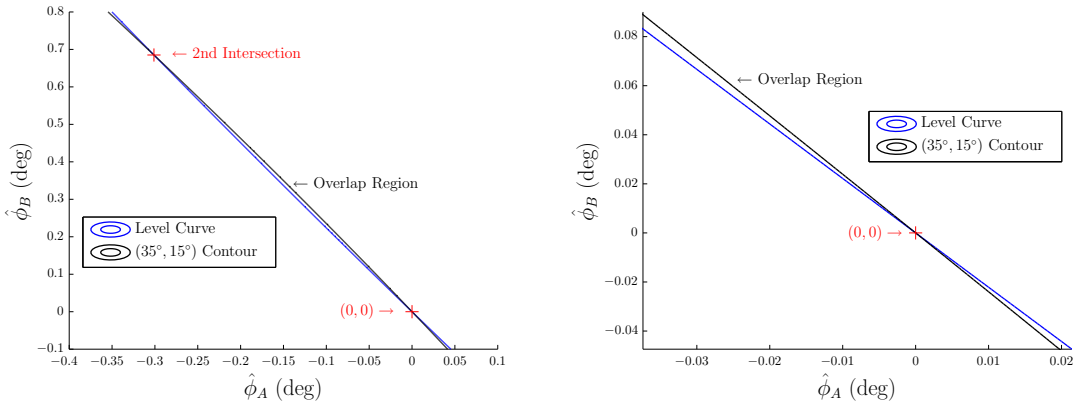

(a) View of entire overlap region

(b) View around the origin

Figure 6.5: Plot of contour associated with $\eta' = 2$ and the level curve associated with V zoomed in to the overlap region near the origin when the true misalignments are $\phi_A = 35°$ and $\phi_B = 15°$

the remainder of this chapter, the area where the $\eta' = 2$ contour passes into the V level curve will be referred to as the "overlap region." The second intersection point can be found by numerically solving a multi-dimensional root-finding problem. For the set of misalignments considered, the second intersection occurs at $\phi_A \approx -0.3011°$ and $\phi_B \approx 0.6851$. Despite how "minuscule" the overlap region is, its appearance prevents the level curve for V from being a region of attraction since the derivative of the Lyapunov function is not negative semi-definite everywhere therein. In fact, the overlap region introduces the possibility that a trajectory could move into the contour (inside the black curve) and the value of the level curve will increase. In any case, the overlap region exists for all sets of misalignments *except* when $\phi_A = \phi_B$. In this case, the intersection that occurs at the origin is the *only* intersection of the two curves; however, this set of misalignments is extremely unique and unlikely in a general sense and therefore cannot be considered.

The region of attraction can still be determined numerically by solving an optimization problem. The problem for a given set of misalignments is to maximize $V = 2\sin^2(\tilde{\phi}_A/2) + 2\sin^2(\tilde{\phi}_B/2)$ subject to the inequality constraint $\eta' \leq 2$.

Note that this solution will be fractionally smaller than the level curve considered above; however, the region of attraction *will not* contain the origin as an initial guess for the estimates of the misalignment angles. As a result, a priori information on the out-of-plane misalignments must be assumed in order to guarantee convergence. This contention is extremely unsatisfying from a practical standpoint. Unfortunately, without a change to the estimation scheme, this issue cannot be avoided through the proposed analysis.

Assuming that the proposed observer was not changed, an allowable set of misalignments could be determined by examining the level curve. Since the region of attraction is only fractionally smaller than the level curve associated with the new estimates being zero, the level curve will be used as a conservative estimate. Now, assume the true misalignments are such that $|\phi_A|, |\phi_B| < \phi_P$, then $V(0) \leq 4\sin^2(\phi_P/2)$. Since V is non-increasing in the region of attraction, it is possible for $\tilde{\phi}_A = 0$ which would maximize how large $\tilde{\phi}_B$ could become because $V(t) \leq V(0)$. If the constraint that $|\hat{\phi}_B| \leq \pi/2$ is added, the expression

$$4\sin^2\left(\frac{\phi_P}{2}\right) = 2\sin^2\left(\frac{\pi/2 - \phi_P}{2}\right)$$

can be solved to find that $\phi_P = \pi/5$. Thus, if $\phi_P \leq 36°$, then there always exists a region of attraction such that $|\hat{\phi}_A|, |\hat{\phi}_B| < \pi/2$. Unfortunately, this is not much of a result since there is no general rule of thumb to selecting the initial guess of the estimates, and projection is not a viable option since η' is not a fixed contour as in the strictly in-plane problem.

6.2.4 Numerical Analysis

Although there is not a proof of convergence for the proposed scheme, it is interesting to examine the numerically simulated behavior of the trajectories for the out-of-plane problem. To begin, the set of misalignments of the previous section are analyzed. For $\phi_A = 35°$ and $\phi_B = 15°$, three trajectories were simulated with a learning rate of $\gamma = 1$. The first trajectory starts at $\hat{\phi}_A(0) = 0$ and $\hat{\phi}_B(0) = 0$ which is at the intersection of the contour and level curve. The second trajectory starts

at $\hat{\phi}_A(0) = -35°$ and $\hat{\phi}_B(0) = 0$ which is inside of the contour. The final trajectory starts at $\hat{\phi}_A(0) = -60°$ and $\hat{\phi}_B(0) = -20°$ which is near to but outside of the contour. The three trajectories are shown along with the contour and level curve in Figure 6.6. In the first set of simulations in Figure 6.6(a), the input is persistently exciting, where

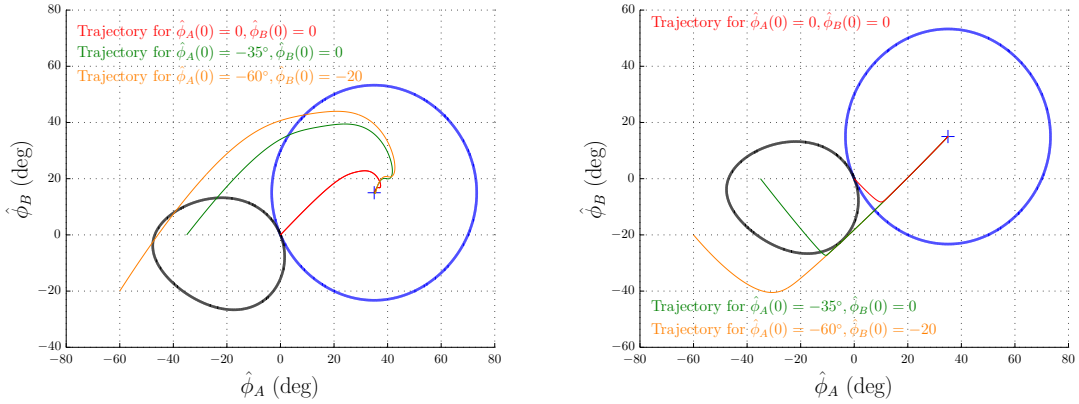

(a) PE input (b) Constant input

Figure 6.6: Plot of several trajectories for $\phi_A = 35°$ and $\phi_B = 15°$ with varying initial estimates

as, the simulations in Figure 6.6(b) only have constant inputs. The two signals are

$$\mathbf{u}_f(t) = \begin{bmatrix} \cos(t/10) \\ -\cos(t/2) \\ \sin t \sin(t/2) \end{bmatrix}; \qquad \mathbf{u}_f = \begin{bmatrix} 1 \\ -1 \\ 1 \end{bmatrix}$$

Regardless of the input signal, the trajectories converge to the true values of the misalignments even when the initial estimates are inside of the $\eta' = 2$ contour (black). For the constant input case, it is clear that the values are initially moving to the stable manifold and then converging. ** When the initial estimate starts inside of the $\eta' = 2$ contour (black) the Lyapunov derivative is positive which means that the V level curve (blue) is increasing; however, the estimates are such that eventually the trajectory (green) leaves the $\eta' = 2$ closed contour at which point the derivative is guaranteed to be negative definite. As long as the trajectory does not re-enter the

**Although it is not clear from the plots, the convergence for the constant input case is much slower than using the PE signal.

$\eta' = 2$ contour, the level curve will decrease to the region of attraction and convergence is then guaranteed. Clearly, this is not a proof of convergence, but it does indicate that convergence is possible (if not expected) outside the region of attraction. This is especially important for the initial guess $\hat{\phi}_A(0) = 0$ and $\hat{\phi}_B(0) = 0$. Starting inside of the $\eta' = 2$ contour occurs because of a terrible guess, where as, $\hat{\phi}_A(0) = 0$ and $\hat{\phi}_B(0) = 0$ would be a desired initial guess when no information on the misalignments is available.

To show the performance of the observer when $\hat{\phi}_A(0) = 0$ and $\hat{\phi}_B(0) = 0$, two Monte Carlo simulations were run for 500 random sets of true misalignments. The first set assumed the PE signal, and the second set assumed the constant input as above. The true misalignments were bounded between $-\pi/4$ and $\pi/4$. The results for the PE and constant signals are shown in Figure 6.7 (a) and (b), respectively. Note that the axes on the plots are the errors $\tilde{\phi}_A$ and $\tilde{\phi}_B$. For every single run the estimates approach their true values regardless of the input signal used. In no way is this a claim of victory for every single possible input signal since a numerical analysis is not a rigorous mathematical proof. It should be noted, however, that in order to converge for $\hat{\phi}_A(0) = 0$ and $\hat{\phi}_B(0) = 0$, the trajectory only needs to avoid the tiny overlap region so that the level curve can be reduced by the fractional amount needed to enter the guaranteed region of attraction. Furthermore, even if the trajectory enters the overlap region, the trajectory only needs to leave the inside of the closed contour at some point to potentially return to the region of attraction. Thus, the numerical analysis *strongly* indicates that $\hat{\phi}_A(0) = 0$ and $\hat{\phi}_B(0) = 0$ will lead to convergence for all reasonable values of the misalignments for the certainty-equivalence like observer.

6.3 Scheduled Axis Decoupling

The discussion of the previous section motivates a control scheme that proves convergence of the observer while still guaranteeing perfect tracking. The observer cannot be proven to converge when $\hat{\phi}_A(0) = 0$ and $\hat{\phi}_B(0) = 0$ because it cannot be proved that the trajectory always moves from the initial condition to the region of

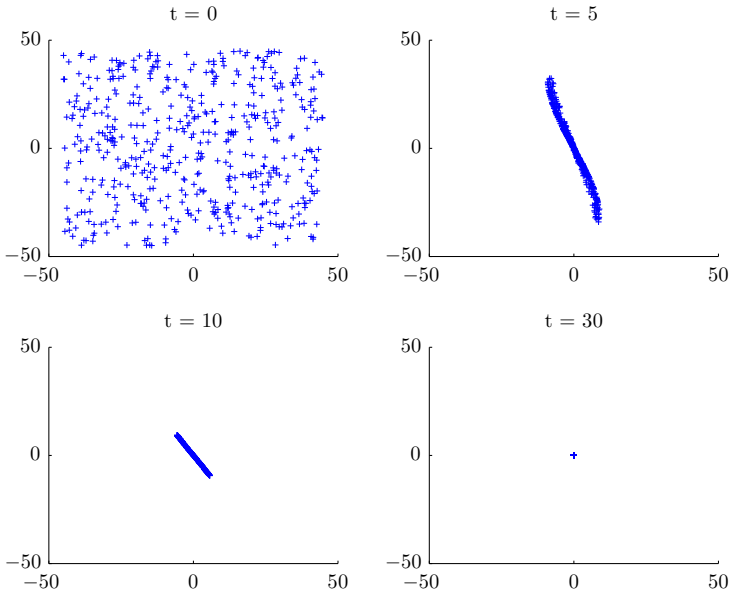

(a) PE input

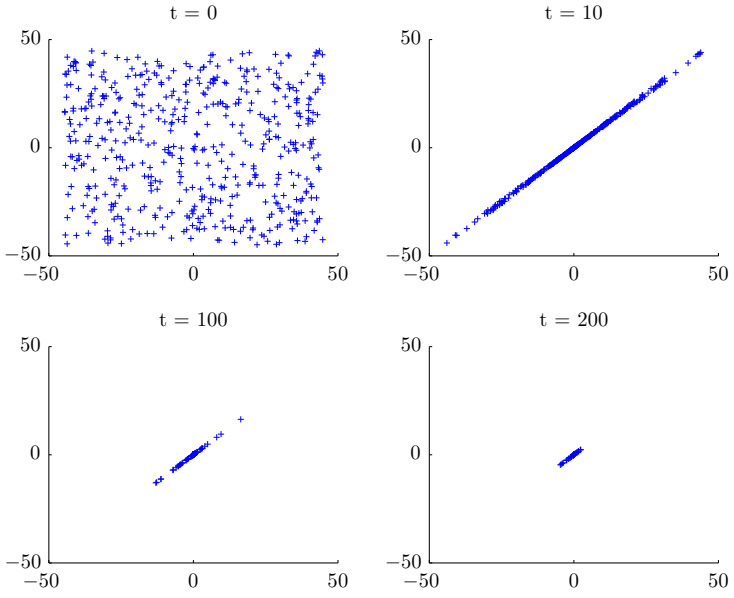

(b) Constant input

Figure 6.7: Monte Carlo simulation for 500 random sets of true misalignments between $-\pi/4$ and $\pi/4$ with initial estimates $\hat{\phi}_A(0) = \hat{\phi}_B(0) = 0$

attraction for *any input signal* $\mathbf{u}_f$. For the control problem, however, the input to the measurement equation is the filtered control signal which can be chosen. Consequently, for a brief period of time say, $T_{\min} > 0$, let $\mathbf{u}_A$ = constant and $\mathbf{u}_B = 0$. [††] Using the certainty-equivalence like observer, this will allow the estimation error on A to converge enough (B will remain constant) for the level curve to be reduced into the region of attraction at which point the designed control signal can be implemented as per usual. This process decouples the estimation down to a single axis.

6.3.1 Determining $T_{\min}$

The open question is whether there exists a $T_{\min}$ for which decoupling the axis to perform estimation guarantees that the estimation values enter the region of attraction for *all* allowable sets of misalignments. To address this question, it is first necessary to relate the decoupled observer to time. Consider the Lyapunov-like function,

$$V_A = 2\sin^2\left(\frac{1}{2}\tilde{\phi}_A\right) \tag{6.7}$$

with the new dynamics for the estimation errors when $u_{f,A}$ is constant and $u_{f,B} = 0$

$$\dot{\tilde{\phi}}_A = -\gamma \sin\tilde{\phi}_A \, u_{f,A}^2 \tag{6.8a}$$

$$\dot{\tilde{\phi}}_B = 0 \tag{6.8b}$$

Taking the derivative of (6.7) and using (6.8a) yields

$$\begin{aligned}
\dot{V}_A &= -\gamma \sin^2\tilde{\phi}_A \, u_{f,A}^2 \\
&= -4\gamma \sin^2\left(\frac{1}{2}\tilde{\phi}_A\right)\cos^2\left(\frac{1}{2}\tilde{\phi}_A\right) \, u_{f,A}^2 \\
&= -\gamma\left[2\sin^2\left(\frac{1}{2}\tilde{\phi}_A\right)\right]\left[2 - 2\sin^2\left(\frac{1}{2}\tilde{\phi}_A\right)\right] \, u_{f,A}^2 \\
&= -\gamma u_{f,A}^2 \left[V_A\left(2 - V_A\right)\right]
\end{aligned} \tag{6.9}$$

[††]Note that the same discussion could be made for the alternate case where $\mathbf{u}_B$ = constant and $\mathbf{u}_A = 0$

This is a differential equation that can be solved using separation of variables and leads to the solution of $V_A(t)$ given by

$$V_A(t) = \frac{2Le^{-2\gamma u_{f,A}^2 t}}{1 + Le^{-2\gamma u_{f,A}^2 t}} \tag{6.10}$$

where

$$L = \frac{V_A(0)}{2 - V_A(0)}$$

Thus, $V_A(t)$ is strictly decreasing with the rate of decay related to γ and the constant value $u_{f,A}$. Let the value $\check{V}_A$ be the value of the level curve associated with the region of attraction, and let $V_A(0)$ be the initial value corresponding to the level curve where $\hat{\phi}_A(0) = 0$ and $\hat{\phi}_B(0) = 0$. Define the ratio

$$\Omega = \frac{\check{V}_A}{V_A(0)} \tag{6.11}$$

which will ultimately be related to the size of the overlap region between the $V_A(0)$ and the $\eta' = 2$ contour discussed in the previous section. It is now possible to search for the value T such that $V_A(T) = \check{V}_A$. Using algebraic manipulation and introducing the ratio in (6.11), T can be represented as

$$T = -\frac{1}{2\gamma u_{f,A}^2} \ \ln\left[\frac{2\Omega - \Omega V_A(0)}{2 - \Omega V_A(0)}\right] \tag{6.12}$$

Note that the value inside of $\ln[\cdot]$ is less than or equal to 1 such that $T \geq 0$. For fixed values of γ and $u_{f,A}$, T increases as Ω decreases and $V_A(0)$ increases. Therefore, if there exists $\Omega_{\min}$ and $V_{A,\max}$ over the allowable set of misalignments then $T_{\min}$ will also exist. $V_{A,\max}(0)$ clearly exists since $V_A(0)$ increases as the magnitude of the misalignment increases. Accordingly,

$$V_{A,\max}(0) = 2\sin^2\left(\frac{1}{2}\phi_P\right) \tag{6.13}$$

The determination of $T_{\min}$ is dependent on the size of the overlap region which must be determined over the entire range of allowable values.

For fixed values of ϕ_A and ϕ_B, the ratio Ω can be determined by solving an optimization problem. Consider the problem of minimizing $\Omega = \check{V}/V(0)$, where V(0)

represents the level curve associated with zero initial estimates and $\check{V}$ represents the level curve which is the region of attraction, subject to the constraint $\eta' = 2$. [‡‡] In order to gain some insight into whether a minimum value exists, the minimization problem can be solved for a grid of misalignments across the allowable set of misalignments, $|\phi_A|, |\phi_B| < \pi/5$ (36°). The results of the analysis are shown in Figure 6.8. The second plot of 6.8(b) is zoomed in on the first octant. The plot shows that the

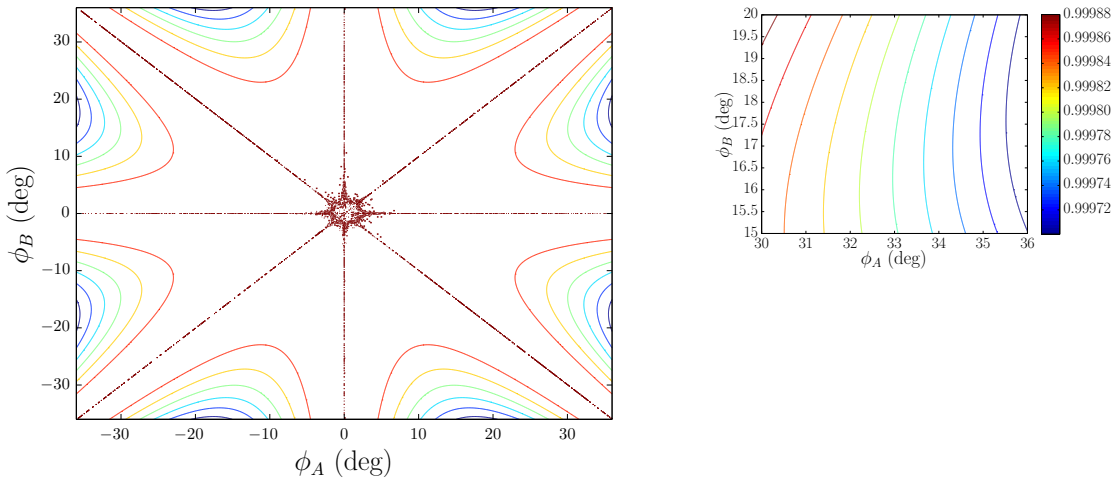

(a) PE input

(b) Constant input

Figure 6.8: Contour plot of the value of Ω for a grid of misalignments in the allowable region. Note that there appears to be 8 minimums which correspond to combinations of the same magnitude ϕ_A and ϕ_B

allowable region is divided into octants which are separated by the contours of 1. These contours occur because there is only one intersection point and the overlap region does not exist. As mentioned previously, this occurs when one of the misalignment angles is zero or the magnitudes of the angles are equal. Within each octant there appears to be one minimum giving a total of 8 minimums; however, the magnitudes of the misalignments can be related for the minimums. One of the angles

[‡‡] All that is being done is determining the region of attraction for a particular set of misalignments as was done before by solving a maximization problem. The reason the same problem is recast as a minimization problem of the ratio is that the misalignments will be allowed to be free variables in order to determine $\Omega_{\min}$.

has a maximized value (36°) while the other appears to be approximately half the maximum value. To find the true minimum, the minimization problem where ϕ_A and ϕ_B are now free but are subject to the constraint $\phi_* \leq (\pi/5)^2$ can be solved. Using MATLAB's constrained optimization function with all tolerances at 1×10^{-10} and an initial guess $\phi_A = 36°$ and $\phi_B = 20°$, the solution $\Omega \approx 0.99968$ is found at $\phi_A = 36°$ and $\phi_B \approx 17.97°$. From these results, let

$$\Omega_{\min} = 0.99965 \tag{6.14}$$

as a conservative choice to account for any numerical errors. Plugging $\Omega_{\min}$ of (6.14) and $V_{A,\max}(0)$ of (6.13) into the expression for T of (6.12) gives the value of $T_{\min}$ as

$$T_{\min}(\gamma, u_{f,A}) = \frac{0.0001935}{\gamma u_{f,A}^2} \tag{6.15}$$

Therefore, if $\gamma = u_{f,A} = 1$ then the scheduled axis decoupling needs to occur for $T > 1.935 \times 10^{-4}$ seconds to ensure that the estimates start in the region of attraction when the desired control signal is implemented.

6.3.2 Control Problem

Consider the control problem for the error system of (2.4) and attempt to determine a control law to perform perfect tracking. Assuming use of the filtered signals on $\mathbf{e}_2$ and $\mathbf{g}$ as shown in (2.19a) and (2.19b) and defining $\mathbf{y}$ as in the standard fashion

$$\mathbf{y} \equiv \dot{\mathbf{e}}_{2,f} - \mathbf{g}_f$$

let the control $\mathbf{u}$ be determined in two parts. First for $0 \leq t < T$, let the control be given by

$$\mathbf{u}(t) = \begin{bmatrix} h \\ 0 \\ 0 \end{bmatrix} \tag{6.16}$$

where h is a scalar constant. For $t \geq T$, let the control be determined through

$$\mathbf{u} = -\hat{\mathbf{\Psi}}^{-1} \left(\mathbf{g} + \alpha \left(k_p \mathbf{e}_1 + \mathbf{e}_2 \right) - \begin{bmatrix} -\sin\hat{\phi}_A & 0 & 0 \\ 0 & -\sin\hat{\phi}_B & 0 \\ \cos\hat{\phi}_A & \cos\hat{\phi}_B & 0 \end{bmatrix} \begin{bmatrix} \dot{\hat{\phi}}_A & 0 & 0 \\ 0 & \dot{\hat{\phi}}_B & 0 \\ 0 & 0 & 0 \end{bmatrix} \hat{\mathbf{\Psi}}^{-1} \hat{\mathbf{y}} \right) \tag{6.17}$$

wherein $k_p, k_v > 0$ are scalar constants. In addition, let the estimates on the vectors $\hat{\mathbf{\Psi}}_A$ and $\hat{\mathbf{\Psi}}_B$ be determined by the standard certainty-equivalence like observers of (5.8) given by

$$\dot{\hat{\mathbf{\Psi}}}_A = -\gamma S\left[(\mathbf{y} - \hat{\mathbf{y}}_B - \mathbf{y}_C) \times \hat{\mathbf{y}}_A\right] \hat{\mathbf{\Psi}}_A$$
$$\dot{\hat{\mathbf{\Psi}}}_B = -\gamma S\left[(\mathbf{y} - \hat{\mathbf{y}}_A - \mathbf{y}_C) \times \hat{\mathbf{y}}_B\right] \hat{\mathbf{\Psi}}_B$$

which using some algebraic manipulation can be represented as update laws on the angles

$$\dot{\hat{\phi}}_A = \gamma\left[\hat{\mathbf{y}}_{A,1}\left(\mathbf{y}_3 - \hat{\mathbf{y}}_{B,3} - u_{f,C}\right) - \hat{\mathbf{y}}_{A,3}\mathbf{y}_1\right] \tag{6.18a}$$
$$\dot{\hat{\phi}}_B = \gamma\left[\hat{\mathbf{y}}_{B,2}\left(\mathbf{y}_3 - \hat{\mathbf{y}}_{A,3} - u_{f,C}\right) - \hat{\mathbf{y}}_{B,3}\mathbf{y}_2\right] \tag{6.18b}$$

The following theorem can then be stated:

Theorem 6.3.1. *Consider the tracking error dynamics of (2.4) where* $\mathbf{f}$ *is such that the system dynamics of (2.2) are input-to-state stable. Suppose that control signal is given by (6.16) and (6.17) with the update laws of (6.18). Then the convergence condition*

$$\lim_{t\to\infty} \begin{bmatrix}\mathbf{e}_1(t)\\ \mathbf{e}_2(t)\end{bmatrix} = \mathbf{0}$$

is applicable for all admissible reference trajectories $\mathbf{r}$ *and initial conditions* $[\mathbf{x}_1(0), \mathbf{x}_2(0)]^\top$ *provided that* $|\phi_A|, |\phi_B| < \pi/5$, $\hat{\phi}_A(0) = \hat{\phi}_B(0) = 0$, *and* $T \geq T_{min}$ *where* T_{min} *is defined as in (6.15). In addition, let the gain* $\alpha = 1$ *when* $t < T$ *and* $\alpha = k_p + k_v$ *when* $t \geq T$.

Proof. As always, the filters can be used to find the filter error dynamics and recover the measurement equation. Now consider the first portion of the control from $0 \leq t < T$. Recall that the definition of the filter signal on the control is $\dot{\mathbf{u}}_f = -\alpha \mathbf{u}_f + \mathbf{u}$. If $\mathbf{u}$ is constant this differential equation can be solved and has the solution

$$\mathbf{u}_f(t) = \frac{1}{\alpha}\mathbf{u} + \left[\mathbf{u}_f(0) - \frac{1}{\alpha}\mathbf{u}\right] e^{-\alpha t} \tag{6.19}$$

Choose $\alpha = 1$ and select $\mathbf{u}_f(0) = h$, then $\mathbf{u}_f = \mathbf{u} =$ constant. Using the discussion of Section 6.5.1, if T is chosen such that $T \geq T_{\min}$, then $\hat{\phi}_A(T)$ and $\hat{\phi}_B(T) = 0$ is

guaranteed to be in the region of attraction of (ϕ_A, ϕ_B). Furthermore, since the system dynamics of (2.2) are ISS, the state will remain bounded during the application of the bounded input $\mathbf{u} = \begin{bmatrix} h & 0 & 0 \end{bmatrix}^\top$. Therefore, the tracking errors are bounded, and the estimates of the misalignment angles are within the region of attraction at $t = T$.

Next consider the second portion of the control which has been designed to achieve perfect tracking of the reference trajectory. Consider the Lyapunov-like function for the estimation terms given by

$$V_E = 2\sin^2\left(\frac{1}{2}\tilde{\phi}_A\right) + 2\sin^2\left(\frac{1}{2}\tilde{\phi}_B\right) \tag{6.20}$$

which has the derivative

$$\begin{aligned}
\dot{V}_E &= -\gamma \sin^2\tilde{\phi}_A\, u_{f,A}^2 - \gamma \sin^2\tilde{\phi}_B\, u_{f,B}^2 \\
&\quad - \gamma\left[\frac{\cos\hat{\phi}_A \cos\left(\frac{1}{2}\bar{\phi}_B\right)}{\cos\left(\frac{1}{2}\tilde{\phi}_B\right)} + \frac{\cos\hat{\phi}_B \cos\left(\frac{1}{2}\bar{\phi}_A\right)}{\cos\left(\frac{1}{2}\tilde{\phi}_A\right)}\right] \sin\tilde{\phi}_A \sin\tilde{\phi}_B\, u_{f,A}\, u_{f,B} \\
&\leq -\gamma|\sin\tilde{\theta}_A\, u_{f,A}|^2 - \gamma|\sin\tilde{\theta}_B u_{f,B}|^2 + \gamma\eta'\,|\sin\tilde{\theta}_A\, u_{f,A}|\,|\sin\tilde{\theta}_B\, u_{f,B}|
\end{aligned}$$

Since the estimates are guaranteed to be within the region of attraction at $t = T$, $\eta' < 2$, and completion of squares can be performed, resulting in

$$\dot{V}_E \leq -\gamma' ||\mathbf{z}(\tilde{\phi})||^2 \leq 0 \tag{6.21}$$

where $\gamma' > 0$ is a scalar constant dependent on the maximum value of η' which is dependent on T. Let $\Lambda \in \mathbb{R}^{3\times 3}$ be given by

$$\Lambda = \begin{bmatrix} \sin\left(\frac{1}{2}\bar{\phi}_A\right) & 0 & 0 \\ 0 & \sin\left(\frac{1}{2}\bar{\phi}_B\right) & 0 \\ -\cos\left(\frac{1}{2}\bar{\phi}_A\right) & -\cos\left(\frac{1}{2}\bar{\phi}_B\right) & 0 \end{bmatrix} \tag{6.22}$$

Note that the $||\Lambda|| < 1$, since the largest eigenvalue of $\Lambda^\top\Lambda$ is 1. Consider the Lyapunov function on the control terms

$$V_C = \frac{1}{2}\mathbf{e}_1^\top\mathbf{e}_1 + \frac{1}{2}\mathbf{e}_{2,f}^\top\mathbf{e}_{2,f} \geq 0 \tag{6.23}$$

which has been shown to have the derivative

$$\begin{aligned}\dot{V}_C &\leq -k_p||\mathbf{e}_1||^2 - k_v||\mathbf{e}_{2,f}||^2 + 2||\mathbf{e}_1 + \mathbf{e}_{2,f}||\,||\Lambda||\,||\mathbf{z}_{1/2}(\tilde{\phi})|| \\ &\leq -k_p||\mathbf{e}_1||^2 - k_v||\mathbf{e}_{2,f}||^2 + 2\sqrt{2}\left(||\mathbf{e}_1|| + ||\mathbf{e}_{2,f}||\right)||\mathbf{z}(\tilde{\phi})|| \end{aligned} \tag{6.24}$$

Finally using the standard combined Lyapunov-like function $V = V_C + \tau V_E$, the derivative can be expressed as

$$\dot{V} \leq -\frac{k_p}{2}||\mathbf{e}_1||^2 - \frac{k_v}{2}||\mathbf{e}_{2,f}||^2 - k_z||\mathbf{z}(\tilde{\phi})||^2 \leq 0 \tag{6.25}$$

where τ has been selected to be large enough to ensure that the estimation error term is negative semi-definite. Note that $k_z > 0$ is a scalar constant whose value depends on the choice of gains. Thus, $\dot{V}$ is negative semi-definite, indicating boundedness for all closed-loop signals. Further, because V is lower-bounded, it is known that $\int_0^\infty \dot{V}(t)\,dt$ exists and is finite which taken together with (6.25) implies that $\mathbf{e}_1, \mathbf{e}_{2,f}, \mathbf{z}(\tilde{\phi}) \in \mathcal{L}_2 \cap \mathcal{L}_\infty$. This also implies that $\dot{\mathbf{e}}_1, \dot{\mathbf{e}}_{2,f} \in \mathcal{L}_\infty$ from (2.4a) and (5.20). Again, it can be shown that $\dot{\mathbf{z}} \in \mathcal{L}_\infty$. Therefore, invoking Barbalat's Lemma yields

$$\lim_{t\to\infty}[\mathbf{e}_1 \quad \mathbf{e}_{2,f} \quad \mathbf{z}(t)] = \mathbf{0}$$

By construction of the filter dynamics, $\mathbf{e}_{2,f}(t) \to \mathbf{0}$ implies $\mathbf{e}_2(t) \to \mathbf{0}$ as $t \to \infty$, and the control objectives are met. The stability analysis reveals that $\mathbf{z}$ also goes to zero asymptotically; however, this does not inherently lead to convergence of the parameter estimates to their true values. Thus, no additional guarantees can be made and upon recovering the control through $\mathbf{u} = \alpha\mathbf{u}_f + \dot{\mathbf{u}}_f$ the proof is complete. □

6.3.3 Remarks

a) The idea of Scheduled Axis Decoupling can only be used for the control problem where the control signal and ultimately the input to the measurement equation can be directly specified by the user. The only requirement for convergence of the tracking errors beyond input-to-state stability is the amount of time of the constant input be greater than $T_{\min}$. This means that T could be arbitrarily long such that the estimate of one axis has time to converge to the true value. In theory, this idea could be applied

equally across all axes to determine the true misalignment for each axis. The issue with increasing T is clearly that the magnitude of the state will most likely increase. This would be especially troublesome for the spacecraft attitude tracking problem since the constant input will have the effect of "spinning-up" the spacecraft. In this case, however, the first portion of the control could be split into two parts. When $t \leq T/2$, the constant control could be applied to a single axis. For the remainder of the time, the opposite constant control could be applied. Thus, the spacecraft would be "spun-up" and then "spun-down" while learning the value of one of the misalignments. Note that this same idea could be applied to the strictly in-plane problem, but it is not necessary to ensure convergence.

b) The requirement of input-to-state stability comes from the possibility of finite-time escapes for nonlinear systems. Therefore, it must be shown that the state of the system will not escape to infinity during the time that the constant input is applied. This will only be guaranteed for a general nonlinear system when $\mathbf{f}(\mathbf{x}_1, \mathbf{x}_2)$ is such that (2.2) is ISS. If $\mathbf{f}$ is such that the terms are linear in $\mathbf{x}_1$ and $\mathbf{x}_2$, then the standard unforced system dynamics are linear which only requires $\mathbf{A}$ to be Hurwitz. Of particular interest in this dissertation is whether the rigid-body attitude dynamics are ISS. Interestingly, the rigid-body attitude dynamics are *not* ISS since the unforced system is only stable in the sense of Lyapunov and not globally asymptotically stable; however, as an alternative, it only needs to be shown that the angular velocity remains bounded while the constant input is being applied. This is guaranteed through the following lemma:

Lemma 6.3.2. *There exist constants δ and ζ such that the solution of the rigid-body attitude dynamics of (3.1) and (3.2) satisfy*

$$||\mathbf{q}(T)|| \leq \delta$$
$$||\boldsymbol{\omega}(T)|| \leq \zeta$$

when the control signal $\mathbf{u}$ = constant is applied from $0 < t < T$.

Proof. Since the attitude must be in a finite direction, and the quaternion satisfies the unit-norm constraint $||\mathbf{q}(t)|| = 1$, it is trivial to select $\delta = 1$ to show boundedness of the quaternion. Therefore, the only significant consideration is to show that the angular velocity remains bounded during the application of the input. Assume that the input $\mathbf{u}$ is constant. Define the scalar signal

$$v(t) = \frac{J_{\min}}{2}\boldsymbol{\omega}^\top \mathbf{J}\boldsymbol{\omega} \tag{6.26}$$

where $J_{\min}$ is the minimum eigenvalue of the positive definite, symmetric matrix $\mathbf{J}$. Note that $v(0) = \boldsymbol{\omega}(0)^\top \mathbf{J}\boldsymbol{\omega}(0)$. Further, recall that for the quadratic form $\boldsymbol{\omega}^\top \mathbf{J}\boldsymbol{\omega}$

$$J_{\min}||\boldsymbol{\omega}||^2 \leq \boldsymbol{\omega}^\top \mathbf{J}\boldsymbol{\omega} \leq J_{\max}||\boldsymbol{\omega}||^2 \tag{6.27}$$

where $J_{\max}$ is the maximum eigenvalue of $\mathbf{J}$. Taking the derivative of (6.26) along (3.1) yields

$$\begin{aligned}\dot{v}(t) &= -J_{\min}\boldsymbol{\omega}^\top S(\boldsymbol{\omega})\mathbf{J}\boldsymbol{\omega} + J_{\min}\boldsymbol{\omega}^\top \mathbf{u} \\ &= J_{\min}\boldsymbol{\omega}^\top \mathbf{u}\end{aligned}$$

where the first term is zero since $\boldsymbol{\omega}^\top S(\boldsymbol{\omega}) = \boldsymbol{\omega} \times \boldsymbol{\omega} = \mathbf{0}$. Adding and subtracting $\frac{1}{2}\boldsymbol{\omega}^\top \mathbf{J}\boldsymbol{\omega}$ and $\frac{1}{2}\mathbf{u}^\top \mathbf{J}\mathbf{u}$, and applying the lower bound inequality of (6.27) produces

$$\begin{aligned}\dot{v}(t) &\leq \frac{1}{2}\boldsymbol{\omega}^\top \mathbf{J}\boldsymbol{\omega} + \frac{1}{2}\mathbf{u}^\top \mathbf{J}\mathbf{u} - \left(\frac{J_{\min}}{2}||\boldsymbol{\omega}||^2 - J_{\min}||\boldsymbol{\omega}||\,||\mathbf{u}|| + \frac{J_{\min}}{2}||\mathbf{u}||^2\right) \\ &\leq \frac{1}{J_{\min}}v(t) + \frac{1}{2}\mathbf{u}^\top \mathbf{J}\mathbf{u} - \frac{J_{\min}}{2}\left(||\boldsymbol{\omega}|| - ||\mathbf{u}||\right)^2 \\ &\leq \frac{1}{J_{\min}}v(t) + \frac{1}{2}\mathbf{u}^\top \mathbf{J}\mathbf{u}\end{aligned}$$

where the non-positive quadratic term has been dropped since it only reduces the upper bound. Next, define the signal $s(t)$ such that

$$\dot{s} = \frac{1}{J_{\min}}s(t) + \frac{1}{2}\mathbf{u}^\top \mathbf{J}\mathbf{u} \tag{6.28}$$

with $s(0) = v(0)$. Note that the dynamics of $s(t)$ has the exact same structure as the upper bound on the derivative of $v(t)$. The differential equation of (6.28) has the solution

$$s(t) = \left[s(0) + \frac{J_{\min}}{2}\mathbf{u}^\top \mathbf{J}\mathbf{u}\right] e^{(t/J_{\min})} - \frac{J_{\min}}{2}\mathbf{u}^\top \mathbf{J}\mathbf{u} \tag{6.29}$$

By direction application of the Comparison Lemma [50], $v(t) \leq s(t)$ for all $t \in [0, T)$. Also, from the quadratic form of $v(t)$, it can be established that

$$\frac{J_{\min}^2}{2}||\boldsymbol{\omega}(T)||^2 \leq s(T)$$

Choosing

$$\zeta = \frac{2\sqrt{s(T)}}{J_{\min}^2} \tag{6.30}$$

guarantees that $||\boldsymbol{\omega}(T)|| \leq \zeta$ for *any* constant input $\mathbf{u}$. Thus, the same condition is met when $\mathbf{u} = \begin{bmatrix} h & 0 & 0 \end{bmatrix}^\top$, and the proof is complete. □

Although the rigid-body attitude dynamics are not input-to-state stable, the trajectories do not escape infinitely fast when a constant input is applied. Obviously, the solution can only be upper bounded by an exponential which means that the angular velocity could become very "large" as T is increased. Fortunately, the Scheduled Axis Decoupling methodology does not require that the constant input be applied for a significant duration. Note that since Lemma 6.3.2. is valid for all constant inputs, the result could be applied for any of the three axes.

c) Note that nothing has been changed in the observer to this point. The exact same vector update laws have been used in the in-plane and out-of-plane results. The ability to chose the input signal of the measurement equation was used to overcome the obstacles associated with estimating the out-of-plane components. In the case of the pure estimation problem, this is not a possibility.

6.4 Estimation Via Switching Observer

The issues with estimating the out-of-plane components can be approached a separate way by changing the structure of the observer and not effecting the control.

6.4.1 Background

Consider the signal $\mathbf{y} = \mathbf{\Psi}\mathbf{u}_f$. For the out-of-plane problem, the structure of $\mathbf{\Psi}$ in (6.1) can be used to recover

$$\mathbf{y} = \begin{bmatrix} y_1 \\ y_2 \\ y_3 \end{bmatrix} = \begin{bmatrix} u_{f,A}\cos\phi_A \\ u_{f,B}\cos\phi_B \\ u_{f,A}\sin\phi_A + u_{f,B}\sin\phi_B + u_{f,C} \end{bmatrix} \tag{6.31}$$

The structure of the out-of-plane problem gives direct knowledge of the magnitude of the misalignment angles through y_1 and y_2 which is not available for the in-plane problem. Therefore, instead of using a certainty-equivalence formulation, The contribution from the other axis can be directly elimnated. To begin, consider only estimation of the x-axis misalignment. An update law of the form $\dot{\hat{\mathbf{\Psi}}}_A = -\gamma S(\mathbf{y}_A \times \hat{\mathbf{y}}_A)\hat{\mathbf{\Psi}}_A$ is desired. Notice that

$$\mathbf{y}_A = \mathbf{\Psi}_A\, u_{f,A} = \begin{bmatrix} y_1 \\ 0 \\ y_3 - u_{f,B}\sin\phi_B - u_{f,C} \end{bmatrix}$$

and the magnitude of ϕ_B is available from y_2. Therefore, if $u_{f,B}\sin\phi_B$ is constructed from available information then the true value of $\mathbf{y}_A$ is obtained without any certainty-equivalence. It is possible to rewrite $u_{f,B}\sin\phi_B$ as

$$u_{f,B}\sin\phi_B = \text{sign}(u_{f,B})|u_{f,B}|\ \ \text{sign}(\sin\phi_B)|\sin\phi_B|$$

where sign$(\cdot)$ is 1 if the value is positive and -1 if the value is negative. From y_2, it can be found that $|u_{f,B}\sin\phi_B| = \sqrt{u_{f,B}^2 - y_2^2}$. Since sign$(u_{f,B})$ is always available, the only unknown is the sign$(\sin\phi_B)$. Fortunately, there are only two possibilities so the following pair of update laws are proposed with the form

$$\dot{\hat{\mathbf{\Psi}}}_{A,j} = -\gamma S\left[\left(\begin{bmatrix} y_1 \\ 0 \\ y_3 \end{bmatrix} + h_j\ \text{sign}(u_{f,B})\begin{bmatrix} 0 \\ 0 \\ \sqrt{u_{f,B}^2 - y_2^2} \end{bmatrix} - \begin{bmatrix} 0 \\ 0 \\ u_{f,C} \end{bmatrix}\right)\hat{\mathbf{y}}_A\right]\hat{\mathbf{\Psi}}_A \tag{6.32}$$

where $j = 1, 2$, $h_1 = -1$ and $h_2 = 1$. Accordingly, when $\sin\phi_B$ is positive, update law "1" will eliminate $u_{f,B}\sin\phi_B$, and the same holds true for update law "2" when the sine of the angle is negative. Therefore, given any scenario, one of the update laws

will have the proper form necessary for convergence. The question remains, however, as to which estimate to implement. For this purpose, define the following signals

$$q_{A,1} \equiv y_1^2 + \left[y_3 + h_1 \text{sign}(u_{f,B}) \sqrt{u_{f,B}^2 - y_2^2} - u_{f,C} \right]^2 - u_{f,A}^2 \tag{6.33a}$$

$$q_{A,2} \equiv y_1^2 + \left[y_3 + h_2 \text{sign}(u_{f,B}) \sqrt{u_{f,B}^2 - y_2^2} - u_{f,C} \right]^2 - u_{f,A}^2 \tag{6.33b}$$

In the event that $\sin \phi_B$ is positive, $q_{A,1} = 0$ for all time. If $\sin \phi_B$ is negative, $q_{A,2} = 0$ for all time. In either case, the other signal will be

$$q_{A,j} = 4 u_{f,B} \, \sin \phi_B \, (y_3 - u_{f,C})$$

which is only zero for all time when $\sin \phi_B$, $y_3(t) - u_{f,C}(t)$, or $u_{f,B}(t)$ is zero for all time. The only practical consideration is when $\sin \phi_B = 0$ since the other two possibilities are very specific. Fortunately, when $\sin \phi_B = 0$, the two update laws are the same. Thus, the signals $q_{A,j}$ can be used to create a switching logic. One might suggest simply choosing the update law that has an initial q value of zero and avoid switching altogether; however, it is possible that both the q values are zero at the initial time. Moreover, it is emphasized that everything that has been derived has been done so under ideal conditions where noise has not been considered. When noise is present, neither q value will be zero and a robust switching method will be needed. As part of a possible solution, the signals $w_{A,j}$ are introduced that are available through low-pass linear dynamics

$$\dot{w}_{A,1} = -w_{A,1} + q_{A,1}^2 \tag{6.34a}$$

$$\dot{w}_{A,2} = -w_{A,2} + q_{A,2}^2 \tag{6.34b}$$

with the initial conditions $w_{A,j}(0) = 1$. Note that both signals will be non-negative for all time. For the correct j, $w_{A,j}$ is a signal that exponentially decays to zero. If the other $q_{A,j}$ is PE, then its associated w signal cannot converge to zero [57]. If the signal is not PE, consider that fact that (assuming $q_{A,1} = 0$ without loss of generality)

$$w_{A,1}(t) = e^{-t}$$

$$w_{A,2}(t) = e^{-t} + \int_{t_0}^{t} e^{-(t-\tau)} q_{A,2}^2(\tau) \, d\tau$$

Taking the difference yields

$$w_{A,2} - w_{A,1} = \int_{t_0}^{t} e^{-(t-\tau)} q_{A,2}^2(\tau)\, d\tau$$

which infers that $w_{A,1}(t) \leq w_{A,2}(t)$ for all time. Therefore as a switching logic, select

$$\hat{\mathbf{\Psi}}_A = \min_{w_{A,j}} \left(\hat{\mathbf{\Psi}}_{A,j} \right) \tag{6.35}$$

where $j = 1, 2$. It is emphasized that the filter construction overcomes the issues of the q values both being zero at initial time, since the switching logic is dependent on time. Furthermore, in the case of high frequency measurement noise, the filter will dampen some of the effects of the noise and still give the same result. In either case, it should be clear that using the filter logic will only cause switching to occur in the transient (i.e. there will not be an infinite number of switches). Therefore, the end result of the switching logic is that the correct $u_{f,B} \sin \phi_B$ is used in the steady-state which gives an update law of the form $\dot{\hat{\mathbf{\Psi}}}_A = -\gamma S(\mathbf{y}_A \times \hat{\mathbf{y}}_A)\hat{\mathbf{\Psi}}_A$ and asymptotic convergence of the estimate to the true value for all but a single initial condition. * Obviously this is a useful result, and it is possible to extend the same logic to estimating the y-axis. The use of switching, however, adds complexity and possible discontinuities in the estimate.

6.4.2 Estimation Problem

Using the discussion of the previous section, the observers for the unknown misalignments are proposed as

$$\dot{\hat{\mathbf{\Psi}}}_{A,j} = -\gamma S \left[\left(\begin{bmatrix} y_1 \\ 0 \\ y_3 \end{bmatrix} + h_j \operatorname{sign}(u_{f,B}) \begin{bmatrix} 0 \\ 0 \\ \sqrt{u_{f,B}^2 - y_2^2} \end{bmatrix} - \begin{bmatrix} 0 \\ 0 \\ u_{f,C} \end{bmatrix} \right) \hat{\mathbf{y}}_A \right] \hat{\mathbf{\Psi}}_A \tag{6.36a}$$

$$\dot{\hat{\mathbf{\Psi}}}_{B,j} = -\gamma S \left[\left(\begin{bmatrix} 0 \\ y_2 \\ y_3 \end{bmatrix} + h_j \operatorname{sign}(u_{f,A}) \begin{bmatrix} 0 \\ 0 \\ \sqrt{u_{f,A}^2 - y_1^2} \end{bmatrix} - \begin{bmatrix} 0 \\ 0 \\ u_{f,C} \end{bmatrix} \right) \hat{\mathbf{y}}_B \right] \hat{\mathbf{\Psi}}_B \tag{6.36b}$$

*This condition is the initial guess of $\hat{\mathbf{q}}_{\mathbf{\Psi}}$ such that $\mathbf{q}_{\mathbf{\Psi}}^\top \hat{\mathbf{q}}_{\mathbf{\Psi}} \neq 0$ as in Chapter 4

where the signals involving "A" are as in (6.33) and (6.34), and the signals involving "B" are defined similarly as

$$q_{B,1} \equiv y_2^2 + \left[y_3 + h_1 \text{sign}(u_{f,A})\sqrt{u_{f,A}^2 - y_1^2} - u_{f,C}\right]^2 - u_{f,B}^2 \tag{6.37a}$$

$$q_{B,2} \equiv y_2^2 + \left[y_3 + h_2 \text{sign}(u_{f,A})\sqrt{u_{f,A}^2 - y_1^2} - u_{f,C}\right]^2 - u_{f,B}^2 \tag{6.37b}$$

and

$$\dot{w}_{B,1} = -w_{B,1} + q_{B,1}^2 \tag{6.38a}$$

$$\dot{w}_{B,2} = -w_{B,2} + q_{B,2}^2 \tag{6.38b}$$

with the initial conditions $w_{B,j}(0) = 1$. For completeness, the update laws on the angles can be found from the vector update laws as

$$\dot{\hat{\phi}}_{A,j} = \gamma\left(\hat{y}_{A,1}\left[y_3 + h_j \,\text{sign}(u_{f,B})\sqrt{u_{f,B}^2 - y_2^2} - u_{f,C}\right] - y_1\hat{y}_{A,3}\right) \tag{6.39a}$$

$$\dot{\hat{\phi}}_{B,j} = \gamma\left(\hat{y}_{B,2}\left[y_3 + h_j \,\text{sign}(u_{f,A})\sqrt{u_{f,A}^2 - y_1^2} - u_{f,C}\right] - y_2\hat{y}_{B,3}\right) \tag{6.39b}$$

To implement this observer, it is necessary to have four update laws instead of the normal two.

Theorem 6.4.1. *Assume that the components of $\mathbf{u}_f$ are such that $u_{f,A}$, $u_{f,B}$ and $u_{f,C}$ and their respective derivatives are bounded. Suppose also that $u_{f,A}$ and $u_{f,B}$ are PE signals and thus cannot remain indefinitely at zero. Then, given the measurement relation $\mathbf{y} = \mathbf{\Psi}\mathbf{u}_f$ together with the update laws of (6.39) with the proposed switching logic of (6.35), the estimation scheme guarantees that $\hat{\phi}_A \to \phi_A$ and $\hat{\phi}_B \to \phi_B$ as $t \to \infty$ provided that $y_3(t) - u_{f,C}(t) \neq 0$ for all time.*

Proof. In the case that there is no noise in the system, there can only be a maximum of one switch for each pair of observers at T_*. For $0 \leq t \leq T_*$ the pair of observers are required to be same provided that $y_3(t) - u_{f,C}(t)$ from 0 to T is not strictly zero, which has been precluded since $y_3(t) - u_{f,C}(t)$ cannot equal zero for all time. [†] Therefore,

[†]When $y_3(t) - u_{f,C}(t) = 0$ for all time, the measurement $\mathbf{y}$ only provides information on the magnitude of the angles. Accordingly, there are two equilibrium points (ϕ_A, ϕ_B) and $(-\phi_A, -\phi_B)$ which are both stable. Therefore, the observer will converge to one of the equilibrium points based on the position of the initial guess of the estimate. This is a naturally occurring issue within the out-of-plane problem that cannot be rectified without additional information.

let $T = \max(T_A, T_B)$. Then for $t \geq T$, the correct observer is being implemented for each axis. For this steady-state period, consider the Lyapunov-like function

$$V_E = 2\sin^2\left(\frac{1}{2}\tilde{\phi}_A\right) + 2\sin^2\left(\frac{1}{2}\tilde{\phi}_B\right) \tag{6.40}$$

which because of the direct elimination of terms has the derivative

$$\begin{aligned}\dot{V}_E &= -\gamma|\sin\tilde{\theta}_A\, u_{f,A}|^2 - \gamma|\sin\tilde{\theta}_B u_{f,B}|^2 \\ &= -\gamma||\mathbf{z}(\tilde{\phi})||^2 \leq 0\end{aligned} \tag{6.41}$$

Note that because the perturbation terms associated with the error of the other axis have been eliminated there are no cross terms, and no need to upper bound the derivative. Thus, $\dot{V}_E$ is negative semi-definite, indicating boundedness for all closed-loop signals. Further, because V_E is lower-bounded, $\int_0^\infty \dot{V}_E(t)\,dt$ exists and is finite which taken together with (6.41) implies that $\mathbf{z}(\tilde{\phi}) \in \mathcal{L}_2 \cap \mathcal{L}_\infty$. Examining $\dot{\mathbf{z}}$ indicates that boundedness of $\dot{\mathbf{z}}$ is only dependent on boundedness of $\dot{\hat{\phi}}_A$ and $\dot{\hat{\phi}}_B$ (as all other values are bounded by definition). From (6.39), it is clear that $\dot{\hat{\phi}}_A, \dot{\hat{\phi}}_B \in \mathcal{L}_\infty$ which implies $\dot{\mathbf{z}} \in \mathcal{L}_\infty$. Therefore, invoking Barbalat's Lemma yields

$$\lim_{t\to\infty} \mathbf{z}(t) = \mathbf{0}$$

Since the components of $\mathbf{u}_f$ are persistently exciting, this implies that

$$\lim_{t\to\infty} \begin{bmatrix}\sin\tilde{\phi}_A \\ \sin\tilde{\phi}_B\end{bmatrix} = \mathbf{0}$$

which considering the definitions on $\tilde{\phi}_*$ implies

$$\lim_{t\to\infty} \begin{bmatrix}\tilde{\phi}_A \\ \tilde{\phi}_B\end{bmatrix} = \begin{bmatrix}\hat{\phi}_A - \phi_A \\ \hat{\phi}_B - \phi_B\end{bmatrix} = \mathbf{0}$$

and the proof is complete. □

6.4.2.1 Remarks

a) When noise is introduced into the measurements, the amount of switches will most certainly increase. Accordingly, during the transient period, it is possible for the

incorrect observer to be implemented causing the estimates to diverge for a period of time. It is noted, however, that there can only be a finite number of switches in finite time. As a result, there exists a value T_* for each observer pair such that the correct observer is used for all $t \geq T_*$. Thus, a Lyapunov analysis could be performed for the steady-state portion after the maximum T_*. Also, the implemented estimate could become discontinuous due to the switching. This has less impact in the estimation problem, but it would cause the control signal to be discontinuous when extending to the control problem. This is not that significant an issue in the absence of noise.

6.4.3 Control Problem

Extension to the control problem is very straightforward. Accordingly the control law will be presented with the corresponding theorem, but the proof will not be included since it is exactly the same as the previous section minus the constant input portion. Therefore, let the control signal be determined through

$$\mathbf{u} = -\hat{\boldsymbol{\Psi}}^{-1}\left(\mathbf{g} + \alpha\left(k_p\mathbf{e}_1 + \mathbf{e}_2\right) - \begin{bmatrix} -\sin\hat{\phi}_{A,j} & 0 & 0 \\ 0 & -\sin\hat{\phi}_{B,j} & 0 \\ \cos\hat{\phi}_{A,j} & \cos\hat{\phi}_{B,j} & 0 \end{bmatrix}\begin{bmatrix} \dot{\hat{\phi}}_{A,j} & 0 & 0 \\ 0 & \dot{\hat{\phi}}_{B,j} & 0 \\ 0 & 0 & 0 \end{bmatrix}\hat{\boldsymbol{\Psi}}_j^{-1}\hat{\mathbf{y}}\right) \tag{6.42}$$

where j will take on the value of the active observer being implemented according to the switching logic.

Theorem 6.4.2. *Consider the tracking error dynamics of (2.4). Suppose that control signal is given by (6.42) with the update laws of (6.39) and the described switching logic of (6.35). Then the convergence condition*

$$\lim_{t\to\infty}\begin{bmatrix}\mathbf{e}_1(t) \\ \mathbf{e}_2(t)\end{bmatrix} = \mathbf{0}$$

is applicable for all admissible reference trajectories $\mathbf{r}$ *and initial conditions* $[\mathbf{x}_1(0), \mathbf{x}_2(0)]^\top$ *provided that that the gain* α *is chosen such that* $\alpha = k_p + k_v$, $|\phi_A|, |\phi_B| < \pi/5$, *and* $\hat{\phi}_A(0) = \hat{\phi}_B(0) = 0$.

6.4.3.1 Remarks

a) The constraints on the misalignments and the value of the initial estimates reappear because of the singularity in the control problem. The constraints guarantee

that $|\hat{\phi}_A|, |\hat{\phi}_B| < \pi/2$ for all time. Note that these constraints could be lifted if a projection scheme was introduced into the observer. The only constraint would then be that the estimates be bounded to the interval $(-\pi/2, \pi/2)$.

b) Since there is assumed to be no noise on the system, the estimates and ultimately the control signal are continuous. As mentioned previously, any noise in the system could lead to discontinuities in the control that would be undesirable. In addition, noise could cause the incorrect observer to be implemented which would destroy the region of attraction argument that automatically bounds the estimates. Thus, a projection scheme would *have* to be implemented to guarantee boundedness of the control signal.

6.5 Estimation via Hybrid Observer

The switching observer in the previous section requires that twice the number of observers be implemented to ensure convergence. In addition, the implemented estimates can be discontinuous in the presence of measurement noise. To overcome these issues, a novel hybrid observer is proposed.

6.5.1 Background

Instead of using h_j to distinguish between the pair of observers, consider the single term

$$\frac{w_{*,1} - w_{*,2}}{w_{*,1} + w_{*,2}} \tag{6.43}$$

If $\text{sign}(\phi_*)$ is positive then $q_{*,1}$ will converge to zero, and the ratio of (6.43) will converge to $-w_{*,2}/w_{*,2} = -1$. If $\text{sign}(\phi_*)$ is negative then $q_{*,2}$ will converge to zero, and the ratio of (6.43) will converge to $w_{*,1}/w_{*,1} = 1$. Therefore, in the steady-state, (6.43) determines the correct value of h_j and ultimately the correct observer *without* switching between a pair of observers. In this way, the number of observers is reduced back down to two, and the estimates are guaranteed to be continuous *even* in the presence of measurement noise. The only issue this could introduce is that the ratio

acts as a perturbation term in the transient since it does not directly eliminate the $\sin(\phi_*)$ term. Fortunately, the perturbation term is exponentially decaying as proved by the following lemma.

Lemma 6.5.1. *Consider the ratio $(w_{A,1} - w_{A,2})/(w_{A,1} + w_{A,2})$ where $w_{A,j}$ is defined as in (6.34). If either $q_{A,1}$ or $q_{A,2}$ as defined in (6.33) is persistently exciting and the other is identically zero for all time, then*

$$\operatorname{sign}(\sin\phi_B) + \left(\frac{w_{A,1} - w_{A,2}}{w_{A,1} + w_{A,2}}\right) \leq c_1 e^{-c_2 t} \tag{6.44}$$

where c_1 and c_2 are positive scalar constants.

Proof. Consider the Lyapunov function given by

$$V_w = \frac{1}{2}\left[\operatorname{sign}(\sin\phi_B) + \frac{w_{A,1} - w_{A,2}}{w_{A,1} + w_{A,2}}\right]^2 \tag{6.45}$$

which has the time derivative

$$\begin{aligned}
\dot{V}_w &= \left[\operatorname{sign}(\sin\phi_B) + \frac{w_{A,1} - w_{A,2}}{w_{A,1} + w_{A,2}}\right]\left[\frac{\dot{w}_{A,1} + \dot{w}_{A,2}}{w_{A,1} + w_{A,2}} - \frac{(w_{A,1} - w_{A,2})(\dot{w}_{A,1} + \dot{w}_{A,2})}{(w_{A,1} + w_{A,2})^2}\right] \\
&= 2\sqrt{V_w}\left[\frac{q_{A,1}^2 - q_{A,2}^2}{w_{A,1} + w_{A,2}} + \frac{(w_{A,1} - w_{A,2})\left(q_{A,1}^2 + q_{A,2}^2\right)}{(w_{A,1} + w_{A,2})^2}\right] \\
&= 2\sqrt{V_w}\left[-\operatorname{sign}(\sin\phi_B)\left(\frac{q_{A,1}^2 + q_{A,2}^2}{w_{A,1} + w_{A,2}}\right) - \frac{(w_{A,1} - w_{A,2})\left(q_{A,1}^2 + q_{A,2}^2\right)}{(w_{A,1} + w_{A,2})^2}\right] \\
&= -2\left(\frac{q_{A,1}^2 + q_{A,2}^2}{w_{A,1} + w_{A,2}}\right) V_w
\end{aligned} \tag{6.46}$$

Since the derivative is of the form $\dot{V}_w = -d(t)^2 V_w$, V_w converges exponentially provided that $d(t)$ is persistently exciting [58, 59]. Given $d(t)$ as in (6.46), assume without loss of generality that $q_{A,1} = 0$ then

$$d(t) = \sqrt{\frac{q_{A,2}^2}{w_{A,1} + w_{A,2}}}$$

If $q_{A,2}$ is persistently exciting, then there exists a lower bound ω such that $0 < \omega \leq w_{A,2}(t)$ for all time [57]. This result combined with the exponential convergence of

$w_{A,1}$ indicates that $d(t) \leq q_{A,2}^2(t)/\omega$. Accordingly, $\dot{V}_w \leq -2(\gamma/\omega)q_{A,2}^2(t)V_w$, and the persistence on $q_{A,2}$ ensures exponential convergence of V_w. Consequently, there exist positive constants c_1 and c_2 such that (6.44) is satisfied. Therefore, the proof is complete. □

Note that the preceding lemma is also valid for the corresponding "B" values. It will be shown that the addition of the ratio introduces an exponentially decaying term into the dynamics, which can be ignored since it does not effect the stability analysis.

6.5.2 Estimation Problem

Using the preceding section, the following hybrid update laws are proposed

$$\dot{\hat{\mathbf{\Psi}}}_A = -\gamma S \left[\left(\begin{bmatrix} y_1 \\ 0 \\ y_3 \end{bmatrix} + \left(\frac{w_{A,1} - w_{A,2}}{w_{A,1} + w_{A,2}} \right) \text{sign}(u_{f,B}) \begin{bmatrix} 0 \\ 0 \\ \sqrt{u_{f,B}^2 - y_2^2} \end{bmatrix} - \begin{bmatrix} 0 \\ 0 \\ u_{f,C} \end{bmatrix} \right) \hat{\mathbf{y}}_A \right] \hat{\mathbf{\Psi}}_A \tag{6.47a}$$

$$\dot{\hat{\mathbf{\Psi}}}_B = -\gamma S \left[\left(\begin{bmatrix} 0 \\ y_1 \\ y_3 \end{bmatrix} + \left(\frac{w_{B,1} - w_{B,2}}{w_{B,1} + w_{B,2}} \right) \text{sign}(u_{f,A}) \begin{bmatrix} 0 \\ 0 \\ \sqrt{u_{f,A}^2 - y_1^2} \end{bmatrix} - \begin{bmatrix} 0 \\ 0 \\ u_{f,C} \end{bmatrix} \right) \hat{\mathbf{y}}_B \right] \hat{\mathbf{\Psi}}_B \tag{6.47b}$$

where h_j has been replaced by the ratio of the w signals in (6.43). After some algebraic manipulation is performed, the update laws on the angles can be represented as

$$\dot{\hat{\phi}}_A = \gamma \left(\hat{y}_{A,1} \left[y_3 + \left(\tfrac{w_{A,1} - w_{A,2}}{w_{A,1} + w_{A,2}} \right) \text{sign}(u_{f,B}) \sqrt{u_{f,B}^2 - y_2^2} - u_{f,C} \right] - y_1 \hat{y}_{A,3} \right) \tag{6.48a}$$

$$\dot{\hat{\phi}}_B = \gamma \left(\hat{y}_{B,2} \left[y_3 + \left(\tfrac{w_{B,1} - w_{B,2}}{w_{B,1} + w_{B,2}} \right) \text{sign}(u_{f,A}) \sqrt{u_{f,A}^2 - y_1^2} - u_{f,C} \right] - y_2 \hat{y}_{B,3} \right) \tag{6.48b}$$

Theorem 6.5.2. *Assume that the components of* $\mathbf{u}_f$ *are such that* $u_{f,A}$, $u_{f,B}$ *and* $u_{f,C}$ *and their respective derivatives are bounded. Moreover,* $u_{f,A}$ *and* $u_{f,B}$ *are persistently exciting. Then, given the relation* $\mathbf{y} = \mathbf{\Psi}\mathbf{u}_f$ *for the strictly out-of-plane problem with the update laws of (6.48) guarantees that* $\hat{\phi}_A \to \phi_A$ *and* $\hat{\phi}_B \to \phi_B$ *as* $t \to \infty$ *for all initial conditions.*

Proof. Using some algebra, it can be shown that the angular update laws can be

written as

$$\dot{\tilde{\phi}}_A = -\gamma u_{f,A}^2 \sin\tilde{\phi}_A + \gamma u_{f,A}\, u_{f,B}\, |\sin\phi_B| \left[\text{sign}(\sin\phi_B) + \frac{w_{A,1} - w_{A,2}}{w_{A,1} + w_{A,2}}\right] \tag{6.49a}$$

$$\dot{\tilde{\phi}}_B = -\gamma u_{f,B}^2 \sin\tilde{\phi}_B + \gamma u_{f,A}\, u_{f,B}\, |\sin\phi_A| \left[\text{sign}(\sin\phi_A) + \frac{w_{B,1} - w_{B,2}}{w_{B,1} + w_{B,2}}\right] \tag{6.49b}$$

which combined with Lemma 6.5.1 indicates that the error dynamics contain an exponentially decaying perturbation term. By selecting the Lyapunov-like function

$$V_{E,exp} = 2\sin^2\left(\frac{1}{2}\tilde{\phi}_A\right) + 2\sin^2\left(\frac{1}{2}\tilde{\phi}_B\right) + \frac{\gamma\delta_A\zeta_B^2|\sin\phi_B|^2}{2}v_A^2 + \frac{\gamma\delta_B\zeta_A^2|\sin\phi_A|^2}{2}v_B^2 \tag{6.50}$$

where ζ_* represents the supremum of the absolute value of $u_{*,f}$, δ_* is a positive scalar constant, $v_A \equiv c_1 e^{-c_2 t}$, and $v_B \equiv c_3 e^{-c_4 t}$, the derivative of the function will be negative semi-definite provided that δ_* is large enough to dominate the decaying exponential terms. This is easily done since δ_* can be chosen sufficiently large without effecting the performance. The same argument was made in Section 2.3.2 for the exponentially decaying term in the filter design. Consequently instead of choosing $V_{E,exp}$, the exponentially decaying term can simply be ignored, and the error dynamics can be written as

$$\dot{\tilde{\phi}}_A = -\gamma u_{f,A}^2 \sin\tilde{\phi}_A \tag{6.51a}$$

$$\dot{\tilde{\phi}}_B = -\gamma u_{f,B}^2 \sin\tilde{\phi}_B \tag{6.51b}$$

without effecting the stability analysis. Then $V_E = 2\sin^2(\tilde{\phi}_A/2) + 2\sin^2(\tilde{\phi}_B/2)$ can be chosen as the Lyapunov like function which has the derivative $\dot{V}_E = -\gamma||\mathbf{z}(\tilde{\phi})||^2$ as demonstrated in the previous section. Using the same signal chasing arguments, the estimation errors are guaranteed to converge provided $u_{f,A}$ and $u_{f,B}$ are PE. □

6.5.2.1 Remarks

a) Clearly the advantage of the hybrid observer is that no switching is necessary to implement the estimates. Moreover, the estimates are required to be continuous even if there is measurement noise.

b) The main drawback of the proposed hybrid observer of (6.48) is the requirement of persistently exciting signals. This is necessary because if the signals are not PE, it is possible for the ratio $(w_1 - w_2)/(w_1 + w_2)$ to be 0/0 in the limit at which point the update law is not implementable. [‡] This issue could be avoided by simply setting the ratio to zero if it becomes too small. In addition, the switching update laws of (6.39) could be implemented. Although this is somewhat less desirable from a computational stand point, the switching observer still converges to the correct update law within a finite number of switches even with noise.

c) In order to definitively prove convergence, $V_{E,exp}$ would always have to be used as opposed to V_E. Although the exponentially decaying term does not effect the overall stability, the size of the level curve is increased significantly. To prove that the estimates remain bounded to the interval $(-\pi/2, \pi/2)$, $V_E(0)$ was used as a level curve to bound the estimates to the desired interval. Inclusion of the two exponential terms into the Lyapunov analysis increases the size of the level curve by

$$\frac{\gamma \delta_A \zeta_B^2 |\sin \phi_B|^2}{2} c_1^2 + \frac{\gamma \delta_B \zeta_A^2 |\sin \phi_A|^2}{2} c_2^2$$

This in turn destroys any natural guarantees on the bounds of the estimates. Therefore, a projection scheme must be implemented to ensure boundedness of the estimates.

6.5.3 Control Problem

Since the control problem is subject to a singularity condition, the estimates must remain bounded, and a projection scheme must be implemented. Consequently, let the estimates on ϕ_* be replaced by estimates of the projection variables ξ_* where the two estimates are related through

$$\phi_* = \frac{\mu_*}{2} (1 - \tanh \xi_*) + \phi_{*,\min} \tag{6.52a}$$

$$\hat{\phi}_* = \frac{\mu_*}{2} \left(1 - \tanh \hat{\xi}_*\right) + \phi_{*,\min} \tag{6.52b}$$

[‡]If there is measurement noise, this issue would automatically be avoided

where $* = A, B$ and $\mu_* = \phi_{*,\max} - \phi_{*,\min}$. Furthermore, let the update laws on $\hat{\xi}_*$ be determined as

$$\dot{\hat{\xi}}_* = -\dot{\hat{\phi}}_* \tag{6.53}$$

where the update laws on $\hat{\phi}_*$ are consistent with hybrid update laws of the previous section given in (6.48). The control signal can the be determined through

$$\mathbf{u} = -\hat{\mathbf{\Psi}}^{-1}\left(\mathbf{g} + \alpha\left(k_p\mathbf{e}_1 + \mathbf{e}_2\right) - \begin{bmatrix} -\sin\hat{\phi}_A & 0 & 0 \\ 0 & -\sin\hat{\phi}_B & 0 \\ \cos\hat{\phi}_A & \cos\hat{\phi}_B & 0 \end{bmatrix}\begin{bmatrix} \frac{\dot{\hat{\phi}}_A}{\cosh^2\xi_A} & 0 & 0 \\ 0 & \frac{\dot{\hat{\phi}}_B}{\cosh^2\xi_B} & 0 \\ 0 & 0 & 0 \end{bmatrix}\hat{\mathbf{\Psi}}^{-1}\hat{\mathbf{y}}\right) \tag{6.54}$$

where the $\cosh^2(\phi_*)$ terms appear because of the projection scheme.

Theorem 6.5.3. *Consider the tracking error dynamics of (2.4). Suppose that the adaptive control law is given by (6.54) with the projection scheme of (6.52) and update laws of (6.53). Then the convergence condition*

$$\lim_{t\to\infty}\begin{bmatrix}\mathbf{e}_1(t) \\ \mathbf{e}_2(t)\end{bmatrix} = \mathbf{0}$$

is applicable for all admissible reference trajectories $\mathbf{r}$ *and initial conditions* $[\mathbf{x}_1(0), \mathbf{x}_2(0)]^\top$ *provided that the gain* α *is chosen such that* $\alpha = k_p + k_v$, $|\theta_A|, |\theta_B| < \pi/2$ *and* $|\hat{\theta}_A(0)|, |\hat{\theta}_B(0)| < \pi/2$.

Proof. The proof is exactly the same as the previous two sections except that the Lyapunov-like function for the estimation terms

$$V_E = \frac{\mu_A}{2}\left[\log\left(\cosh\hat{\xi}_A\right) - \tilde{\xi}_A\tanh\xi_A\right] + \frac{\mu_B}{2}\left[\log\left(\cosh\hat{\xi}_B\right) - \tilde{\xi}_B\tanh\xi_B\right] \geq 0$$

is used to account for the smooth projection scheme. All other aspects of the analysis remain the same resulting in the convergence of the tracking errors. □

6.6 Out-of-Plane with Single In-Plane Component Misalignment Problem

Much like the previous chapter, the natural extension to the strictly out-of-plane problem would be to add a single in-plane component to one of the axes. If

the in-plane component were assumed to be on the x-axis, the misalignment matrix would have the columns

$$\boldsymbol{\Psi}_A = \begin{bmatrix} \cos\theta_A \cos\phi_A \\ \sin\theta_A \cos\phi_A \\ \sin\phi_A \end{bmatrix} \qquad \boldsymbol{\Psi}_B = \begin{bmatrix} 0 \\ \cos\phi_B \\ \sin\phi_B \end{bmatrix} \qquad \boldsymbol{\Psi}_C = \begin{bmatrix} 0 \\ 0 \\ 1 \end{bmatrix} \tag{6.55}$$

where ϕ_* signifies the out-of-plane misalignments, and θ_A is the in-plane misalignment on the x-axis. Again, the z-axis is assumed to have no misalignment. A graphical representation is shown in Figure 6.9. In this case, $\boldsymbol{\Psi}$ would have $\det(\hat{\boldsymbol{\Psi}}) =$

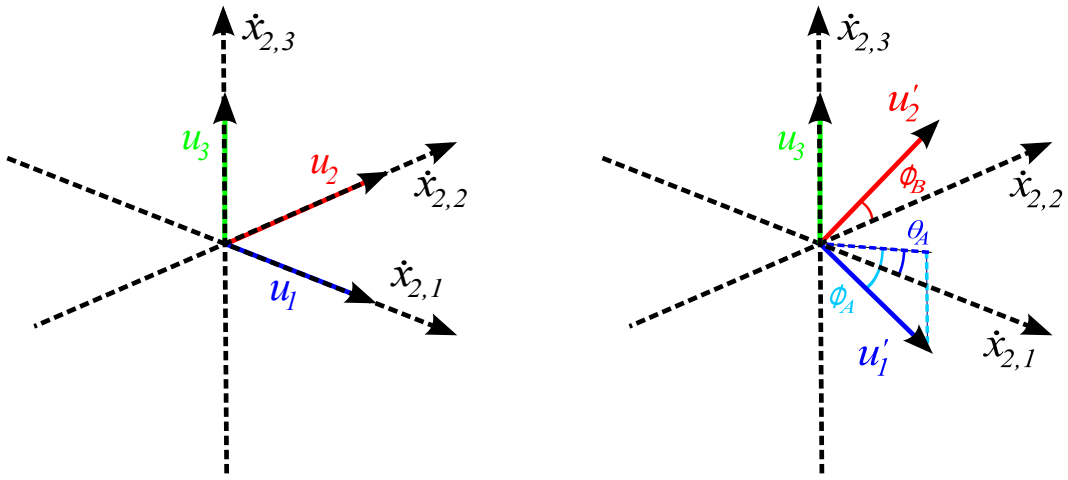

(a) $\boldsymbol{\Psi} = \mathbf{I}_{3\times3}$ (b) $\boldsymbol{\Psi} \neq \mathbf{I}_{3\times3}$

Figure 6.9: Graphical representation of the effect of $\boldsymbol{\Psi}$ for the out-of-plane misalignments with a single in-plane component on the independent control axes

$\cos\hat{\theta}_A \cos\hat{\phi}_A \cos\hat{\phi}_B$, which would make the singularity condition $\hat{\theta}_A, \hat{\phi}_A, \hat{\phi}_B = \pm\pi/2$. Thus, neither axis can be aligned with the z-axis nor can the x-axis move into the yz-plane. In general, this condition is not very restricting when compared to the strictly in-plane problem which has a pair of in-plane components.

Unfortunately, the out-of-plane analysis discussed thus far in the chapter cannot be readily extended to form a proof for this particular problem. A possibility would be to try and extend on the idea discussed in the switching and hybrid ob-

servers; however, when one considers the output

$$\mathbf{y} = \begin{bmatrix} y_1 \\ y_2 \\ y_3 \end{bmatrix} = \begin{bmatrix} u_{f,A} \cos\theta_A \cos\phi_A \\ u_{f,A} \sin\theta_A \cos\phi_A + u_{f,B} \cos\phi_B \\ u_{f,A} \sin\phi_A + u_{f,B} \sin\phi_B + u_{f,C} \end{bmatrix} \tag{6.56}$$

it is clear that the magnitude of the out-of-plane angles are no longer directly available. The magnitude of the "B" term has been corrupted by the in-plane component of the x-axis. Furthermore, the magnitude of the "A" term is scaled by the magnitude of the in-plane component. As a result, the magnitudes are not directly available to eliminate the $\sin(\phi_*)$ terms in y_3 which was the purpose of the switching and hybrid observers. The only way to recover the true magnitudes is to use estimated values (e.g. divide y_1 by $\cos\hat{\theta}_A$ to try and recover $\cos\phi_A$) which is no better than using the certainty-equivalence like approach. Thus, the switching and hybrid observers can not be extended.

A second approach would be to try and determine a $T_{\min}$ such that Scheduled Axis Decoupling algorithm could be implemented. Again, it can be shown that this will not be feasible. Recall, the general procedure of the strictly out-of-plane problem, and to simplify the algebra, consider three scalar variables x, y, and z. [§] The derivative of the Lyapunov-like function for the strictly out-of-plane problem could be represented like

$$\dot{V} \leq -x^2 - y^2 + \eta' |x|\,|y|$$

where there are two non-positive quadratic terms and a *single* sign indefinite cross term. If $\eta' < 2$, then completion of squares can be used to dominate the cross term. Therefore, the the key idea with most of the analysis is to limit the magnitude of the cross terms. When a single in-plane component is added, however, the derivative of the Lyapunov function changes to the form

$$\dot{V} \leq -x^2 - y^2 - z^2 + \eta' |x|\,|y| + \Delta_{xz} |x|\,|z| + \Delta_{yz} |y||z|$$

where there are now three non-positive quadratic terms and *three* sign indefinite cross terms. In order to complete squares, each quadratic term must contribute two parts

[§] A formalized discussion for this particular problem is available in Appendix D

to dominate all the terms. Assume that each quadratic term is split equally (i.e. η', Δ_{xz} and Δ_{yz} are allowed to be equally as large), then the condition $\eta', \Delta_{xz}, \Delta_{yz} < 1$ follows. Further, assume that Δ_{xz} and Δ_{yz} are such that a projection scheme can be implemented to ensure that the condition is met. The only question that remains is how must η' be constrained to meet the condition. To show that this condition cannot be arbitrarily met, η' is determined when $\hat{\phi}_A = \phi_A$ and $\hat{\phi}_B = \phi_B$ as

$$\eta' = 2\cos\phi_A \cos\phi_B$$

Therefore, the Lyapunov derivative cannot be shown to be negative semi-definite for all values of ϕ_A and ϕ_B such that $\cos\phi_A \cos\phi_B > 1/2$. Since this cannot be shown *at the true misalignment*, it certainly cannot be shown in the neighborhood of the true misalignment. The argument could be made that equally splitting the quadratic terms was a poor choice; however, it can be shown that there exists no choice which can recover the $\eta' < 2$ constraint. In fact, enforce the constraint that $0 < \Delta_{xz}, \Delta_{yz} < \epsilon << 1$ which leads to the condition that $\eta' < 2\sqrt{1-\epsilon}$. Even in this extremely contrived scenario, all misalignments such that $\cos\phi_A \cos\phi_B > \sqrt{1-\epsilon}$ cannot possibly be part of the convergence analysis which means that using this representation, the certainty-equivalence like observer cannot be shown to converge even for infinitesimally small misalignments. Moreover, Scheduled Axis Decoupling cannot be used since it can only force the misalignment errors to be small in finite time. Therefore, a convergence proof cannot be shown using a standard approach.

Again, this is not to say that the certainty-equivalence like observer will not converge to the true values if implemented with a non-zero input. To show that the observer is at minimum locally asymptotically stable for constant inputs, a linear analysis can be performed as in Section 6.2.2. Using the estimation error dynamics of (D.1), the linear error dynamics can be determined as

$$\begin{bmatrix} \dot{\tilde{\theta}}_A \\ \dot{\tilde{\phi}}_A \\ \dot{\tilde{\phi}}_B \end{bmatrix} = \gamma \mathbf{M} \begin{bmatrix} \tilde{\theta}_A \\ \tilde{\phi}_A \\ \tilde{\phi}_B \end{bmatrix} \tag{6.57}$$

where $\mathbf{M}$ is given by

$$\mathbf{M} = \begin{bmatrix} -u_{f,A}^2 & 0 & u_{f,A}u_{f,B}\,\mathrm{c}\theta_A\,\mathrm{c}\phi_A\,\mathrm{s}\phi_B \\ 0 & u_{f,A}^2 & -u_{f,A}u_{f,B}\left(\mathrm{c}\phi_A\,\mathrm{c}\,\phi_B + \mathrm{s}\phi_A\,\mathrm{s}\phi_B\,\mathrm{c}\theta_A\right) \\ u_{f,A}u_{f,B}\frac{\mathrm{c}\theta_A\,\mathrm{s}\phi_B}{\mathrm{c}\phi_A} & -u_{f,A}u_{f,B}\left(\mathrm{c}\phi_A\,\mathrm{c}\phi_B + \mathrm{s}\phi_A\mathrm{s}\phi_B\mathrm{s}\theta_A\right) & -u_{f,B}^2 \end{bmatrix}$$

and 'c' and 's' are shorthand for $\cos(\cdot)$ and $\sin(\cdot)$, respectively. Thus, if $\mathbf{M}$ is negative semi-definite then the observer is locally asymptotically stable. It can be shown through tedious algebra that the eigenvalues of $\mathbf{M}$ are strictly in the left-half plane except when $\phi_A = \phi_B = 0$. In this case, the eigenvalues are given by $-u_{f,A}^2$, $-u_{f,A}^2 - u_{f,B}^2$ and 0. Therefore, a center manifold exists at $\phi_A = \phi_B = 0$ as before, and the system can be reduced to first-order to see that the reduced-order system is also asymptotically stable as in Section 6.2.2. Accordingly, the certainty-equivalence like observer is locally asymptotically stable for constant inputs.

In addition, the convergence of the observer can be examined empirically through a numerical analysis. A Monte Carlo simulation was run with 500 sets of random misalignments between $(-\pi/4, \pi/4)$ for a persistently exciting input signal. The initial estimates assumed no a priori knowledge on the misalignments and were chosen to be zero. The results of the simulation are shown in Figure 6.10. Note that the axes on the plot are the three estimation errors, and the red disk represents the origin (i.e. convergence of the errors). Each of the 500 runs converges within 30 seconds to within a tolerance of 1×10^{-3}. Although this is not a proof of convergence, it does indicate that the addition of a single in-plane component does not effect the stability of the observer; consequently, the issues with completing the stability proof lie solely with the analysis techniques and not with the proposed observer. At present, the only degree of freedom available in the analysis process is the choice of the Lyapunov-like function. Despite considerable effort, however, a different Lyapunov-like function has not been found which addresses the issues previously discussed. More importantly, this discussion not only applies to this problem, but also to any more generalized problem which contains a pair of out-of-plane components. Therefore, until this particular problem can be solved, there can be no hope proving that the observer will converge for the full three-axis misalignment problem.

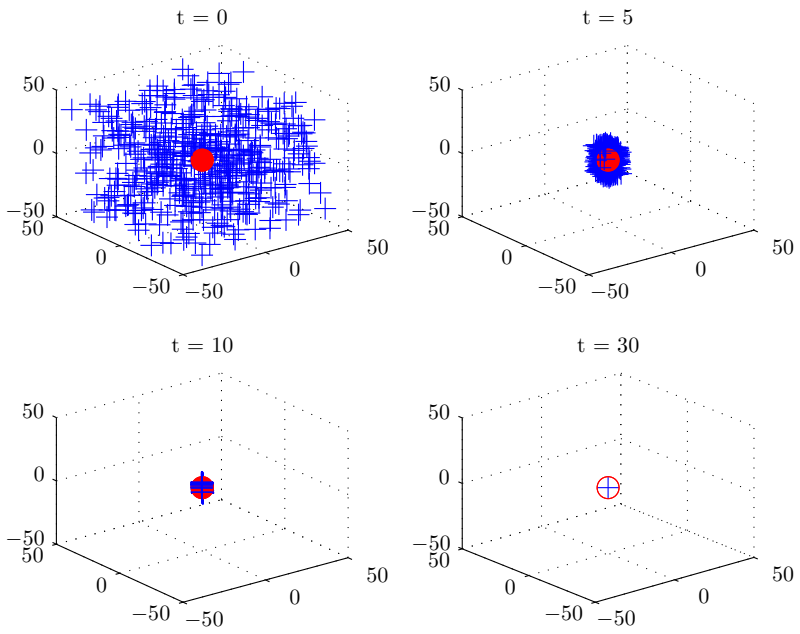

Figure 6.10: Monte Carlo simulation for 500 random sets of true misalignments between $-\pi/4$ and $\pi/4$ and with initial estimates $\hat{\phi}_A(0) = \hat{\theta}_A(0) = \hat{\phi}_B(0) = 0$

6.7 Numerical Simulations

To demonstrate the performance of the proposed control schemes, a series of simulations were performed where $\phi_A = -15°$ and $\phi_B = 25°$. The length of each simulation was varied to show the convergence of the tracking and parameter errors. For all the simulations, the initial conditions for $\mathbf{g}_f$ and $\mathbf{e}_{2,f}$ were set to zero. In addition, the gains were selected as $k_p = k_v = 3$ and $\gamma = 10$. The remainder of the values will be discussed in the appropriate section.

6.7.1 Scheduled Axis Decoupling

To begin, the performance of the Scheduled Axis Decoupling method is examined. As a comparison, the certainty-equivalence like observer and controller are implemented without the constant input from 0 to T. It is emphasized that there is no stability proof associated with this result for the initial conditions $\hat{\phi}_A(0) = \hat{\phi}_B(0) = 0$

since the estimates start outside of the region of attraction. The reference trajectory is taken to be the PE signal

$$\mathbf{r}(t) = \begin{bmatrix} \cos t \\ \sin t \cos 2t \\ \sin t \sin 2t \end{bmatrix}$$

and the system is assumed to have the drift term

$$\mathbf{f} = -\mathbf{x}_1 - \mathbf{x}_2$$

In this case, the unforced system is linear with state matrix

$$\mathbf{A} = \begin{bmatrix} 0 & 1 \\ -1 & -1 \end{bmatrix}$$

Note that $\mathbf{A}$ is Hurwitz since the eigenvalues are $-1/2 \pm \sqrt{3}/2$ which guarantees that the system is BIBO stable which automatically implies that the system is ISS. Accordingly, the constant input $h = 1$ is applied for $T = 1$ second. The T is purposely chosen to be significantly greater than $T_{\min}$ to show the effect of the Scheduled Axis Decoupling. The system was assumed to initially be at rest. The tracking error results are shown in Figure 6.11. Despite the lack of stability proof, the standard ob-

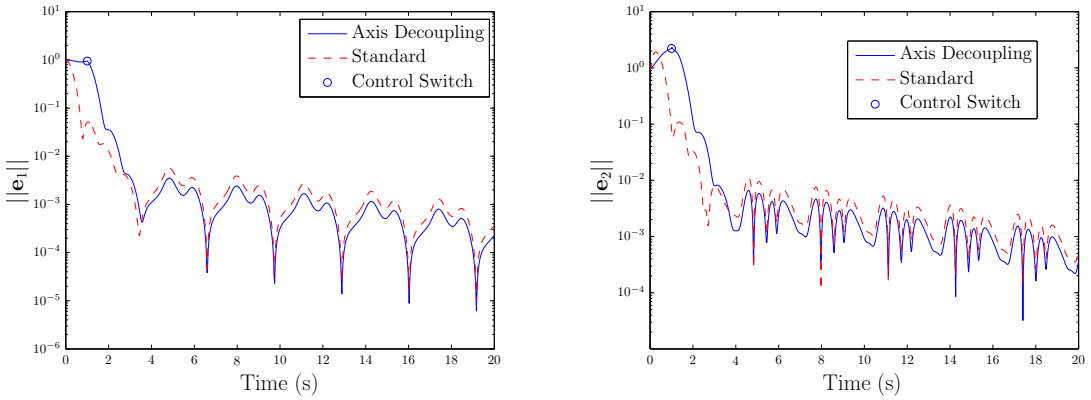

(a) Position error

(b) Velocity error

Figure 6.11: Simulation results for the tracking errors for the Scheduled Axis Decoupling method compared with the standard controller

server/controller combination is able to converge along with Axis Decoupling method.

In the steady-state, both methods are practically the same, but the transient behaviors are obviously different. The standard method is able to respond quicker since the control signal has been designed to track the reference trajectory. The use of the constant input causes the errors to grow slightly; however, the length of time is short enough that the effect on the system is minimal. ¶ The simulation results for the estimation errors is shown in Figure 6.12 in the $\hat{\phi}_A\hat{\phi}_B$-plane and in Figure 6.13 with respect to time. Although it is difficult to see, the estimates start outside of

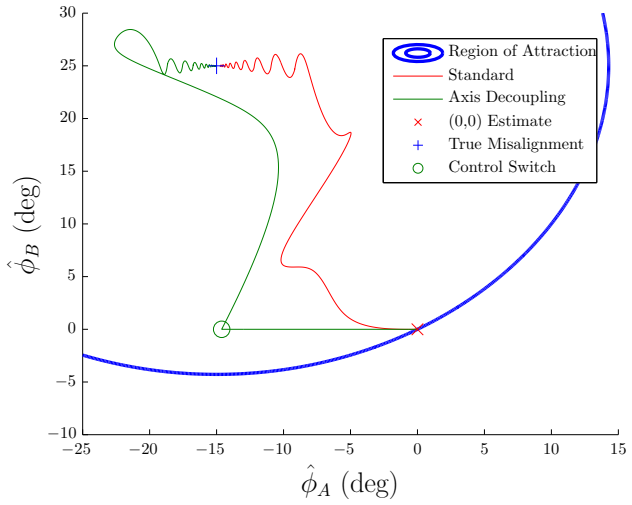

Figure 6.12: Plot of the region of attraction with the trajectories for the Scheduled Axis Decoupling method compared with the standard controller. Although it is difficult to see, the trajectories start outside the region of attraction

the region attraction but both methods enter and ultimately converge to the true misalignment. Note that there is no guarantee that the standard observer will enter the region of attraction. On the other hand, the Scheduled Axis Decoupling method follows a $\hat{\phi}_B$ = constant line into the region of attraction as designed. Since T is greater than $T_{\max}$, the reduction in the estimation error associated with ϕ_A is significant (almost to zero) which is better than with the standard method. As the control switch occurs, however, the effect of the "B" estimate causes the error to increase

¶If T were chosen to be $T_{\min}$, the change in transient behavior would be hard to see; however, convergence would be guaranteed for the Scheduled Axis Decoupling method

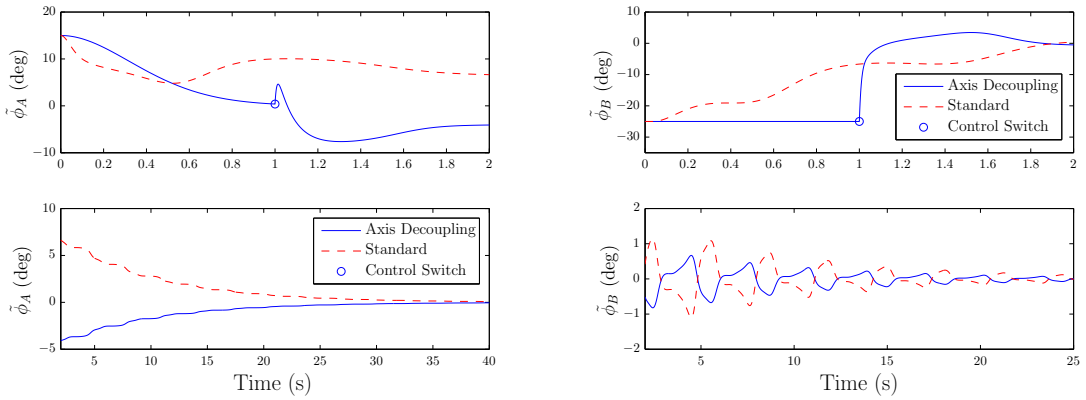

(a) A estimation error

(b) B estimation error

Figure 6.13: Simulation results for the estimation errors for the Scheduled Axis Decoupling method compared with the standard controller

before re-settling to zero. Thus, both methods perform approximately the same in the steady-state and eventually converge to the true values because of the PE reference trajectory.

6.7.2 Hybrid Observer Without Noise

Next, the control problem is simulated using the hybrid observer. To begin, the states are assumed to be perfectly measured. The gains, reference trajectory, and initial conditions are assumed to remain the same but the drift term is given by

$$\mathbf{f} = \text{diag}(\mathbf{x}_1)\mathbf{x}_2$$

which coincides with the drift term used during the in-plane simulations. Note that input-to-state stability is no longer required to ensure convergence. The simulation results are shown in Figure 6.14. As expected, both the tracking and estimation errors converge to the true values. The more interesting behavior appears when one examines the ratio of (6.43) shown in Figure 6.15. Recall that the ratio was introduced to avoid any switching and maintain continuity in the estimates and control signal. Since ϕ_B is positive, the "A" ratio should become -1 to eliminate the out-of-plane component of the y-axis. Since ϕ_A is negative, the "B" ratio should become 1 to

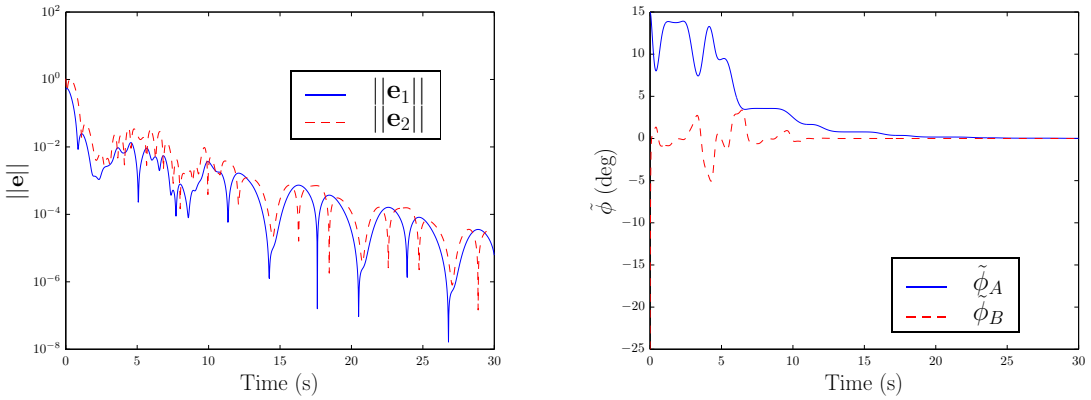

(a) Tracking error

(b) Estimation error

Figure 6.14: Simulation results for the tracking and estimation errors with the hybrid observer for the strictly out-of-plane problem without measurement noise

eliminate the x-axis out-of-plane component. As can be seen this is precisely what happens although it does take approximately 10 seconds for the ratios to converge. During the transient period, the values associated with the other axis are not being directly eliminated; however, this does not have a significant impact on the overall performance of the system.

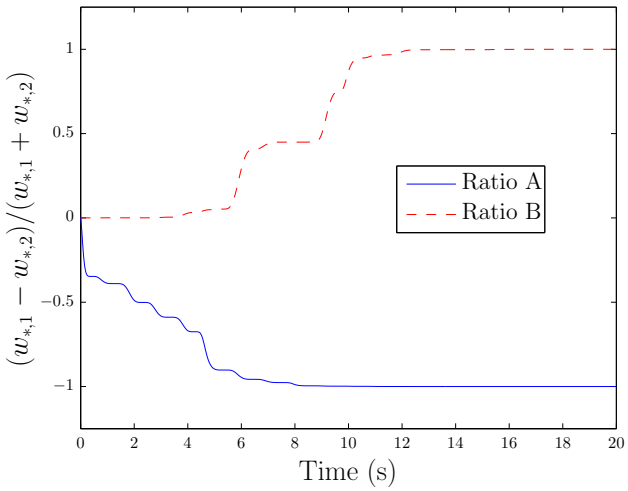

Figure 6.15: Simulations results for the hybrid ratio for the strictly out-of-plane problem without measurement noise

6.7.3 Hybrid Observer With Noise

Although no stability proof is available, the performance of the hybrid observer is examined in the control problem with measurement noise. In this case, $\mathbf{x}_1$ and $\mathbf{x}_2$ are available through the measurements

$$\mathbf{x}_{1,m} = \mathbf{x}_1 + \boldsymbol{\nu}_1$$

$$\mathbf{x}_{2,m} = \mathbf{x}_2 + \boldsymbol{\nu}_2$$

where $\boldsymbol{\nu}_1$ and $\boldsymbol{\nu}_2$ are zero-mean, white noise with a variance of $\sigma^2 = 1 \times 10^{-4}$. All other aspects of the simulation were the same. The results of the simulation are shown in Figure 6.16. Both the tracking and estimation errors are reduced during the

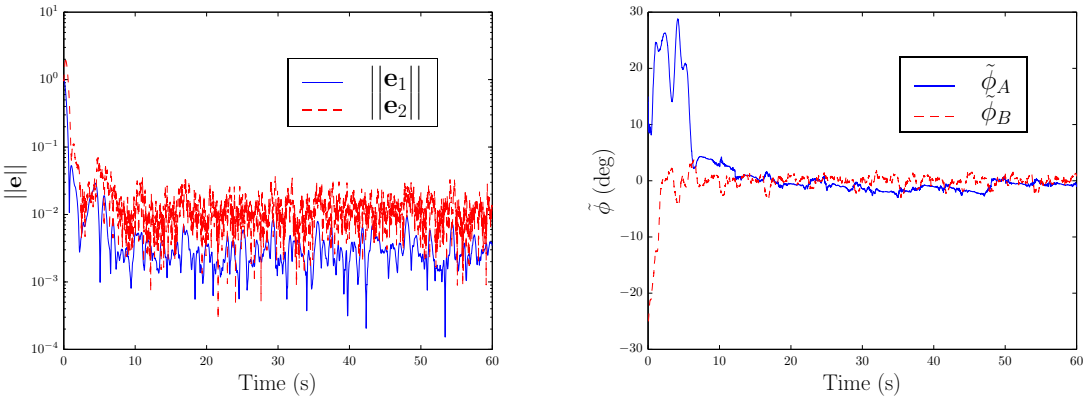

(a) Tracking error

(b) Estimation error

Figure 6.16: Simulation results for the tracking and estimation errors with the hybrid observer for the strictly out-of-plane problem with measurement noise and a PE reference trajectory

transient period. Eventually, the errors become small enough that the measurement noise makes a significant contribution to the error signal. Accordingly, the errors enter into a residual set whose size is determined by the variance of the white noise (i.e. the smaller the variance, the smaller the residual set). The errors will remain within this residual set for all time but will never become smaller. The noise not only effects the system errors but also the values of the ratio as can be seen in Figure 6.17. Without noise, the ratios converge to ± 1; however, the noise prevents the w_* values

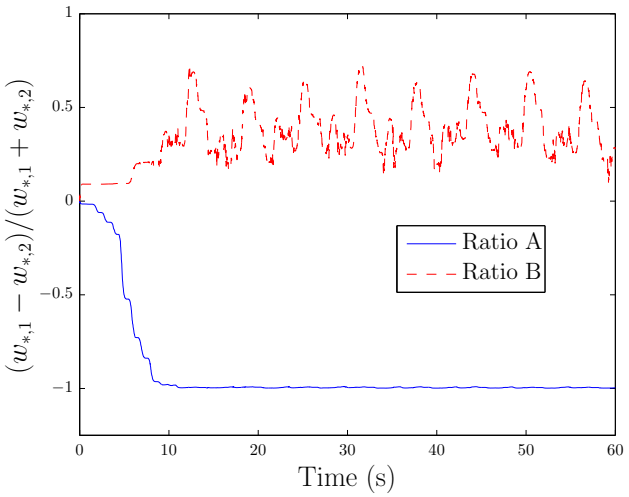

Figure 6.17: Simulations results for the hybrid ratio for the strictly out-of-plane problem with measurement noise and a PE reference trajectory

associated with the true sign of the angle from converging to zero. As a result, the ratio is corrupted by the addition of the second value. The steady-state value of the "A" ratio is determined by the magnitude of

$$4u_{f,B}|\sin\phi_B|\left(u_{f,B}|\sin\phi_B| + u_{f,A}\sin\phi_A\right)$$

in relation to the variance of the noise. Note that the "B" ratio would be the same with the values switched. In this case, the value of $u_{f,B}$ and $\sin\phi_B$ are larger than $u_{f,A}$ and $\sin\phi_A$. Thus, the "A" ratio is hardly affected by the noise but the "B" ratio does not come close to 1 since the average value is not much greater than that of the noise. In both cases, the estimation errors are able to converge to a residual set.

Recall that for perfect measurements, the hybrid observer cannot be used for stabilization problems because the ratio will converge to 0/0. When noise is included, however, this is not an issue. Therefore, a simulation was run for the stabilization problem with initial conditions $\mathbf{x}_1(0) = \begin{bmatrix}1 & -0.5 & 0.1\end{bmatrix}^\top$ and $\mathbf{x}_2(0) = \begin{bmatrix}-0.05 & -0.05 & 0\end{bmatrix}^\top$. The noise was assumed to have the same variance as before. The simulation results for the errors is shown in Figure 6.18. As before, the tracking errors reduce to a residual set that is dependent on the variance. Note that the

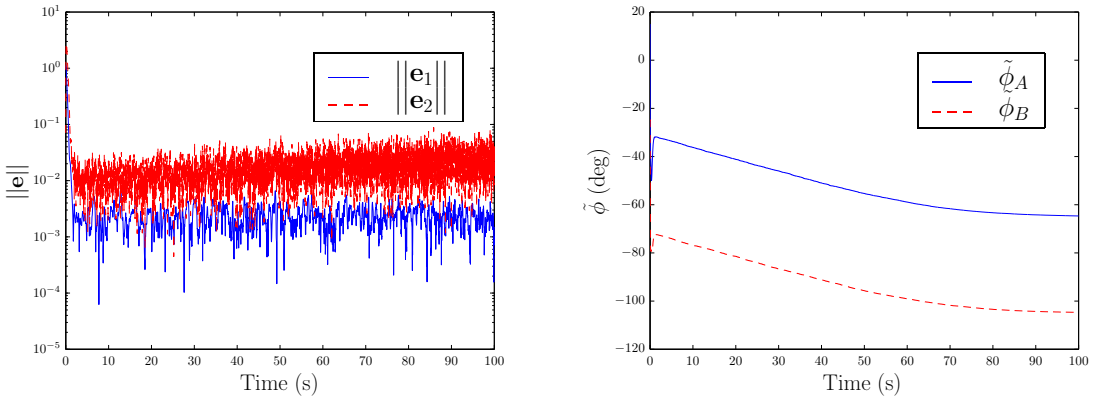

(a) Tracking error

(b) Estimation error

Figure 6.18: Simulation results for the tracking and estimation errors with the hybrid observer for the strictly out-of-plane problem with measurement noise and stabilization

residual set is approximately the same as with a PE reference trajectory since the variance of the noise has not changed. The estimation errors are unable to converge because the reference trajectory is not rich enough; however, there are no continuity issues because the ratio converges to a finite value as can be seen in Figure 6.19. In

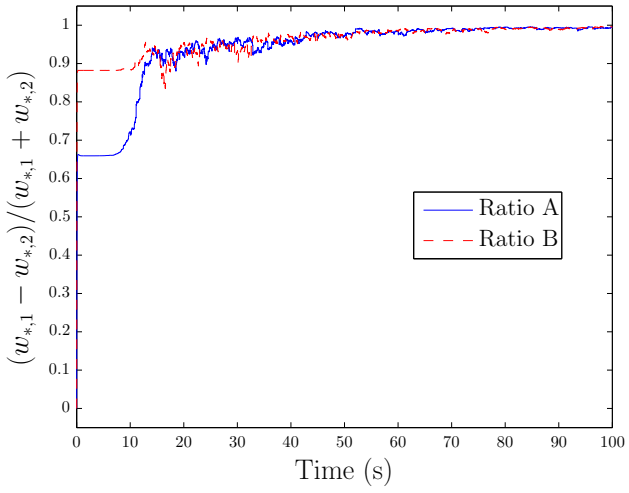

Figure 6.19: Simulations results for the hybrid ratio for the strictly out-of-plane problem with measurement noise and stabilization

this case, both of the ratios appear to be close to 1. This is not particularly significant since in the steady state $u_{f,A}$ and $u_{f,B}$ are near zero so the entire estimation process has very little meaning. It is significant that the ratios remain bounded and that the hybrid observer can be implemented when noise is expected (as it would be for a practical system).

6.8 Concluding Remarks

This chapter examines the problem of controlling a system where two of the control axes are independently misaligned. Furthermore, the misalignments are assumed to be predominately out of the plane. The geometry of the out-of-plane problem coupled with the structure of the update laws leads to difficulties in the stability analysis. A straightforward application of the certainty-equivalence like observers with the standard Lyapunov like function indicates that each set of out-of-plane misalignments has a region of attraction. Unfortunately, the region of attraction is directly dependent on the misalignments; moreover, the region of attraction does not contain the initial estimate $\hat{\phi}_A(0) = \hat{\phi}_B(0) = 0$ which means that a priori information must be available. Thus, a general set of allowable misalignments cannot be determined as in the previous chapter.

As an alternative, the Scheduled Axis Decoupling and hybrid methods are proposed. The Scheduled Axis Decoupling method is only valid in the control problem because it requires the ability to change the input to the measurement equation so that the axes can be decoupled. This method introduces a minimum time that a constant input needs to be applied such that the estimates are guaranteed to enter the region of attraction from the initial guess $\hat{\phi}_A(0) = \hat{\phi}_B(0) = 0$. Using this strategy, no prior information needs to be known about the misalignments. The switching and hybrid methods come from the specific geometry of the strictly out-of-plane problem where the magnitude of the misalignment angles is directly available. The magnitude can then be used to eliminate the error directly from the other axis by implementing a pair of observers and a sensible switching logic. The hybrid method uses a novel filtering

ratio to combine the pair of observers and overcome the discontinuity issues evident in the switching observer. These alternatives can be applied to both the estimation and control problems and are only restricted by the natural control singularity of the strictly out-of-plane problem. Unfortunately, these alternatives cannot be used to prove convergence when a single in-plane component is added to the misalignment. This deficiency is not attributed to the proposed observer, rather, the issues seem to be an artifact of the stability analysis since a numerical analysis indicates that the observer is stabilizing for this problem in addition to the strictly out-of-plane problem. Therefore, without a change to the standard stability analysis, any misalignments that contain a pair of out-of-plane components cannot readily be proven.

Chapter 7

Independent Three-Axis Misalignments

This chapter examines the problem of determining unknown actuator misalignments across all three axes. The full independent three-axis misalignment problem would require that each axes have an unknown in-plane and out-of-plane angle. The results of the previous chapter show that any set of misalignments that contain a pair of out-of-plane components plus a third component whose magnitude cannot be directly determined cannot be proven to converge. There does exist, however, a class of three-axis misalignments that can be shown to converge in the control problem using the standard certainty equivalence approach combined with the insights gained from the switching/hybrid observer and the Scheduled Axis Decoupling methodology. The class is limited to any set of misalignments where two of the axes have strictly in-plane components, and the third axis has either an in-plane or out-of-plane component but not both. This particular set of misalignments allows for the use of certainty equivalence to handle the in-plane portion while the misalignment of the third axis is eliminated directly Accordingly, a new methodology is introduced that allows for extension to the three-axis control problem. As before, the goal is to determine an allowable set of misalignments such that the observer is guaranteed to converge.

The remainder of the chapter is organized as follows. Section 7.1 introduces the set of independent three-axis misalignment problems that can be solved. Section 7.2 discusses the methodology employed for the estimates and presents stability proofs for the control problem for one of sets of misalignments. Section 7.3 highlights the performance of the proposed method through numerical simulations. Section 7.4 presents a brief discussion on the full three-axis misalignment problem. Finally, Section 7.5 discusses some concluding remarks.

7.1 Allowable Three-Axis Misalignments

At this point, there are only 4 sets of independent three-axis misalignments for which a stability proof can be completed. Since the idea of in-plane and out-of-plane loses a little bit of meaning in the three-axis problem, the convention is established that the in-plane angle for the z-axis is in the xz-plane and is denoted by θ_C. Out-of-plane for the z-axis is thus in the yz-plane and is denoted as ϕ_C to be consistent with the other axes. Using this convention, the 4 sets of misalignments are as follows:

$$\boldsymbol{\Psi}_A = \begin{bmatrix} \cos\theta_A \\ \sin\theta_A \\ 0 \end{bmatrix} \qquad \boldsymbol{\Psi}_B = \begin{bmatrix} -\sin\theta_B \\ \cos\theta_B \\ 0 \end{bmatrix} \qquad \boldsymbol{\Psi}_C = \begin{bmatrix} -\sin\theta_C \\ 0 \\ \cos\theta_C \end{bmatrix} \tag{7.1a}$$

$$\boldsymbol{\Psi}_A = \begin{bmatrix} \cos\theta_A \\ \sin\theta_A \\ 0 \end{bmatrix} \qquad \boldsymbol{\Psi}_B = \begin{bmatrix} -\sin\theta_B \\ \cos\theta_B \\ 0 \end{bmatrix} \qquad \boldsymbol{\Psi}_C = \begin{bmatrix} 0 \\ \sin\phi_C \\ \cos\phi_C \end{bmatrix} \tag{7.1b}$$

$$\boldsymbol{\Psi}_A = \begin{bmatrix} \cos\phi_A \\ 0 \\ \sin\phi_A \end{bmatrix} \qquad \boldsymbol{\Psi}_B = \begin{bmatrix} 0 \\ \cos\phi_B \\ \sin\phi_B \end{bmatrix} \qquad \boldsymbol{\Psi}_C = \begin{bmatrix} -\sin\theta_C \\ 0 \\ \cos\theta_C \end{bmatrix} \tag{7.1c}$$

$$\boldsymbol{\Psi}_A = \begin{bmatrix} \cos\phi_A \\ 0 \\ \sin\phi_A \end{bmatrix} \qquad \boldsymbol{\Psi}_B = \begin{bmatrix} 0 \\ \cos\phi_B \\ \sin\phi_B \end{bmatrix} \qquad \boldsymbol{\Psi}_C = \begin{bmatrix} 0 \\ \sin\phi_C \\ \cos\phi_C \end{bmatrix} \tag{7.1d}$$

Considering the measurement equation $\mathbf{y} = \boldsymbol{\Psi}\mathbf{u}_f$, it is clear that all 4 misalignments have a particular structure. In each set, there is a cosine term that is directly available which allows for direct elimination, albeit with a different approach then discussed in the previous chapter. The remainder of the misalignment is the same as the strictly in-plane problem which using a projection scheme can be proven to converge for all misalignments in the interval $(-\pi/4, \pi/4)$. Thus, the path is clear except that the singularity conditions must also be known. For each of the misalignments, the in-plane components must not become parallel, and the other component cannot move into the plane $(\pm\pi/2)$. Thus if all the misalignments are restricted to $(-\pi/4, \pi/4)$, then the singularity condition cannot be reached.

7.2 Control for Particular Three-Axis Misalignment

Since each of the 4 misalignments have the same structure, only the misalignment of (7.1a) is presented with the understanding that the other misalignments could be proven in a similar manner. A graphical representation of this scenario is shown in Figure 7.1. Note that there are actually two pairs of out-of-plane components in this

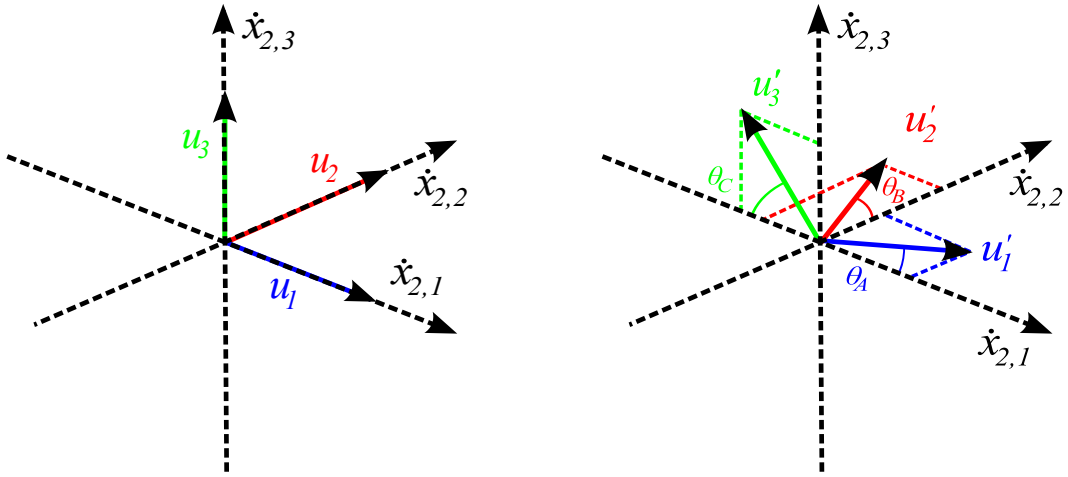

(a) $\mathbf{\Psi} = \mathbf{I}_{3\times 3}$ (b) $\mathbf{\Psi} \neq \mathbf{I}_{3\times 3}$

Figure 7.1: Graphical representation of the effect of $\mathbf{\Psi}$ for the three-axis problem where all the axes have an unknown in-plane component on the independent control axis

problem, but the specific geometry will allow for a convergence prove in the control problem. First, some background information will be given first that motivates how the estimates can be properly updated. It will then be shown that a proper choice of the control signal allows for convergence of the tracking and estimation errors. Furthermore, smooth parameter projection will be used to guarantee that the control singularity is avoided.

7.2.1 Background

Consider the measurement equation $\mathbf{y} = \mathbf{\Psi}\mathbf{u}_f$ for which the misalignment of (7.1a) can be written as

$$\mathbf{y} = \begin{bmatrix} y_1 \\ y_2 \\ y_3 \end{bmatrix} = \begin{bmatrix} u_{f,A}\cos\theta_A - u_{f,B}\sin\theta_B - u_{f,C}\sin\theta_C \\ u_{f,A}\sin\theta_A + u_{f,B}\cos\theta_B \\ u_{f,C}\cos\theta_C \end{bmatrix} \tag{7.2}$$

Note that the $\cos\theta_C$ is directly available through y_3. Therefore, only the sign of θ_C is needed to directly eliminate the effect of the z-axis misalignment. In the previous chapter, this led to implementation of the switching and hybrid observers which were dependent on first-order, low-pass filters to determine the unknown sign. An important step to that analysis was defining the $q_{*,j}$ signals. The goal of these signals was to implement both possibilities of the sign of the angle. If the correct sign of the B axis misalignment were determined, the measurement $\mathbf{y}$ could be reduced to $\mathbf{y}_A$. This was of particular importance because the norm of $\mathbf{y}_A$ is known and is equal to $u_{f,A}^2$; consequently, this value could be subtracted, and one of the q values would be equal to zero for all time. Now consider the measurement equation of (7.2). Directly eliminating the sine of the C axis misalignment only reduces $\mathbf{y}$ to $\mathbf{y}_A + \mathbf{y}_B$ which has the norm

$$u_{f,A}^2 + u_{f,B}^2 - 2u_{f,A}u_{f,B}\sin(\theta_A - \theta_B)$$

Thus for the three axis problem, it is impossible to arrive at a q value of zero since $\sin(\theta_A - \theta_B)$ is unknown. Note that the other q value will also be non-zero but will contain terms involving the C misalignment. This fact motivates a solution for this three axis-problem when the input signal can be chosen as for the control problem. Let $u_{f,A} = u_{f,B} = 0$ and $u_{f,C} =$ constant as in the Scheduled Axis Decoupling methodology. Define the signals

$$q_{C,1} \equiv y_1 + \text{sign}(u_{f,C})\sqrt{u_{f,C}^2 - y_3^2} \tag{7.3a}$$

$$q_{C,2} \equiv y_1 - \text{sign}(u_{f,C})\sqrt{u_{f,C}^2 - y_3^2} \tag{7.3b}$$

For the case of the correct sign, $q_{C,j} = 0$, and the other q value will be $2u_{f,C}\sin\theta_C$. This allows for the stable first-order filters to be given by

$$\dot{w}_{C,1} = -w_{C,1} + q_{C,1}^2 \tag{7.4a}$$

$$\dot{w}_{C,2} = -w_{C,2} + q_{C,2}^2 \tag{7.4b}$$

with the initial conditions $w_{C,j}(0) = 1$. For the case of the correct sign, the w value will converge to zero while the other value will be non-zero for all time as in the previous chapter. In addition, the correct w value will always be less than or equal to the wrong value. Using this fact, define the value of T to be when

$$\left|\frac{w_{C,1} - w_{C,2}}{w_{C,1} + w_{C,2}}\right| > \epsilon$$

for some chosen value of ϵ such that $0 < \epsilon << 1$. In theory, ϵ could be infinitesimally small since any difference automatically indicates the sign of the angle; however, ϵ can be chosen larger to account for numerical errors in calculating the w values. Next define the value

$$p \equiv \text{sign}\left[w_{C,1}(T) - w_{C,2}(T)\right] \tag{7.5}$$

and the auxiliary signal

$$\bar{\mathbf{y}}_C \equiv \begin{bmatrix} p\,\text{sign}(u_{f,C})\sqrt{u_{f,C}^2 - y_3^2} \\ 0 \\ y_3 \end{bmatrix} \tag{7.6}$$

Of particular important is that $\bar{\mathbf{y}}_C$ is the same as the true $\mathbf{y}_C$ at time T. Thus, the certainty-equivalence like vector update laws can be chosen as

$$\dot{\hat{\mathbf{\Psi}}}_A = -\gamma S\left[(\mathbf{y} - \hat{\mathbf{y}}_B - \bar{\mathbf{y}}_C) \times \hat{\mathbf{y}}_A\right]\hat{\mathbf{\Psi}}_A \tag{7.7a}$$

$$\dot{\hat{\mathbf{\Psi}}}_B = -\gamma S\left[(\mathbf{y} - \hat{\mathbf{y}}_A - \bar{\mathbf{y}}_C) \times \hat{\mathbf{y}}_B\right]\hat{\mathbf{\Psi}}_B \tag{7.7b}$$

$$\dot{\hat{\mathbf{\Psi}}}_C = -\gamma S\left(\bar{\mathbf{y}}_C \times \hat{\mathbf{y}}_C\right)\hat{\mathbf{\Psi}}_C \tag{7.7c}$$

which is implemented at T. Note that the use of the Scheduled Axis Decoupling in the initial time period has allowed for decoupling of the estimation of the x and y

axes from the z-axis. From (7.7), algebraic manipulation can be used to determine the update laws on the angles as

$$\dot{\hat{\theta}}_A = \gamma \hat{\mathbf{y}}_A^\top \Gamma_{AB} \left(\mathbf{y} - \hat{\mathbf{y}}_B - \bar{\mathbf{y}}_C \right) \tag{7.8a}$$

$$\dot{\hat{\theta}}_B = \gamma \hat{\mathbf{y}}_B^\top \Gamma_{AB} \left(\mathbf{y} - \hat{\mathbf{y}}_A - \bar{\mathbf{y}}_C \right) \tag{7.8b}$$

$$\dot{\hat{\theta}}_C = \gamma \hat{\mathbf{y}}_C^\top \Gamma_C \bar{\mathbf{y}}_C \tag{7.8c}$$

where

$$\Gamma_{AB} = \begin{bmatrix} 0 & 1 & 0 \\ -1 & 0 & 0 \\ 0 & 0 & 0 \end{bmatrix} \qquad \Gamma_C = \begin{bmatrix} 0 & 0 & 1 \\ 0 & 0 & 0 \\ -1 & 0 & 0 \end{bmatrix}$$

The estimates of the pair of in-plane components need to be restricted to stay within the region of attraction and avoid the inherent control singularity. Accordingly, the smooth projection scheme is adopted as in 2.3.3. Let the estimates on θ_* be replaced by estimates of the projection variables ξ_* where the three estimates are related through

$$\theta_* = \frac{\mu_*}{2} \left(1 - \tanh \xi_* \right) + \theta_{*,\min} \tag{7.9a}$$

$$\hat{\theta}_* = \frac{\mu_*}{2} \left(1 - \tanh \hat{\xi}_* \right) + \theta_{*,\min} \tag{7.9b}$$

where $* = A, B, C$ and $\mu_* = \theta_{*,\max} - \theta_{*,\min}$. Furthermore, let the update laws on $\hat{\xi}_*$ be determined as

$$\dot{\hat{\xi}}_* = -\dot{\hat{\theta}}_* \tag{7.10}$$

where the update laws on $\hat{\theta}_*$ are consistent with (7.8). Since the problem has been decoupled into a strictly in-plane problem and a single rotation problem, the previous results already established indicate that the observers are convergent for a PE input signal which is valid for $t \geq T$.

7.2.2 Control Problem

As shown numerous times before, the observer can simply be introduced into the control design by modifying the estimation term of the control law in order to show that perfect tracking is achievable. At this point, it is nearly trivial to show the

extension to the control problem. Assume the implementation of the standard filters on the system dynamics, and let the control signal be determined in two parts. First for $0 \leq t < T$ (where T is defined as in the previous section), let the control be given by

$$\mathbf{u}(t) = \begin{bmatrix} 0 \\ 0 \\ h \end{bmatrix} \tag{7.11}$$

where h is a non-zero scalar constant. Note that this forces the requirement that $\mathbf{f}(\mathbf{x}_1, \mathbf{x}_2)$ be such that the dynamics are ISS. For $t \geq T$, let the control be determined through

$$\mathbf{u} = -\hat{\mathbf{\Psi}}^{-1}\left[\mathbf{g} + \alpha\left(k_p\mathbf{e}_1 + \mathbf{e}_2\right) - \dot{\hat{\mathbf{\Psi}}}\hat{\mathbf{\Psi}}^{-1}\hat{\mathbf{y}}\right] \tag{7.12}$$

where

$$\dot{\hat{\mathbf{\Psi}}} = \begin{bmatrix} -\sin\hat{\theta}_A & -\cos\hat{\theta}_B & -\cos\hat{\theta}_C \\ \cos\hat{\theta}_A & -\sin\hat{\theta}_B & 0 \\ 0 & 0 & -\sin\hat{\theta}_C \end{bmatrix} \begin{bmatrix} \frac{\dot{\hat{\theta}}_A}{\cosh^2\xi_A} & 0 & 0 \\ 0 & \frac{\dot{\hat{\theta}}_B}{\cosh^2\xi_B} & 0 \\ 0 & 0 & \frac{\dot{\hat{\theta}}_C}{\cosh^2\xi_C} \end{bmatrix} \tag{7.13}$$

The following theorem can then be stated:

Theorem 7.2.1. *Consider the tracking error dynamics of (2.4) where* $\mathbf{f}$ *is such that the system dynamics of (2.2) are input-to-state stable. Suppose that the adaptive control law is given by (7.11) and (7.12) with the smooth projection scheme for* θ_* *and update laws of (7.10). Then the convergence condition*

$$\lim_{t\to\infty} \begin{bmatrix} \mathbf{e}_1(t) \\ \mathbf{e}_2(t) \end{bmatrix} = \mathbf{0}$$

is applicable for all admissible reference trajectories $\mathbf{r}$ *and initial conditions* $[\mathbf{x}_1(0), \mathbf{x}_2(0)]^\top$ *provided that the gain* α *is chosen such that* $\alpha = k_p + k_v$, $|\theta_A|, |\theta_B| < \pi/4$, $|\theta_C| < \pi/2$, $|\hat{\theta}_A(0)|, |\hat{\theta}_B(0)| < \pi/4$, *and* $|\hat{\theta}_C(0)| < \pi/2$.

Proof. This proof is nearly identical to the other control problem proofs with a few minor changes. Therefore, a condensed proof is presented which highlights the only changes. Let $\Lambda \in \mathbb{R}^{3\times 3}$ be re-defined as

$$\Lambda = \begin{bmatrix} \sin\left(\frac{1}{2}\bar{\theta}_A\right) & \cos\left(\frac{1}{2}\bar{\theta}_B\right) & \cos\left(\frac{1}{2}\bar{\theta}_C\right) \\ -\cos\left(\frac{1}{2}\bar{\theta}_A\right) & \sin\left(\frac{1}{2}\bar{\theta}_B\right) & 0 \\ 0 & 0 & \sin\left(\frac{1}{2}\bar{\theta}_C\right) \end{bmatrix} \tag{7.14}$$

Note that the $||\Lambda|| < 1$, since the largest eigenvalue of $\Lambda^\top \Lambda$ is 1. Let the Lyapunov like function on the control be defined as in (5.23) at which point the derivative can be represented as

$$\begin{aligned}\dot{V}_C &\leq -k_p||\mathbf{e}_1||^2 - k_v||\mathbf{e}_{2,f}||^2 + 2||\mathbf{e}_1 + \mathbf{e}_{2,f}||\,||\Lambda||\,||\mathbf{z}_{1/2}(\tilde{\theta})|| \\ &\leq -k_p||\mathbf{e}_1||^2 - k_v||\mathbf{e}_{2,f}||^2 + 2\sqrt{2}\left(||\mathbf{e}_1|| + ||\mathbf{e}_{2,f}||\right)||\mathbf{z}(\tilde{\theta})|| \end{aligned} \tag{7.15}$$

The Lyapunov-like function for the estimation terms is given by

$$\begin{aligned}V_E = \frac{\mu_A}{2}\left[\log\left(\cosh\hat{\xi}_A\right) - \tilde{\xi}_A \tanh\xi_A\right] + \frac{\mu_B}{2}\left[\log\left(\cosh\hat{\xi}_B\right) - \tilde{\xi}_B \tanh\xi_B\right] \\ + \frac{\mu_C}{2}\left[\log\left(\cosh\hat{\xi}_C\right) - \tilde{\xi}_C \tanh\xi_C\right] \geq 0 \end{aligned} \tag{7.16}$$

which using previous results can be shown to have the derivative

$$\dot{V}_E \leq -\gamma\beta||\mathbf{z}(\tilde{\theta})||^2 \leq 0 \tag{7.17}$$

where β is a positive scalar constant. Now, consider the joint Lyapunov-like function which combines the estimation and control functions of (5.16) and (7.16)

$$V = V_C + \tau V_E \geq 0 \tag{7.18}$$

where τ is a positive scalar constant. The associated derivative of V comes from (5.17) and (7.17) and can be manipulated using completion of squares to get the result

$$\dot{V} \leq -\frac{k_p}{2}||\mathbf{e}_1||^2 - \frac{k_v}{2}||\mathbf{e}_{2,f}||^2 - k_z||\mathbf{z}(\tilde{\theta})||^2 \leq 0 \tag{7.19}$$

where τ has been selected to be large enough to ensure that the estimation error term is negative semi-definite. Using the same signal chasing arguments and invoking Barbalat's Lemma yields

$$\lim_{t\to\infty}[\mathbf{e}_1 \quad \mathbf{e}_{2,f} \quad \mathbf{z}(t)] = \mathbf{0}$$

By construction of the filter dynamics, $\mathbf{e}_{2,f} \to \mathbf{0}$ implies $\mathbf{e}_2 \to \mathbf{0}$ as $t \to \infty$, and the control objectives are met. Upon recovering the control signal, the proof is complete.

□

7.3 Numerical Simulations

To demonstrate the performance of the proposed control scheme, a simulation was performed where $\theta_A = -15°$, $\theta_B = 20°$, and $\theta_C = 25°$. The system dynamics was assumed to have the drift term

$$\mathbf{f} = -\mathbf{x}_1 - \mathbf{x}_2$$

which has already been shown to be ISS. The persistently exciting reference trajectory

$$\mathbf{r}(t) = \begin{bmatrix} \cos t \\ \sin t \cos 2t \\ \sin t \sin 2t \end{bmatrix}$$

was used with the system initially at rest. Furthermore, the initial conditions for $\mathbf{g}_f$ and $\mathbf{e}_{2,f}$ were set to zero, and the initial estimates were assumed to be $\hat{\theta}_A(0) = \hat{\theta}_B(0) = \hat{\theta}_C(0) = 0$. In addition, the gains were selected as $k_p = k_v = 3$ and $\gamma = 10$ with $\epsilon = 0.01$. The simulation results are shown in Figure 7.2. As expected, the tracking

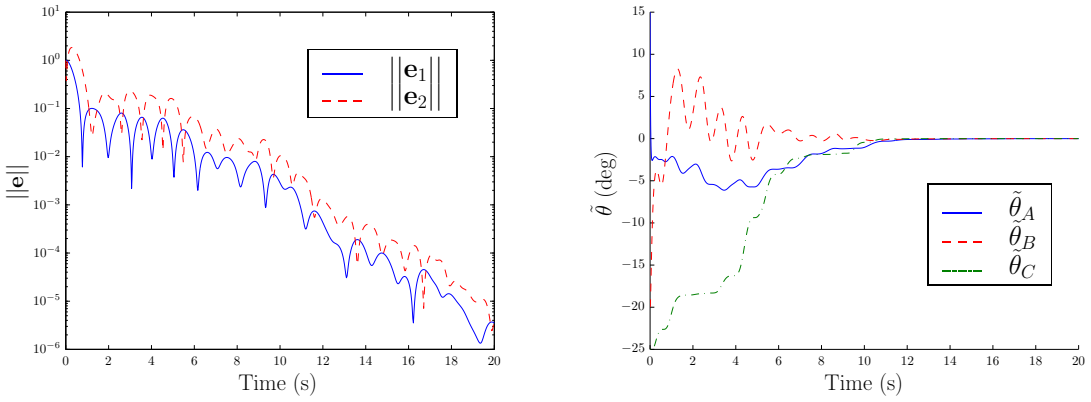

(a) Tracking error

(b) Estimation error

Figure 7.2: Simulation results for the tracking and estimation errors for the allowable set of three-axis misalignments

errors converge to zero. In addition, the estimation errors are able to converge because of the PE reference trajectory. Note that T for this problem occurs at ≈ 0.05 seconds and as such is not visible on the plots.

7.4 Full Three-Axis Misalignment Problem

As mentioned previously, the full three-axis misalignment problem cannot be proven since the out-of-plane problem cannot be proven with additional components. This is not to say that the proposed observers do not result in convergence of the estimates to the true values even when each axis has an uncertain in-plane and out-of-plane misalignment. The general certainty-equivalence like observers for the full three-axis problem are given by

$$\dot{\hat{\mathbf{\Psi}}}_A = -\gamma S\left[(\mathbf{y} - \hat{\mathbf{y}}_B - \hat{\mathbf{y}}_C) \times \hat{\mathbf{y}}_A\right] \hat{\mathbf{\Psi}}_A \tag{7.20a}$$

$$\dot{\hat{\mathbf{\Psi}}}_B = -\gamma S\left[(\mathbf{y} - \hat{\mathbf{y}}_A - \hat{\mathbf{y}}_C) \times \hat{\mathbf{y}}_B\right] \hat{\mathbf{\Psi}}_B \tag{7.20b}$$

$$\dot{\hat{\mathbf{\Psi}}}_C = -\gamma S\left[(\mathbf{y} - \hat{\mathbf{y}}_A - \hat{\mathbf{y}}_B) \times \hat{\mathbf{y}}_C\right] \hat{\mathbf{\Psi}}_C \tag{7.20c}$$

To show that the observer *appears* to be convergent for a large set of unknown misalignments, a Monte Carlo simulation was run with 2000 random misalignments. The number was increased to 2000 since there is no known proof associated with this problem. Note that no additional mechanisms (e.g. projection, hybrid, etc.) were implemented to subsidize the estimation process. Each misalignment was assumed to lie in the interval $(-\pi/4, \pi/4)$ since this is required to avoid the control singularities. The initial estimates were all assumed to be zero. For this problem, the error for each axis was assumed to be the magnitude of the angle between $\mathbf{\Psi}_*$ and $\hat{\mathbf{\Psi}}_*$ for $* = A, B, C$. The magnitude of the error, ρ_* is available through the dot product since $\mathbf{\Psi}_*^\top \hat{\mathbf{\Psi}}_* = \cos\rho_*$. The results of the Monte Carlo simulation is shown in Figure 7.3. For 2000 different initial conditions, the observer converges for every single set of misalignments. This indicates, at least empirically, that the proposed observers converge for a significant set of misalignments across all three axes. The only remaining step is to overcome the issues that appear in the stability analysis and develop a proof for this most general problem.

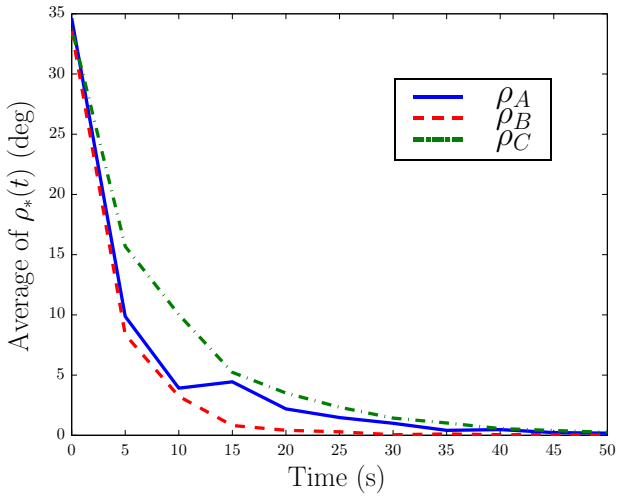

Figure 7.3: Monte Carlo simulation for 2000 random sets of true misalignments between $-\pi/4$ and $\pi/4$ and with initial estimates on all misalignments set to zero

7.5 Concluding Remarks

This chapter examines extending the results from the two-axis misalignments to the full three-axis problem. Since the two-axis problem cannot be proven for the out-of-plane problem with additional uncertain components, only a set of 4 three-axis misalignment problems can be proven to converge. All 4 misalignments have a structure of two in-plane components combined with a component from the third axis whose magnitude is directly available. For this structure, a stability proof can be made for both the estimation and control problems using a combination of the standard certainty-equivalence like and hybrid observers. The proof allows for the estimates to evolve everywhere such that the constraint imposed by the control singularity is not violated. Unfortunately, proofs can only be completed for this small set of three-axis misalignments. The inability to prove convergence seems to be an artifact of the stability analysis since a numerical analysis of a large set misalignments for the full three-axis misalignment problem shows convergence for every misalignment using the standard certainty-equivalence like observers.

Chapter 8

Conclusion

8.1 Summary

The primary goal of this dissertation has been to investigate realistic issues due to actuator misalignment through the use of adaptive estimation and control. Although there is a significant amount of literature which uses adaptive control, most assume that measurements are perfectly available or that sensors and actuators are perfectly aligned. This dissertation attempted to rectify or at minimum investigate some of these deficiencies especially focusing on the issue of actuator misalignment. As a whole, a new adaptive control scheme is introduced for rigid-body attitude tracking where realistic measurement models are used and the body inertia matrix is constant and unknown. In addition, several observers are investigated for the actuator misalignment problem where the control axes are independently misaligned. Although the observers can be proven to converge with varying success, this work represents the first significant effort to consider possible misalignments effecting the control signal.

Specifically, Chapter 3 introduces an adaptive control scheme for the rigid-body attitude tracking problem with the attitude available through vector measurements and the angular velocity measurement subject to a constant unknown bias. A Lyapunov stability analysis shows that the control scheme meets the control objectives regardless of where the body inertia matrix is known or unknown. In the case that the inertia matrix is known, it can be guaranteed that all of the estimation errors converge without any persistence of excitation conditions. When inertia uncertainty is introduced, certain PE conditions are required for the inertia (and other overparameterized values) estimates to converge. In addition to the stability guar-

antees, simulations suggest that the adaptive control scheme is robust to both noise and time-varying bias to within a residual set.

In Chapter 4, the problem of an actuator misalignment as an unknown rotation matrix is introduced. Although it is not expected that a realistic actuator misalignment would be represented through a pure rotation matrix, the solution to the problem introduces two key aspects to the general actuator misalignment problem. The first is that the measurement equation must somehow be recovered from the system dynamics, which was shown to be possible through the filtering process. The second aspect is that the estimate of the misalignment must remain invertible to avoid the control signal from becoming unbounded. In general, the evolution of the estimates cannot be limited by many standard observers; however, the nonlinear observer structure used throughout the dissertation maintains either the $SO(3)$ or unit-vector constraints for all time. Therefore, the only singularities that must be avoided come from the structure of the misalignment. In Chapter 4, the rotation matrix estimate is always invertible but the addition of the unknown scaling requires that the scaling never pass through zero. This is accomplished through a smooth projection scheme which is applied to noticeable effect throughout the dissertation.

The remainder of the chapters focus on the idea of actuator misalignments that are independent across all three control axes. Thus, each of the control axes is a unit vector which has been shifted away from the ideal direction. Although the ultimate goal was to show convergence for the full three-axis misalignment problem, the problem was approached by dividing into simpler sub-problems which would give specific insights. To begin, one axis was assumed to be ideal while the other two axes were assumed to be uncertain. When the misalignments were restricted to the plane, the proposed certainty-equivalence like update laws were proven to be convergent using a fairly straightforward stability analysis for both the estimation and control problems. The only issue arose from restricting the allowable misalignments and their estimates to a region of attraction which was accomplished through parameter projection. Unfortunately, when the misalignments have pairs of components which are out-of-plane, the analysis from Chapter 5 breaks down because of the unique geome-

try of the out-of-plane problem combined with restrictions inherent to the procedure adopted for the stability analysis. In fact, it is found that infinitesimally small out-of-plane errors contribute the most to the "cross-terms" that are to be dominated as part of the stability analysis. Accordingly, a general region of attraction cannot be readily determined as was the case with in-plane only misalignments. It is proven that a region of attraction exists but it does not include the initial estimates being equal to zero which would be the initial guess when no additional information is available on the misaligned values. To overcome these inherent issues, the Scheduled Axis Decoupling methodology and switching/hybrid observers are developed which do guarantee convergence of the estimates to the true values for the strictly out-of-plane problem. Inclusion of any additional misalignment components, however, does not allow for extension of any of these alternate methods to prove convergence. As a result, a majority of three-axis misalignments cannot be proven using the stability analysis described herein. Chapter 7 does prove convergence of the tracking errors for a set of four three-axis misalignments by combining aspects of the observers from Chapters 5 and 6, but the misalignments discussed represent very specific instances which do not include the full-problem. Therefore, no proof is available for the full three-axis problem, but a numerical analysis indicates that the proposed observer is convergent for a large set of three-axis misalignments which would suggest that the issue is solely with the stability analysis and not the observer itself.

8.2 Statement of Contributions

This dissertation has made several original contributions to the field of adaptive control. These are outlined in no particular order as follows:

1. An adaptive control scheme was developed for the problem of rigid-body attitude tracking with the attitude available through vector measurements and the angular velocity subject to a constant and unknown bias. Existing literature on this problem [32, 33] was restricted to the body inertia matrix being perfectly known. The main contribution here is that this problem can be extended

to the situation where the inertia matrix is constant but unknown which has never been shown previously [53, 54]. In addition, the use of immersion and invariance techniques aided with the appearance of the inertia matrix affinely in the control allows for superior performance of the proposed control scheme compared to the existing literature. Furthermore, the proposed scheme is far less susceptible to the effects of measurement noise on the vector measurements.

2. An adaptive control scheme was developed and shown to meet the control objectives for a standard set of dynamics and the rigid-body attitude tracking problem when an unknown rotation matrix and scaling pre-multiply the control signal. Although an appropriate observer already existed in prior literature for an unknown rotation matrix, this is the first time the special orthogonal matrix was assumed to act as an actuator misalignment. Moreover, the completion of the tracking objectives is not straightforward and requires the implementation of the first-order low-pass filters to recover the necessary measurement equation. Again, although a considerable amount of literature exists on using adaptive control on scalar high frequency gains (the unknown scaling in this problem), the appearance of the scaling and the misalignment causes a non-affine representation of the uncertainty. In general this is a significant difficulty in the area of adaptive controls, which was readily overcome in this dissertation through the novel implementation of the filter process and parameter projection [56].

3. To the author's best knowledge, this is the first systematic formulation of the problem of actuator misalignments where it is assumed that each of the ideal control axes are shifted independently to a different direction. Most of the existing literature approaches misalignment uncertainty through consideration of the actuator dynamics which reduces the problem to accounting for uncertain plant parameters albeit with overparameterization. Although this is certainly a valid approach, the results are far more specific to the system dynamics. The idea that uncertainty in actuators is manifested as a "net" misalignment is far more general and potentially applicable to a larger set of problems. Thus, all the

results contained herein related to independent actuator misalignments are the first attempt at understanding a more fundamental theoretic control problem.

4. The proposed certainty-equivalence like observer is shown to have a region of attraction (i.e. stabilizing) for a large set of misalignments for the strictly in-plane problem and the in-plane problem with an additional out-of-plane component. The observer is shown to be convergent by itself, but when endowed with the additional features of smooth parameter projection, the set of allowable misalignments is greatly increased. For the in-plane problems, the region of attraction is independent of the values of the misalignment. * A region of attraction is also determined for the out-of-plane problem; however, the region of attraction is directly dependent on the values of the unknown misalignments which does not allow for generalization of the stability result.

5. The two-axis actuator misalignment problem with strictly out-of-planes components is introduced. The particular structure of the out-of-plane components causes issues with the stability analysis since infinitesimally small misalignments require that all the of the non-positive quadratic terms be used to dominate the cross terms. This is not the case for the in-plane problem where infinitesimally small errors lead to infinitesimally small magnitudes in the cross terms. Thus, there is a fundamental challenge with proving convergence using the proposed stability analysis techniques for the out-of-plane problem. For the strictly out-of-plane problem, the issues can be overcome by applying a switching observer coupled with a novel filter switching logic. Although this adds complexity, the switching observer is valid for all possible misalignments. To avoid the potential discontinuities in the estimates, a novel hybrid observer was developed which maintains continuity of the estimates while still keeping the stability properties of the switching observer.

*Provided that the magnitude of the misalignments is less than $\pi/4$ which is assumed since misalignments greater than this would automatically lead to singularity issues in the control problem.

6. Throughout the dissertation, the observers are readily extended to the control problem because a separation property is established for the control design. That is to say, the filter control design can simply be combined with the stabilizing observers to guarantee that the control objectives are met. The only consideration is that eliminating the unknown misalignment from the dynamics requires inversion of the estimated misalignment matrix. Therefore, the actuator misalignment problem has intrinsic singularities in the control which are manifested through the independent control axes becoming parallel. [†] To avoid the control singularities, smooth parameter projection is implemented to bound the estimates and guarantee that the control signal remains bounded. Thus, the extension to the control problem is fairly straightforward.

8.3 Future Work

The work contained in this dissertation introduces many interesting questions that could be fruitful research directions in the future. These are outlined in no particular order as follows:

1. In Chapter 3, a solution for the control objectives of the rigid-body attitude tracking problem with vector measurements, unknown bias, and unknown body inertia is shown. Although this is a significant step in including more realistic effects into the adaptive controller, there are still assumptions that are made and could be addressed. Of particular importance is the assumption that there is an infinite amount of control effort available. In practice, this is obviously not the case, and the input is subject to actuator saturation. This problem has been studied separately [13, 16, 17] but not in the context of the problem shown here. In addition, other more realistic effects such as unknown external disturbances could be included. Finally, one of the limiting properties of the

[†]The use of azimuth and elevation as the minimal two parameter set in the dissertation also introduces possibility singularities. Fortunately, these are very specific misalignments that in most cases are outside the proven convergence region of the observers.

proposed solution is that two constant vector measurements must be available because the stability analysis of Mahoney et al. [28] is used to show convergence. Akella et. al [27] establish the same result without the gyro bias but with time-varying measurements. If the stability analysis of [27] could be extended to include the bias estimate, then the results contained in this dissertation would be valid for a single time-varying measurement.

2. In Chapter 4, uncertainties are assumed to only exist on the control through the unknown scaling and rotation matrix. Although the focus was placed on studying the actuator misalignment, it would also be useful to consider uncertainties in the plant parameters. This represents a particularly complex set of circumstances since the effects of the plant and misalignment uncertainties would essentially be mixed together. If this problem could be solved, however, the results contained within this dissertation could be extended to the rigid-body attitude tracking problem with unknown body inertia matrix. This would be a considerable step forward in the study of the tracking problem with adaptive control.

3. In Chapter 4, additional complexity was introduced through an unknown constant scalar. The scaling is assumed to effect the entire control signal. A more realistic approach would be to have a scaling on each axis that represents performance degradation across each axis as is assumed in the existing literature on fault-tolerant control. Combining this concept of performance degradation with the actuator misalignment representation proposed in this dissertation would lead to a very general model of actuator uncertainty that would apply to a large set of control problems.

4. Clearly, the most useful future work would be to resolve the issues in the stability analysis of the strictly out-of-plane problem. Although a region of attraction exists in the current form, the exclusion of the zero initial estimates means that a priori knowledge must be known about the misalignments. Furthermore, in the current form, the region of attraction is directly dependent on the unknown

misalignments. Thus, the goal would be to demonstrate a general region of attraction for the certainty-equivalence like observer at which point the result could be extended to the full three-axis independent misalignment problem.

5. The majority of this work has focused on the actuator misalignment problem but several mentions have also been made to the sensor misalignment problem. In general, the sensor misalignment problem is the estimation problem discussed throughout the dissertation since the sensor misalignment would directly affect the measurements. This should be clear from Chapter 3 where the sensor misalignment examined is actually the attitude of the vehicle. The main open question is whether sensor misalignments are manifested in the way described in the dissertation where individual sensor axes are misaligned. The idea of "net effect" makes sense for actuator misalignments but that might not necessarily be the case for sensors. This idea needs to be studied more carefully and perhaps different structures would need to be investigated for sensor misalignments.

8.4 Concluding Remarks

This dissertation attempts to extend the range of practical applications encompassed by adaptive control. If there has been a weakness to adaptive control theory and its applications, it is that they are far too restricting in their assumptions despite their rigorous stability proofs. Therefore any adaptive methods which eliminate these assumptions is useful to the application community. Of particular interest is the study of actuator alignment uncertainties on the control signal which has received far less attention in the existing literature. Although general results exist in the form of the unknown high frequency gain problem, the appearance of control misalignments in practical applications is far more structured. Therefore, examination of actuator uncertainties where the control axes are independently misaligned is of practical and fundamental importance. Despite the fact that the dissertation falls short of resolving the full three-axis misalignment problem, the insights gained from

the detailed study of the various sub-problems represents an important step in using adaptive control to counteract the effects of actuator misalignments, and ultimately also sensor misalignments that can appear in a variety of practical systems.

Appendices

Appendix A

Proof for Rigid-Body Attitude Tracking with Unknown Rotation and Scaling

Using the filter discussion of Section 2.3.2, the filtered error dynamics can be represented as

$$\dot{\boldsymbol{\omega}}_f = \mathbf{J}^{-1}\left(\mathbf{W}_f + c\boldsymbol{\Psi}\mathbf{u}_f\right) \tag{A.1}$$

Re-arranging the terms in (A.1), $\bar{\mathbf{y}}$ can be defined as in (4.42) and the measurement equation of (4.11) is recovered. Then define

$$\hat{\mathbf{y}} \equiv \hat{\boldsymbol{\Psi}}\mathbf{u}_f \tag{A.2}$$

where $\hat{c}$ has not been included as in the observer. Next, choose the filtered control signal as

$$\mathbf{u}_f = -\frac{1}{\hat{c}}\hat{\boldsymbol{\Psi}}^\top\left(\mathbf{W}_f + k_p\mathbf{J}\delta\mathbf{q}_v + k_v\mathbf{J}\boldsymbol{\omega}_f\right) \tag{A.3}$$

If the estimates were to converge, the unknown values on the control would be eliminated and only the standard control problem would remain. Consider the Lyapunov-like function on the estimation values given by

$$V_E = \tau\frac{\mathbf{z}_v^\top\mathbf{z}_v}{2cz_0^2} + \frac{\mu}{2\lambda}\left[\log\left(\cosh\hat{\xi}\right) - \tilde{\xi}\tanh\xi\right] \tag{A.4}$$

where the second term is consistent with (2.30) and the discussion of the smooth projection scheme. Using the derivatives from (4.18) and (2.31), the rate of change of the Lyapunov-like function is

$$\dot{V}_E = -\gamma\tau||\mathbf{z}_v \times \mathbf{u}_f||^2 - \frac{1}{\lambda}\tilde{c}\,\dot{\hat{\xi}} \tag{A.5}$$

Next, consider the Lyapunov-like function involving the control values

$$V_C = \frac{1}{2}\boldsymbol{\omega}_f^\top\boldsymbol{\omega}_f + 2\left(1 - \delta q_0\right) \tag{A.6}$$

Taking the derivative of (A.6) and recognizing that $c = \hat{c} - \tilde{c}$ yields

$$\begin{aligned}
\dot{V}_C &= \boldsymbol{\omega}_f^\top \dot{\boldsymbol{\omega}}_f - 2\delta\dot{q}_0 \\
&= \boldsymbol{\omega}_f^\top \dot{\boldsymbol{\omega}}_f + \delta\mathbf{q}_v^\top \boldsymbol{\omega} \\
&= \alpha\delta\mathbf{q}_v^\top \boldsymbol{\omega}_f + (\delta\mathbf{q}_v + \boldsymbol{\omega}_f)^\top \dot{\boldsymbol{\omega}}_f \\
&= \alpha\delta\mathbf{q}_v^\top \boldsymbol{\omega}_f + (\delta\mathbf{q}_v + \boldsymbol{\omega}_f)^\top \mathbf{J}^{-1}(\mathbf{W}_f + c\boldsymbol{\Psi}\mathbf{u}_f) \\
&= \alpha\delta\mathbf{q}_v^\top \boldsymbol{\omega}_f + (\delta\mathbf{q}_v + \boldsymbol{\omega}_f)^\top \mathbf{J}^{-1}\left[\mathbf{W}_f + c\hat{\boldsymbol{\Psi}}\mathbf{u}_f + c\left(\boldsymbol{\Psi} - \hat{\boldsymbol{\Psi}}\right)\mathbf{u}_f\right] \\
&= \alpha\delta\mathbf{q}_v^\top \boldsymbol{\omega}_f + (\delta\mathbf{q}_v + \boldsymbol{\omega}_f)^\top \mathbf{J}^{-1}\left[\mathbf{W}_f + (\hat{c} - \tilde{c})\hat{\boldsymbol{\Psi}}\mathbf{u}_f + c\boldsymbol{\Psi}\left(\mathbf{I} - \boldsymbol{\Psi}^\top\hat{\boldsymbol{\Psi}}\right)\mathbf{u}_f\right] \\
&= \alpha\delta\mathbf{q}_v^\top \boldsymbol{\omega}_f + (\delta\mathbf{q}_v + \boldsymbol{\omega}_f)^\top \mathbf{J}^{-1}\left[-k_p\mathbf{J}\delta\mathbf{q}_v - k_v\mathbf{J}\boldsymbol{\omega}_f + \tilde{c}\hat{\mathbf{y}} - c\boldsymbol{\Psi}\left(\mathbf{I} - \boldsymbol{\Psi}^\top\hat{\boldsymbol{\Psi}}\right)\mathbf{u}_f\right] \\
&= -k_p||\delta\mathbf{q}_v||^2 - k_v||\boldsymbol{\omega}_f||^2 + (\alpha - k_p - k_v)\,\delta\mathbf{q}_v^\top\boldsymbol{\omega}_f \\
&\quad + c\,(\delta\mathbf{q}_v + \boldsymbol{\omega}_f)^\top \mathbf{J}^{-1}\boldsymbol{\Psi}\left(\mathbf{I} - \boldsymbol{\Psi}^\top\hat{\boldsymbol{\Psi}}\right)\mathbf{u}_f - \tilde{c}\,(\delta\mathbf{q}_v + \boldsymbol{\omega}_f)^\top \mathbf{J}^{-1}\hat{\mathbf{y}} \\
&= -k_p||\delta\mathbf{q}_v||^2 - k_v||\boldsymbol{\omega}_f||^2 \\
&\quad + c\,(\delta\mathbf{q}_v + \boldsymbol{\omega}_f)^\top \mathbf{J}^{-1}\boldsymbol{\Psi}\left(\mathbf{I} - \boldsymbol{\Psi}^\top\hat{\boldsymbol{\Psi}}\right)\mathbf{u}_f - \tilde{c}\,(\delta\mathbf{q}_v + \boldsymbol{\omega}_f)^\top \mathbf{J}^{-1}\hat{\mathbf{y}}
\end{aligned} \tag{A.7}$$

where the constraint on the control gains has been used. Define the joint Lyapunov-like function V by combining (A.4) and (A.6) as

$$V = V_C + V_E \tag{A.8}$$

which from (A.5) and (A.7) has the derivative

$$\begin{aligned}
\dot{V} = &-k_p||\delta\mathbf{q}_v||^2 - k_v||\boldsymbol{\omega}_f||^2 - \gamma\tau||\mathbf{z}_v \times \mathbf{u}_f||^2 \\
&+ c\,(\delta\mathbf{q}_v + \boldsymbol{\omega}_f)^\top \mathbf{J}^{-1}\boldsymbol{\Psi}\left(\mathbf{I} - \boldsymbol{\Psi}^\top\hat{\boldsymbol{\Psi}}\right)\mathbf{u}_f - \tilde{c}\left[(\delta\mathbf{q}_v + \boldsymbol{\omega}_f)^\top \mathbf{J}^{-1}\hat{\mathbf{y}} + \frac{1}{\lambda}\dot{\hat{\xi}}\right]
\end{aligned} \tag{A.9}$$

This is the point where the update law on $\hat{\xi}$ is chosen such that the term proceeding $\tilde{c}$ is zero. Thus, using the observer for $\hat{\xi}$ in (4.44), completing squares, and relating the matrix norm to the eigenvalues, equation (A.9) becomes

$$\begin{aligned}
\dot{V} &\leq -k_p||\delta\mathbf{q}_v||^2 - k_v||\boldsymbol{\omega}_f||^2 - \gamma\tau||\mathbf{z}_v \times \mathbf{u}_f||^2 \\
&\quad + ||c\,(\delta\mathbf{q}_v + \boldsymbol{\omega}_f)^\top \mathbf{J}^{-1}\boldsymbol{\Psi}\left(\mathbf{I} - \boldsymbol{\Psi}^\top\hat{\boldsymbol{\Psi}}\right)\mathbf{u}_f|| \\
&\leq -k_p||\delta\mathbf{q}_v||^2 - k_v||\boldsymbol{\omega}_f||^2 - \gamma\tau||\mathbf{z}_v \times \mathbf{u}_f||^2
\end{aligned}$$

$$
\begin{aligned}
&+ |c| \, || \left(\delta\mathbf{q}_v + \boldsymbol{\omega}_f\right) || \, ||\mathbf{J}^{-1}|| \, ||\boldsymbol{\Psi}|| \, || \left(\mathbf{I} - \boldsymbol{\Psi}^\top \hat{\boldsymbol{\Psi}}\right) \mathbf{u}_f || \\
&\leq -k_p ||\delta\mathbf{q}_v||^2 - k_v ||\boldsymbol{\omega}_f||^2 - \gamma\tau ||\mathbf{z}_v \times \mathbf{u}_f||^2 \\
&\quad + 4|c| \, J_{\max}^{-1} \, ||\mathbf{z}_v \times \mathbf{u}_f|| \\
&\leq -\frac{k_p}{2} ||\delta\mathbf{q}_v||^2 - \frac{k_v}{2} ||\boldsymbol{\omega}_f||^2 - \gamma\tau \left[1 - \frac{8c^2}{\gamma\tau J_{\max}^2} \left(\frac{1}{k_p} + \frac{1}{k_v}\right)\right] ||\mathbf{z}_v \times \mathbf{u}_f||^2 \\
&\quad - \frac{k_p}{2} \left[||\delta\mathbf{q}_v|| - \left(\frac{4|c|J_{\max}^{-1}}{k_p}\right) ||\mathbf{z}_v \times \mathbf{u}_f||\right]^2 \\
&\quad - \frac{k_v}{2} \left[||\boldsymbol{\omega}_f|| - \left(\frac{4|c|J_{\max}^{-1}}{k_v}\right) ||\mathbf{z}_v \times \mathbf{u}_f||\right]^2 \\
&\leq -\frac{k_p}{2} ||\mathbf{e}_1||^2 - \frac{k_v}{2} ||\mathbf{e}_{2,f}||^2 - \gamma' ||\mathbf{z}_v \times \mathbf{u}_f||^2
\end{aligned} \tag{A.10}
$$

where an appropriate choice of τ was made to ensure that the factor on the rotation error term remains positive. Thus, $\dot{V}$ is negative semi-definite, indicating boundedness for all closed-loop signals. Further, because V is lower-bounded, $\int_0^\infty \dot{V}(t)\, dt$ exists and is finite which implies that $\delta\mathbf{q}_v$, $\boldsymbol{\omega}_f$ and $\mathbf{z}_v \times \mathbf{u}_f \in \mathcal{L}_2 \cap \mathcal{L}_\infty$. It follows that $\delta\dot{\mathbf{q}}_v$, $\dot{\boldsymbol{\omega}}_f$ and $\dot{\mathbf{z}}_v$ are $\mathcal{L}_\infty$ from (3.7), (A.1), and (2.14a). Thus by Barbalat's lemma, $\delta\mathbf{q}_v$ and $\boldsymbol{\omega}_f \to 0$ as $t \to \infty$. Furthermore, because of the definition of the filter of (4.41), $\boldsymbol{\omega}_f \to 0$ implies $\delta\boldsymbol{\omega} \to 0$ as $t \to \infty$. Therefore, the control objective is met. In addition, from Barbalat's lemma, $||\mathbf{z}_v \times \mathbf{u}_f|| \to 0$ as $t \to 0$. This, however, does not guarantee convergence of $\mathbf{z}_v \to 0$ and ultimately $\hat{\boldsymbol{\Psi}} \to \boldsymbol{\Psi}$ in all cases; yet, it is emphasized that even without convergence of the misalignment matrix, the attitude and angular velocity errors still converge to zero. For completeness, the process of recovering the control signal $\mathbf{u}$ is shown from the filter definition $\mathbf{u} = \alpha\mathbf{u}_f + \dot{\mathbf{u}}_f$.

$$
\begin{aligned}
\mathbf{u} &= -\alpha \frac{1}{\hat{c}} \hat{\boldsymbol{\Psi}}^\top \left(\mathbf{W}_f + k_p \mathbf{J}\delta\mathbf{q}_v + k_v \mathbf{J}\boldsymbol{\omega}_f\right) - \frac{d}{dt}\left(\frac{1}{\hat{c}}\right) \hat{\boldsymbol{\Psi}}^\top \mathbf{u}_f \\
&\quad - \frac{1}{\hat{c}} \frac{d}{dt}\left(\hat{\boldsymbol{\Psi}}^\top\right) \mathbf{u}_f - \frac{1}{\hat{c}} \hat{\boldsymbol{\Psi}}^\top \left(\dot{\mathbf{W}}_f + k_p \mathbf{J}\delta\dot{\mathbf{q}}_v + k_v \mathbf{J}\dot{\boldsymbol{\omega}}_f\right) \\
&= -\frac{1}{\hat{c}} \hat{\boldsymbol{\Psi}}^\top \left(\left(\alpha\mathbf{W}_f + \dot{\mathbf{W}}_f\right) + k_v \mathbf{J}\left(\alpha\boldsymbol{\omega}_f + \dot{\boldsymbol{\omega}}_f\right) + \alpha k_p \mathbf{J}\delta\mathbf{q}_v + \frac{1}{2} k_p \mathbf{J}\left[\delta q_0 \mathbf{I} + S(\delta\mathbf{q}_v)\right]\delta\boldsymbol{\omega}\right) \\
&\quad - \frac{\mu}{2\hat{c}^2}\left(1 - \tanh^2\hat{\xi}\right)\dot{\hat{\xi}}\mathbf{u}_f - \frac{1}{\hat{c}}\left[-\gamma S(\bar{\mathbf{y}} \times \hat{\mathbf{y}})\hat{\boldsymbol{\Psi}}\right]^\top \mathbf{u}_f \\
&= -\frac{1}{\hat{c}} \hat{\boldsymbol{\Psi}}^\top \left[\mathbf{W} + k_v \mathbf{J}\delta\boldsymbol{\omega} + k_p \mathbf{J}\left(\alpha\delta\mathbf{q}_v + \frac{1}{2} k_p \mathbf{J}\left[\delta q_0 \mathbf{I} + S(\delta\mathbf{q}_v)\right]\delta\boldsymbol{\omega}\right)\right]
\end{aligned}
$$

$$
\begin{aligned}
&- \frac{\mu}{2\hat{c}^2}\left(1-\tanh^2\hat{\xi}\right)\dot{\hat{\xi}}\,\hat{\boldsymbol{\Psi}}^\top\hat{\mathbf{y}} - \frac{\gamma}{\hat{c}}\hat{\boldsymbol{\Psi}}^\top S(\bar{\mathbf{y}}\times\hat{\mathbf{y}})\hat{\boldsymbol{\Psi}}^\top\hat{\mathbf{y}} \\
\mathbf{u} = -\frac{1}{\hat{c}}\hat{\boldsymbol{\Psi}}^\top\Big[&\mathbf{W} + k_v\mathbf{J}\delta\boldsymbol{\omega} + k_p\mathbf{J}\Big(\alpha\delta\mathbf{q}_v + \frac{1}{2}\left[q_0\mathbf{I}_{3\times3} + S(\delta\mathbf{q}_v)\right]\delta\boldsymbol{\omega}\Big) \\
&+ \frac{\mu}{2\hat{c}}\left(1-\tanh^2\hat{\xi}\right)\dot{\hat{\xi}}\,\hat{\boldsymbol{\Psi}}^\top\hat{\mathbf{y}} + \gamma S\left(\bar{\mathbf{y}}\times\hat{\mathbf{y}}\right)\hat{\boldsymbol{\Psi}}^\top\hat{\mathbf{y}}\Big]
\end{aligned}
$$

which is equivalent to (4.45).

Appendix B

Determining the Upper Bounds on Δ

Consider upper bounding the term $\Delta_{\tilde{\theta}_A,\tilde{\phi}_A}$ for a fixed value of $\theta_P > 0$. This can be done as follows:

$$\begin{aligned}
\Delta_{\tilde{\theta}_A,\tilde{\phi}_A} &= \sqrt{\frac{\cos\hat{\phi}_A}{\cos\phi_A}}\sqrt{\frac{\tilde{\theta}_A\sin\tilde{\phi}_A}{\tilde{\phi}_A\sin\tilde{\theta}_A}}\delta_{\tilde{\phi}_A,\tilde{\theta}_A} \\
&= \sqrt{\frac{\cos\hat{\phi}_A}{\cos\phi_A}}\sqrt{\frac{\tilde{\theta}_A\sin\tilde{\phi}_A}{\tilde{\phi}_A\sin\tilde{\theta}_A}}\tan\left(\frac{1}{2}\tilde{\theta}_A\right)\sin\hat{\phi}_A\cos\phi_A \\
&= \sqrt{\cos\phi_A\cos\hat{\phi}_A}\sin\hat{\phi}_A\tan\left(\frac{1}{2}\tilde{\theta}_A\right)\sqrt{\frac{\tilde{\theta}_A\sin\tilde{\phi}_A}{\tilde{\phi}_A\sin\tilde{\theta}_A}} \\
&\leq \left|\sqrt{\cos\phi_A\cos\hat{\phi}_A}\sin\hat{\phi}_A\tan\left(\frac{1}{2}\tilde{\theta}_A\right)\sqrt{\frac{\tilde{\theta}_A\sin\tilde{\phi}_A}{\tilde{\phi}_A\sin\tilde{\theta}_A}}\right| \\
&\leq \underbrace{\left|\sqrt{\cos\phi_A\cos\hat{\phi}_A}\right|}_{\leq 1}\underbrace{\left|\sin\hat{\phi}_A\sqrt{\frac{\sin\tilde{\phi}_A}{\tilde{\phi}_A}}\right|}_{\text{max when }\hat{\phi}_A=\theta_P}\underbrace{\left|\tan\left(\frac{1}{2}\tilde{\theta}_A\right)\sqrt{\frac{\tilde{\theta}_A}{\sin\tilde{\theta}_A}}\right|}_{\text{max when }\tilde{\theta}_A=2\theta_P} \\
&\leq |\sin\theta_P|\left|\tan\theta_P\sqrt{\frac{2\theta_P}{\sin(2\theta_P)}}\right| \\
&\leq \tan\theta_P\sqrt{\frac{2\theta_P\sin^2\theta_P}{2\sin\theta_P\cos\theta_P}}
\end{aligned} \tag{B.1}$$

Using (B.1) define the value

$$\Delta^{\max}_{\tilde{\theta}_A,\tilde{\phi}_A} = \sqrt{\theta_P\tan\theta_P}\ \tan\theta_P \tag{B.2}$$

which guarantees that $\Delta_{\tilde{\theta}_A,\tilde{\phi}_A} \leq \Delta^{\max}_{\tilde{\theta}_A,\tilde{\phi}_A}$.

Consider upper bounding the term $\Delta_{\tilde{\theta}_A,\tilde{\theta}_B}$ for a fixed value of $\theta_P > 0$. This

can be done as follows:

$$\begin{aligned}
\Delta_{\tilde{\theta}_A,\tilde{\theta}_B} &= \sqrt{\frac{\cos\hat{\phi}_A}{\cos\phi_A}}\left(\sqrt{\frac{\tilde{\theta}_A\sin\tilde{\theta}_B}{\tilde{\theta}_B\sin\tilde{\theta}_A}}\delta_{\tilde{\theta}_A,\tilde{\theta}_B}+\sqrt{\frac{\tilde{\theta}_B\sin\tilde{\theta}_A}{\tilde{\theta}_A\sin\tilde{\theta}_B}}\delta_{\tilde{\theta}_B,\tilde{\theta}_A}\right)\\
&= \sqrt{\frac{\tilde{\theta}_A\sin\tilde{\theta}_B}{\tilde{\theta}_B\sin\tilde{\theta}_A}}\frac{1}{\sqrt{\cos\phi_A\cos\hat{\phi}_A}}\frac{\sin\left(\hat{\theta}_A-\frac{1}{2}\bar{\theta}_B\right)}{\cos\left(\frac{1}{2}\tilde{\theta}_B\right)}\\
&\quad+\sqrt{\frac{\tilde{\theta}_B\sin\tilde{\theta}_A}{\tilde{\theta}_A\sin\tilde{\theta}_B}}\frac{\sin\left(\frac{1}{2}\bar{\theta}_A-\hat{\theta}_B\right)}{\cos\left(\frac{1}{2}\tilde{\theta}_A\right)}\sqrt{\frac{\cos\hat{\phi}_A}{\cos\phi_A}}\cos\left(\frac{1}{2}\tilde{\phi}_A\right)\cos\left(\frac{1}{2}\bar{\phi}_A\right)\\
&\leq \underbrace{\left|\sqrt{\frac{\tilde{\theta}_A}{\sin\tilde{\theta}_A}}\right|}_{\text{max when }\tilde{\theta}_A=2\theta_P}\underbrace{\left|\sqrt{\frac{\sin\tilde{\theta}_B}{\tilde{\theta}_B}}\frac{\sin\left(\hat{\theta}_A-\frac{1}{2}\bar{\theta}_B\right)}{\cos\left(\frac{1}{2}\tilde{\theta}_B\right)}\right|}_{\text{max when }\tilde{\theta}_B=2\theta_P,\hat{\theta}_A=\theta_P}\underbrace{\left|\frac{1}{\sqrt{\cos\phi_A\cos\hat{\phi}_A}}\right|}_{\text{max when }\phi_A=\hat{\phi}_A=\theta_P}\\
&\quad+\underbrace{\left|\sqrt{\frac{\tilde{\theta}_B}{\sin\tilde{\theta}_B}}\right|}_{\text{max when }\tilde{\theta}_B=2\theta_P}\underbrace{\left|\sqrt{\frac{\sin\tilde{\theta}_A}{\tilde{\theta}_A}}\frac{\sin\left(\frac{1}{2}\bar{\theta}_A-\hat{\theta}_B\right)}{\cos\left(\frac{1}{2}\tilde{\theta}_A\right)}\right|}_{\text{max when }\tilde{\theta}_A=2\theta_P,\hat{\theta}_B=\theta_P}\underbrace{\left|\frac{1}{2}\left(\sqrt{\cos\phi_A\cos\hat{\phi}_A}+\sqrt{\frac{\cos^3\hat{\phi}_A}{\cos\phi_A}}\right)\right|}_{\leq\sqrt{2}/2}\\
&\leq \left|\sqrt{\frac{2\theta_P}{\sin(2\theta_P)}}\right|\left|\sqrt{\frac{\sin(2\theta_P)}{2\theta_P}}\right|\left|\frac{\sin\theta_P}{\cos\theta_P}\right|\left|\frac{1}{\cos\theta_P}\right|\\
&\quad+\frac{\sqrt{2}}{2}\left|\sqrt{\frac{2\theta_P}{\sin(2\theta_P)}}\right|\left|\sqrt{\frac{\sin(2\theta_P)}{2\theta_P}}\right|\left|\frac{\sin\theta_P}{\cos\theta_P}\right|\\
&\leq \frac{\tan\theta_P}{\cos\theta_P}+\frac{\sqrt{2}}{2}\tan\theta_P \qquad \text{(B.3)}
\end{aligned}$$

Using (B.3) define the value

$$\Delta^{\max}_{\tilde{\theta}_A,\tilde{\theta}_B} = \frac{1}{2}\left(\frac{2}{\cos\theta_P}+\sqrt{2}\right)\tan\theta_P \qquad \text{(B.4)}$$

which guarantees that $\Delta_{\tilde{\theta}_A,\tilde{\theta}_B} \leq \Delta^{\max}_{\tilde{\theta}_A,\tilde{\theta}_B}$.

Consider upper bounding the term $\Delta_{\tilde{\phi}_A,\tilde{\theta}_B}$ for a fixed value of $\theta_P > 0$. This can be done as follows:

$$\Delta_{\tilde{\phi}_A,\tilde{\theta}_B} = \sqrt{\frac{\tilde{\phi}_A\sin\tilde{\theta}_B}{\tilde{\theta}_B\sin\tilde{\phi}_A}}\delta_{\tilde{\phi}_A,\tilde{\theta}_B}+\sqrt{\frac{\tilde{\theta}_B\sin\tilde{\phi}_A}{\tilde{\phi}_A\sin\tilde{\theta}_B}}\delta_{\tilde{\theta}_B,\tilde{\phi}_A}$$

$$
\begin{aligned}
&= \sqrt{\frac{\tilde{\phi}_A \sin\tilde{\theta}_B}{\tilde{\theta}_B \sin\tilde{\phi}_A}} \sin\hat{\phi}_A \frac{\cos\left(\hat{\theta}_A - \frac{1}{2}\bar{\theta}_B\right)}{\cos\left(\frac{1}{2}\tilde{\theta}_B\right)} \\
&\quad \sqrt{\frac{\tilde{\theta}_B \sin\tilde{\phi}_A}{\tilde{\phi}_A \sin\tilde{\theta}_B}} \frac{\sin\left(\frac{1}{2}\bar{\phi}_A\right)}{\cos\left(\frac{1}{2}\tilde{\phi}_A\right)} \cos\left(\frac{1}{2}\tilde{\theta}_A\right) \cos\left(\frac{1}{2}\bar{\theta}_A - \hat{\theta}_B\right) \\
&\leq \underbrace{\left|\sqrt{\frac{\tilde{\phi}_A}{\sin\tilde{\phi}_A}} \sin\hat{\phi}_A\right|}_{\text{max when } \tilde{\phi}_A = 2\theta_P, \hat{\phi}_A = -\theta_P} \underbrace{\left|\cos\left(\hat{\theta}_A - \frac{1}{2}\bar{\theta}_B\right)\right|}_{\leq 1} \underbrace{\left|\frac{1}{\cos\left(\frac{1}{2}\tilde{\theta}_B\right)} \sqrt{\frac{\sin\tilde{\theta}_B}{\tilde{\theta}_B}}\right|}_{\text{max when } \tilde{\theta}_B = 2\theta_P} \\
&\quad + \underbrace{\left|\sqrt{\frac{\sin\tilde{\phi}_A}{\tilde{\phi}_A}} \frac{\sin\left(\frac{1}{2}\bar{\phi}_A\right)}{\cos\left(\frac{1}{2}\tilde{\phi}_A\right)}\right|}_{\text{max when } \bar{\phi}_A = 2\theta_P, \tilde{\phi}_A = 0} \underbrace{\left|\sqrt{\frac{\tilde{\theta}_B}{\sin\tilde{\theta}_B}}\right|}_{\text{max when } \tilde{\theta}_B = 2\theta_P} \underbrace{\left|\cos\left(\frac{1}{2}\tilde{\theta}_A\right) \cos\left(\frac{1}{2}\bar{\theta}_A - \hat{\theta}_B\right)\right|}_{\leq 1} \\
&\leq \sqrt{\frac{2\theta_P}{\sin(2\theta_P)}} \sin\theta_P + \sqrt{\frac{2\theta_P}{\sin(2\theta_P)}} \sin\theta_P \qquad \text{(B.5)} \\
&\leq 2\sqrt{\frac{2\theta_P \sin^2\theta_P}{2\sin\theta_P \cos\theta_P}} \qquad \text{(B.6)}
\end{aligned}
$$

Using (B.6) define the value

$$
\Delta^{\max}_{\tilde{\phi}_A, \tilde{\theta}_B} = 2\sqrt{\theta_P \tan\theta_P} \qquad \text{(B.7)}
$$

which guarantees that $\Delta_{\tilde{\phi}_A, \tilde{\theta}_B} \leq \Delta^{\max}_{\tilde{\phi}_A, \tilde{\theta}_B}$.

Appendix C

Center Manifold for Strictly Out-of-Plane Estimation

For the strictly out-of-plane estimation problem using the certainty-equivalence like observer, a linear analysis shows that $\phi_A = \phi_B = 0$ which causes one of the eigenvalues to be zero when the inputs are assumed to be constant. Thus, a center manifold analysis is necessary to determine the stability of this point as described in [50]. To simplify the notation, let $u_{f,A} = u_1$ and $u_{f,B} = u_2$ where u_1 and u_2 are non-zero constants. In addition, let $\mathbf{u} = \begin{bmatrix} u_1 & u_2 \end{bmatrix}^\top$. For this case, the matrix $\mathbf{M}$ of (6.6) reduces to

$$\mathbf{M} = \begin{bmatrix} -u_2^2 & -u_1 u_2 \\ -u_1 u_2 & -u_2^2 \end{bmatrix} \tag{C.1}$$

The eigenvalues and eigenvectors can be found as

$$\lambda_1 = 0,\ \mathbf{v}_1 = \begin{bmatrix} u_2 \\ -u_1 \end{bmatrix}; \qquad \lambda_2 = -||\mathbf{u}||^2,\ \mathbf{v}_2 = \begin{bmatrix} u_1 \\ u_2 \end{bmatrix} \tag{C.2}$$

Let $\mathbf{P}$ be a similarity transformation where

$$\mathbf{P} = \begin{bmatrix} \mathbf{v}_1 & \mathbf{v}_2 \end{bmatrix} \tag{C.3}$$

then $\mathbf{M}$ can be transformed into a block diagonal matrix of the eigenvalues, that is,

$$\mathbf{P}^{-1}\mathbf{M}\mathbf{P} = \begin{bmatrix} 0 & 0 \\ 0 & -||\mathbf{u}||^2 \end{bmatrix}$$

The change of variables

$$\begin{bmatrix} s \\ d \end{bmatrix} = \mathbf{P}^{-1} \begin{bmatrix} \tilde{\phi}_A \\ \tilde{\phi}_B \end{bmatrix} \tag{C.4}$$

transforms the nonlinear error dynamics of (6.5) into

$$\dot{s} = \frac{\gamma u_1 u_2}{||\mathbf{u}||^2}\big(u_1 \sin(u_1 d + u_2 s)\left[\cos(u_2 d - u_1 s) - 1\right] + u_2 \sin(u_2 d - u_1 s)\left[1 - \cos(u_1 d + u_2 s)\right]\big) \tag{C.5a}$$

$$\dot{d} = -\frac{\gamma}{||\mathbf{u}||^2}\big(u_1 \sin(u_1 d + u_2 s)\left[u_1^2 + u_2^2 \cos(u_2 d - u_1 s)\right] + u_2 \sin(u_2 d - u_1 s)\left[u_2^2 + u_1^2 \cos(u_1 d + u_2 s)\right]\big) \tag{C.5b}$$

From Theorem 8.1 of [50], there exists a continuously differentiable function $h(s)$ such that $d = h(s)$ is a center manifold of (C.5). Furthermore, if $d(0) = h(s(0))$, then the solution $(s(t), d(t))$ will lie in the manifold for all time. In this case, the motion of the center manifold is described by the reduced order system of (C.5a). Thus, the center manifold is asymptotically stable if the reduced order system can be shown to be asymptotically stable. In general, the function h is a solution of the partial differential equation

$$h'(s)\dot{s} = \dot{d}[s, h(s)] \tag{C.6}$$

Fortunately, the solution can be approximated using a Taylor series in s. For this problem,

$$h(s) = h_2 s^2 + O(|s|^3) \tag{C.7}$$

where h_2 is a to be determined coefficient which is found by applying the partial differential equation of (C.6). Using a Taylor series expansion of both sine and cosine, the trigonometric values in (C.5) can be reduced to

$$\sin(u_1 d + u_2 s) = u_2 s + u_1 h_2 s^2 + O(|s|^3) \tag{C.8a}$$

$$\cos(u_1 d + u_2 s) = 1 - \frac{1}{2}u_2^2 s^2 - u_1 u_2 h_2 s^3 + O(|s|^4) \tag{C.8b}$$

$$\sin(u_2 d - u_1 s) = -u_1 s + u_2 h_2 s^2 + O(|s|^3) \tag{C.8c}$$

$$\cos(u_1 d - u_1 s) = 1 - \frac{1}{2}u_1^2 s^2 + u_1 u_2 h_2 s^3 + O(|s|^4) \tag{C.8d}$$

Using (C.8) and keeping only the lowest order terms, it can be shown that

$$\dot{d}[s, h(s)] = -\gamma ||\mathbf{u}||^2 h_2 s^2 + O(|s|^3) \tag{C.9a}$$

$$h'(s)\dot{s} = O(|s|^4) \tag{C.9b}$$

Equating (C.9a) and (C.9b), it is clear that $h_2 = 0$; consequently, $h(s) = O(|s|^3)$ which can be used to determine the stability of the reduced order system. Since $h(s)$ is a center manifold, the motion in the center manifold can be described by plugging $h(s)$ into (C.5a) such that

$$\dot{s}[s, h(s)] = -\gamma u_1^2 u_2^2 s^3 + O(|s|^5) \tag{C.10}$$

Choosing the Lyapunov function $V = s^2/2$, the derivative becomes

$$\begin{aligned}
\dot{V} &= -\gamma u_1^2 u_2^2 s^4 + s\, O(|s|^5) \\
&\leq -\gamma u_1^2 u_2^2 s^4 + k s^6 \\
&\leq -\frac{1}{2}\gamma u_1^2 u_2^2 s^4 - \frac{1}{2} s^4 \left(\frac{\gamma u_1^2 u_2^2}{2} - k y^2 \right)
\end{aligned}$$

where $k > 0$ is a scalar constant. Thus, in some neighborhood of the origin where

$$s^2 < \frac{\gamma u_1^2 u_2^2}{2k}$$

the Lyapunov function derivative can be upper bounded by

$$\dot{V} \leq -\frac{1}{2}\gamma u_1^2 u_2^2 s^4$$

which indicates that the origin of the reduced order system is asymptotically stable. As a result, the origin of the linear system with constant inputs is stable when $\phi_A = \phi_B = 0$; moreover, the linearized dynamics of (6.6) are locally asymptotically stable for all ϕ_A and ϕ_B such that $\phi_A, \phi_B \in (-\pi/2, \pi/2)$.

Appendix D

Addition of Single In-Plane Component

Consider the measurement equation $\mathbf{y} = \mathbf{\Psi}\mathbf{u}_f$ where $\mathbf{\Psi}$ coincides with the x-axis having an in-plane and out-of-plane component and the y-axis only has an out-of-plane component as in (6.55). Using the standard certainty-equivalence like update laws of (5.8) given by

$$\dot{\hat{\mathbf{\Psi}}}_A = -\gamma S\left[(\mathbf{y} - \hat{\mathbf{y}}_B - \mathbf{y}_C) \times \hat{\mathbf{y}}_A\right] \hat{\mathbf{\Psi}}_A$$
$$\dot{\hat{\mathbf{\Psi}}}_B = -\gamma S\left[(\mathbf{y} - \hat{\mathbf{y}}_A - \mathbf{y}_C) \times \hat{\mathbf{y}}_B\right] \hat{\mathbf{\Psi}}_B$$

the estimation error dynamics for the angles θ_A, ϕ_A, and ϕ_B can be determined as

$$\dot{\tilde{\theta}}_A = \dot{\hat{\theta}}_A = -\gamma \left(\frac{\cos\phi_A}{\cos\hat{\phi}_A}\right) \sin\tilde{\theta}_A \, u_{f,A}^2 + \gamma \delta_{\tilde{\theta}_A,\tilde{\phi}_B} \sin\tilde{\phi}_B \, u_{f,A} \, u_{f,B} \tag{D.1a}$$

$$\dot{\tilde{\phi}}_A = \dot{\hat{\phi}}_A = -\gamma \sin\tilde{\phi}_A \, u_{f,A}^2 + \gamma \delta_{\tilde{\phi}_A,\tilde{\theta}_A} \sin\tilde{\theta}_A \, u_{f,A}^2 - \gamma \delta_{\tilde{\phi}_A,\tilde{\phi}_B} \sin\tilde{\phi}_B \, u_{f,A} \, u_{f,B} \tag{D.1b}$$

$$\dot{\tilde{\phi}}_B = \dot{\hat{\phi}}_B = -\gamma \sin\tilde{\phi}_B \, u_{f,B}^2 + \gamma \delta_{\tilde{\phi}_B,\tilde{\theta}_A} \sin\tilde{\theta}_A \, u_{f,A} \, u_{f,B} - \gamma \delta_{\tilde{\phi}_B,\tilde{\phi}_A} \sin\tilde{\phi}_A \, u_{f,A} \, u_{f,B} \tag{D.1c}$$

where

$$\delta_{\tilde{\theta}_A,\tilde{\phi}_B} = \frac{\sin\left(\frac{1}{2}\bar{\phi}_B\right)\cos\hat{\theta}_A}{\cos\left(\frac{1}{2}\tilde{\phi}_B\right)\cos\hat{\phi}_A} \tag{D.2a}$$

$$\delta_{\tilde{\phi}_A,\tilde{\theta}_A} = \tan\left(\frac{1}{2}\tilde{\theta}_A\right)\sin\hat{\phi}_A\cos\phi_A \tag{D.2b}$$

$$\delta_{\tilde{\phi}_A,\tilde{\phi}_B} = \frac{\cos\hat{\phi}_A\cos\left(\frac{1}{2}\bar{\phi}_B\right)}{\cos\left(\frac{1}{2}\tilde{\phi}_B\right)} + \frac{\sin\hat{\theta}_A\sin\hat{\phi}_A\sin\left(\frac{1}{2}\bar{\phi}_B\right)}{\cos\left(\frac{1}{2}\tilde{\phi}_B\right)} \tag{D.2c}$$

$$\delta_{\tilde{\phi}_B,\tilde{\theta}_A} = \frac{\sin\hat{\phi}_B\left(\cos\phi_A + \cos\hat{\phi}_A\right)\cos\left(\frac{1}{2}\bar{\theta}_A\right)}{2\cos\left(\frac{1}{2}\tilde{\theta}_A\right)} \tag{D.2d}$$

$$\delta_{\tilde{\phi}_B,\tilde{\phi}_A} = \frac{\cos\hat{\phi}_B\cos\left(\frac{1}{2}\bar{\phi}_A\right)}{\cos\left(\frac{1}{2}\tilde{\phi}_A\right)} + \frac{\left(\cos\theta_A + \cos\hat{\theta}_A\right)\sin\hat{\phi}_B\sin\left(\frac{1}{2}\bar{\phi}_A\right)}{2\cos\left(\frac{1}{2}\tilde{\phi}_A\right)} \tag{D.2e}$$

Consider the Lyapunov-like function

$$V_E = 2\sin^2\left(\frac{1}{2}\tilde{\theta}_A\right) + 2\sin^2\left(\frac{1}{2}\tilde{\phi}_A\right) + 2\sin^2\left(\frac{1}{2}\tilde{\phi}_B\right) \tag{D.3}$$

Next, define the scalar signals

$$x \equiv \sqrt{\gamma}\sin\tilde{\phi}_A\, u_{f,A} \tag{D.4a}$$

$$y \equiv \sqrt{\gamma}\sin\tilde{\theta}_B\, u_{f,B} \tag{D.4b}$$

$$z \equiv \sqrt{\gamma\frac{\cos\phi_A}{\cos\hat{\phi}_A}}\sin\tilde{\theta}_A\, u_{f,A} \tag{D.4c}$$

Using these signals, the derivative of the Lyapunov-like function can be represented as

$$\dot{V}_E \leq -x^2 - y^2 - z^2 + \Delta_{xy}|x|\,|y| + \Delta_{xz}|x|\,|z| + \Delta_{yz}|y|\,|z| \tag{D.5}$$

where

$$\Delta_{xy} \equiv \eta' + \frac{\sin\hat{\theta}_A\sin\hat{\phi}_A\sin\left(\frac{1}{2}\bar{\phi}_B\right)}{\cos\left(\frac{1}{2}\tilde{\phi}_B\right)} + \frac{\left(\cos\theta_A + \cos\hat{\theta}_A\right)\sin\hat{\phi}_B\sin\left(\frac{1}{2}\bar{\phi}_A\right)}{2\cos\left(\frac{1}{2}\tilde{\phi}_A\right)} \tag{D.6a}$$

$$\Delta_{yz} \equiv \sqrt{\frac{\cos\phi_A}{\cos\hat{\phi}_A}}\left[\frac{\sin\left(\frac{1}{2}\bar{\phi}_B\right)\cos\hat{\theta}_A}{\cos\left(\frac{1}{2}\tilde{\phi}_B\right)\cos\hat{\phi}_A} + \frac{\sin\hat{\phi}_B\left(\cos\phi_A + \cos\hat{\phi}_A\right)\cos\left(\frac{1}{2}\bar{\theta}_A\right)}{2\cos\left(\frac{1}{2}\tilde{\theta}_A\right)}\right] \tag{D.6b}$$

$$\Delta_{xz} \equiv \sqrt{\cos\phi_A\cos\hat{\phi}_A}\,\sin\hat{\phi}_A\tan\left(\frac{1}{2}\tilde{\theta}_A\right) \tag{D.6c}$$

From this point, the standard procedure would be to try and dominate the cross terms by limiting the magnitude of the Δ's. It should be clear that Δ_{yz} and Δ_{xz} can be made arbitrarily small by limiting the magnitude of the misalignment angles and their estimates. This can be done because of the sine terms that appear throughout these terms. Moreover, the additional terms in Δ_{xy} will also be arbitrarily small; however, η' will remain the same as (6.2) because it contains only cosine terms. Thus, as before, the Δ_{xy} term cannot be made arbitrarily small by requiring small deviations. In fact, $\Delta_{xy} > \eta'$ in some cases. Therefore, the addition of the extra terms makes it impossible to dominate Δ_{xy} since $\Delta_{xy} > 2$ even for infinitesimally small angles. Furthermore, the constraint $\Delta_{xy} < 2$ cannot even be applied since other portions of the quadratic terms must also be used to dominate Δ_{xz} and Δ_{yz}.

Bibliography

[1] A. A. Nofi. Defining and measuring shared situational awareness. *CRM D0002895.A1/Final*, 2000.

[2] A. Cebrowski and J. Raymond. Operationally responsive space: A new defense business model. *Parameters*, 35(2):67–77, 2005.

[3] J. T. Y. Wen and K. Kreutz-Delgado. The attitude control problem. *Automatic Control, IEEE Transactions on*, 36(10):1148 –1162, Oct. 1991.

[4] B. Wie, H. Weiss, and A. Arapostathis. Quarternion feedback regulator for spacecraft eigenaxis rotations. *Journal Of Guidance, Control, And Dynamics*, 12(3), May-June 1989.

[5] S. Sastry and M. Bodson. *Adaptive Control: Stability, Convergence, and Robustness*. Prentice-Hall, Upper Saddle River, NJ, 1989, Chap. 3.

[6] D. Seo and M. R. Akella. High-performance spacecraft adaptive attitude-tracking control through attracting-manifold design. *Journal of Guidance, Control, and Dynamics*, 31(4):884–891, July-Aug. 2008.

[7] A. Sanyal, A. Fosbury, N. Chaturvedi, and D.S. Bernstein. Inertia-free spacecraft attitude tracking with disturbance rejection and almost global stabilization. *Journal of Guidance, Control and Dynamics*, 32(4):1167–1178, July-Aug. 2009.

[8] F. Lizarralde and J. T. Y. Wen. Attitude control without angular velocity measurement: A passivity approach. *Automatic Control, IEEE Transactions on*, 41:468 –472, 1996.

[9] P. Tsiotras. Further passivity results for the attitude control problem. *IEEE Transactions on Automatic Control*, 43(11):1597–1600, Nov. 1998.

[10] M. R. Akella. Rigid body attitude tracking without angular velocity feedback. *Systems & Control Letters*, 42(4):321 – 326, 2001.

[11] A. Tayebi. Unit quaternion-based output feedback for the attitude tracking problem. *IEEE Transactions on Automatic Control*, 53(6):1516 –1520, July 2008.

[12] B. T. Costic, D. M. Dawson, M. S. de Queiroz, and V. Kapila. Quaternion-based adaptive attitude tracking controller without velocity measurements. *Journal of Guidance, Control, and Dynamics*, 24(6):1214–1222, 2001.

[13] R.J. Wallsgrove and M.R. Akella. Globally stabilizing saturated attitude control in the presence of bounded unknown disturbances. *Journal of Guidance, Control and Dynamics*, 28(5):957–963, 2005.

[14] Qinglei Hu. Robust adaptive sliding mode attitude maneuvering andvibration damping of three-axis-stabilized flexible spacecraft with actuator saturation limits. *Nonlinear Dynamics*, 55:301–321, 2009.

[15] Qinglei Hu and Bing Xiao. Fault-tolerant sliding mode attitude control for flexible spacecraft under loss of actuator effectiveness. *Nonlinear Dynamics*, 64:13–23, 2011.

[16] P. Tsiotras and J.H. Luo. Control of underactuated spacecraft with bounded inputs. *Automatica*, 36(8):1153–1169, 2000.

[17] J.D. Boskovic, S.M. Li, and R.K. Mehra. Robust tracking control design for spacecraft under control input saturation. *Journal of Guidance, Control and Dynamics*, 27(4):627–633, 2004.

[18] S. Harvey, M. Balas, F. Chavez, and L. Robertson. A gradient estimation scheme of an external unknown torque on a satellite. In American Controls Conference, pages 2454–2458, 2007.

[19] W. MacKunis, K. Dupree, N. Fitz-Coy, and W. E. Dixon. Adaptive satellite attitude control in the presence of inertia and cmg gimbal friction uncertainties. *The Journal of the Astronautical Sciences*, 56(1):121–134, Jan.-March 2008.

[20] J. Ahmed, V. T. Coppola, and D. S. Bernstein. Adaptive asymptotic tracking of spacecraft attitude motion with inertia matrix identication. *Journal of Guidance, Navigation and Control*, 21(5):684–691, 1998.

[21] H. Wong, M. S. de Queiroz, and V. Kapila. Adaptive tracking control using synthesized velocity from attitude measurements. *Automatica*, 37(6):947–953, 2001.

[22] J. L. Crassidis, F. Markley, and Y. Cheng. Survey of nonlinear attitude estimation methods. *Journal of Guidance, Control, and Dynamics*, 30(1):12–28, Jan.-Feb. 2007.

[23] E. Lefferts, F. Markley, and M. Schuster. Kalman filtering for spacecraft attitude estimation. *Journal of Guidance, Control, and Dynamics*, 5(5):417–429, Sept.-Oct. 1982.

[24] J. L. Crassidis and F. Markley. Unscented filtering for spacecraft attitude estimation. *Journal of Guidance, Control, and Dynamics*, 26(4):536–542, July-Aug. 2003.

[25] C. Fan and Z. You. Highly efficient sigma point filter for spacecraft attitude and rate estimation. *Mathematical Problems in Engineering*, 2009, 2009.

[26] J. D. Boskovic, S. Li, and R. K. Mehra. Fault tolerant control of spacecraft in the presence of sensor bias. In American Controls Conference, Chicago, IL, June 2000.

[27] M. R. Akella, D. Seo, and R. Zanetti. Attracting manifolds for attitude estimation in flatland and otherlands. *Journal of the Astronautical Sciences*, 54(3 & 4):635–655, July-Dec. 2006.

[28] R. Mahony, T. Hamel, and J. M. Pflimlin. Nonlinear complementary filters on the special orthogonal group. *IEEE Transactions on Automatic Control*, 53(5):1203 –1218, June 2008.

[29] D. Seo and M. R. Akella. Separation property for rigid-body attitude tracking control problem. *Journal of Guidance, Control, and Dynamics*, 30(6):1569–1576, Nov.-Dec. 2007.

[30] J. Thienel and R. M. Sanner. A coupled nonlinear spacecraft attitude controller and observer with an unknown constant gyro bias and gyro noise. *IEEE Transactions on Automatic Control*, 48(11):2011 – 2015, Nov. 2003.

[31] J.D. Boskovic, S.M. Li, and R.K. Mehra. A globally stable scheme for spacecraft control in the presence of sensor bias. In *Aerospace Conference Proceedings, 2000 IEEE*, volume 3, pages 505–511, 2000.

[32] T. Hamel and R. Mahony. Attitude estimation on so[3] based on direct inertial measurements. In *Robotics and Automation, 2006. ICRA 2006. Proceedings 2006 IEEE International Conference on*, pages 2170–2175, May 2006.

[33] P. Pounds, T. Hamel, and R. Mahony. Attitude control of rigid body dynamics from biased imu measurements. In 46th IEEE Conference on Decision and Control, New Orleans, LA, Dec. 2007.

[34] K. S. Narendra and A. M. Annaswamy. *Stable Adaptive Systems*. Prentice-Hall, Englewood Cliffs, NJ, 1989.

[35] A.S. Morse. Towards a unified theory of parameter adaptive control: Certainty equivalence and implicit tuning. *IEEE Transactions on Automatic Control*, 37(1):15 –29, Jan. 1992.

[36] A. Chakrabortty, M. Arcak, and P. Tsiotras. Robust design of a spacecraft attitude tracking control system with actuator uncertainties. In *Proceedings 47th IEEE Conference on Decision and Control*, December 2008.

[37] H. Yoon and P. Tsiotras. Adaptive spacecraft attitude tracking control with actuator uncertainties. *The Journal of the Astronautical Sciences*, 56(2):251–268, April-June 2008.

[38] Y. Xudong. Asymptotic regulation of time-varying uncertain nonlinear systems with unknown control directions. *Automatica*, 35(5):929 – 935, 1999.

[39] Z. Ding. Adaptive output regulation of a class of nonlinear systems with completely unknown parameters. In *American Control Conference*, volume 2, pages 1566 – 1571, 4-6, 2003.

[40] L. Yan, L. Hsu, R.R. Costa, and F. Lizarralde. Variable structure model reference adaptive control for systems with unknown high frequency gain. In *42nd IEEE Conference on Decision and Control*, volume 4, pages 3525 – 3530, Dec. 2003.

[41] P. Ioannou and J. Sun. *Robust Adaptive Control*. Prentice-Hall, Upper Saddle River, NJ, 1996.

[42] Ortega R., L. Hsu, and A. Astolfi. Immersion and invariance adaptive control of linear multivariable systems. *Systems and Control Letters*, 49:37 – 47, 2003.

[43] J. D. Boskovic, S. Li, and R. K. Mehra. Intelligent control of spacecraft in the presence of actuator failures. In *Proceedings 38th IEEE Conference on Decision and Control*, pages 1587–1592, December 1999.

[44] Tandale M. D. and J. Valasek. Fault-tolerant structured adaptive model inversion control. *Journal Of Guidance, Control, And Dynamics*, 29(3), May-June 2006.

[45] D. Ye and Guang-Hong Yang. Adaptive fault-tolerant tracking control against actuator faults with application to flight control. *IEEE Transactions on Control Systems Technology*, 14(6):1088 –1096, Nov. 2006.

[46] Z. Zuo, D. W. C. Ho, and Y. Wang. Fault tolerant control for singular systems with actuator saturation and nonlinear perturbation. *Automatica*, 46(3):569 – 576, 2010.

[47] A. M. Fosbury and C. K. Nebelecky. Spacecraft actuator alignment estimation. In *Proceedings AIAA Guidance, Navigation, and Control Conference*, pages 1–18, Chicago, IL, August 2009.

[48] Peck. M. A. Estimation of wheel and cmg alignments from on-orbit telemetry. In 2001 Flight Mechanics Symposium, June 2001.

[49] M. C. Norman, Peck. M. A., and D. J. O'Shaughnessy. In-orbit estimation of inertia and momentum-actuator alignment parameters. In AAS Spaceflight Mechanics Conference, AAS 11-164, New Orleans, LA, February 2011.

[50] H. K. Khalil. *Nonlinear Systems*. Prentice Hall, Upper Saddle River, NJ, 3rd edition, 2002.

[51] Bakker R. and Annaswamy A. M. Stability and robustness properties of a simple adaptive controller. *IEEE Transactions on Automatic Control*, 41(7):1352 – 1358, 1996.

[52] M. R. Akella and K. Subbarao. A novel parameter projection mechanism for smooth and stable adaptive control. *Systems and Control Letters*, 54:43–51, 2005.

[53] T. H. Mercker and M. R. Akella. Rigid-body attitude tracking with vector measurements and unknown gyro bias. *Journal of Guidance, Control, and Dynamics*, 44(5):1474–1484, 2011.

[54] T. Mercker and M. R. Akella. Rigid-body attitude tracking with vector measurements and unknown gyro bias. In AAS Spaceflight Mechanics Conference, New Orleans, LA, Feb. 2011.

[55] H. Schaub and J. L. Junkins. *Analytical Mechanics of Space Systems*, chapter 3. AIAA Education Series, AIAA, Reston, VA, 2003.

[56] T. H. Mercker and M. R. Akella. Onboard adaptive compensation for large-scale actuator misalignments in responsive space systems. In *AAS Guidance and Controls Conference*, AAS 10-092, Breckenridge, CO, February 2010.

[57] S. Srikant and M. R. Akella. Persistence filter-based control for systems with time-varying control gains. *Systems and Control Letters*, 58:413–420, 2009.

[58] A. Morgan and K. Narendra. On the uniform asymptotic stability of certain nonautonomous differential equations. *SIAM Journal of Control and Optimization*, 15:5–24, 1977.

[59] A. Morgan and K. Narendra. On the stability of nonautonomous differential equations $\dot{x} = [a + b(t)]x(t)$ with skew symmetric matrix b(t). *SIAM Journal of Control and Optimization*, 15:163–176, 1977.

[60] A. Tayebi, S. McGilvray, A. Roberts, and M. Moallem. Attitude estimation and stabilization of a rigid body using low-cost sensors. In *Proceedings of the Forty-Sixth IEEE Conference on Decision and Control*, New Orleans, LA, Dec. 2007.

Vita

Travis H. Mercker was born to Thomas Mercker and Janet Hentges on October 11, 1983. Travis attended the University of Texas at Austin earning his Bachelors of Science in Aerospace Engineering in the Spring of 2006. He entered graduate school at the University of Texas at Austin in the Fall of 2006 as part of the Department of Aerospace Engineering to study guidance and controls. He completed his Masters of Science in Engineering in the Spring of 2008. While conducting his Ph.D. research, Travis was a SMART scholar and worked with the Air Force Research Labs. In addition, Travis was an Assistant Instructor and taught several undergraduate classes in the Department of Aerospace Engineering.

Permanent address: 17507 Avena Valley Drive
Pflugerville, Texas 78660

This dissertation was typeset with LaTeX[†] by the author.

[†]LaTeX is a document preparation system developed by Leslie Lamport as a special version of Donald Knuth's TeX Program.